AD-A157 958 MODULATIONS OF DRIVEN NONLINEAR SURFACE WAVES ON WATER AND LIQUID HELIUM-4(U) CALIFORNIA UNIV LOS ANGELES DEPT OF PHYSICS R M KEOLIAN JUN 85 TR-44 N00014-85-K-0370 1/3

UNCLASSIFIED F/G 20/4 NL

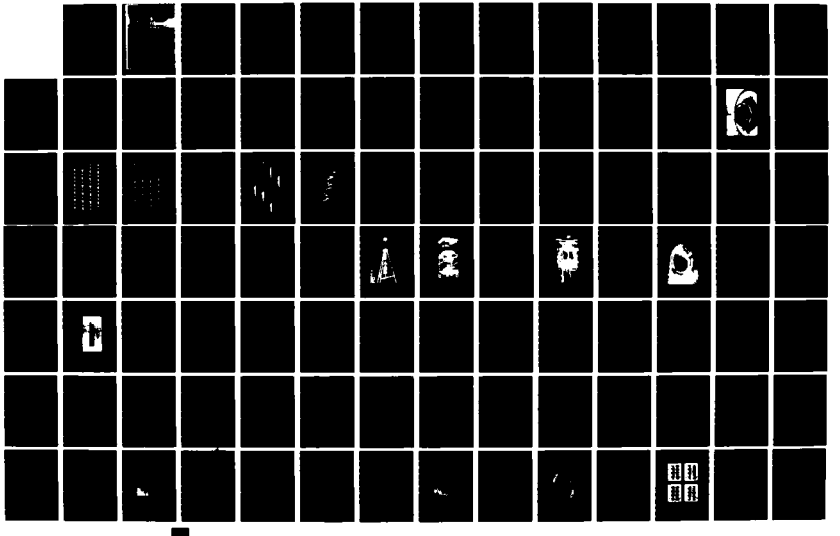

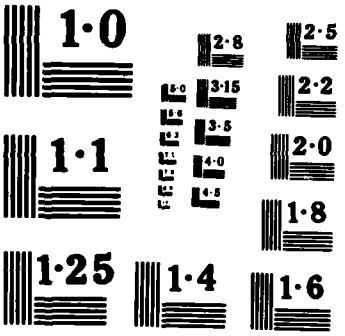


# Modulations of Driven Nonlinear Surface Waves On Water and Liquid Helium-4

By

Robert Mitchel Keolian



LOS ANGELES 90024
CALIFORNIA

TECHNICAL REPORT No. 44

June 1985

Submitted by

I. Rudnick, Project Director

Contract N00014-85-K-0370

# Modulations of Driven Nonlinear Surface Waves On Water and Liquid Helium-4

By

Robert Mitchel Keolian

Office of Naval Research
Contract
4-484024-25895

Department of Physics
University of California
Los Angeles, California 90024

to my Parents,

Grandparents,

and family

Table of Contents

List of Figures

CHAPTER I. INTRODUCTION.

Section 1. History and Data Summary



CHAPTER II. APPARATUS

Section 2. Concept and Design of the Experiment.



Section 3. Water Resonator.

Section 4. Helium Apparatus.

CHAPTER III. DATA AND INTERPRETATION.

Section 5. Cockscombs.

Section 6. Ultra Deep Modulations.



Sec. 7. Subharmonics and Quasiperiodicity in a Paddle Driven Trough.



Section 8. Smooth Modulations.

Appendix 5. Quasiperiodicity Demonstrations.



Appendix 6. Video Tape to Computer Interface.



Appendix 7. Schematics of Homemade Electronics.

## List of Tables

## Acknowledgments

I have had a fantastic time in graduate school largely because of the support and joy given me by many friends, among which are Liz, Mary Lil, John, Scott, Roset, Dave, Joe, Mary Beth, Narbik, Shen, Zhou, Vince, Antonio, Mike, the guys in the lounge, the loyal members of the Steak of the Week Club, Harold, Molly, Ellen, and the other Dave.

The reader should join me in thanking Merdeka Do and the ever so beautiful Tanya Dickenson who kept me from bungling the language more than I would have otherwise, and did their best to squeeze sugar from the text. It could have been worse.

I wish to thank Professor Robert Kelly, Professor Friedrich Busse, and Professor Paul Chaiken for their advice while serving on my doctoral committee, and Lee Turkevich for initiating such an interesting problem. I wish to also thank the physics department staff for putting up with my sometimes irrational behavior.

Jay Maynard said kind things about me that got me into grad school, and once there, the intense ball of energy that is Steven Garrett sparked and maintained my interest in acoustics.

Steve Baker has been a reliable source of information and ideas, and along with Junru Wu always gave me wise, honest advice that was often needed.

Joe Rudnick could see value in my disorganized results and gave

me needed encouragement. It is an honor when people occasionally confuse me for him. Tom Erber often offered good advice. It was also my pleasure to discuss problems and receive suggestions over the years from Gary Williams (who wishes to take no responsibility for the syntax used in this thesis).

True unsung heros are Scott Hannahs and Art Cabral, who selflessly gave their time to improve on the UCSD Pascal operating system making it much more useful, wrote utilities that pervade my programs, and taught me how and how not to use a computer.

I will dearly miss Bruce Denardo, Andres Larraza, and their advisor Seth Putterman, who have a genuine love of things nonlinear. The interactions we have are extremely important, and their enthusiasm keeps me going.

And now, I can finally do what I have long waited to do, thank My Mentor,

Professor Isadore Rudnick,

who nurtured me, gave me acoustics, taught me physics and where to find it, and showed me a way of life. He has no equal.

## VITA

| | |
|---|---|
| August 28, 1954 | Born, Los Angeles, California |
| 1976 | B.S., University of California, Los Angeles |
| 1976-1980 | Teaching Assistant, Department of Physics, University of California, Los Angeles |
| 1978 | Outstanding Teaching Assistant Award, Department of Physics, University of California, Los Angeles |
| 1978 | M.S., University of California, Los Angeles |
| 1980-1984 | Research Assistant, Department of Physics, University of California, Los Angeles |

## PUBLICATIONS AND PRESENTATIONS

"The Role of Phase Locking in Quasiperiodic Surface Waves on Liquid Helium and Water," R. Keolian and I. Rudnick, Proceedings of the International School of Physics, "Enrico Fermi," Course XCIII, "Frontiers in Physical Acoustics," Varenna, Italy, July 1984, to be published.

"Discovery of a Non-Propagating Hydrodynamic Soliton," J. Wu, R. Keolian and I. Rudnick, Proceedings of the International School of Physics, "Enrico Fermi," Course XCIII, "Frontiers in Physical Acoustics," Varenna, Italy, July 1984, to be published.

"Observation of a Nonpropagating Hydrodynamic Soliton," J. Wu, R. Keolian, I. Rudnick, Phys. Rev. Lett. 52, 1421-1424 (1984).

"Smooth Modulation of Parametrically Driven Surface Waves on Liquid Helium-4," R. Keolian and I. Rudnick, Proceedings of LT-17, Karlsruhe, W. Germany, 1121-1122 (1984).

"Subharmonic Sequences in the Faraday Experiment: Departures from Period Doubling," R. Keolian, L.A. Turkevich, S.J. Putterman, I. Rudnick, J.A. Rudnick, Phys. Rev. Lett. 47, 1133 (1981).

"A Surface Wave Instability on Liquid Helium and Water," R. Keolian and I. Rudnick, J. Acoust. Soc. Am. 77, Suppl. 1, S21, (1985). Paper presented at the meeting of the Acoustical Society of America, Austin, Texas.

"Demonstrations of Nonlinear Oscillators and Solitons," R. Keolian, J. Wu, I. Rudnick, J. Acoust. Soc. Am. 77, Suppl. 1, S35, (1985). Paper presented at the meeting of the Acoustical Society of America, Austin, Texas.

"Space Applications of Acoustics," T. Wang, E. Trinh, M. Barmatz, J.L. Allen, S.R. Baker, R. Keolian, I. Rudnick, J. Acoust. Soc. Am. 76, Suppl. 1, S56, (1984). Plenary session paper presented at the meeting of the Acoustical Society of America, Minneapolis, Minnesota.

"Discovery of a Solitary, Localized, Stationary Water Wave," J. Wu, R. Keolian, I. Rudnick, J. Acoust. Soc. Am. 74, Suppl. 1, S11, (1983). Invited paper presented at the meeting of the Acoustical Society of America, San Diego, California.

"Subharmonic Phenomena in Normal and Superfluid Helium," R. Keolian and I. Rudnick, J. Acoust. Soc. Am. 73, Suppl. 1, S82 (1983). Paper presented at the meeting of the Acoustical Society of America, Cincinnati, Ohio.

"Deep Subharmonics in High Amplitude Surface Waves on Superfluid Helium," R. Keolian and I. Rudnick, Bull. Am. Phys. Soc. 28, 253 (1983). Paper presented at the meeting of the American Physical Society, Los Angeles, California.

"Ultra-deep Subharmonics in High Amplitude Shallow Water Waves," R. Keolian and I. Rudnick, J. Acoust. Soc. Am. 72, Suppl. 1, S13 (1982). Paper presented at the meeting of the Acoustical Society of America, Orlando, Florida.

"Subharmonics, Bifurcations, Chaos and all that Jazz," I. Rudnick and R. Keolian, J. Acoust. Soc. Am. 70, Suppl. 1, S89 (1981). Invited paper presented at the meeting of the Acoustical Society of America, Miami, Florida.

"An Afternoon Interlude of Demonstration Experiments in Acoustics," I. Rudnick, S.R. Baker, R. Keolian, A. Huffman, J. Acoust. Soc. Am. 68, Suppl. 1, S22 (1980). Plenary session paper presented at the meeting of the Acoustical Society of America, Los Angeles, California.

"Acoustic Measurement of Isotopic Concentration of Gases," R. Keolian, S. Garrett, J. Maynard, I. Rudnick, J. Acoust. Soc. Am. 64, Suppl. 1, S61 (1978); Bull. Am. Phys. Soc. 24, 623 (1979). Papers presented at the meeting of the Acoustical Society of America, Honolulu, Hawaii, and the American Physical Society, Washington, D.C.

ABSTRACT OF THE DISSERTATION

Modulations of Driven Nonlinear Surface Waves
on Water and Liquid Helium-4

by

Robert Mitchel Keolian
Doctor of Philosophy in Physics
University of California, Los Angeles, 1985
Professor Isadore Rudnick, Chair

When a trough of water or liquid helium-4 is oscillated vertically at frequency f, waves can form on the surface through the process of parametric resonance (described in an appendix) at half the frequency of the drive, at f/2. The principle measurement is the liquid height at the end of the trough as a function of time. Nonlinearities determine the response amplitude and give rise to hysteresis. At larger drive amplitudes, the signal at f/2 becomes modulated at frequencies much lower than that of the drive in a variety of ways.

One such modulation is smooth with a frequency near one of the low modes of the trough, even though it is one of the higher modes that is driven. The surface amplitude is first larger on one end of the trough then larger on the other, oscillating back and forth at the

modulation frequency which is of the order of f/20. Several of these frequencies can be present at once; they may be incommensurate (irrationally related) with each other or the drive, or they may phase lock. The cause of these modulations are three wave resonant triads formed by a low mode, an intermediate mode, and the driven mode of the trough.

Another modulation is characterized by short, sudden drops in amplitude. These sudden drops are localized in space and propagate back and forth in the trough at nearly the gravity wave velocity. Several drops may be present at once.

A third modulation is characterized by extremely deep frequencies -- as low as f/2000. It seems to be caused by two adjacent modes, nonlinearly coupled together, slowly exchanging energy back and forth.

At still higher drive amplitudes the surface response is chaotic.

All these effects are present in both water and liquid helium. Helium appears to act essentially the same in either its normal or superfluid states.

In addition, subharmonic response at f/2 or f/3 and incommensurate response near f/3 is found when surface waves on water are directly (rather than parametrically) driven with a paddle.

Five appendices describe properties and demonstrations of anharmonic oscillators: bent tuning curves, parametrics, doubly bent tuning curves, phase locking, and quasiperiodicity.

# Chapter I. Introduction.

> "Only once or twice in a millennium is there a true scientific revolution, a real paradigm shift -- Newtonian mechanics and the invention of calculus in the seventeenth century was the last one." "The current scientific revolution will synthesize the whole intellectual discourse of the species."
>
> A well known nonlinear dynamicist talking about his field in "Connoisseurs of Chaos," Omni magazine, June 1983.

## Section 1. History and Data Summary.

One day, an article in Physics Today (Lubkin, 1981) caught my mentor's eye. The article describes a theory on how the oscillations of a nonlinear system might change from being simple to erratic as some parameter of the system is varied -- like temperature, the resonant frequency of a mode, or how hard the system is being driven. It says, for some range of one of the parameters, the motion might be periodic, with period T. But as the parameter is varied past a certain threshold, it takes twice as long for the motion to repeat, and the period doubles to 2T. As the parameter crosses another threshold the period doubles again to 4T. This goes on and on; after m thresholds the period becomes $2^m T$, the intervals between the

thresholds becoming smaller and smaller until the intervals geometrically accumulate to a parameter value where the period is infinite -- where the motion never repeats.

Beyond the parameter value for the last period doubling, where the period becomes infinite, the theory says there will be chaos. The motion will, to some extent, fluctuate erratically. The behavior is still determined by deterministic laws and the initial conditions, but the motion will depend on the initial condition so sensitively that no one can tell you what happens after some finite time. Measurements will jump around and appear to be noisy, but the source of the noise is not external, but comes from within the system itself. For the nonlinear mechanical systems that can be modeled by this theory, noise is intrinsic to Newton's laws.

Meanwhile, Lee Turkevich, a post-doc working at UCLA at the time, was reading Lord Rayleigh's collected works and came across a discussion (1883 b) of some experiments by Michael Faraday, which Lee brought to my mentor's attention. Faraday, in his paper (1831), was correcting a mistake made by Savart on the nature of the vibration of plates. When the plates of Chladni are excited with the bow of a violin, sand will collect on the quiescent parts of the surface of the plate, tracing out the nodal lines. Chladni and Oersted found, however, that shavings from the hairs of the bow or light powders would also collect where the vibration was most vigorous, at the antinodes. Savart stated "that every time a body emits sounds, not only is it the seat of many modes of division which are superposed,"

(which we now call orthogonal modes) "but amongst all these modes there are always two which are more distinctly established than all the rest." Faraday replied, "A secondary mode of division, so subordinate to the principal as to be always superposed by it, might have great influence in reasonings upon other points in the philosophy of vibrating plates; to prove its existence therefore is an important matter. But its existence being assumed and supported by such high authority as the name of Savart, to prove its non-existence, supposing it without foundation, is of equal consequence." He then proves that the light material collects at the antinodes because of circulating currents of air driven by the vibrating plate.

In the process of burying the misconception, Faraday placed a layer of water on Chladni's plates. In a long Appendix, "On the Forms and States assumed by Fluids in contact with vibrating elastic surfaces," he reports that "the water usually presents a beautifully crispated appearance in the neighbourhood of the centres of vibration. This appearance has been observed by Oersted, Wheatstone, Weber, and probably others." He then details his many experiments on these surface waves, which usually appear as arrays of uniformly spaced small heaps. He saw them on water, alcohol, oil of turpentine, white of egg, ink, milk, mercury, and on the head of an upright cask in a brewer's van passing over stones. Faraday physically understood their generation, explained more fully in Appendix 2 and diagrammed in fig. 1: (a) the plate accelerates up to meet the heaps of liquid coming down and spread them laterally, (b) the plate then recedes from

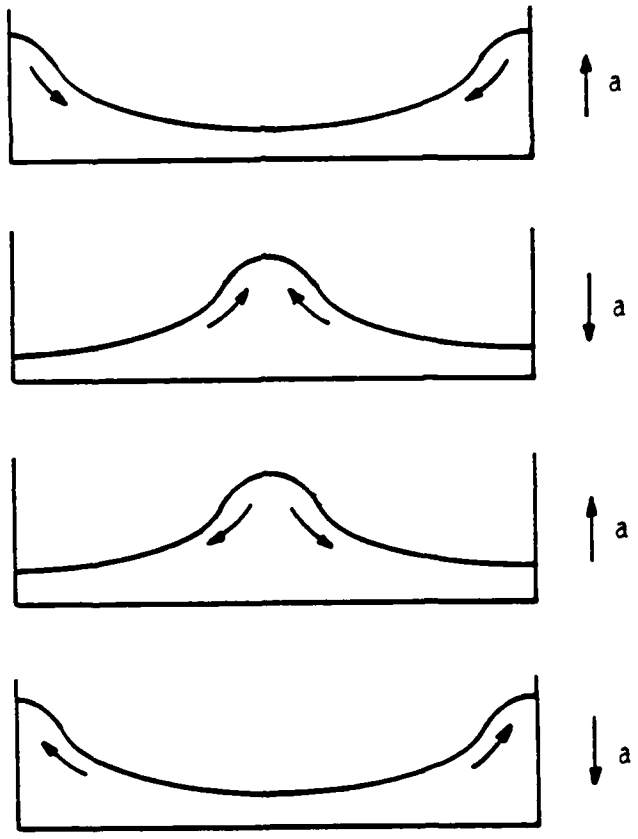


Figure 1. Parametric growth mechanism for heaps of liquid. The acceleration a of the dish effectively increases gravity when the heaps are flattening.

the new heaps as they form at positions intermediate to the old heaps, (c) these new heaps are then met and spread by the upward accelerating plate again, and (d) the heaps re-form in the original configuration. Notice, as Faraday did, that the liquid goes through one cycle as the plate goes through two. The liquid responds at half the frequency of the drive.

However, thirty seven years later a Dr. L. Matthiessen reported (1868,1870) that the waves have the same frequency as the plate. This led Rayleigh to repeat Faraday's experiments. The two great men were in complete agreement, and Rayleigh went on to develop the first mathematical theory for parametric resonance (1883 a). He, by the way, was not too kind to Matthiessen.

In more recent times though, Benjamin and Ursell (1954) solved the hydrodynamics for surface waves on an inviscid liquid contained in a vertically vibrating vessel. They showed that, depending on the drive parameters, the observations of Faraday and Rayleigh, and of Matthiessen, could have both been right.

The chaos article inspired The Mentor to try Faraday's experiment again. I came into the lab one day to see The Mentor oscillating a Petri dish containing some water by placing it on the cone of a loudspeaker. He showed me nice concentric rings, that suddenly changed into stars, which switched to nasty complicated patterns, that then decided to dance around in time as he crossed one threshold after another, driving the dish harder and harder.

We were fascinated by the behavior's touchy dependence on amplitude; we had never seen anything like this before. In this lab we are used to measuring the amplitude of response vs. drive frequency -- we love those tuning curves --but now we have a whole new dimension to explore, Drive Amplitude. The next three or four years of my life were then determined. The major part of this dissertation is spent describing the zoology of phenomena that occur in this nonlinear system as we vary drive amplitude and drive frequency.

Soon after seeing all the action in the Petri dish, we decided that this two dimensional geometry was unnecessarily complicated and a one dimensional trough would be easier to handle. Our next version of Faraday's experiment therefore used an annular Plexiglas resonator which to good approximation is a one dimensional waveguide closing on itself. It is shown in fig. 2 on a loudspeaker driving large amplitude waves of water. The water is mixed with a wetting agent, Kodak Photo-Flo 200, to decrease surface pinning effects (Heckerman, 1979). The barrier, shown in the figure and typically in place, fixes the position of the antinodes of the wave. The height of the water is recorded vs. time, usually at the barrier, by measuring the conductance between pairs of copper blocks machined into the walls. An accelerometer measures the amplitude of the drive.

Later experiments, setup as sketched in fig. 3, were performed at low temperatures with liquid helium, which is a more ideal fluid than water. Another annular trough, sealed and then partially filled with normal or superfluid helium, is oscillated vertically and supported

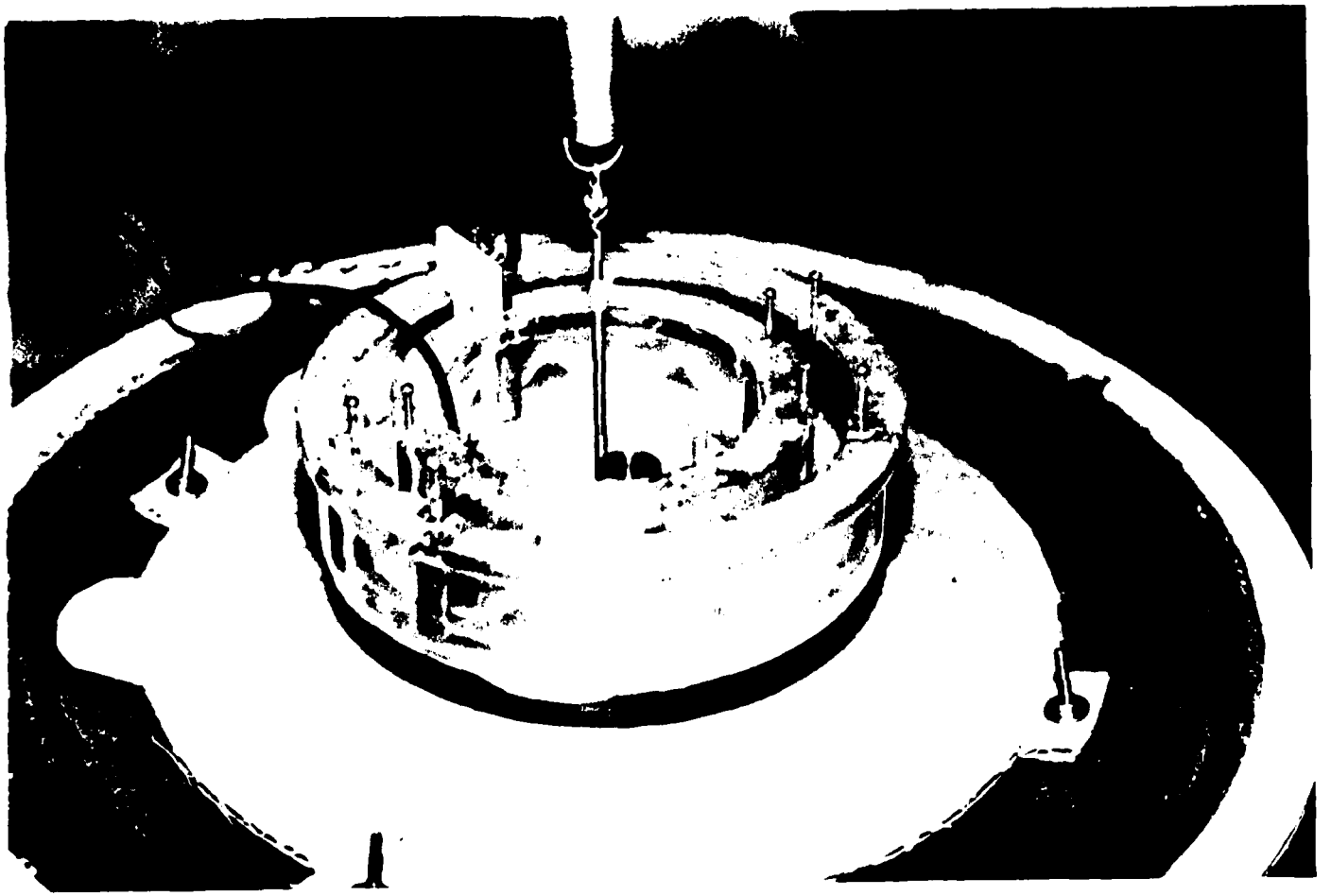

Figure 2. Annular trough of water on a loudspeaker.

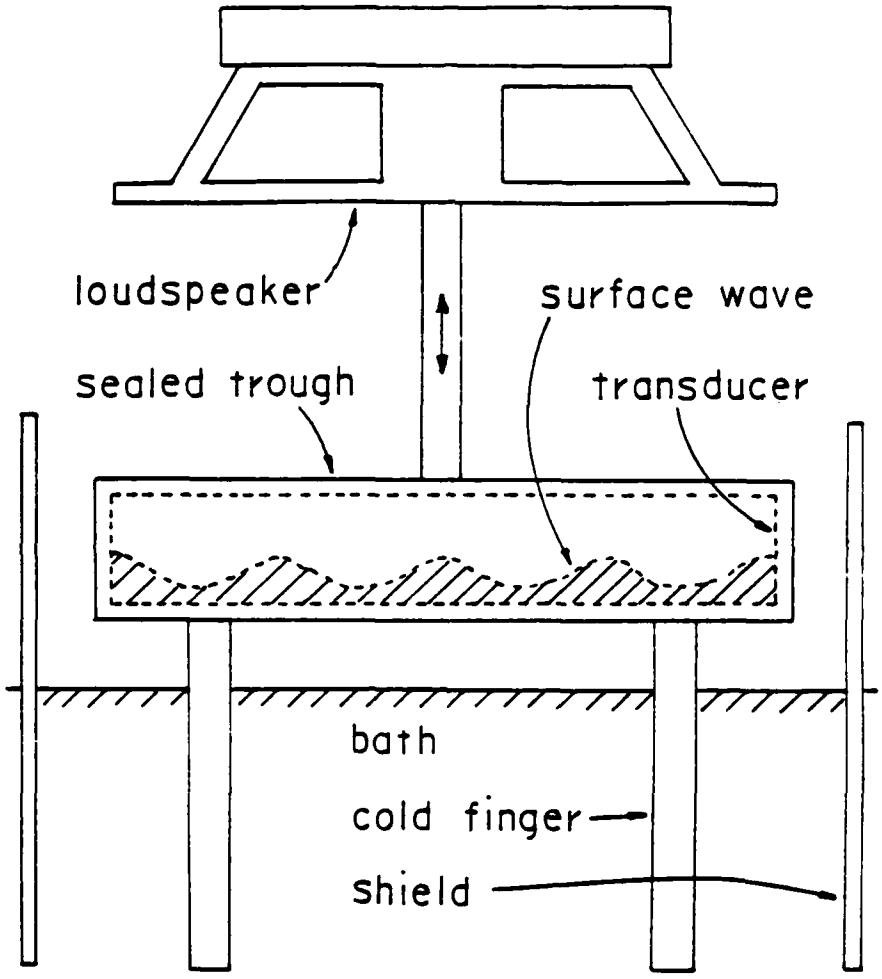


**Figure 3. Schematic of the helium experiment.**

from above by a shaft which is driven by a loudspeaker. The trough is kept cold above a bath of liquid helium with cold fingers and a heat shield. The main signal is the height of the helium vs. time measured capacitively at a barrier which blocks the width of the trough.

Three prominent sorts of behavior are seen in both helium and water. One is characterized by sudden drops in amplitude of the f/2 oscillations, nearly to zero. Figure 4 is a typical example. It is a plot of the surface height vs. time at the end of the trough of helium at 3.8 K. Because it resembles the comb of a rooster, we call this waveform a cockscomb. This example has two sudden drops per cycle of the cockscomb — they can have one, two, three, and probably more. More often than not, the period of this modulation is an exact integer multiple of the period of the drive, and is nearly the period of the fundamental mode of the trough -- although there are exceptions. It is remarkable how, in a waveform this complicated, even minute details repeat.

Another behavior, smooth modulations, is characterized by waveforms in time that smoothly, rather than suddenly, vary in amplitude. A waveform from the end of the trough, Fig. 5, resembles beating, but this is not a linear phenomena. These modulations are usually quasiperiodic, that is their period is (in principle) an irrational multiple of the drive period. More than one modulation may be present at the same time. They may either proceed independently or phase lock on each other or the drive -- their frequencies pulling into syncronism. Like the cockscombs, smooth modulations occur near

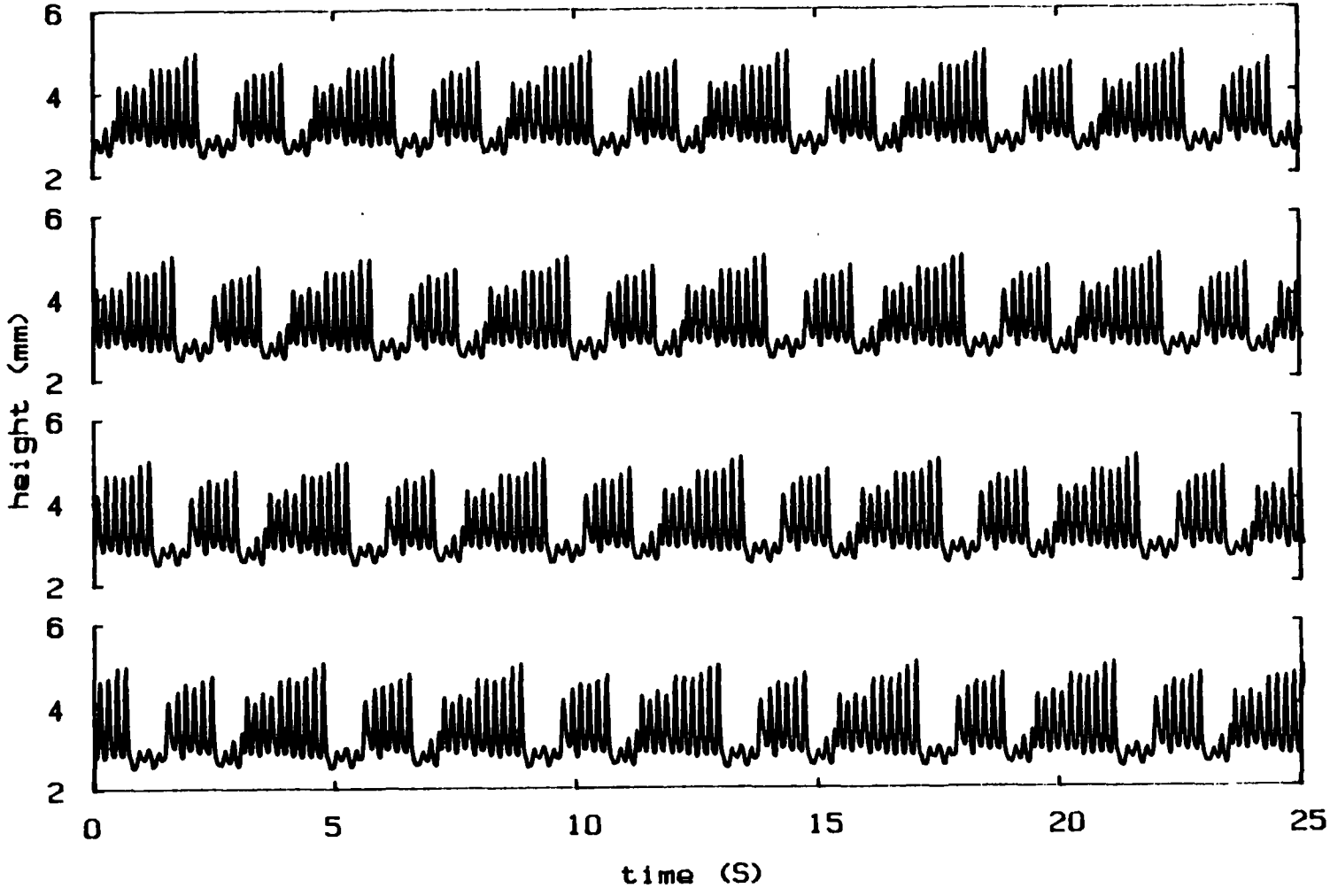


Figure 4. A cockscomb in 2.81 mm of helium at 3.8 K. The trough is driven at 11.000 Hz with 156 μm rms amplitude.

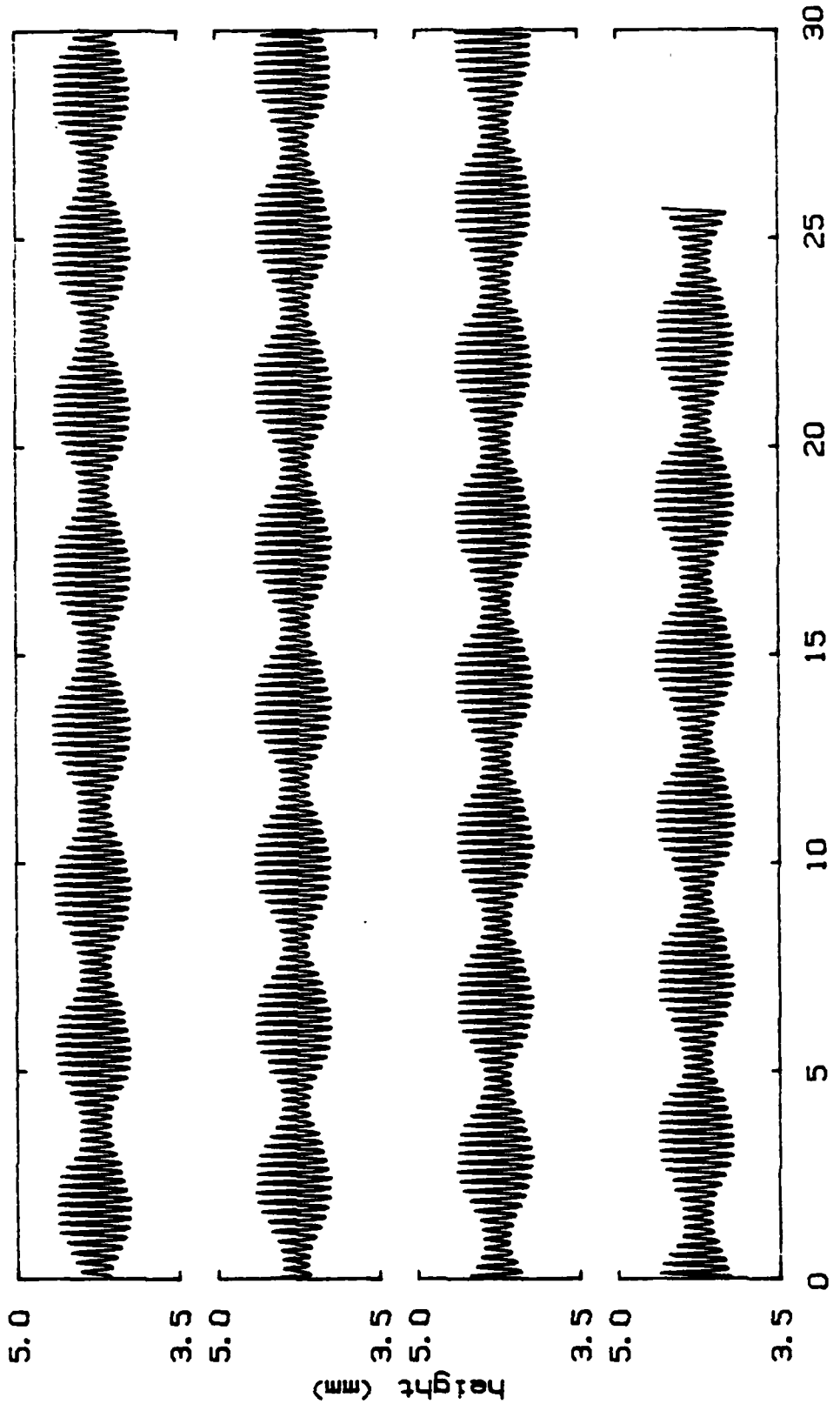


Figure 5. A smooth modulation in 4.20 mm of helium at 1.25 K. The trough is driven at 8.850 Hz with 35.4 μm rms amplitude.

the frequency of the lowest linear mode of the trough.

The third common behavior, ultra deep modulations, has a surprisingly long time scale. The amplitude at the transducer, Fig. 6, slowly rises and falls, typically taking around 1000 cycles of the drive to complete a cycle. Its frequency is two orders of magnitude lower than any mode of the trough.

Turbulent or chaotic waveforms persist at high drive levels, but these are not properly characterized. I spent my time trying to understand the low amplitude phenomena first.

Subharmonic and quasiperiodic modulations can also exist in a trough driven with a paddle, rather than by vertically oscillating the trough. These are described later.

Incidentally, we never saw a clean signature of the period doubling route to chaos. The signiture would be a spectrum from the trough driven at frequency f with a series of peaks at f/2 and its harmonics, with a smaller set at f/4 and its harmonics, with a still smaller set at f/8 and its harmonics, and so on with as many of these superimposed sets of peaks as there have been doublings of the motion's period. The second spectrum ever taken with the plastic annular resonator, Fig. 7, shows clear peaks at the harmonics of f/4, perhaps the result of the motion's period doubling once after the initial f/2 period doubling due to the parametric drive. There are also some peaks at the harmonics of f/8 and f/16, beneath the tick marks, but they are rather ambiguous. As the experiment evolved and

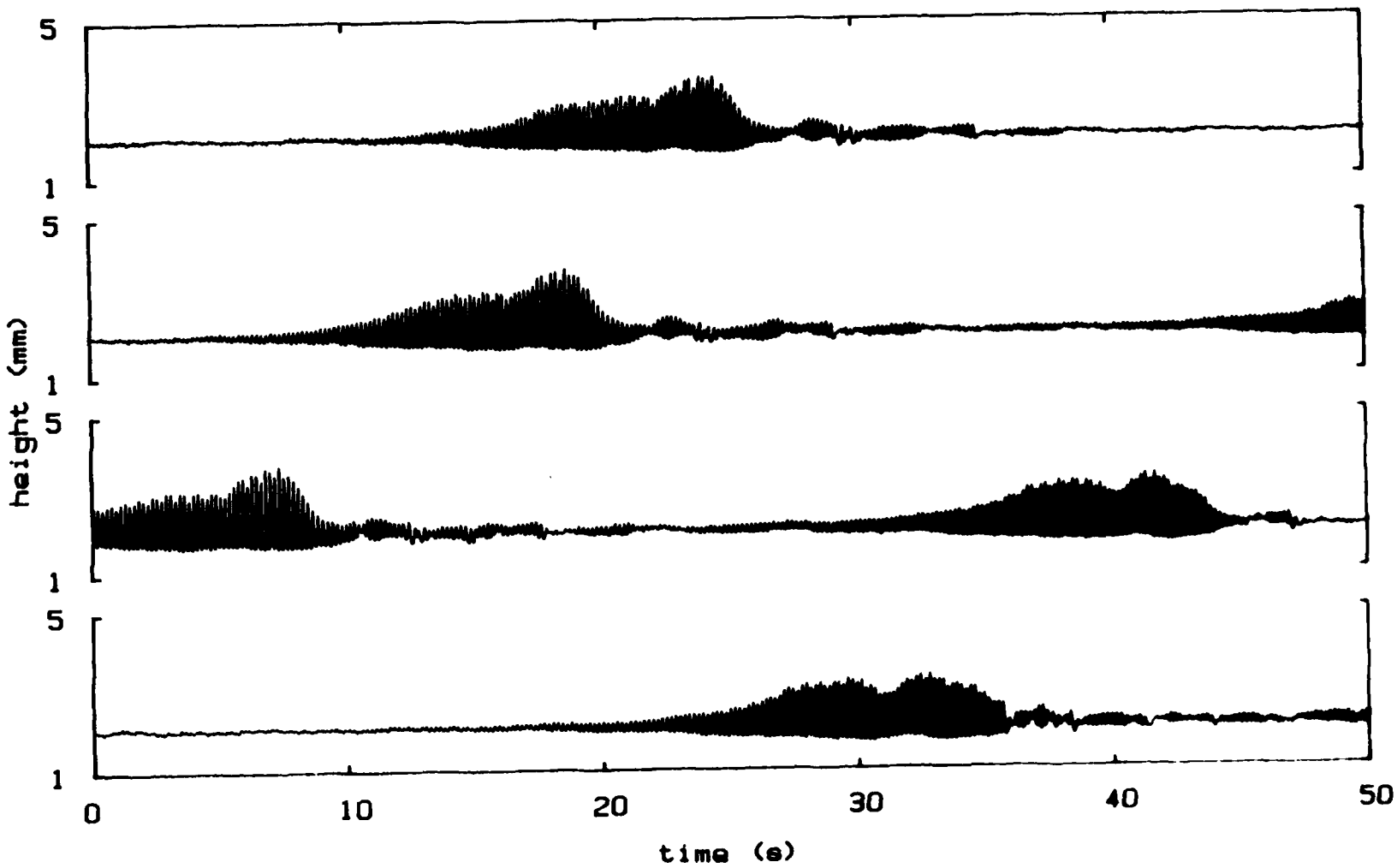


Figure 6. An ultra deep modulation in 2.06 mm of helium at 4.2 K. The trough is driven at 11.000 Hz with 142 μm rms amplitude.

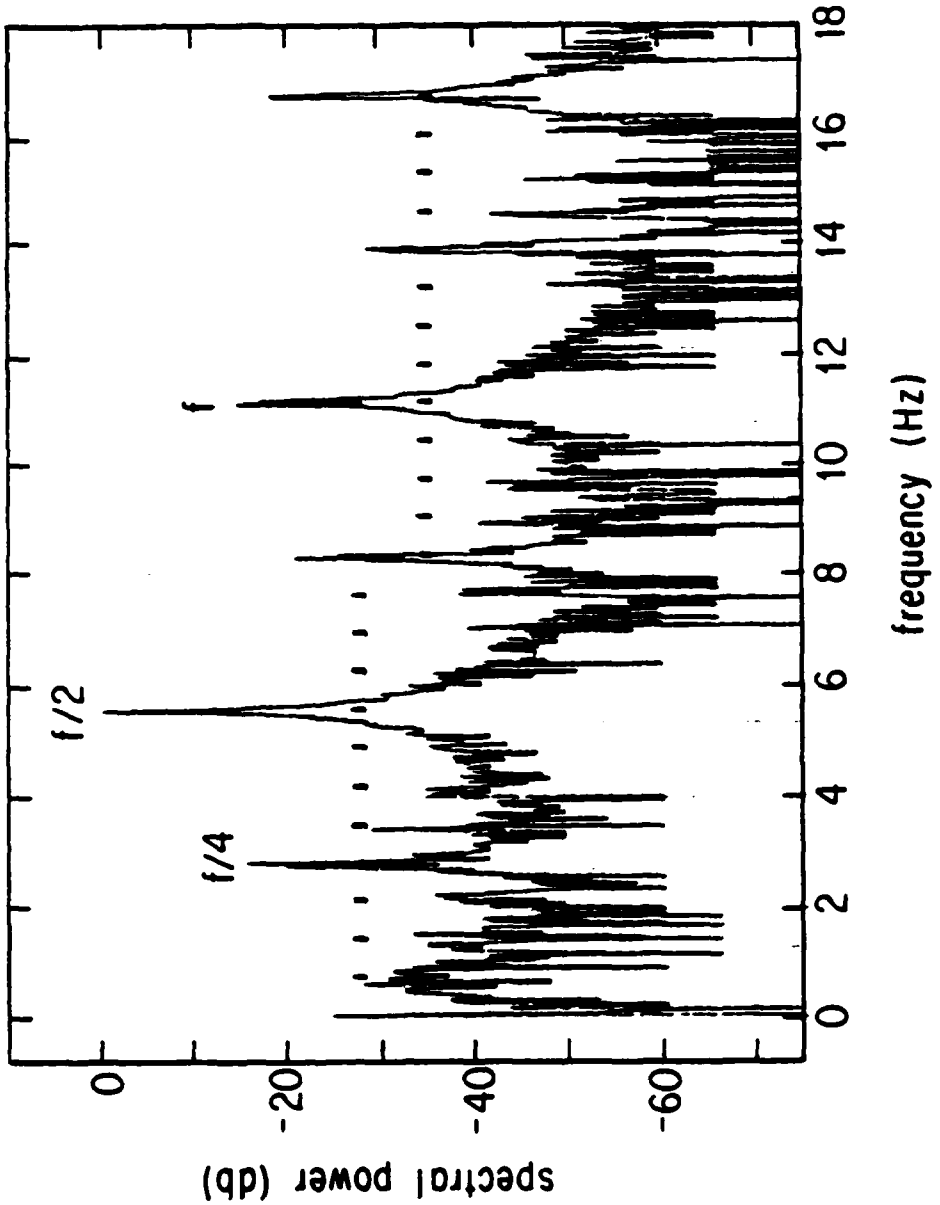


**Figure 7. An early spectrum showing two and perhaps four period doublings. Tick marks are spaced f/16 apart as a guide to the eye.**

the drive was cleaned up, these peaks no longer appeared. Perhaps they were in the drive -- interesting in its own right as a nonlinear mechanical system, though not studied here. In retrospect, period doubling seems to be a property of single degree of freedom systems, such as the drive itself but not the water with its multitude of modes. However, as is seen above, modes in this system tend to lock together into collective motion, and I suspect that the dynamics of these collective motions may one day display the period doubling route to chaos. Regardless, the hope of seeing period doubling influenced the design of the experiment. We thought we would see the period doubling route because the adjective "universal" was used to describe it.

Organization. Experiments are presented in the chronological order with which they were performed with water. Helium experiments, which were generaly performed afterwards, are presented with the water experiments. Perhaps the most useful part of the dissertation are the first five appendices, on nonlinear oscillators. They are meant as a supplement to the last chapters of Pippard's remarkable book, The Physics of Vibration, Vol. 1 (1978). One may wish to read the appendices first in lieu of a theory section. Experience has shown that the reader without prior background in nonlinear oscillations will at times probably find the experimental results opaque (as they once were to me) -- unless he refers to the appendicies. There is even a bit of original work in them; I think that the doubly bent tuning curve idea and the parametric interpretation of the hanging

chain is new, although I do not know the literature very well.

# Chapter II. Apparatus.

## Section 2. Concept and Design of the Experiment.

### 2a. Resonator acoustics.

We decided to use a one dimensional trough to simplify the physics and transduction. Making a trough long and narrow suppresses wave motion for small amplitude waves across the width of the trough as long as the wave frequency is below that where the width is half a wavelength (Rayleigh, 1896). (Incidently, one might wonder what happens when the waves are driven to nonlinearity near this frequency. Waves across the width can coalesce to form an interesting nonpropagating soliton [Wu, 1984]. I have always, naively, stayed well below this frequency.)

A long narrow trough has another advantage. We wanted to use the resonances of the container to encourage the system to go through a succession of period doublings. The way to do this, it seemed, was to let each subharmonic -- f/2, f/4, f/8 ... -- and their harmonics -- 2f/8, 3f/8, 4f/8, 5f/8 ... -- all lie on top of resonances. What was needed was a resonator whose modes were spaced uniformly in frequency, driven at a $2^n$th mode. That way by driving the resonator at the 32nd mode say, f/2, f/4, f/8, f/16, and f/32 would all be resonantly

enhanced as well as any harmonics of these subharmonics. A one dimensional resonator enclosing a dispersionless (constant wave speed) medium has this property -- no other geometry will do.

Surface waves on a liquid (Landau and Lifshitz, Fluid Mechanics, p. 40 and p. 238, or Benjamin and Ursell, 1954) travel with a phase velocity $\omega/k$ which has been plotted vs. k (and mode number for later reference) in fig. 8 for (a) water at the depth used in the straight glass trough to study smooth modulations, 2.9 mm, (b) water at the depth typically used in other experiments, 5.6 mm, and for liquid helium at the (c) maximum and (d) minimum depths used, 4.2 mm and 2.0 mm ($\omega$ is the wave's angular frequency, k is its wavenumber which is $2\pi$ divided by its wavelength). The velocity has three regimes. When k and $\omega$ are high the wave motion is confined near the surface, surface tension is the dominant restoring force, and the phase velocity increases as $k^{1/2}$. With intermediate k, the deep gravity wave regime, the motion is still confined near the surface but gravity becomes the more important restoring force, and the velocity becomes $(g/k)^{1/2}$, where g is the acceleration due to gravity. But in the shallow gravity wave regime, at low k and low $\omega$, the wave motion reaches to the bottom of the trough and the wave speed becomes a constant independent of k, $(gh)^{1/2}$, where h is the liquid's depth. Since the resonances of a one dimensional trough are spaced evenly in k by $\pi/L$, where L is the length of the trough, and $\omega/k$ approaches a constant for low k, the resonances are spaced evenly in frequency too, as desired.

In practice, the desire to have the resonances spaced evenly in

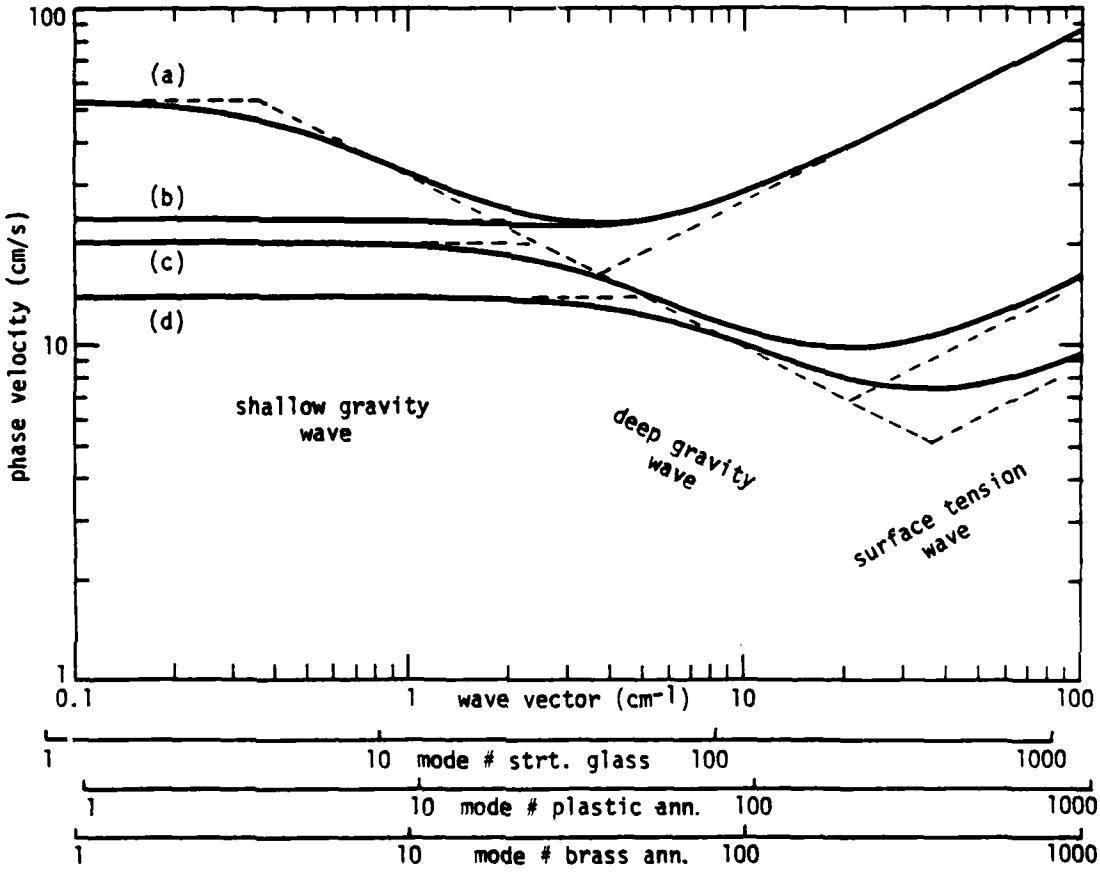


**Figure 8.** Phase velocity of a surface wave vs. wave vector, with dashed asymptotes, calculated for (a) and (b) pure water with depths 29 mm and 5.6 mm, and (c) and (d) helium at 1.2 K and 4.22 K with depths 4.2 mm and 2.0 mm. Axes at the bottom give plane wave mode numbers for the straight glass trough (38.1 cm long), the plastic annular trough (30.13 cm long), and the brass annular trough (32.01 cm long).

frequency was not realized for several reasons. By force of habit, for instance, the liquid level was not reduced low enough to be completely in the shallow gravity wave regime. In addition, the wave speed in water, though not in helium, tends to be higher than calculated because the surface pins to the walls (Heckerman, 1979 and the next subsection) which adds another restoring force. Thirdly, a parametric drive guarantees that nonlinearities will be important. Once the drive frequency is close enough to twice the resonant frequency of a mode and the drive amplitude is high enough to initiate parametric growth, the response amplitude rises exponentially until it is limited by a nonlinearity; typically the resonant frequency changes (Appendix 2). So the resonant frequencies, when the modes are actually excited, are no longer spaced evenly. In spite of this, there was plenty of physics.

We were initially pessimistic (unnecessarily as it turned out) about being able to see any subharmonic signal so we wanted to make the quality factor Q of the modes ($2\pi$ * energy stored / energy dissipated per cycle) as high as possible. (I did not realize back then that high dissipation rather than low probably favors the period doubling route.) It can be shown rigorously and remembered easily (Heiserman 1976) that the Q of a one dimensional resonator due to viscous damping at the walls is twice the ratio of the cross-sectional area of the channel to the cross sectional area around the walls within a small viscous penetration depth $\delta$ of $(2\eta/\rho\omega)^{1/2}$, where $\eta$ is the dynamic viscosity (Landau and Lifshitz, Fluid Mechanics, p. 89).

For surface waves in a trough, the channel area is wh, where w is the width and h is the liquid depth, and the area around the perimeter where the dissipation takes place is $\delta(2h+w)$, so the Q becomes $wh/(\delta(2h+w))$. The penetration depth scales as $L^{1/2}$ since $\omega$ scales as $L^{-1}$. Therefore, for a given shape trough, making w and h scale with L, the Q increases with size as $L^{1/2}$. The Q can be increased by making the trough as large as possible. For this reason, the trough was bent into an annulus so as to fit as much length as possible into a round dewar for the experiments to be done in helium.

2b. Why helium?

Good question. We wanted high Q along with a shallow depth which points to a liquid with low dissipation. Helium is the best; it has the lowest viscosity of any classical fluid. Furthermore, by comparing water with helium at different temperatures, one might measure the effect of damping on chaos. Something ought to happen if you lower the kinematic viscosity $\eta/\rho$ by 2 orders of magnitude.

Besides, water has all kinds of problems. The properties of water, like its surface tension and electrical conductivity, are easily changed by contamination. Things like to grow in it. The worst problem is that the walls wet reluctantly so that the surface pins to the wall, as discussed below. These problems are eliminated in helium. My advisors are fond of saying that normal helium is the ideal Navier-Stokes fluid.

Surface pinning should not be confused with surface tension. Surface tension arises from the work needed to increase the amount of surface between two media. Surface pinning arises from the lack of translational invariance of the energy stored by this work. If it is moved slightly, the surface feels a restoring force proportional to its displacement, rather than its velocity, because its meniscus must distort around grease, finger prints, scum, or minute irregularities on the wall. Beyond a certain stress, the surface suffers dissipation as it irreversibly breaks minute bonds to the wall and remakes others at different positions. Pinning is the principal disadvantage of using water, and the lack of it is the principal advantage of using liquid helium. In water, the wave wets the wall up to the maximum excursion of the wave and the wall would dry in a fraction of a minute if it were not wet again in the next cycle. This adds extra hysteresis which is very undesirable; the wave shape changes reluctantly in response to a change of drive because the surface has to slowly hammer away at the old wetting line. The problem is serious even after adding Kodak Photo-Flo 200, a wetting agent used to keep drops of water from forming on print paper. Without the Photo-Flo, it is difficult to excite any wave at all. With liquid helium however, a helium film covers everything. All the wall is always wet so the surface is free to move, and any hysteresis is due to more interesting physics.

Moreover, superfluid helium obeys two-fluid hydrodynamics with quantized circulation. How does this effect the chaos? What happens

as you go through the lambda transition?

From the beginning we had helium in mind, this being a combination low temperature and acoustics lab. We finally got to the point, after seeing so many neat effects in water, of thinking that sooner or later someone is going to want to try helium, so let's do it and see what happens.

In retrospect, not much was learned with helium that could not have been learned with water, although the helium data is better. The smooth modulations were recognized first in helium, but they were later seen in water as well. Both water and helium display essentially the same behavior, it seems, because the inertia of the liquid, the restoring force of gravity, and the acceleration of the container dominate over the viscous forces on either liquid. After all, viscosity controls the amplitude of a driven mass on a spring only near resonance, where the inertia of the mass and the stiffness of the spring tend to cancel. Off resonance, the main effect of viscosity is to damp out transients -- but in the steady state they do not matter and the chaotic state was never properly studied, and with a parametric drive (Appendix 2) growth and decay rates can be easily determined by the drive amplitude -- not viscosity.

The lambda transition remains a mystery because I was not familiar enough with the behavior above it and below it to know a nonlinear effect from a superfluid effect.

Perhaps the time would have been better spent on some other

classical liquid like alcohol or mercury that is more controllable than water and easier to deal with than helium, but then there was no way of knowing this until we tried. However, I certainly do not regret using helium -- it was great fun.

Actually though, I always suspected that the real reason for using helium --although my mentor has denied this -- is that one must do something hard to get a Ph.D. Helium is hard.

## Section 3. Water Resonators.

A plastic annular resonator was designed for use in helium, but I tried it out in water first, collected enough data to stay busy for awhile, and never successfully used it with helium. A photograph of the resonator on a loudspeaker appeared earlier as Fig. 2. Later water data was taken with the same resonator oscillated more reliably by the early probe (see Fig. 32 for a photograph). The trough's average circumference is 30.29 cm, its width is 0.808 cm, and its depth is 2.54 cm.

The body is Plexiglas because I mistakenly thought it should be an insulator if helium was to be detected capacitively. Helium has a dielectric constant of 1.045-1.057, depending on temperature, so an oscillating surface can be detected by measuring the small capacitance change as this weak dielectric fills the space between capacitor plates. Copper blocks are machined into the walls to act as the capacitor plates. Since we wanted the trough to oscillate above the liquid helium bath so as to not be disturbed by turbulence from the outside, these blocks were to also sink heat to the bath with copper wires that run from the blocks down to the bath.

When using water, the conductance rather than the capacitance between the blocks was measured to detect the surface. Later, a barrier made of printed circuit board, similar to the one used in

helium and described in the next section, was used as a transducer. Calibrations are difficult because the conductivity of the water changes by orders of magnitude over days of sitting in the trough. Old water is the best -- its conductance is stable and high --but there is no guarantee on the value of its surface tension.

Because of a mistaken sentimental attachment to this resonator after taking water data with it, I couldn't bear to seal it by permanently gluing on a lid as originally planned. Instead, two demountable seals, a soap-glycerin solution and indium O-rings, were tried without success. As this was a losing battle, the plastic resonator was saved for water, and a new brass resonator was made for helium.

For the last experiments, a straight trough, 38.1 cm long x 2.65 cm wide x 7.2 cm high, was made of glass glued together with RTV silicone rubber adhesive/sealant.

## Section 4. Helium Apparatus.

When I started the design of the helium experiment, I did not know what I could get away with and feared my results would be offhandedly attributed to an obscure flaw in the drive; hence the probe is quite complicated — but it works rather well.

If one uses brute force and lots of parts, a simple calculation points out a problem concerning reliability. An experiment should work "most" of the time, say nine times out of ten. With well over 1000 parts on the probe, this means each part can have a failure rate of only one in 10,000. It is not enough to say "this ought to work"; each part needs to be built with overkill. In particular, seals mustn't leak, transducers mustn't fail, and leads mustn't break; these are the common causes for failure. But perhaps I overdid it a bit.

An overview of the probe is shown in fig. 9 and closeups of the drive and resonator areas of the probe are shown in figs. 10-13. At the top of the probe is an outlet box where the fill tube and electrical connections are made. The fill tube and leads run down to the drive area inside a stainless steel tube which can slide through a seal in the top plate. The drive area holds a loudspeaker that oscillates a shaft that runs down to the resonator. The drive amplitude is sensed capacitively in the tube between the drive and resonator areas, and thermal radiation shields and leads run along

this tube. Since the resonator oscillates above the bath, it and some of the parts in the resonator area need to be heat sunk to the bath with cold fingers at the bottom of the probe. Not photographed are a section of the liquid helium transfer tube that hangs from the top plate and a copper heat shield tube that surrounds the resonator area and hangs from the drive area. All electrical shields are isolated from the probe, which is at the plumbing's ground, to avoid any 60 Hz pickup. The body of the resonator is also electrically isolated because it is driven by a capacitance bridge circuit that detects the oscillating helium surface inside the resonator.

The following is a detailed description of the apparatus. It is intended for new grads, skeptics, and those not in any rush to get to the interesting parts of the dissertation.

## 4a. Resonator.

Trough. As was described on p. 20, the largest trough possesses the highest Q. Therefore, the trough is annular and the experiment is performed in a large 15 cm dewar to maximize the trough length. It is made of brass, for brass is easily machined and soldered. The rest of the design is a compromise between acoustics and the ability of the machinist. The trough should be as narrow and as long as possible to maximize the number of modes below the frequency where the width is half a wavelength; it should be as deep as possible so that high amplitude waves do not hit the lid; and the whole assembly should be

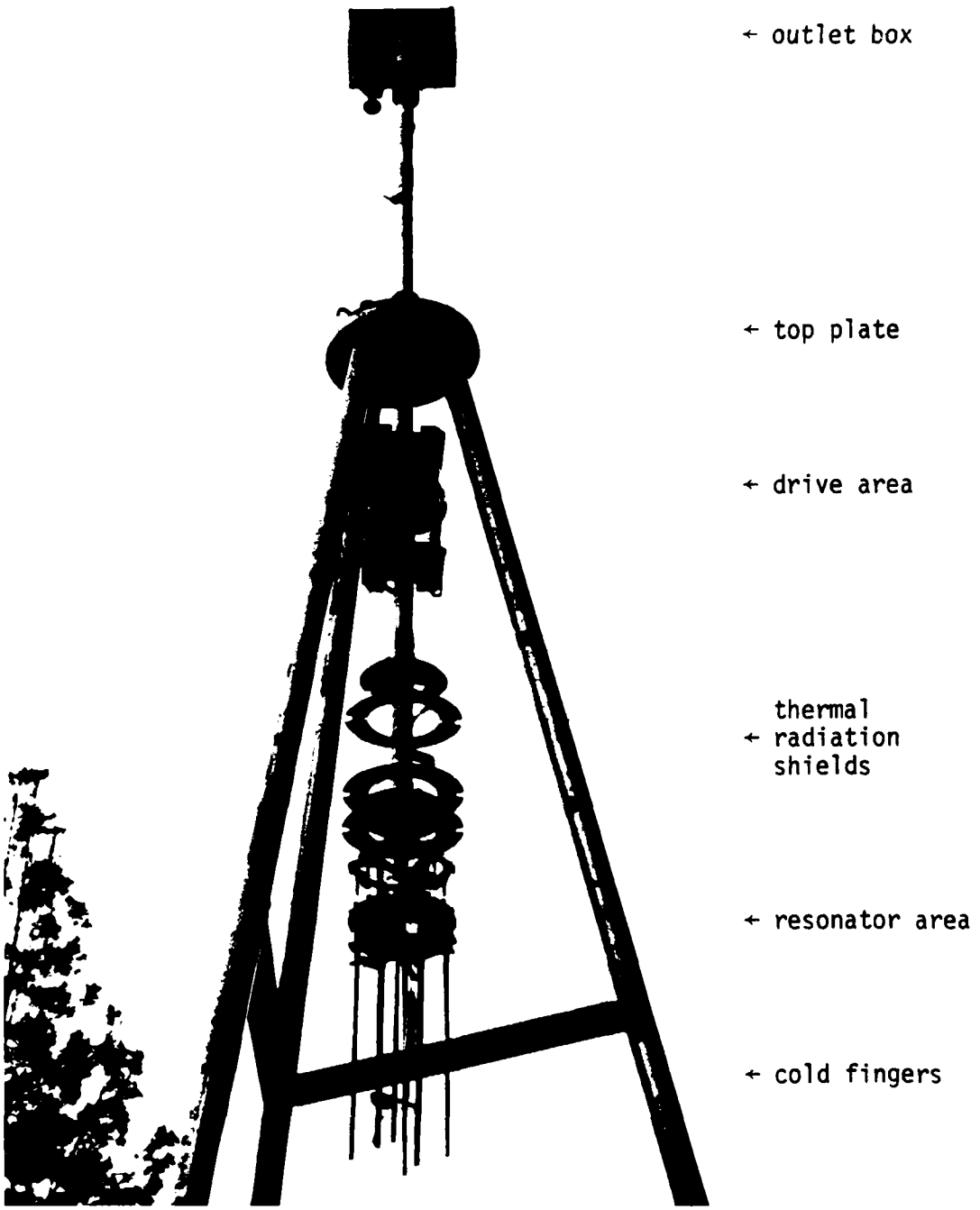


**Figure 9. Overview of the probe.**

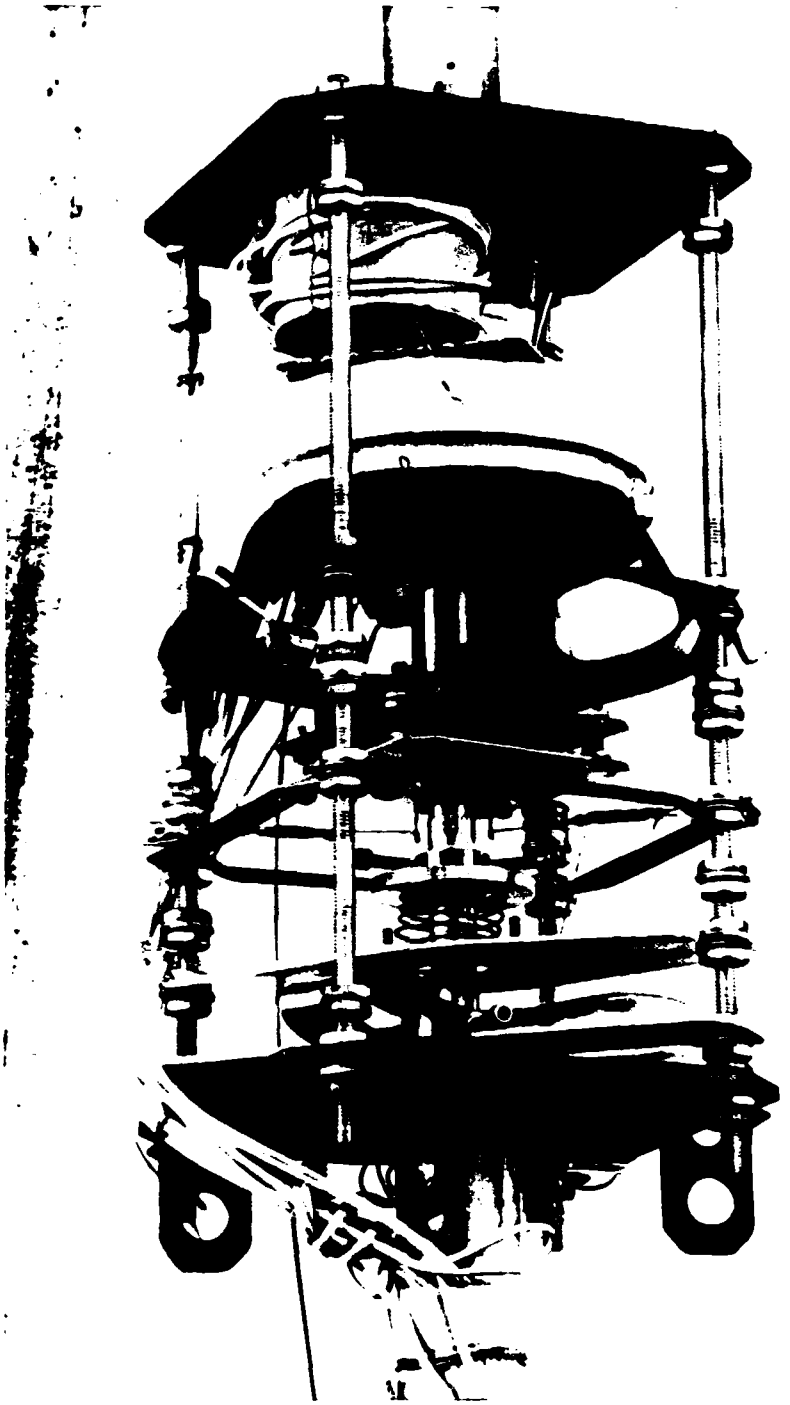

Figure 10. Photo of the probe drive area.

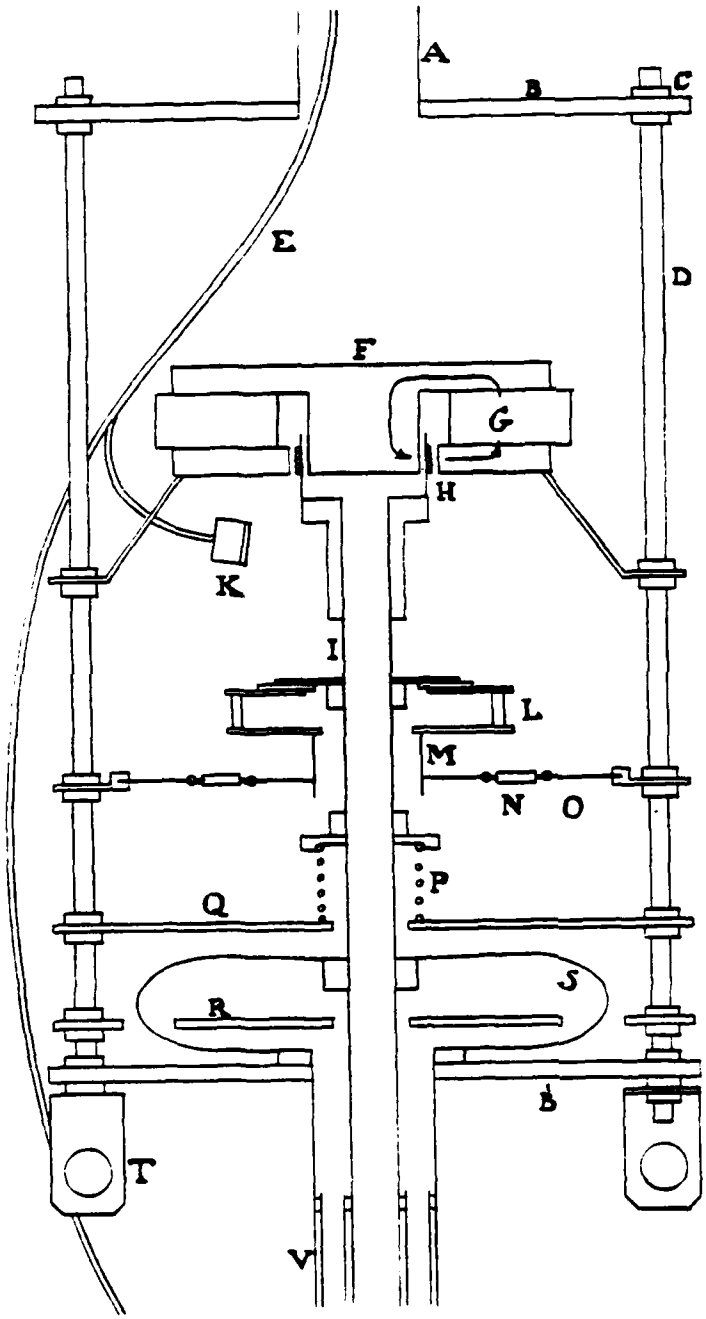


Figure 11.
Drawing of the probe drive area, showing stainless tube A, upper and lower plates B and B', nut C, threaded rod D, leads and fill tube E, loudspeaker F, loudspeaker magnet and field lines G, voice coil in loudspeaker gap H, central vertically oscillating shaft I, microphone K, centering gizmo L, spider leaf spring M, spider turnbuckle N, spider wire O, coil spring P, upper and lower stops Q and R, main leaf spring S, hooking point for heat shield wires T, and drive amplitude sensing capacitor V.

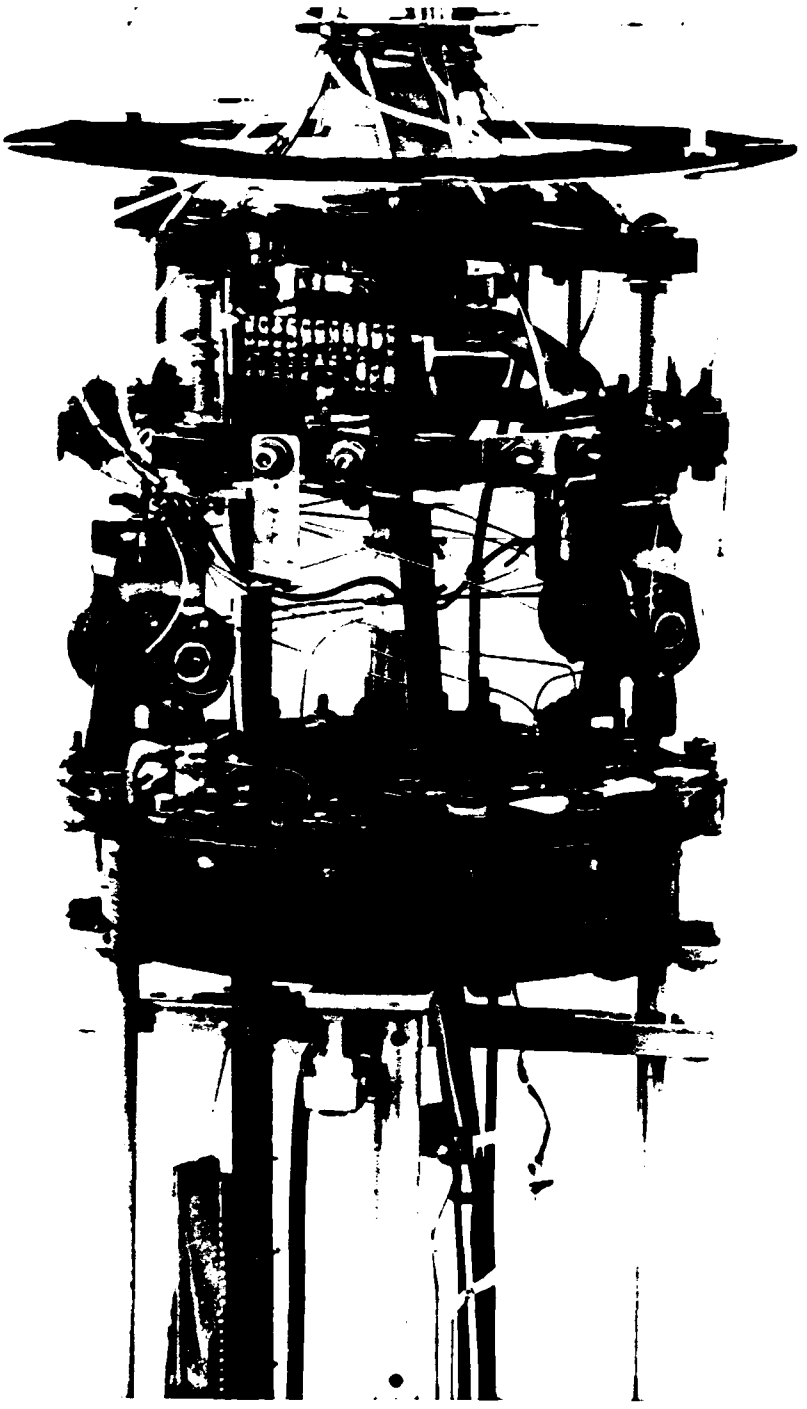

Figure 12. Photo of the probe resonator area.

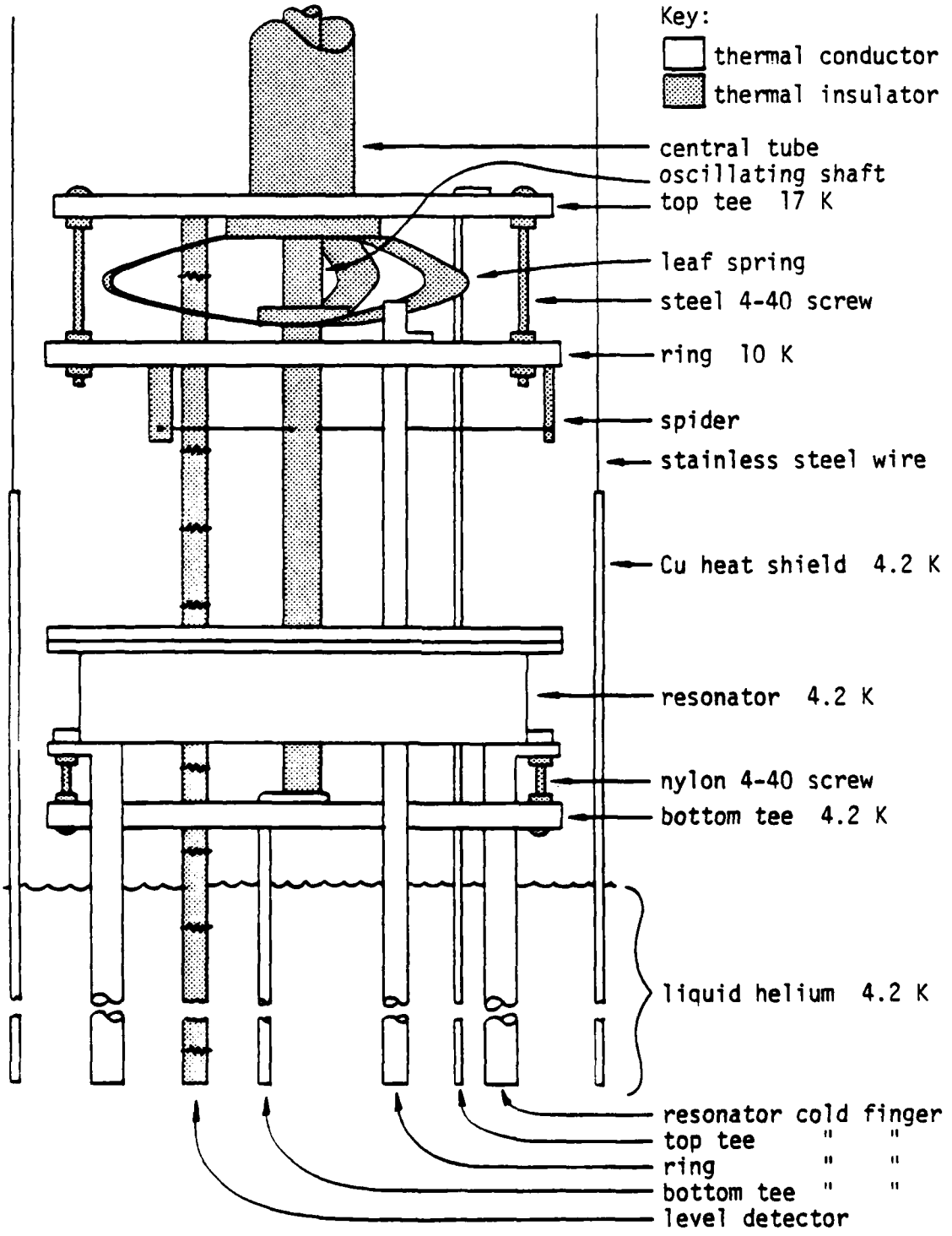


**Figure 13. Drawing of the probe resonator area.**

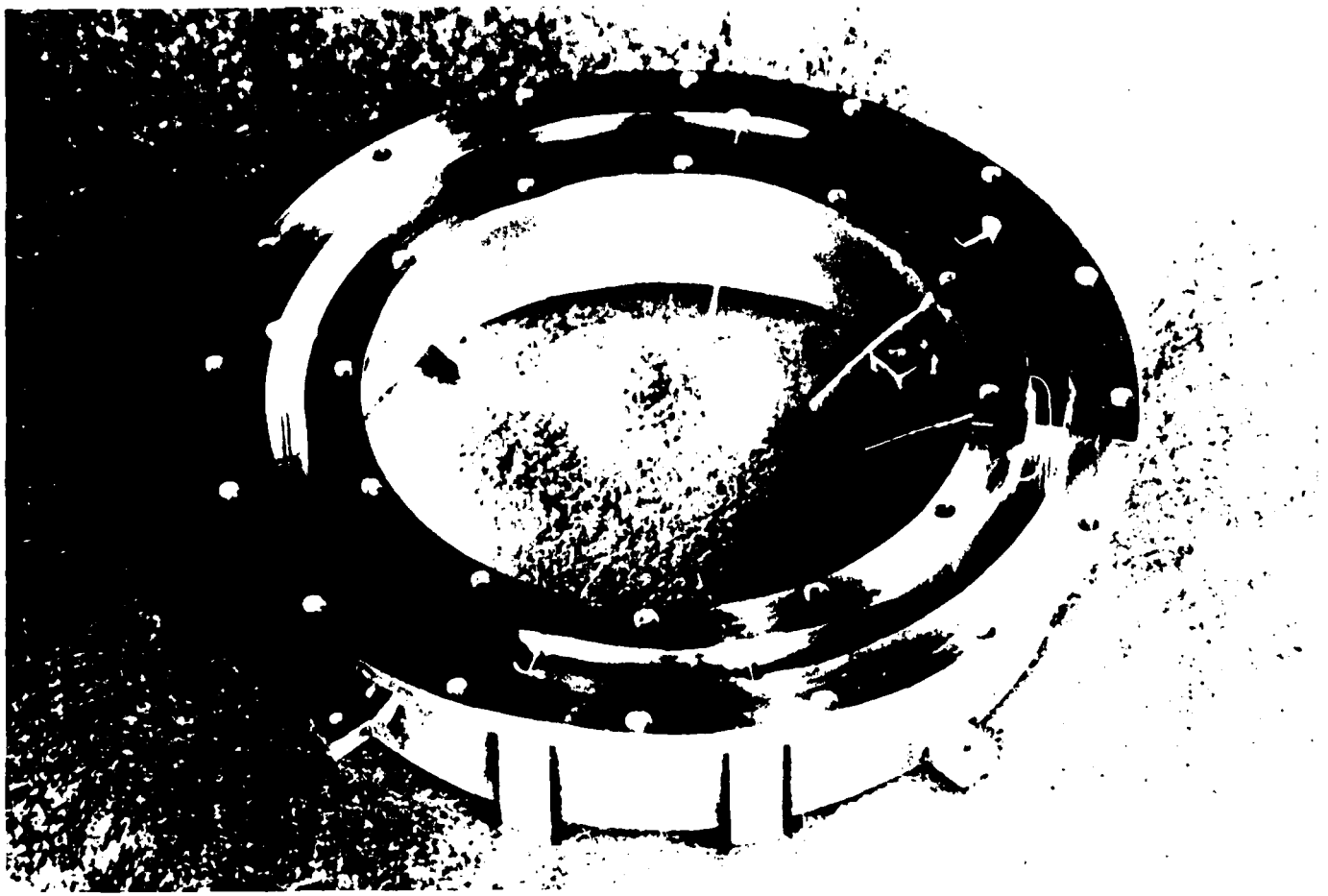

Figure 14. Photo of the open brass resonator with barrier in place.

light weight so that it can be oscillated easily. After negotiations with the shop, the trough was cut with an end mill to 0.505 cm width and 2.54 cm depth, and the walls were thinned down to a thickness of 0.10 cm. The acoustic length of the trough (the average circumference minus the barrier thickness) is 32.01 cm. Figure 14 is a photograph of the resonator before the lid was sealed on. The shop did an impressive job.

Transducers. Capacitance transducers are machined into the outer wall of the resonator at various angles, and are detailed in fig. 15. They are 1.6 mm diameter brass pins that were epoxied into 3.2 mm diameter holes in the resonator before the trough was cut. Small Plexiglas pieces on the top and bottom held the pins in place as the epoxy cured. The pins were positioned to be cut in half when the trough was machined, and they extend slightly below the floor of the trough. A 30 gauge (0.25 mm diam.) wire is indium soldered to the top of the pin, crosses the trough, and extends out a feedthrough on the inner wall.

These wall transducers work by measuring the capacitance between the pin and the body of the resonator. The pin is attached to the low (sensitive) side of the capacitance bridge described on p. 55. The body is attached to the high (driven) side. Typically 4.2 pf of the capacitance is "dead," due to the electric field lines that pass through the epoxy, Plexiglas, feedthroughs, or outside the resonator where the connections to coax cables are made. This capacitance is constant in time and is nulled out by the bridge. Fortunately though,

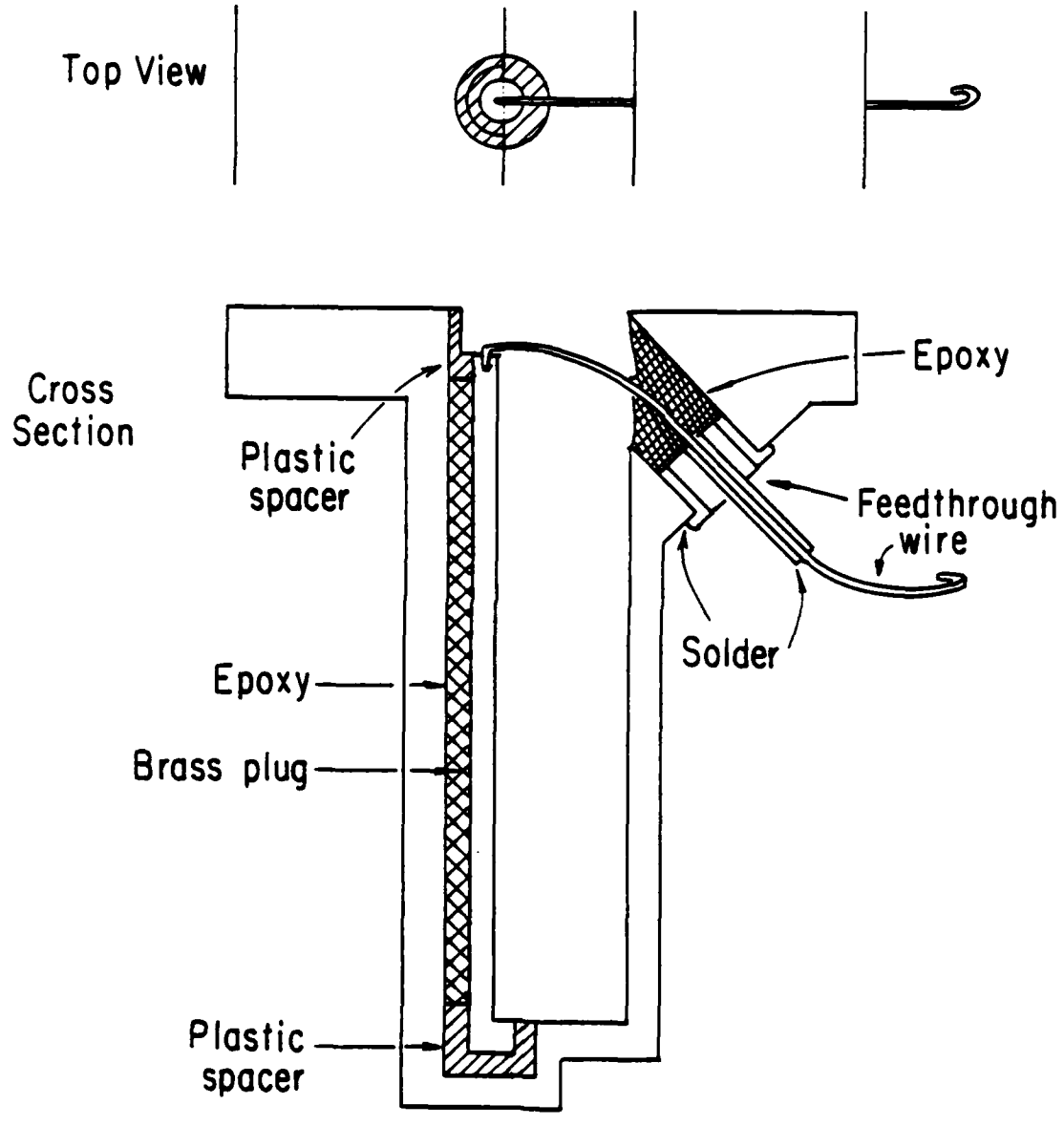


Figure 15. Wall transducer.

nearly 0.74 pf is "active," due to the field lines that fringe around the epoxy or cross the trough. Helium, with its dielectric constant of about 1.05, increases this capacitance when it is present. The transducer is most sensitive to the helium level at very low heights because of the concentration of field lines near the semi-circle on the trough floor. Above heights of about 0.5 mm, the capacitance increases nearly linearly with height with a typical sensitivity of 0.29 pf/cm. The output of the bridge, which is the principle measurement of this experiment, is then proportional to the oscillations of the surface, relative to the body, at the particular position of the transducer.

A barrier spans the trough, as in the water experiments. It pins an antinode (maximum) of the surface oscillations to it, thus converting the annular resonator, with its periodic boundary conditions, to fixed-fixed boundary conditions.

The barrier is also a pair of transducers, one on each side. These were the primary transducers for most experiments. The barrier, photographed in fig. 16, is made from two 1.6 mm thick printed circuit boards, epoxied on either side of a thin copper shield. Vertical conductors spaced 0.72 mm apart are etched into the faces, and alternate conductors connect at the top. Again, it is the fringing field between these two sets of conductors that senses the helium surface. The set that includes the outer conductors are the high side of the bridge. Two wires, soldered to the inner walls of the trough, pass through each upper corner of the barrier, thus connecting the

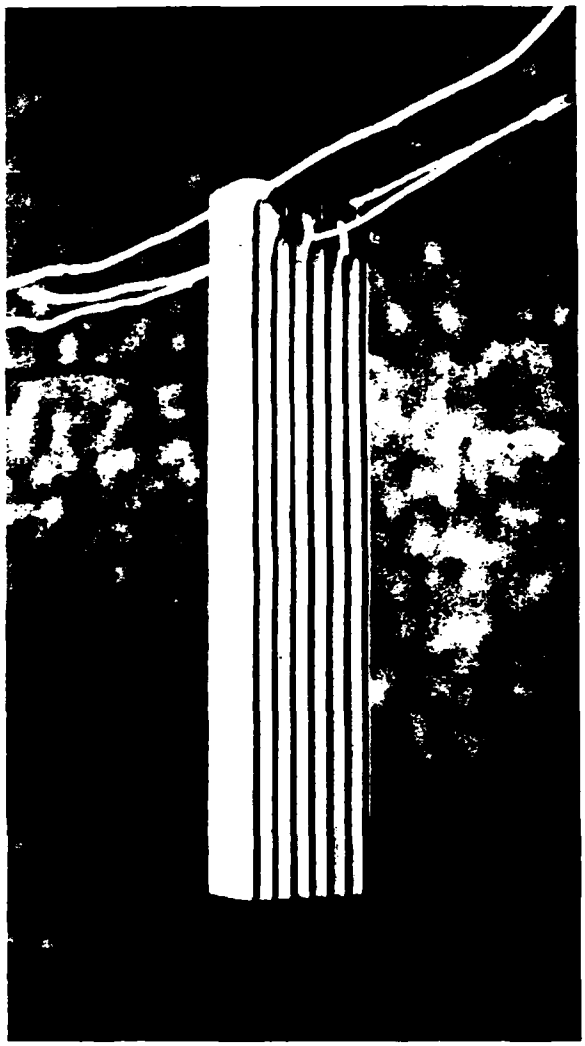

Figure 16. Barrier.

high side conductors on both faces to the shield and to the resonator body. The other three vertical conductors form the low side of the bridge. Wires soldered to the tops of these conductors pass through tiny holes and connect just behind the barrier face. The wire passing through each middle conductor goes on to a feedthrough in the resonator wall. The spaces between the shield and the faces where the connections are made are potted with epoxy so that helium cannot collect there. The dimensions of the conductors were kept very small so that the capacitance would vary with the helium height as linearly as possible.

Seals. A brass lid seals the trough with two indium O-rings. The fill tube passes through a feedthrough in the lid. The feedthrough is necessary since the resonator is electrically driven and the fill tube is grounded. The fill tube has a strain relief to guarantee that the feedthrough will not crack and leak.

Feedthroughs were gingerly soldered into holes in the inner resonator wall. (This is how I avoided leaks: The outer wall was kept under water to protect the wall transducers during soldering. The feedthroughs and hole were tinned, cleaned, and refluxed. The inner wall was then quickly reheated with a small torch and the feedthrough set in the hole with tweezers. The heat from the wall heated the feedthrough and pulled it in; the torch was never allowed near the feedthrough. If anything looked even slightly suspicious, the feedthroughs were removed and replaced.) After the wires were passed through the feedthroughs and soldered in place, the portion of

the hole not filled with the feedthrough was potted with epoxy to keep helium from collecting there, and to make a redundant seal.

Leads. Low noise coaxial cable (Microtech LN-3) for the transducers runs between the outlet box and the ring in the resonator area. Tiny (0.8 mm o.d.) solid stainless steel and Teflon coax runs between the ring and the oscillating resonator. The tiny coax conducts little heat to the resonator and takes millions of flexings without breaking. A splice at the ring joins the two coax, makes thermally contact to the ring, and mechanically supports the tiny coax.

## 4b. Drives.

Main drive. A cheap 4 inch (10 cm) loudspeaker was gutted for its magnet assembly and voice coil to drive the resonator vertically. The magnet sits inverted in a cage formed by four 10-32 threaded steel rods at the center of the probe. During a run, the magnet gets cold, but survives surprisingly well. After two runs it permanently loses about half its strength; afterwards it loses no more. Since thermal cycling mechanically stresses the magnet, the loss mechanism is probably the same as for dropping the magnet.

One of the principle experimental problems was drifting drive amplitude. Drifts in the magnet strength and coil resistance versus temperature caused this. The coil problem might have been solved by

driving the coil with a high impedance amplifier (which specifies output current), but to damp the oscillations of the resonator, the coil must be driven by a low impedance amplifier (which specifies output voltage). The solution was feedback from the computer (p. 61).

Leaf springs that were stiff to sideways motion (Imai, 1969), assisted by a coil spring, support the weight of the central shaft and resonator and keep them centered. Centering the shaft is critical since the coil has only about 0.1 mm clearance in the gap of the magnet, and sideways motion of the resonator is unacceptable. A curious problem, though, was subharmonics in the drive. (Should I have studied the nonlinear dynamics of the probe?) The cause was a little sideways motion in the leaf springs. The springs needed to be supplemented with some sort of spider, the objects in loudspeakers that keep the cone centered. Months were spent building several complicated gadgets that never worked. Finally, my advisor remarked that if he were doing the experiment he would use something simple, like bailing wire, and get on with the experiment. That worked fine. Stainless steel wires that radiate from the top and bottom of the shaft are anchored to stiff supports that give a little when the shaft oscillates vertically. A centering gizmo allows fine adjustment of the coil's position in the loudspeaker's gap.

The drive amplitude, a most important parameter, is measured from the capacitance between a tube on the shaft partially inserted into a stationary concentric tube on the probe (fig. 17). As long as the fringing fields from the ends of these active pieces are far from each

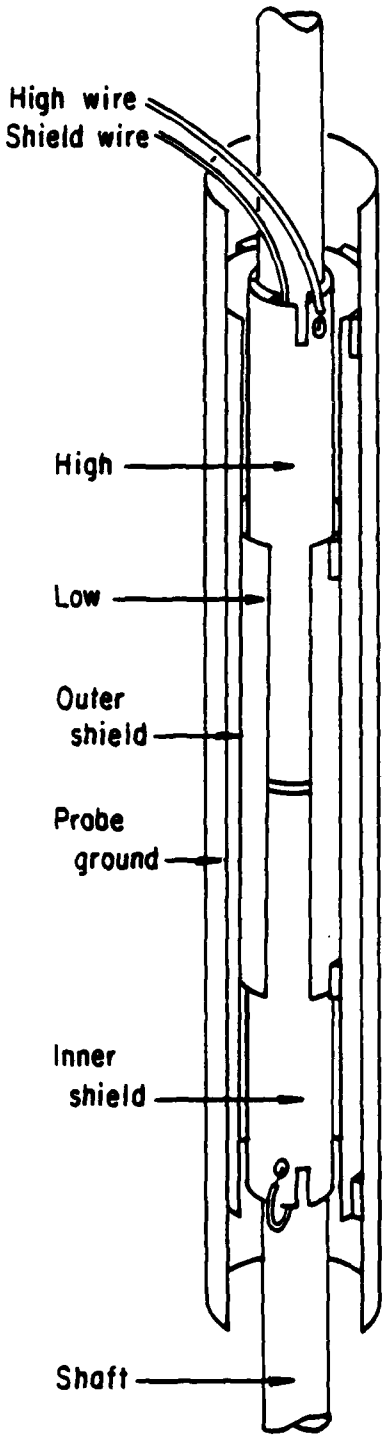


Figure 17. Drive amplitude sensing capacitor, cutaway.

other, this sort of capacitor is exceedingly linear.

A small electret microphone is placed near the coil to listen for scraping sounds from the gap, the shaft banging against its stops when the drive amplitude is too high, and to assist in transferring helium. It is typically used throughout the run.

On this probe there are many tubes and fingers dipping into the bath like tines of a tuning fork. All mechanical resonances were kept above 20 Hz so they would not be driven.

Torque drive. A second, independent drive can torque the resonator about its axis. This allows the barrier to act as a paddle which drives every other mode directly instead of parametrically. Two 18 mm permanent disk magnets are attached to opposite sides of the resonator with their axes along the resonator's circumference. On either side of each magnet are stationary superconducting coils wound on plastic sewing machine bobbins. The coils push the magnets which torque the resonator against the stiffness of the leaf springs. Although not normally used, this drive provides a check of the mode structure and thus the helium height in the resonator.

## 4c. Low Temperature Systems.

Thermal paths. The resonator is kept above the bath so as not to be disturbed by it when oscillating. Therefore, the probe must be designed to keep the resonator cold. Thermal paths are diagramed in

fig. 13 on p. 33. The top cross, which supports the ring, is thermally anchored to the bath with a 12 gauge (0.2 cm diam.) copper wire. The ring is the thermal anchor for all leads and the fill tube, and is kept cold with a 6.4 mm o.d. copper tube to the bath. (For convenience, the ring is connected to the electrical rather than the plumbing ground.) The bottom cross, on the end of the central shaft, is anchored to the bath with an 3.2 mm copper tube. Finally, the resonator is held 10 mm above the bottom cross with four 4-40 nylon screws, and is thermally anchored with four aluminum alloy 7.9 mm cold finger tubes. All this turned out to be insufficient -- the rising helium vapor has enough thermal conductivity to dump hundreds of milliwatts into the resonator from the dewar wall. The trick was to shield everything below the ring with an 3.2 mm thick copper tube that dips into the bath. The shield stays in the dewar; the stainless steel wires that support it hook onto the probe below the drive area as the probe is inserted into the dewar.

Level detector. A level detector for the bath is necessary since the the dewar is made of stainless steel and is quite opaque. The first, a superconducting wire, failed since the resistivity of the normal fraction of the wire above the bath depended on temperature. The second, a capacitor formed by a wire inside a tube, failed since the capacitance was more sensitive to the tube flexing and the temperature dependence of the dielectrics used to center the wire than to the helium level. The third try worked. Twenty three 1/8 watt Allen-Bradley carbon resistors are positioned along the probe. Wires

from each run down to the bath to be heat sunk and then up to the outlet box. With 4 volts applied, the current through the resistors drops from 8mA to 6mA when they become covered with liquid, regardless of bath temperature. The circuit used is shown in Appendix 6. These resistors were also used as thermometers to diagnose the vapor heat leak problem mentioned above.

Thermometry and temperature control. A capacitance manometer (MKS Baratron 220BHS) is the principal thermometer for the resonator when the resonator contains helium. The manometer, placed in the fill line, outputs a DC voltage proportional to the vapor pressure of helium in the resonator. This voltage is measured with a DVM and read by the computer which then converts the vapor pressure to temperature.

Electronic feedback provides resonator temperature regulation. A calibrated 1/2 watt Allen-Bradley carbon resistor senses the temperature while resistance wire, wound around the resonator, provides the heat. Leads pass through the bath to be heat sunk. Figure 18 shows the resistor's calibration (Scott Hannahs wrote the program that does the fit).

Bath temperature is controlled with the bath vapor pressure. The bath is pumped partially through a non-lubricated latex condom which has had its end cut off. A volume outside the condom contains gas at the desired vapor pressure which pinches off or opens the condom when the vapor pressure is too low or too high.

Transfer tube. The transfer tube for the bath is in three

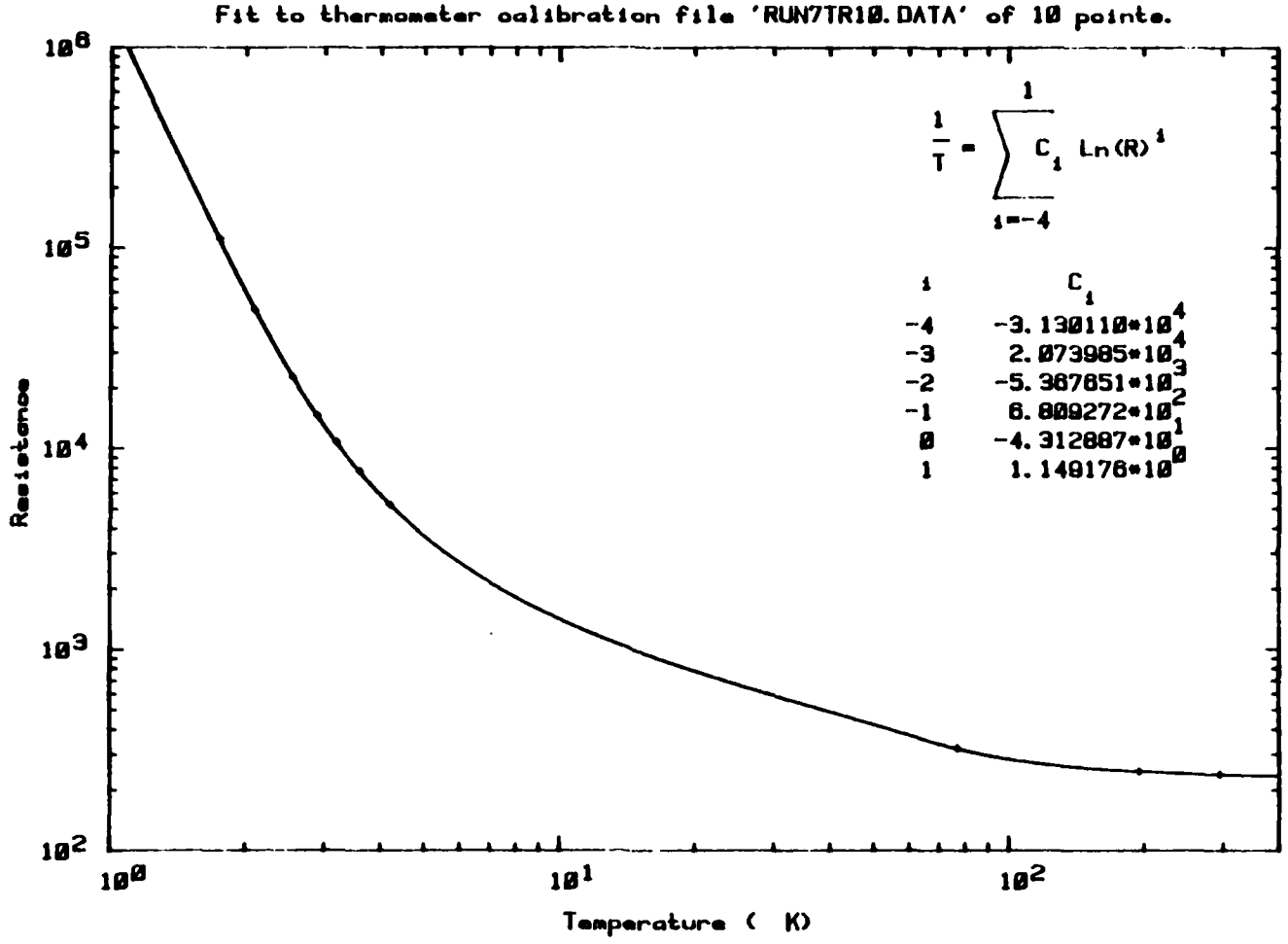


Figure 18. Allen-Bradley 1/2 W carbon resistor calibration, taken at helium, nitrogen, dry ice, and room temperatures.

sections with one section remaining on the top plate to avoid damage to the probe. To prevent Taconis oscillations during a run, the section remaining is vented to the bath with a hose from the top plate, rather than being plugged with a stopper.

Plumbing. A sliding seal in the top plate allows the probe to be lowered as the bath level drops.

The 18cm diameter stainless steel dewar has a liquid nitrogen jacket and is supported with the usual plumbing.

The resonator fill panel is diagramed in fig. 19. To fill the resonator, helium is admitted through the cold trap from the known volume. The pressure drop and temperature of the volume determine the amount of mass that left the volume. The cold trap is kept between popoff valve and the resonator so that an air leak will not clog the fill line, which could be quite dangerous. There is a subtle problem, though: at higher vapor pressures a significant fraction of the helium mass remains in the cold trap. As the liquid nitrogen boils away this fraction decreases enough to increase the helium height in the resonator by a few percent. This raises the resonant frequencies by a percent or so, which can be a large fraction of the spacing between modes and enough to ruin the experiment. A copper shield around the cold trap minimizes this effect by keeping the entire cold trap at liquid nitrogen temperature.

The liquid height in the resonator is a surprisingly strong function of the resonator's temperature because of the temperature

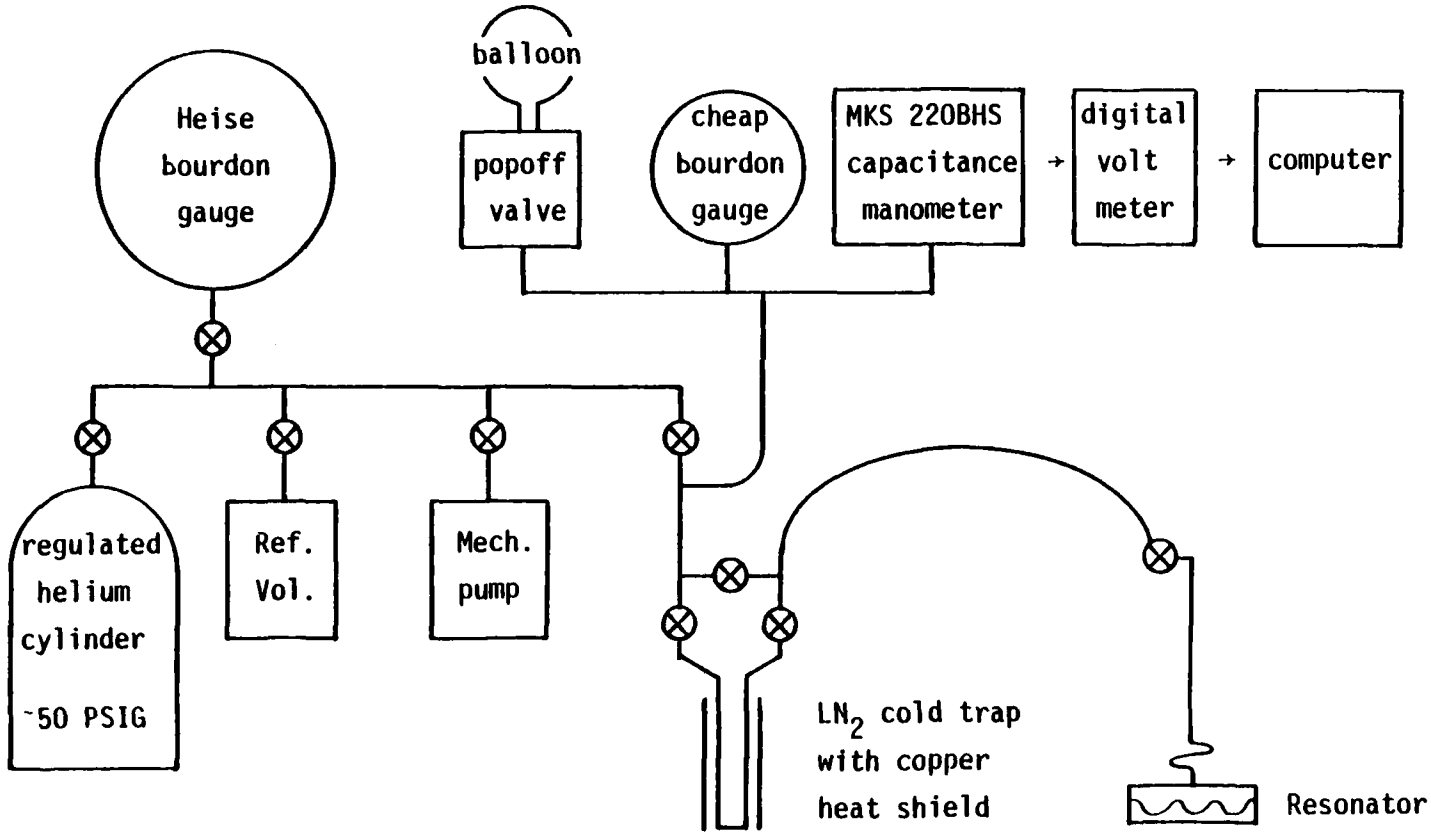


**Figure 19. Resonator fill plumbing.**

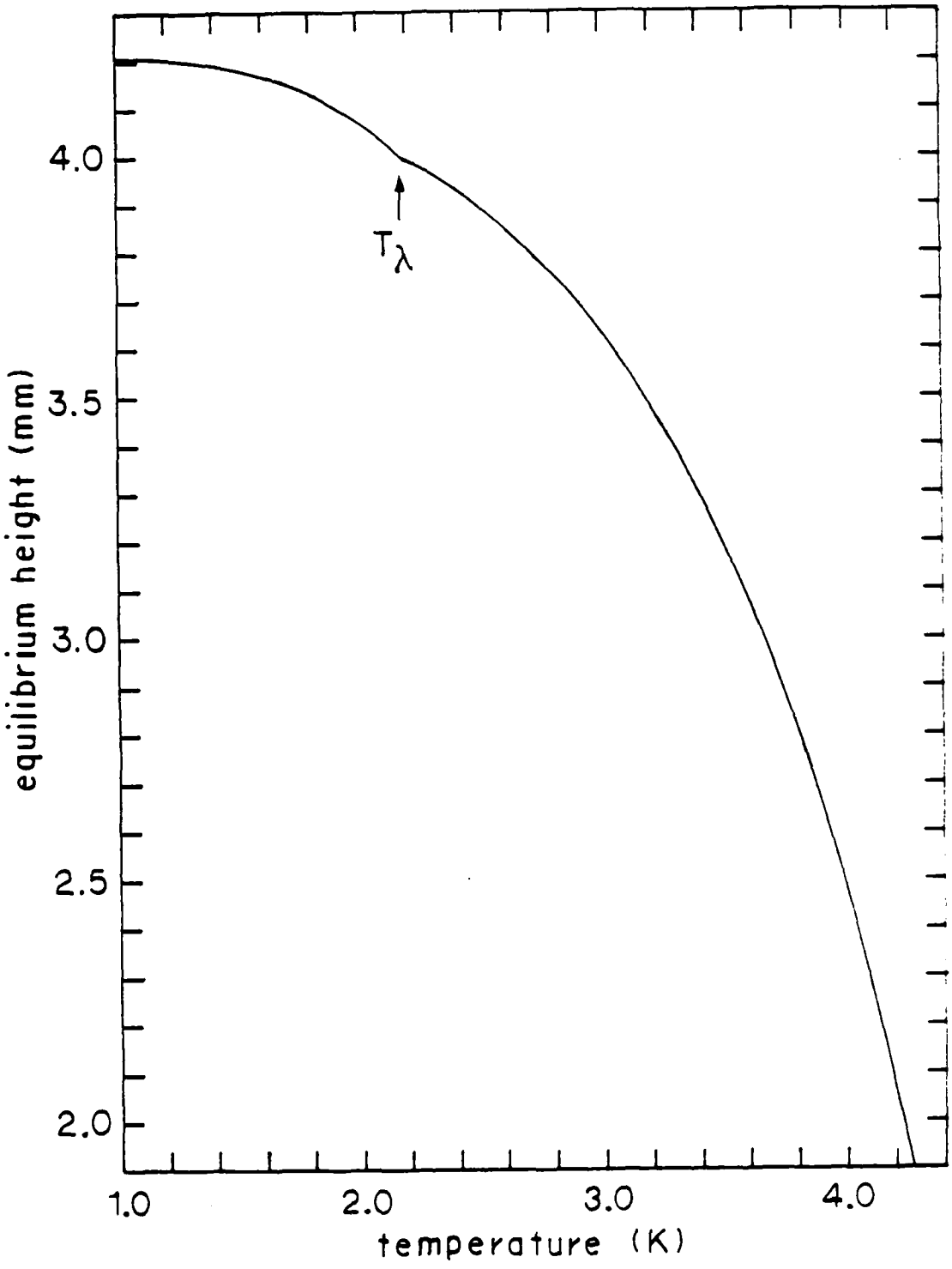


**Figure 20. Helium height vs. temperature for a fixed amount, 1.000 gm, of mass delivered by the fill panel.**

dependence of the liquid's density, and the vapor pressure dependence of the mass that remains in the dead volume of the cold trap and plumbing left connected to the resonator and the vapor space above the liquid in the resonator. The calculated dependence due to all these effects is plotted in fig. 20 for 1.00 grams of helium delivered by the known volume, which was the same for all the runs.

## 4d. Electronics.

Overview. Electronics is needed to acquire and monitor signals from the helium surface and drive amplitude sensing capacitor, power the drive, trigger the data sampling, and some miscellaneous chores. Figures 21(a)-(c) are block diagrams of the electronics used. Schematics for all of the home made electronics are collected in Appendix 6.

Signal Acquisition. To detect the small capacitance changes of $1.8 \times 10^{-3}$ pf/mm from the oscillating helium surface or of $4 \times 10^{-4}$ pf from the drive sensing capacitor at small (3 μm) drive levels, a separate capacitance bridge and lock-in amplifier is needed for each transducer. Commercially, they would cost around $10,000 per channel, and so they were home made. The main signal, from one of the barrier transducers, and the drive amplitude signal were acquired with nearly identical channels of electronics; for later experiments a third simplified channel was built to monitor a second transducer.

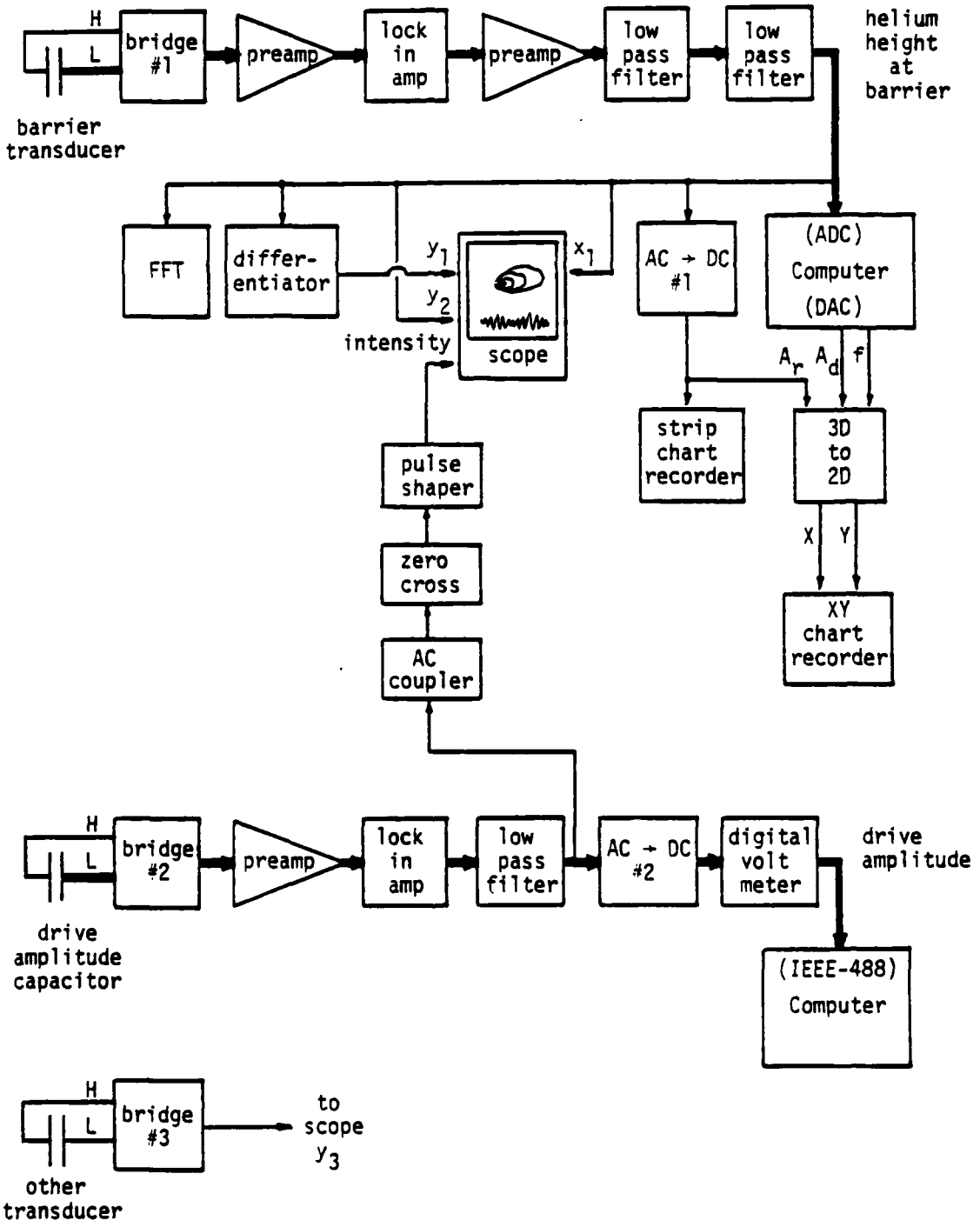


**Figure 21(a). Electronics block diagram, signal path.**

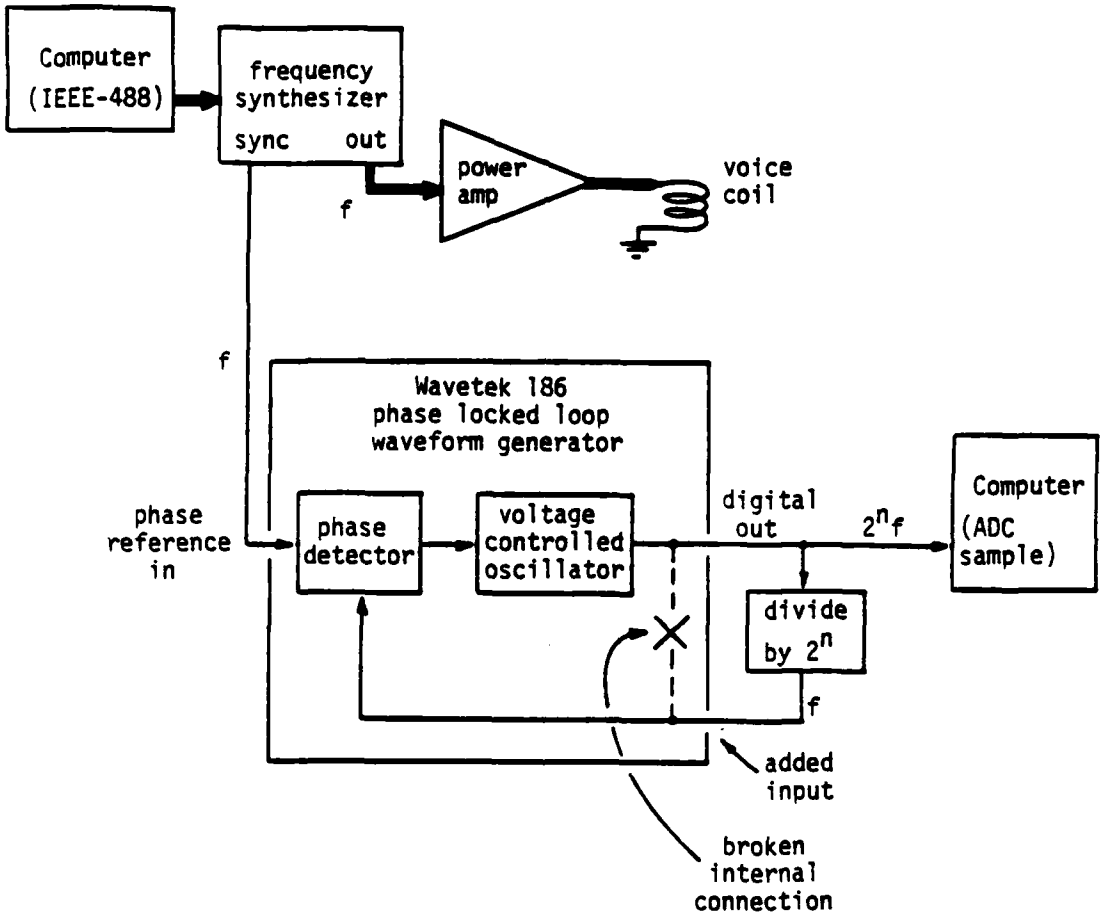


**Figure 21(b). Electronics block diagram, drive power and data sampling.**

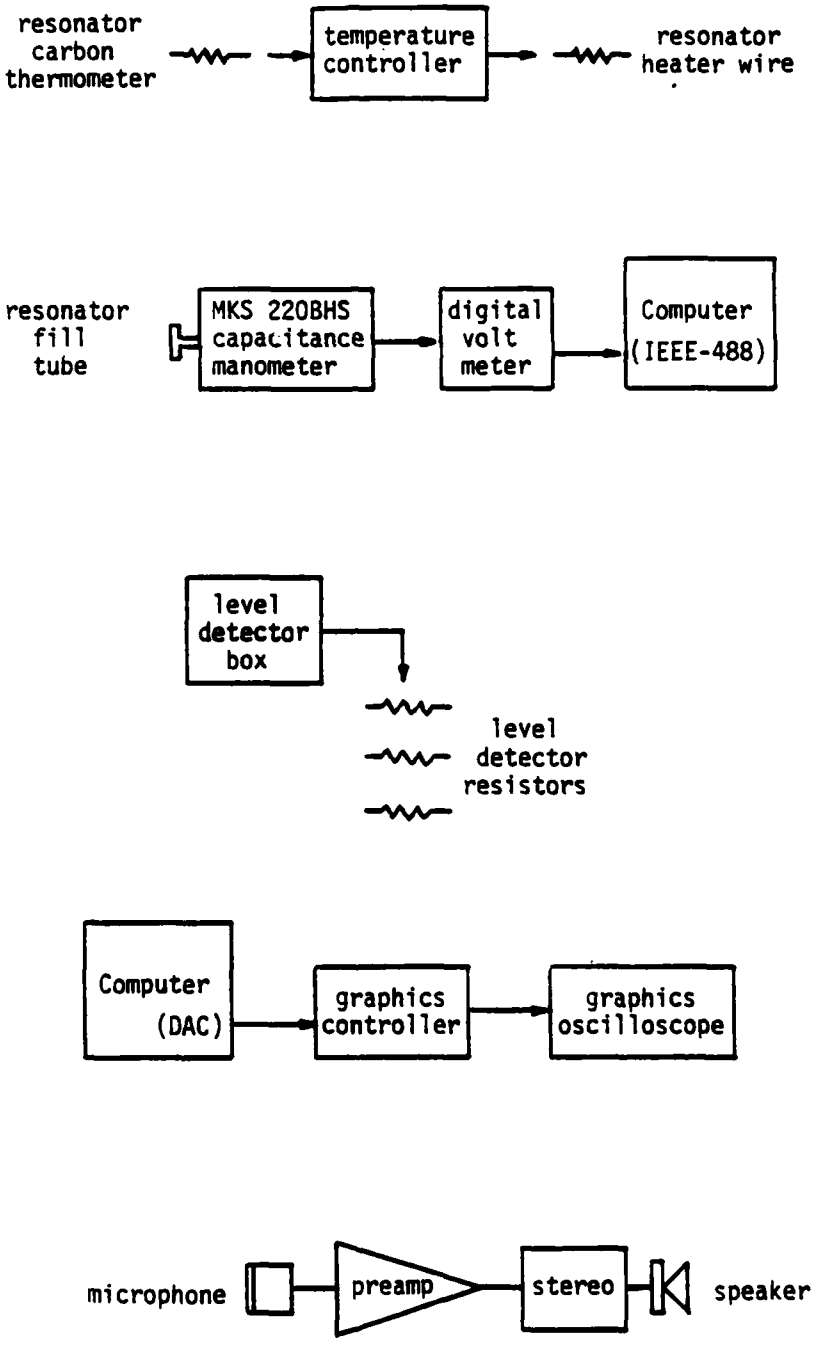


**Figure 21(c). Electronics block diagram, miscellaneous chores.**

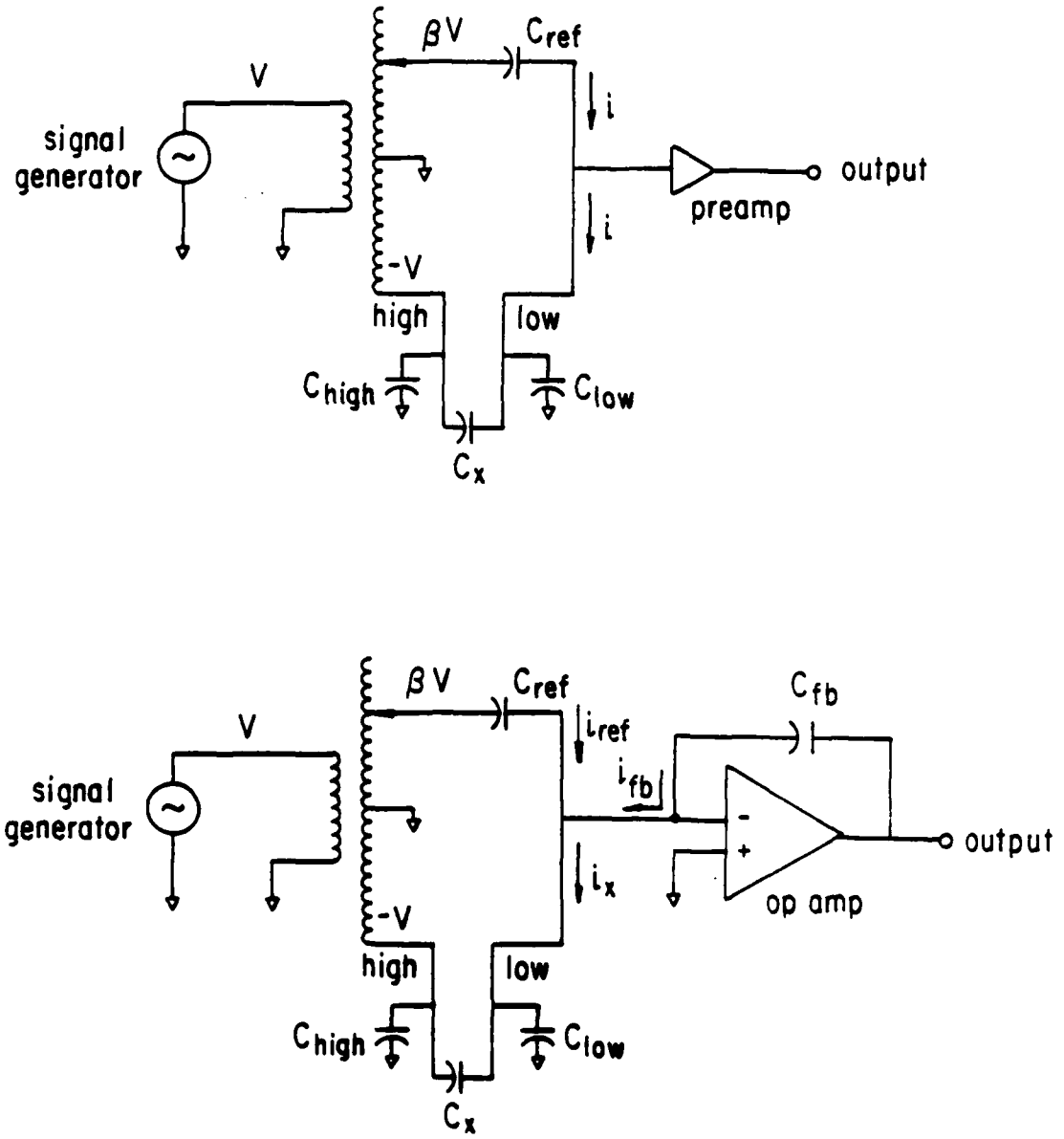


Figure 22. Capacitance bridges; (a) typical commercial method, and (b) improved method for better linearity and insensitivity cable capacitance $C_{low}$ off null.

To work, the bridges must be insensitive to the large, unstable capacitance of several hundred picofarads of the cables that run to the probe. The typical commercial method is shown in fig. 22(a). The transformer splits the input sine wave into two waves $180^{o}$ out of phase. One side of the transformer has variable taps and drives the known reference capacitor $C_{ref}$ with a known fraction $\beta$ of the input voltage V. The other side, called the high side of the bridge, drives the unknown capacitor $C_x$ with V. The junction of the two capacitances, the low side of the bridge, is monitored by an amplifier. Long coaxial cables run from the high and low sides to $C_x$ with cable capacitances $C_{high}$ and $C_{low}$. In operation, $\beta$ is varied until the low side is nulled. At null, the ratio of the voltage across $C_{ref}$ to $C_x$ is $\beta$. But the current through both capacitors is the same since no current is lost to either $C_{low}$ or the amplifier because there is no voltage across them. Therefore, by Ohm's law, $C_x$ is $\beta C_{ref}$, independent of $C_{low}$. Since the high side's only job is to deliver voltage to $C_x$ from a transformer which has a low output impedance, current can flow through $C_{high}$ without affecting the null. Note, however, that the amplitude of the off null signal, the signal desired from the oscillating surface, depends on $C_{low}$ since some current is diverted through it.

For this experiment, the off null signal should be linearly proportional to the helium height or drive position, and thus $C_x$, and the proportionality constant should be insensitive to $C_{low}$ so that absolute calibrations can be made. The one modification shown in

fig. 22(b) makes this possible. The amplifier is replaced by an operational amplifier (op amp for short) with a feedback capacitor $C_{fb}$. The op amp constantly keeps the low side nulled like a see-saw. If current flows into the low side from $C_{ref}$ or $C_x$, the op amp sees a rising voltage which it cancels by decreasing its output and pulling current through $C_{fb}$. This happens at the frequency of the input voltage, typically 10 KHz; the amplitude of the output voltage is proportional to the amplitudes of $i_{ref}$ and $i_x$. Thus, the output is amplitude modulated by changes in $C_x$, the proportionality constant being $V/C_{fb}$, and the offset amplitude is set by $\beta$, a constant. The calibration is independent of $C_{low}$ because the bridge is always nulled. Actually, the bridge is just the traditional op amp summing circuit made with capacitors instead of resistors.

Preamps and lock-in amplifiers, made with op amps and analog multiplier chips, amplify and demodulate the signals from the bridges. The voltage from one channel represents the helium surface height at the barrier, the other represents the vertical displacement of the resonator.

Signal Monitoring. The signal representing the surface height is anti-alias filtered (two 24 db/octave Butterworth filters in series, typically set to 30 Hz), digitized by the computer (a copy of a Digital Equipment Corporation LSI-11 computer with a 12 bit analog to digital converter), and stored in memory or floppy disk (sec. 4e). This is the main signal path.

While the experiment is running, the signal is monitored by a hardware FFT, oscilloscope, and stripchart recorder. The FFT (Fast Fourier Transform) continually displays the signal's spectrum, so that subharmonics, quasiperiodicity, or turbulence become obvious.

The oscilloscope simultaneously displays the signals from the barrier and the drive position vs. time, and a Lissajous figure -- the barrier signal vs. its time derivative. The derivative is taken with an op amp circuit. When the drive position passes through zero, the traces are momentarily intensified with a pulse to the Z axis of the oscilloscope from a zero cross circuit and pulse shaper. This causes bright spots on the Lissajous figure which are used for measuring the phase shift between the drive and response, a precursor of a sharp change in behavior (Appendix 2, p. 191).

To determine the long term behavior of the surface, the barrier signal passes through an AC to DC converter that filters the absolute value of the signal with a 1 second time constant; its output is the envelope of the signal. The average and peak to peak levels of the envelope, and long term (minute) oscillations of these levels, are useful indicators of the state of the surface. The envelope is recorded throughout the run on a strip chart recorder. Tick marks are placed on the strip chart by the computer whenever it samples the signal.

On the last run, the envelope of the barrier signal $A_r$ was also plotted at run time versus both drive frequency f and drive amplitude

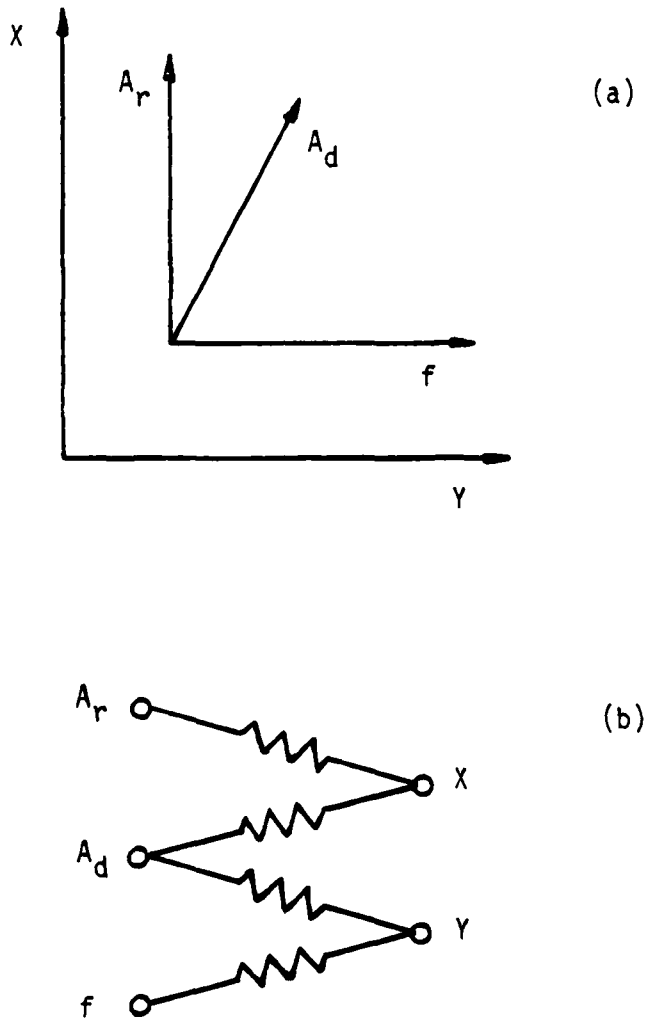


**Figure 23. (a) Three axes to be projected onto two. (b) A circuit to do this.**

$A_d$ to provided a guide in selecting the next frequency or amplitude sweep. Voltages proportional to f and $A_d$ come from the computer's digital to analog converters. This projection of three axes onto two can be made with surprising ease, especially for axes as in fig. 23(a), where X and Y are the axes of the chart recorder making the plot. We want f to influence X but not Y, $A_r$ to influence Y but not X, and $A_d$ to influence both X and Y. This can be trivially implemented with resistors as in (b), as long as the sources of $A_r$, $A_d$, and f have negligible output impedance and the input impedance of the chart recorder is high. The circuit used (Appendix 6) is essentially this. The computer also stored $A_r$ vs. f and $A_d$ so that the 3-dimensional plot, fig. 67 on p. 151, could be made later with various projections.

To measure the drive amplitude, another AC to DC converter determines the amplitude of the drive position signal which is then read on a digital volt meter monitored by the computer.

Drive Power and Data Sampling. To power the drive, the computer controls a frequency synthesizer whose output is amplified and fed to the voice coil on the probe.

The synthesizer also controls the sampling of data, so that data will be sampled commensurate with the drive. This is important for the construction of return maps (p. 112) and clean looking time records. A phase locked loop is tricked into operating at a multiple of the drive frequency by inserting a digital frequency divider

between the loop's oscillator and phase detector input. A Wavetek 186 was modified as shown in fig. 21(b) for this purpose. The output of the loop, typically set to 4 times the drive frequency, triggers the analog to digital converter on the computer to sample the surface.

Graphics Controller. A graphics controller allows another oscilloscope to be used as a graphics display. Pairs of points periodically put out by the computer's digital to analog converters are connected by straight lines to display time records and frequency spectrums. It is essentially a graphics card for a terminal; building it was not a particularly wise investment of time.

## 4e. Computer.

Hardware. The computer, an Andromeda Systems 11-B, is a copy of a Digital Equipment Corporation (DEC) LSI-11, the smallest of the DEC PDP-11 family of computers ever made. The computer has 30K of 16 bit memory, two floppy disks, a 16 channel 12 bit analog to digital converter, four 12 bit digital to analog converters, a programmable clock, an IEEE-488 (HP-IB) bus for lab equipment, a Hewlett- Packard 7225A digital plotter, a Hazeltine 1500 terminal, a printer, and three parallel interfaces. A homemade "graphics controller" (above), oscilloscope, and two of the digital to analog converters display graphics.

Software. The computer monitors and controls nearly all aspects of the experiment. This was a serious mistake. Such a huge program is cumbersome to change and makes a poor substitute for a lab book.

The program, written in Pascal and assembly language, is a collection of segment procedures which are large chunks of code loaded into memory from floppy disk. Table 1 lists the segments with their functions. Most of the segments are menu driven, a convenient way of entering values and desired actions from the keyboard, but the price for this convenience is a lot of software.

Time records. Time records are collected by sampling the surface height at a transducer at a rate determined by either the computer's internal clock or, with later experiments, commensurate with the drive (p. 59). Nearly all the experimental parameters that one might fancy are combined with the time record when it is taken.

Ramps. The frequency and amplitude of the drive can be set by typing the desired values or by letting the computer ramp them up or down. The ramped parameter increments in small discrete steps that depend on the ramp rate and step time of typically 2 or 5 seconds. The computer can take time records at regular intervals (holding the ramped parameter fixed while sampling the barrier signal) or it can record the the envelope of the barrier signal (p. 57) vs. the parameter, instead of time, to obtain the 3 dimension plot on p. 151. These ramps are a good way of collecting hundreds of time records.

Drive amplitude feedback. Drifts in the loudspeaker magnet

Table 1. Segment procedures.

| Name | Function |
|---|---|
| Task | Controls the experiment and data taking |
| Filer | Manages memory, disks, data, etc. |
| Plotter | Plots data on paper |
| Display | Displays data on oscilloscope screen |
| QFFT | Takes Fast Fourier Transforms |
| Ret | Makes return maps |
| Threshplt | Plots thresholds for parametric growth |
| Omniplot | Plots reams of data on tractor feed paper |
| Prnthead | Prints experimental parameters (data headers) |
| PR11 | Makes 3-D plots: Response vs. drive Freq and Amp |
| Videodigtz | For digitizing video tapes by hand |

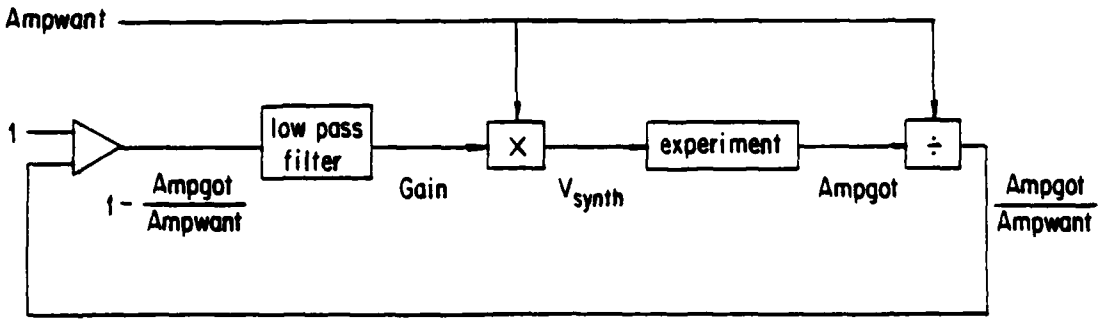


**Figure 24. Software feedback loop to control drive amplitude.**

strength and coil resistance caused the drive amplitude to drift (p. 40), which rendered the experiment uncontrollable until they were compensated for with a software feedback loop, which is diagramed in fig. 24. The difference between 1 and the ratio of measured drive amplitude, Ampgot, to the desired amplitude, Ampwant, corrects a value, Gain, that accumulates in a low pass filter. Gain then multiplies Ampwant to produce the proper voltage, $V_{synth}$, to drive the experiment. Gain follows the long time drifts in the probe while Ampwant can change quickly since it is multiplied into and then divided out of the loop. Gain also compensates for the main probe resonance of 5 Hz from the trough's mass being supported by springs. Whenever the frequency is changed, Gain is instantly corrected using the probe's known tuning curve, without losing the accumulated information about the drifts. The loop is stable because only amplitude information is fed back and the low pass filter is the numerical equivalent of a simple RC with at most a phase shift of $90^{o}$. (A previous attempt at electronic feedback on the drive wave shape failed because mechanical resonances, higher than the main one which was compensated for, added phase shifts into the loop. When an extra $180^{o}$ is added to a feedback loop, negative feedback becomes positive and combined with enough gain, the loop breaks into oscillation.)

The loop, being digital, poses a subtle problem. Discrete values are all that Ampgot can take because the frequency synthesizer used to drive the experiment and the meter used to measure the drive amplitude both have finite discrete resolution. Presented with this, the loop

would want to hunt between the two values that straddle Ampwant, trying to keep the average Ampgot correct, but foul up the experiment with an incommensurate frequency modulating the drive. To stop this from happening, the loop was given a dead band, or slop; it does not respond to values of Ampwant-Ampgot less than the calculated resolution. As a bonus, the drive level was made insensitive to noise in the measurement of Ampgot by increasing the dead band a little bit more.

# Chapter III. Data and Interpretation.

## Section 5. Cockscombs

### 5a. Cockscombs in water.

The plastic annular resonator, described on p. 25, was tried out with water before use with helium. The results turned out to be interesting, so work in helium was delayed for quite a while.

The resonator is partially filled with a 200:1 mixture of water and Kodak Photo-Flo 200, a wetting agent that helps keep the water surface from sticking to the walls (p. 22), and some salt to increase the conductance between the transducer electrodes. Bridge circuits made the salt unecessary by the time the ultra deep modulation experiments of the next section were performed.

When the resonator oscillates vertically with relatively small amplitude, the standing waves seen by Faraday form at half the frequency of the drive. At higher drive levels, with accelerations of around g/3, we find behavior that is periodic, quasiperiodic, and turbulent. The waves have high amplitude; peaks can be as high as 20 mm and troughs as low as 3mm.

A typical periodic waveform is shown in fig. 25(a). The

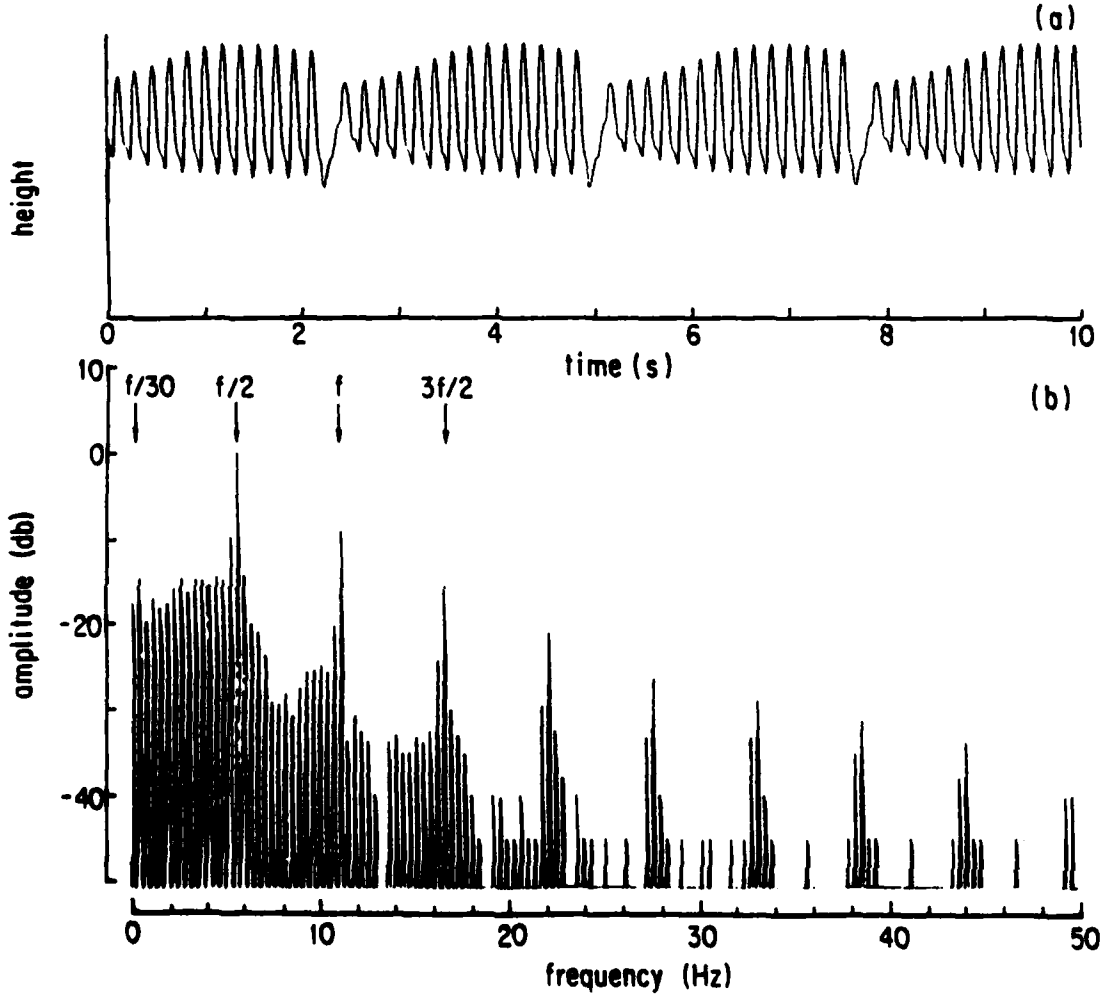


Figure 25. Cockscomb at f/30, in 5.3 mm of water driven at 11.00 Hz.

amplitude builds up and suddenly dies in a characteristic "cockscomb" pattern, in this case, every 15 cycles of f/2 where the drive frequency is f. Note how even minute details repeat. These states, and most others, are robust; they persist for hours, and are stable to small drive amplitude changes. Note too that the first heap after the sudden drop is delayed quite a bit in time. This phase delay will turn up again in the "conspiracy theory" of p. 103. It should be mentioned that the signals from the transducers were AC coupled in these early water experiments. This causes the baseline to rise and fall keeping the average voltage constant. To undo this distortion, keep in mind fig. 4 of the introduction, taken in helium.

The periodicity is reflected in the power spectrum, fig. 25(b). Subharmonic response is response with a period which is an exact integral multiple of the period of the drive. There is no ambiguity in identifying this as subharmonic response at f/30 since all harmonics of f/30 are present to beyond f and there are no unaccounted for peaks. For these periodic waveforms, the peaks are given by pf/m, where p and m are integers, and m most often is even. This is unlike the period doubling route to chaos where m is restricted to powers of two.

The m'th subharmonic series is encouraged by driving the trough near its m'th mode. In other words, the cockscomb frequency is nearly the same as the first mode of the trough.

There can be double cockscombs, with two sudden drops per cycle,

as in fig. 26(a), as well. First seven then nine heaps rise before the sudden drop. By counting peaks in fig. 26(b), the frequency is seen to be f/32. Spontaneously though, the sudden drop moved up a heap in fig. 27(a), making two identical sets of eight heaps. The frequency becomes f/16, causing every other peak to disappear in fig. 27(b).

At larger drive amplitudes, for example in fig. 28, the cockscombs rise and fall erratically. Even though there is still quite a bit of structure, this causes the spectrum (b) to develop a noise floor.

The qualitative results of stepping the drive amplitude are shown in fig. 29. This data was taken without the barrier in place. The spectrums are arranged by increasing drive voltage, and therefore by increasing drive amplitude, although they were taken in the order (g) to (a), then (h). They show the system converting energy from the sinusoidal drive into noise in the water with larger drive amplitude. Up to a voltage of about 0.4 V, the response (a) is at the drive frequency f. Very small waves radiating from the walls at f cause this and can be easily seen in containers that oscillate with low amplitude. The cause most likely is the meniscus, which flattens out with greater gravity and therefore with the upward accelerations of the container occurring at f. Between 0.4 V and 0.65 V the response is at f/2 as in (b). Between 0.6 V and 0.87 V f/4 appears with satellite peaks. This f/4 is curious. Perhaps it is due to f/2 in the drive, or it may have something to do with the barrier not being

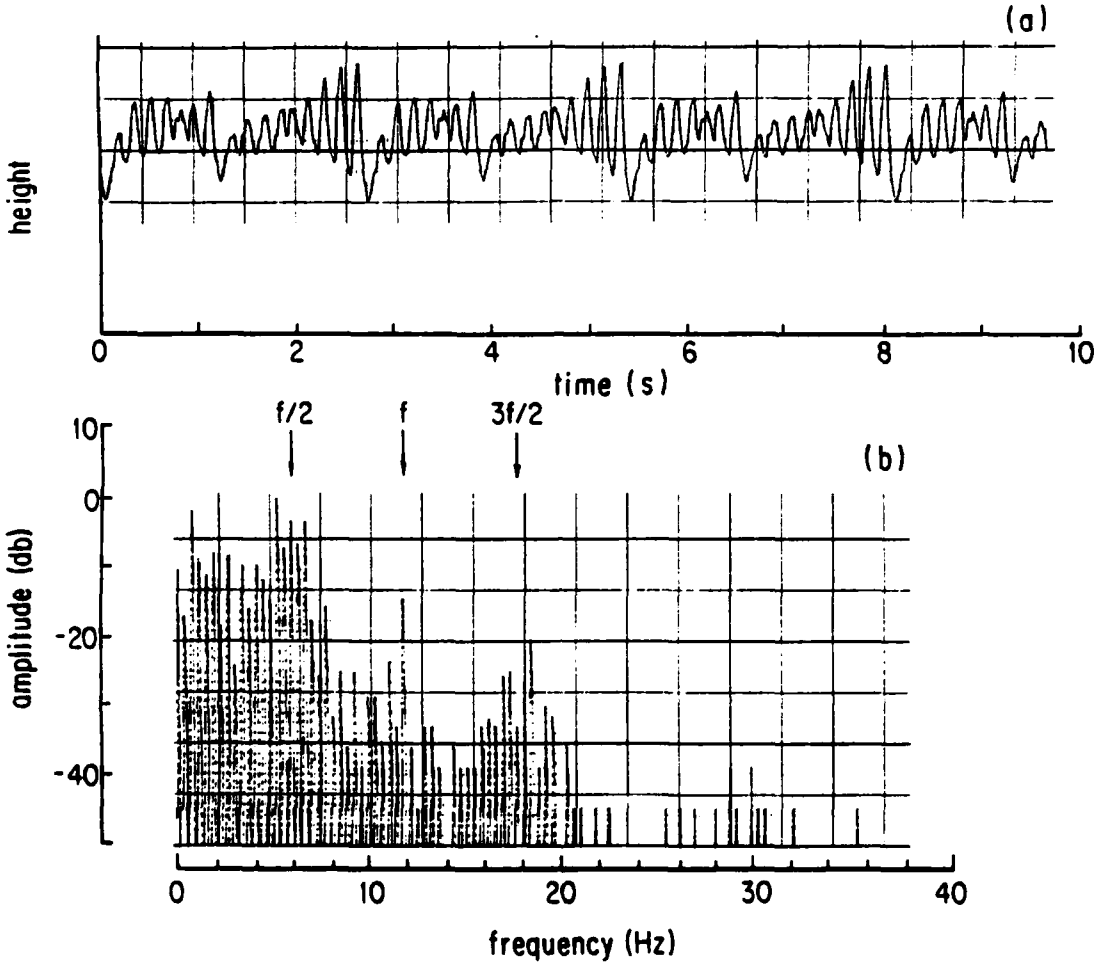


Figure 26. Double cockscomb with 7 and 9 heaps, in 5.3 mm of water. The trough is driven at 11.876 Hz with 180 μm rms amplitude.

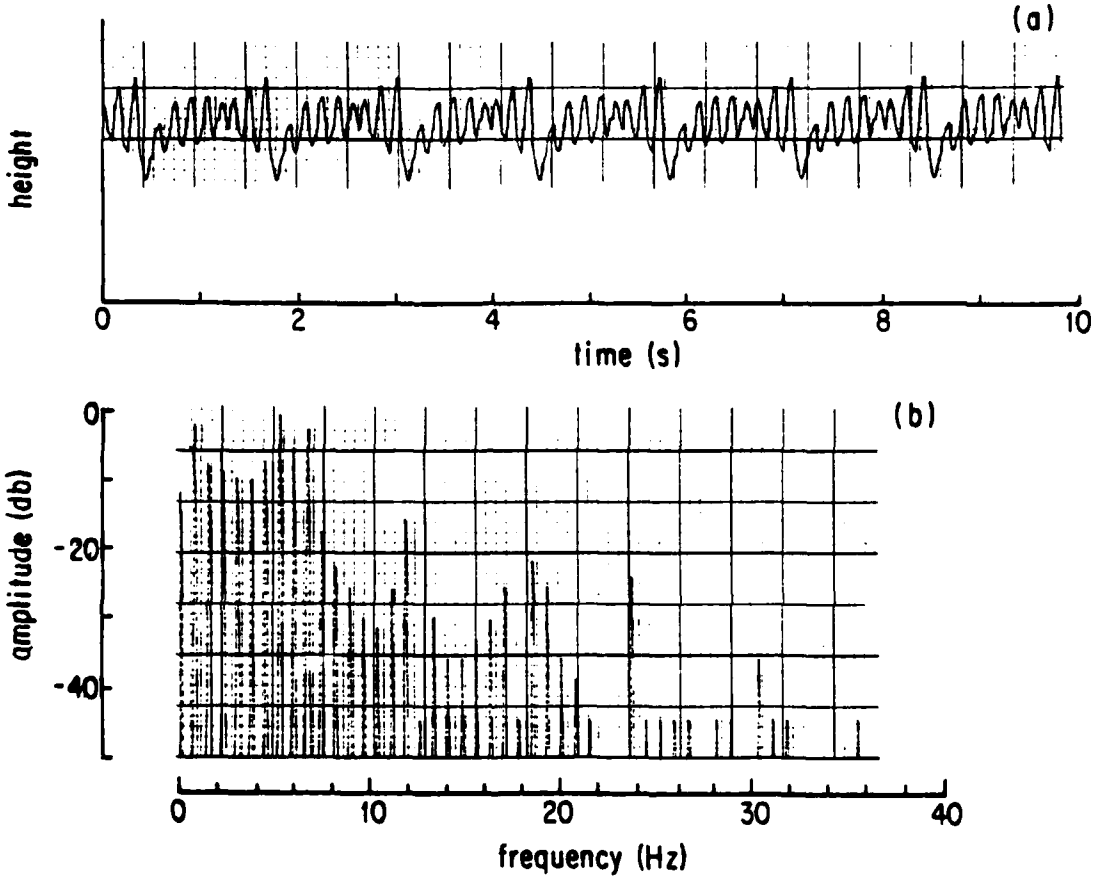


**Figure 27. Double cockscomb in water with two groups of 8 heaps; same conditions as the previous figure.**

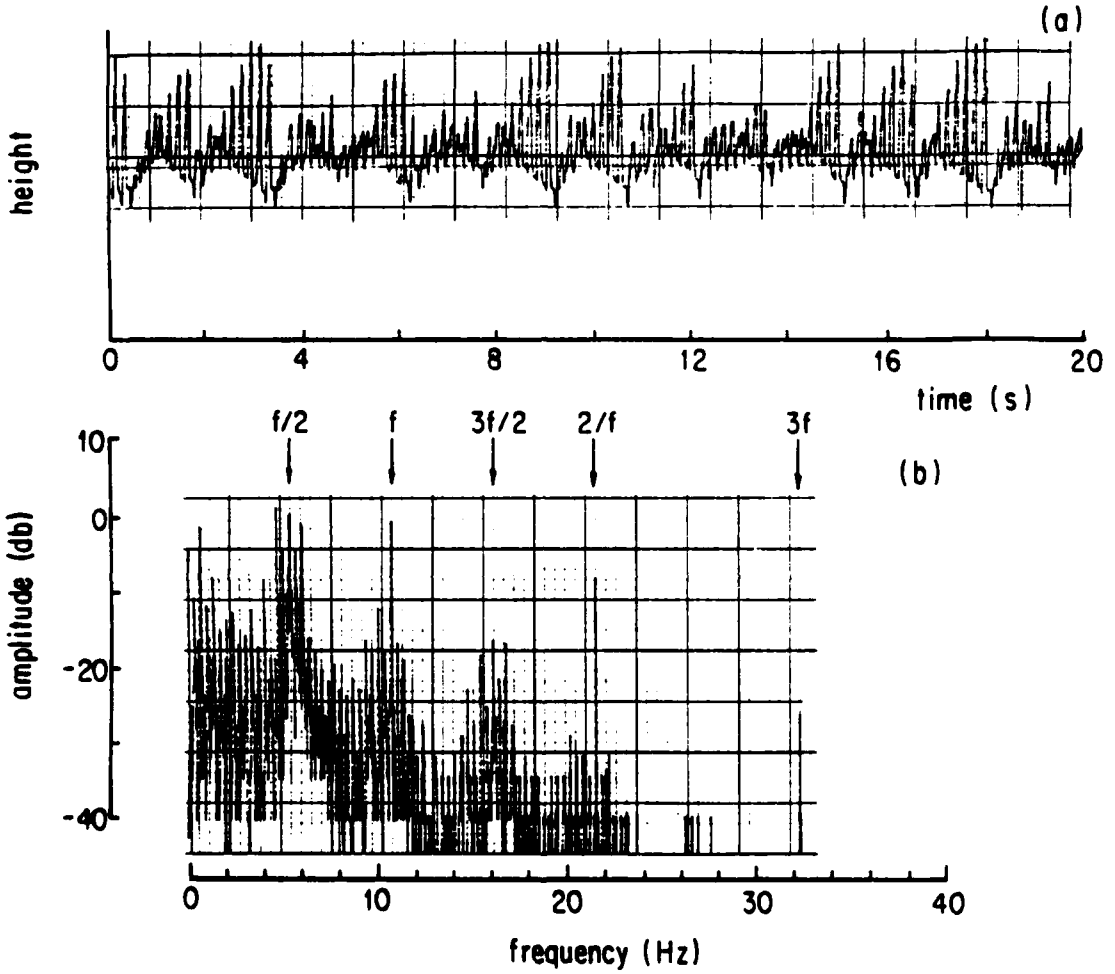


**Figure 28. Chaotic cockscomb in 5.3 mm of water. Trough is driven at 10.769 Hz with 910 μm rms amplitude.**

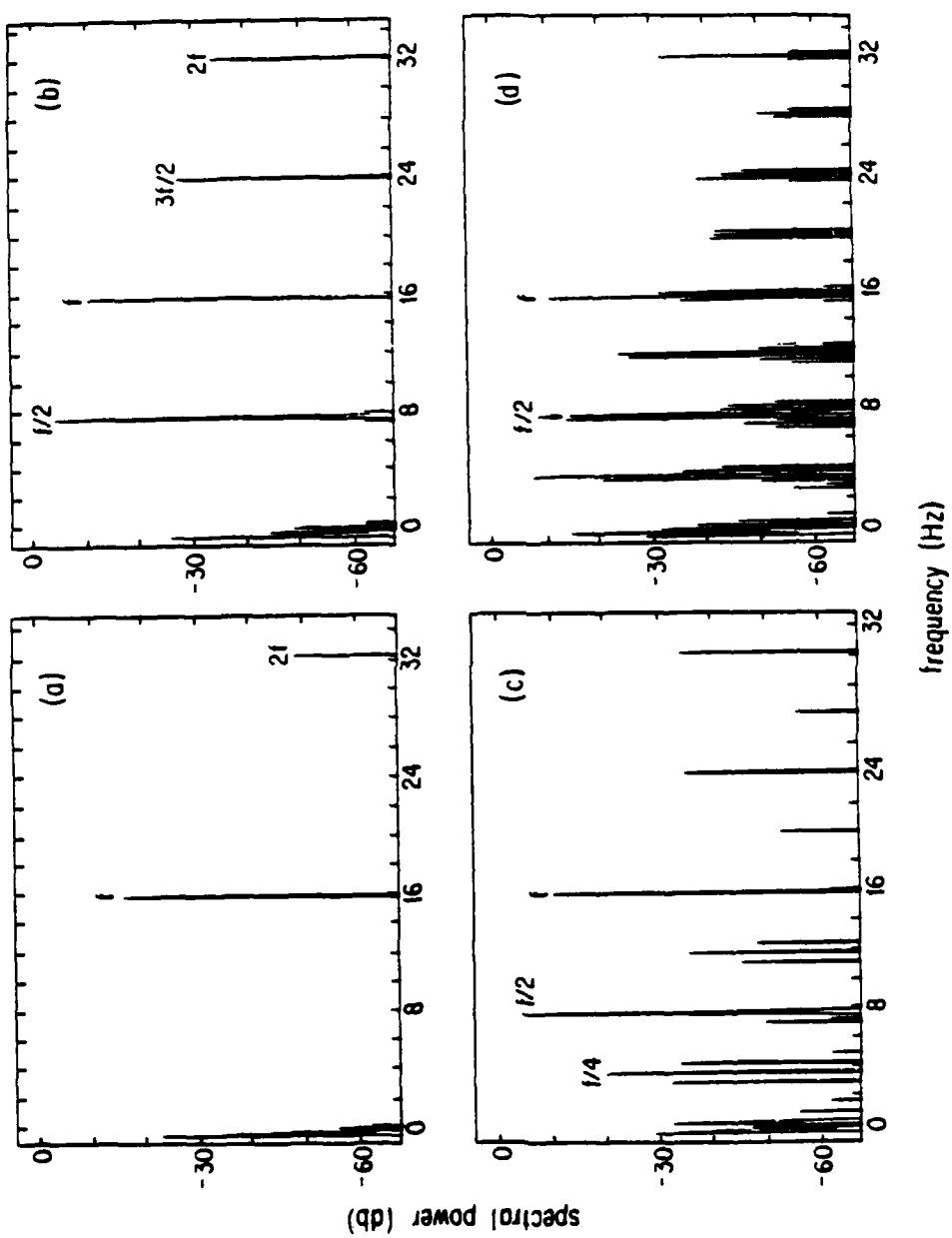


Figure 29(a)-(d). Cockscombs vs. drive amplitude in 5.3 mm of water with drive frequency 16.37 Hz. The drive voltages are: (a) 0.37 V, (b) 0.55 V, (c) 0.66 V, and (d) 0.70 V.

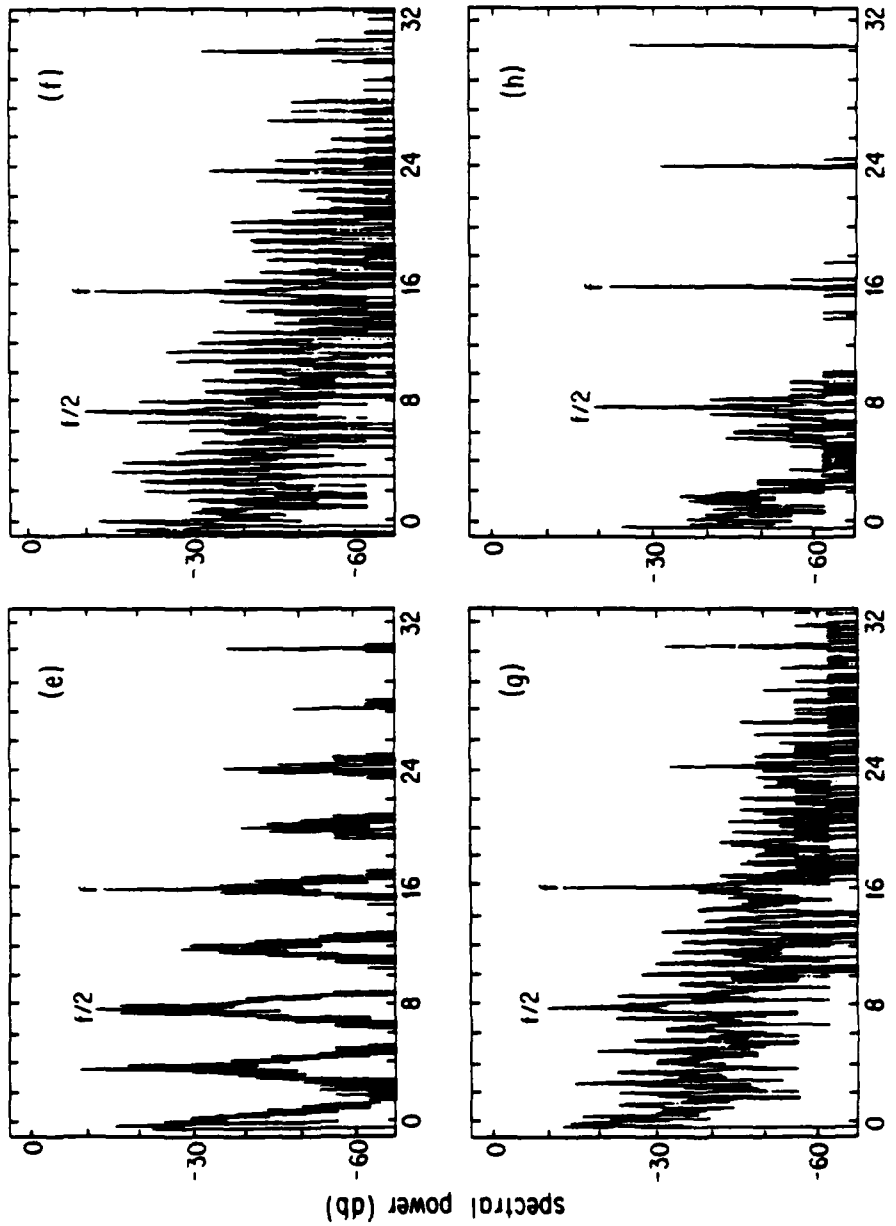


**Figure 29(e)-(h). More cockscombs vs. drive amplitude. The drive voltages are: (e) 0.80 V, (f) 0.87 V, (g) 1.14 V, and (h) 1.20 V.**

in place. The clean satellite peaks in (c), (d), and (e) may be due to the pattern slowly rotating around the resonator which it is free to do if there is no barrier to fix it. In (e) however, a continuous noise floor is added around the f/4 peaks. The noise floor is also present in (f) along with peaks at roughly f/24 and its harmonics. In (g) the f/24 has become f/22. Finally, in (h) the voltage is so high that water creeps up the walls and is lost.

In another experiment with the barrier in place, the transducers machined into the walls at various locations away from the barrier suggest what is going on in space. The top trace of fig. 30(a), taken at the barrier, shows a cockscomb with a single sudden drop in amplitude. The bottom trace, taken from a transducer $45^{\circ}$ away from the barrier, shows two drops, one just before and the other just after the drop at the barrier. This suggests that the sudden drop is an object propagating past the $45^{\circ}$ transducer, bouncing off the barrier, and passing the $45^{\circ}$ transducer again as it goes the other way. In the lower trace of (b), it can be seen passing the transducer at $135^{\circ}$ just before and after it went past $45^{\circ}$, using the drop in the top trace, again taken from the barrier, as reference. At $180^{\circ}$ (c) the drops are uniformly spaced in time, shifted 1/4 of the cockscomb cycle from the drop at the barrier, as they should with this point of view. And almost all the way around at $292.5^{\circ}$, (d), the waveform drops just before and just after a time 1/2 cycle from the drop at the barrier -- presumably just before and after the object bounces off the barrier's back side.

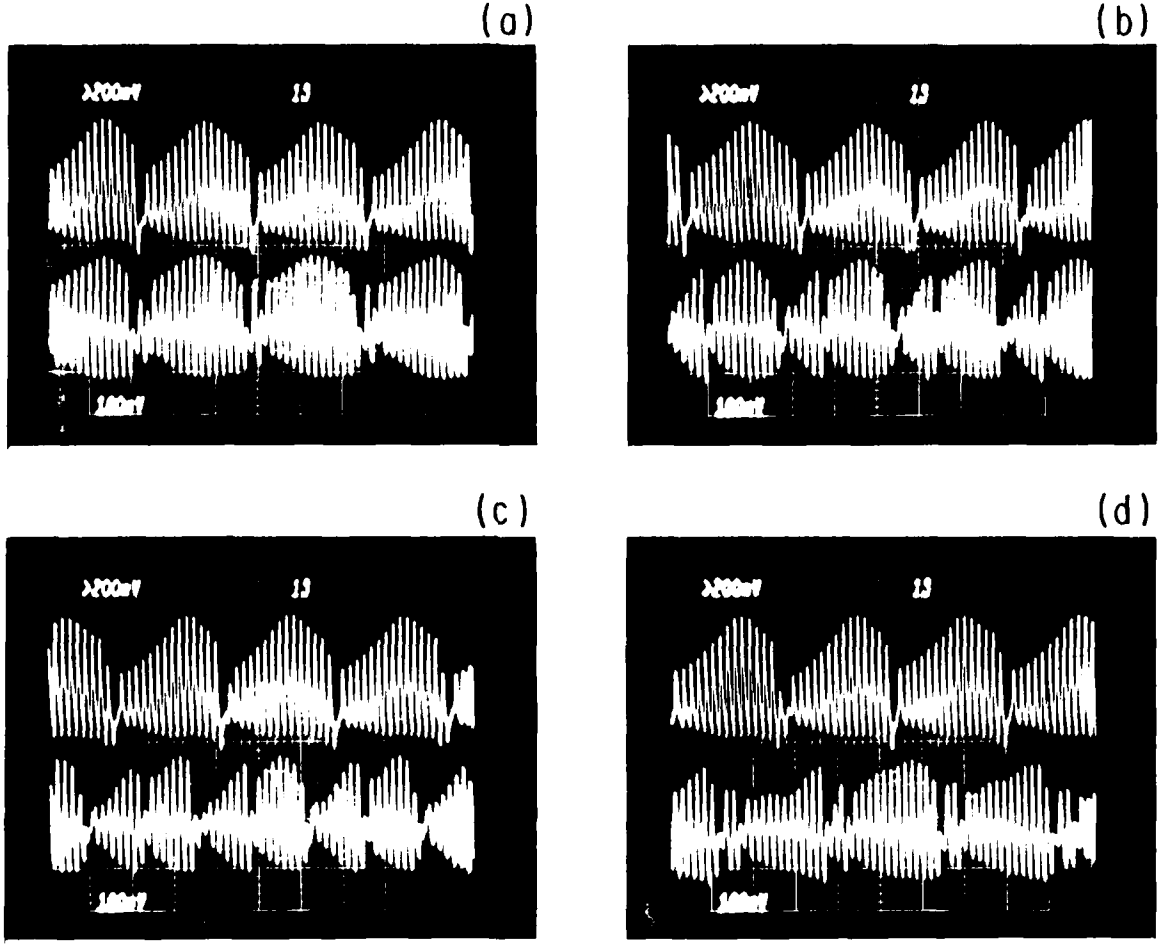


Figure 30. Cockscomb in water at various transducers along the trough. Top traces are from the barrier, while bottom traces are taken (a) 45°, (b) 135°, (c) 180°, and (d) 292.5° away.

The existence of double and triple cockscombs fits in nicely with this picture. They would be due to two or three of the objects bouncing around in the trough. The objects would have to pass through each other, supporting the claim that they are some sort of soliton.

5b. Soliton ideas.

The following is a guess on the nature of the cockscombs, based on "kink" solitons in the phase of the heaps. It is appealing enough to present because it explains most features of all the data, in spite of some evidence that it is not true.

Consider a hypothetical linear trough with a barrier placed in the center, as in fig. 31(a). Whenever the response to a parametric drive is at f/2, there are two equivalent states possible, shifted in phase by $180^{\circ}$ of f/2 or $360^{\circ}$ of f. Suppose that the water in the left side of the trough is in one state and the water on the right side is in the other, so that the waves on either side of the barrier are out of phase, as drawn. What happens if the barrier is suddenly removed? The guess and hope is that the phase discontinuity stays localized, picks a direction to go, and propagates in the trough at nearly the speed of the surface wave.

Figure 31(b) is a proposed phasor diagram of the discontinuity. Each phasor represents a half wavelength. The phase from the downward vertical is the phase of the drive relative to the response. The diagram suggests an analogy with the sine-Gordon "kink" or

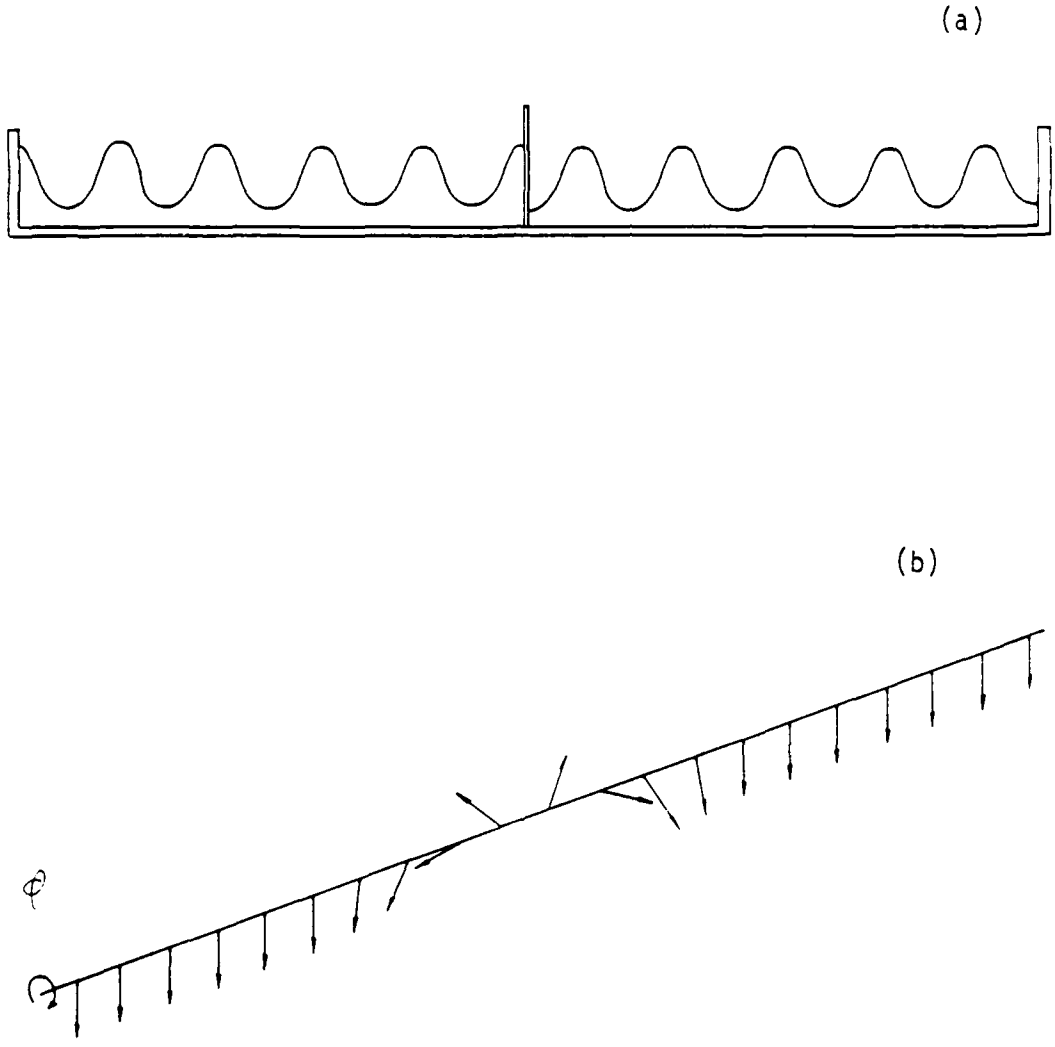


Figure 31. Soliton ideas. (a) Opposite phases in either side of a hypothetical trough. (b) Kink in the phase of the drive with respect to each heap.

AD-A157 958 MODULATIONS OF DRIVEN NONLINEAR SURFACE WAVES ON WATER 2/3
AND LIQUID HELIUM-4(U) CALIFORNIA UNIV LOS ANGELES DEPT
OF PHYSICS R M KEOLIAN JUN 85 TR-44 N00014-85-K-0370
UNCLASSIFIED F/G 20/4 NL

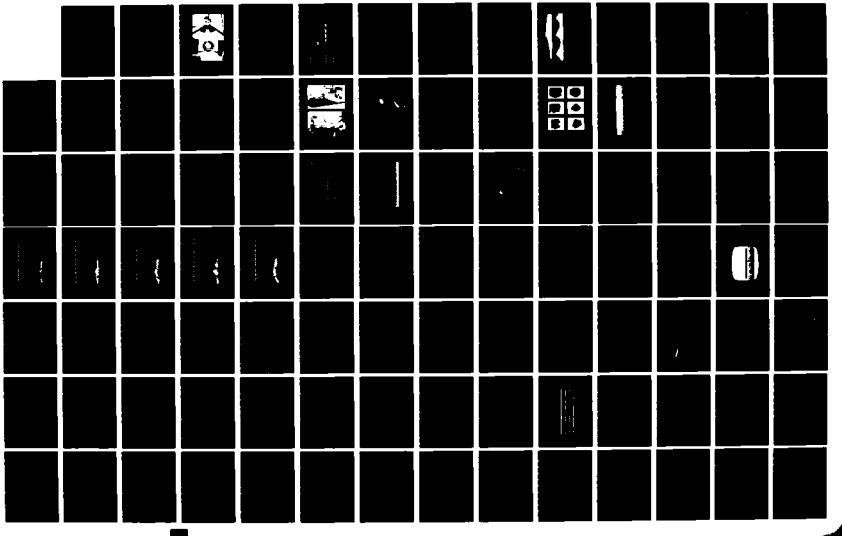

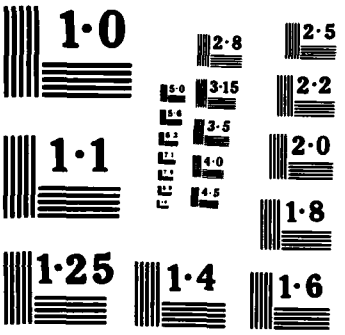

"topological" solitons on a rubber band which is stuck with pins and possesses a twist that stays localized. The twist can propagate since the energy stored in the rubber band and raised pins is very nearly translationally invariant.

Before this idea came up, a video tape was made, using a conical mirror and flat mirror oriented as in fig. 32. The conical mirror, constructed of shiny flexible plastic, encircles the resonator. The reflection of the resonator in the conical mirror is viewed from below with a flat mirror raised off the floor at an angle. The image one sees, though distorted, shows the entire surface at once. When the tape was reviewed in slow motion and frame by frame, the localized "object" of depressed amplitude was seen bouncing off the barrier and propagating around the trough, but the predicted $180^{o}$ phase shift across it could not be detected. Clearly, the experiment to perform in the future is to carefully analyze a video tape of a cockscomb in a linear trough, perhaps as was done with the smooth modulations of Sec. 8.

It may be that cockscombs are not the result of solitons, but fig. 30 does at least show that cockscombs are not relaxation oscillations occuring everywhere in the trough simultaneously; there is spatial structure. Two other ideas on their nature are presented on p. 103 and p. 159.

5c. Cockscombs in helium.

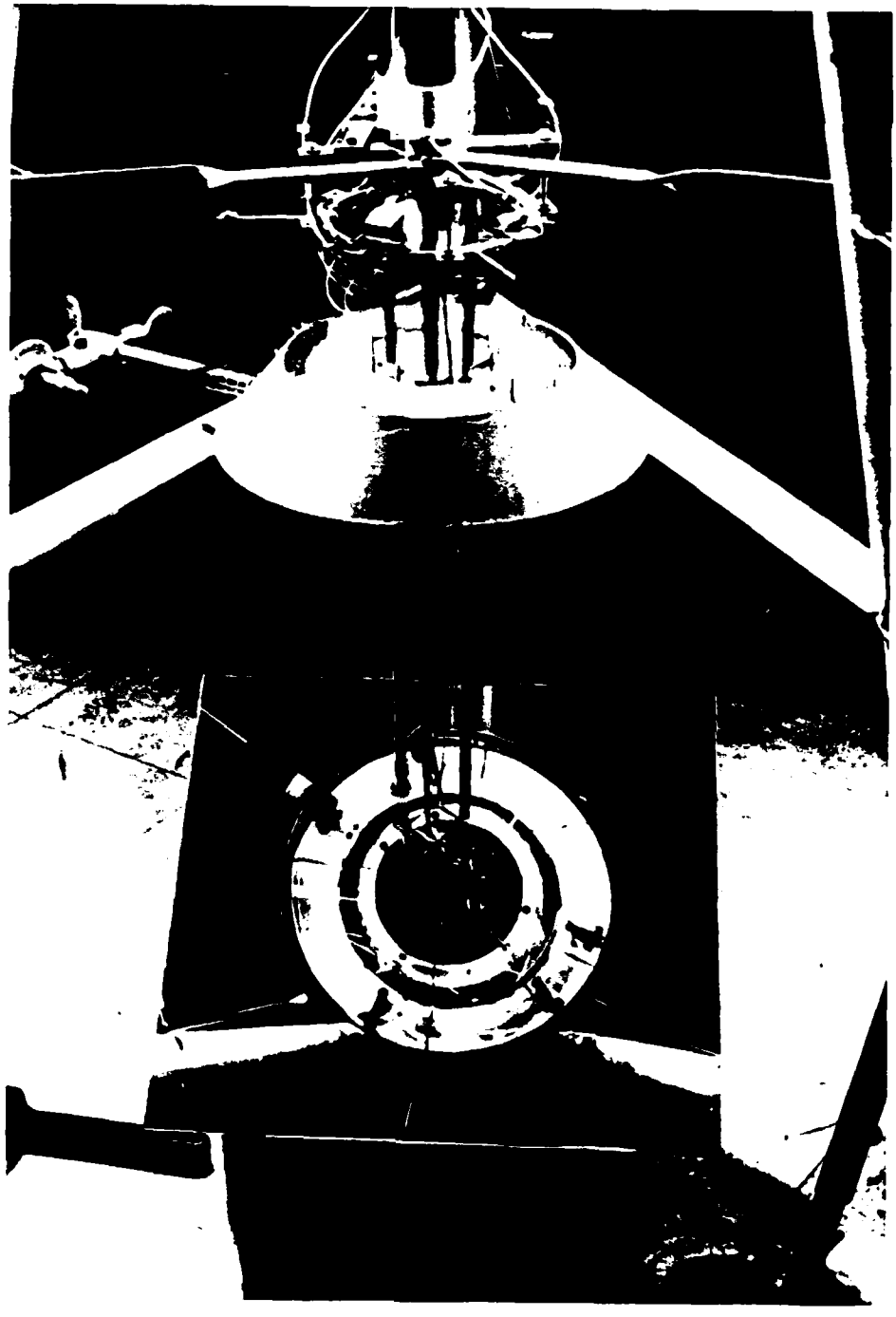

Figure 32. Conical mirror showing a cockscomb along the trough.

Cockscombs in helium are nearly identical to those in water, except that they are a bit more dramatic. Notice the crispness of the envelope shown in fig. 4 in the introduction.

As the drive amplitude is ramped up, cockscombs tend to get more sudden drops, as if more "stress" induces more "kinks." I have seen as many as three drops in a waveform (see fig. 75 on p. 167 for an example). Once a cockscomb gets a sudden drop, it is reluctant to give it up as the drive amplitude is ramped back down.

Chaotic waveforms, those without a pattern discernible to the eye (mine at least) on a short or long time scale and possessing energy in a wide band of frequencies, typically occur at higher drive levels. These waveforms were not characterized well as I spent most of my time trying to figure out the low drive amplitude behavior. This is a loose end. Usually, in the range of parameters explored, chaotic waveforms have roughly the same response amplitude as cockscombs. Sometimes, chaotic waveforms had double the typical amplitude; one is shown in fig. 33. Intermittently there is a burst of amplitude at the transducer that saturated the electronics and clipped the waveform (while I was asleep and the computer ran the experiment). Possibly helium is hitting the lid.

A particular cockscomb waveform decayed as the drive amplitude was slowly lowered below the threshold needed to sustain it. The decay, shown in fig. 34 through seven cycles of the cockscomb, is interesting because it shows that the cockscomb has energy in the

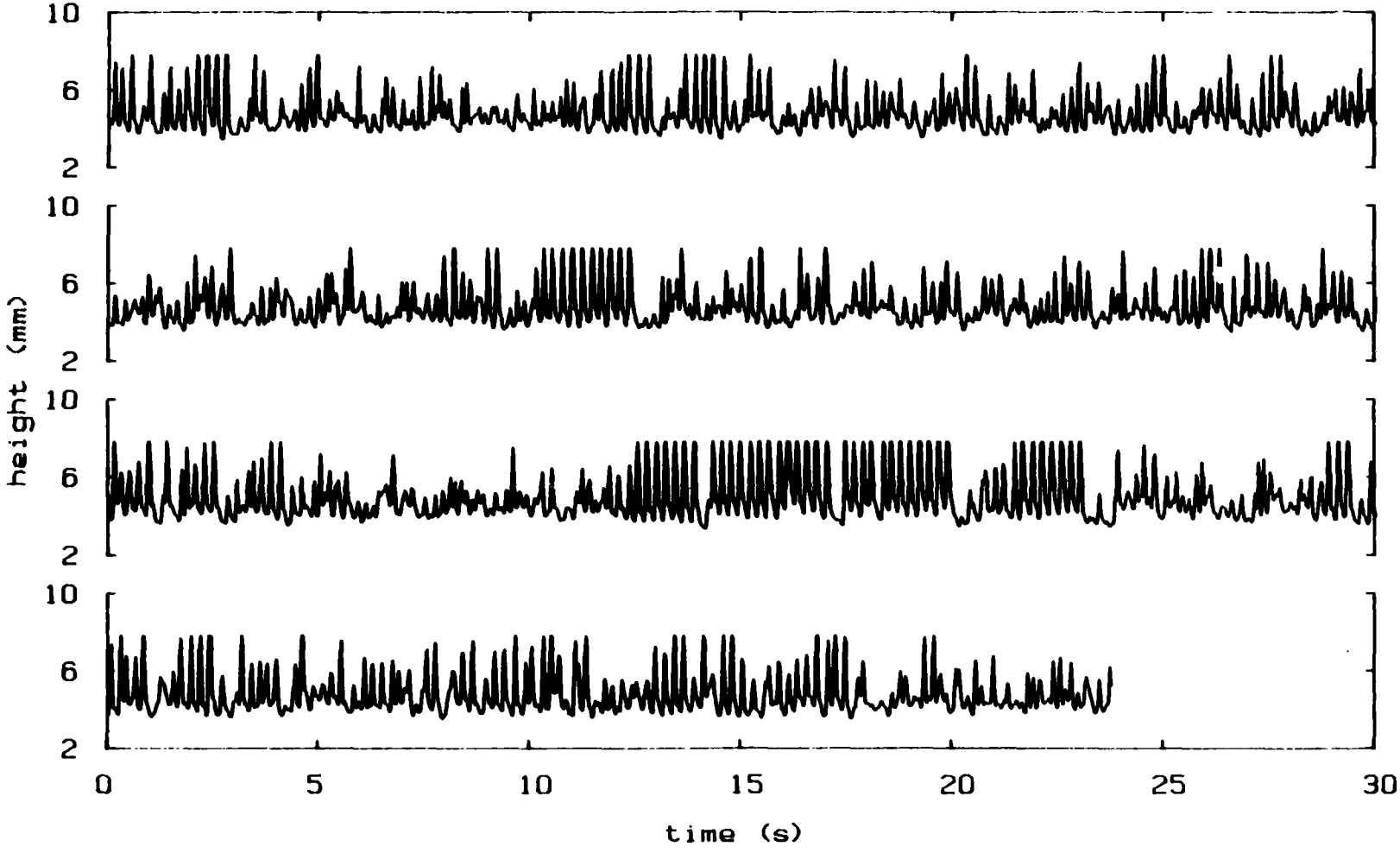


**Figure 33.** Chaotic cockscomb in helium, showing bursts of large amplitude, unfortunately clipped by the electronics. Helium at 1.28 K and height 4.20 mm is driven at 9.000 Hz with 476 μm rms amplitude.

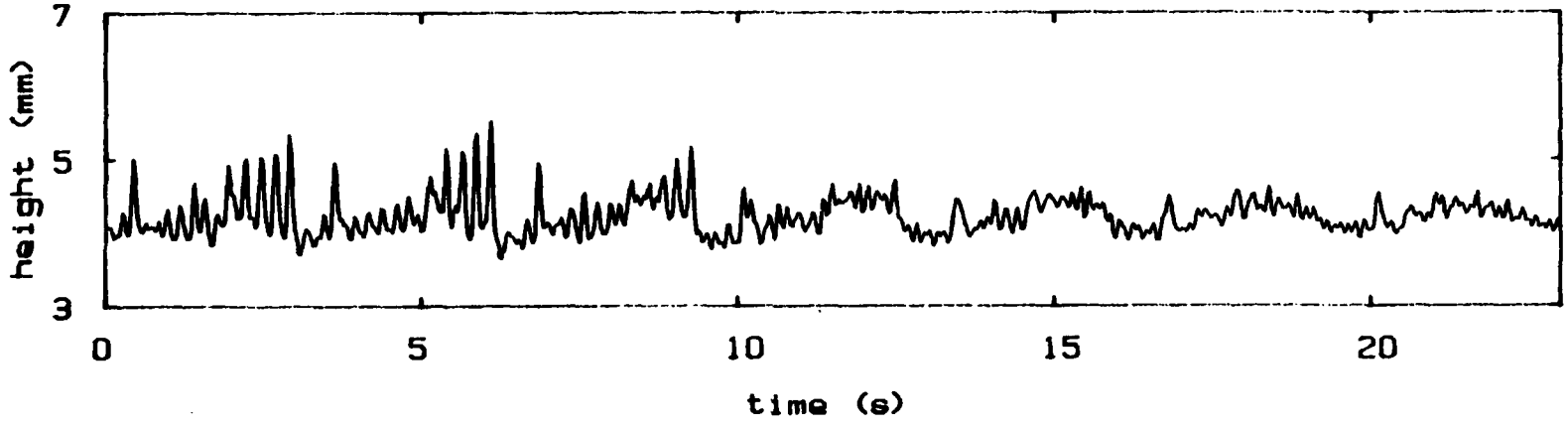




Figure 34. Decay of a cockscomb in 4.19 mm of helium at 1.42 K driven at 8.790 Hz with 181 μm rms amplitude.

lowest modes of the trough -- it carries fluid along in between the sudden drops. Notice that the f/2 wiggles die off first leaving the average of the envelope to bounce around in the trough. This may be the reason why the cockscomb frequency is close to the fundamental frequency of the trough.

Cockscombs are compared to smooth modulations in Sec. 10, and their transitions to and from ultra deep modulations are shown on pp. 88 and 89.

## Section 6. Ultra Deep Modulations.

I fired up the resonator at 11 Hz one day, and to my surprise the amplitude of the f/2 waveform continued to slowly rise and fall, taking just over a minute to complete a cycle. On several occasions, these "ultra deep modulations" were seen with periods that range from 500 to 2000 cycles of the drive, two orders of magnitude deeper than the lowest mode of the trough. In fig. 35(a), a waveform from the barrier is expanded enough to show individual cycles of f/2. Note how the amplitude takes only a few cycles to switch from the rising to the falling state. On a longer time scale (b), this modulation is seen rising faster than it falls. The periodicity of the modulation on a very long time scale is recorded in (c) by a strip chart pen that could only move fast enough to respond to the averaged amplitude of f/2. The modulation is periodic to the eye, but the time between each cycle may vary 10%. The average frequency of the modulation here is f/890, where f is 11.0 Hz, the drive amplitude is 429μm rms, and the equilibrium height is $5.97 \pm 0.1$ mm.

I believe these modulations are not due to an external cause. They have persisted for 25 hours, through a million cycles of the drive, on through the night after passing trucks and air conditioning have ceased to operate. They were seen on two different water runs, months apart, after substantial modifications were made to the probe's suspension. And the modulations occur in helium, as was shown by

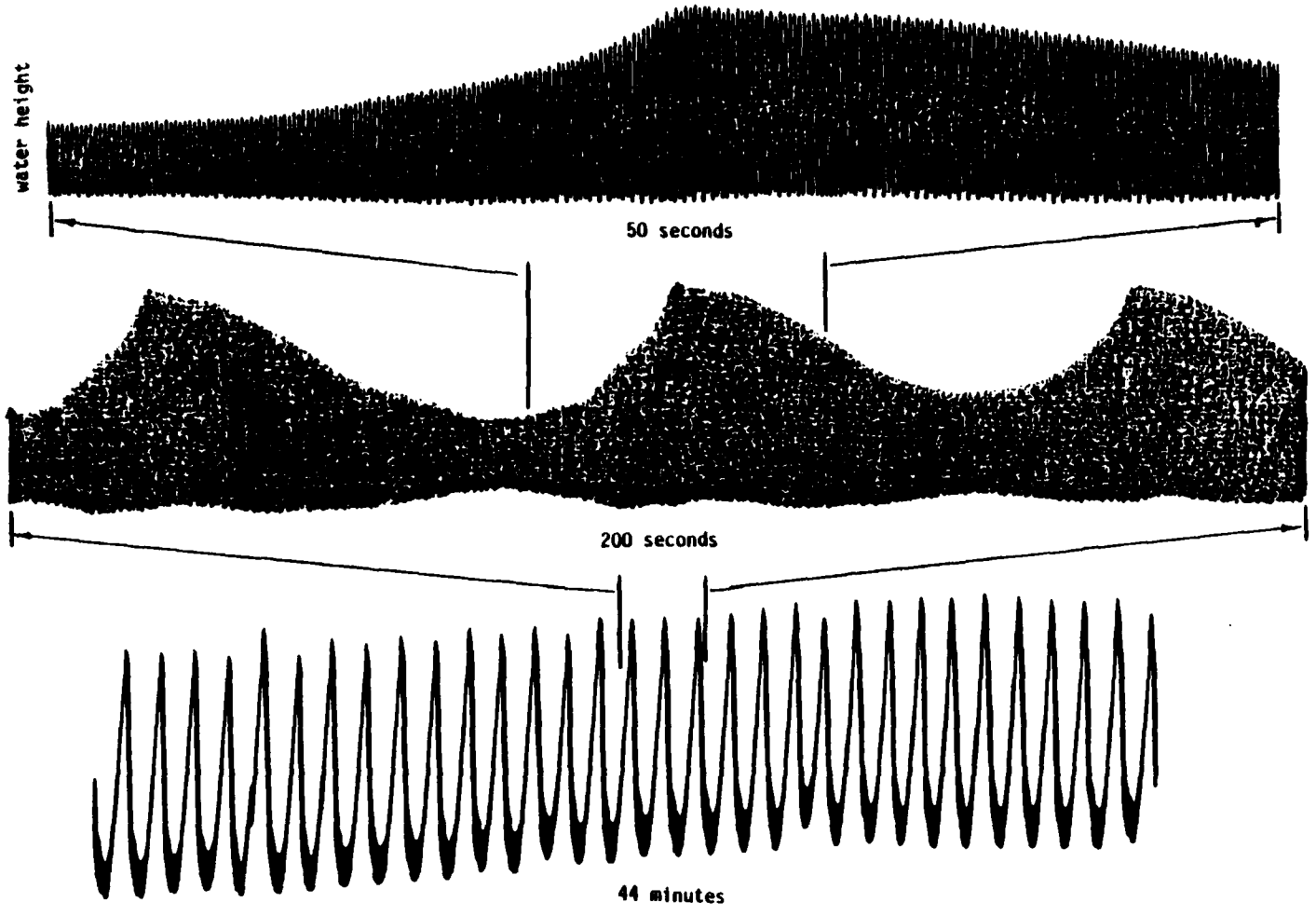


Figure 35. Ultra deep modulation in 5.97 mm of water driven at 11.00 Hz with 429 μm rms amplitude.

fig. 6 in the introduction.

Ultra deep modulations are a distinct behavior. A transition from an ultra deep modulation to a cockscomb is shown in fig. 36, as the temperature of normal helium near 3.89 K drifts upward (which besides increasing its viscosity, increases the equilibrium height and therefore the resonant frequencies of the helium). The opposite transition is shown in fig. 37. One other spurt of modulations occurs in between.

In water, some rather incomplete observations were made of the spatial dependence of the modulations. The observations were made unnecessarily difficult by the annular shape of the resonator, so I concentrated on the water on either side of the barrier. Starting from very low amplitude everywhere in the trough, the amplitude starts to rise on one side of the barrier, say the left, before the other. The amplitude gets quite high on the left side, and quickly drops off along the circumference of the resonator, being negligible on the right side. After a few seconds, the large amplitude appears to penetrate farther around the resonator, so that the water on the right side of the barrier starts vibrating, initially out of phase with the water on the left. There are now an odd number of half wavelengths along the circumference, my recollection is 15 of them when f is 11 Hz. By now the water on the left has risen to nearly its maximum amplitude, but about when the right side's amplitude makes it halfway up, it starts to fall again, then rise again, this time with the vibrations in phase with the water on the left since there are now 14

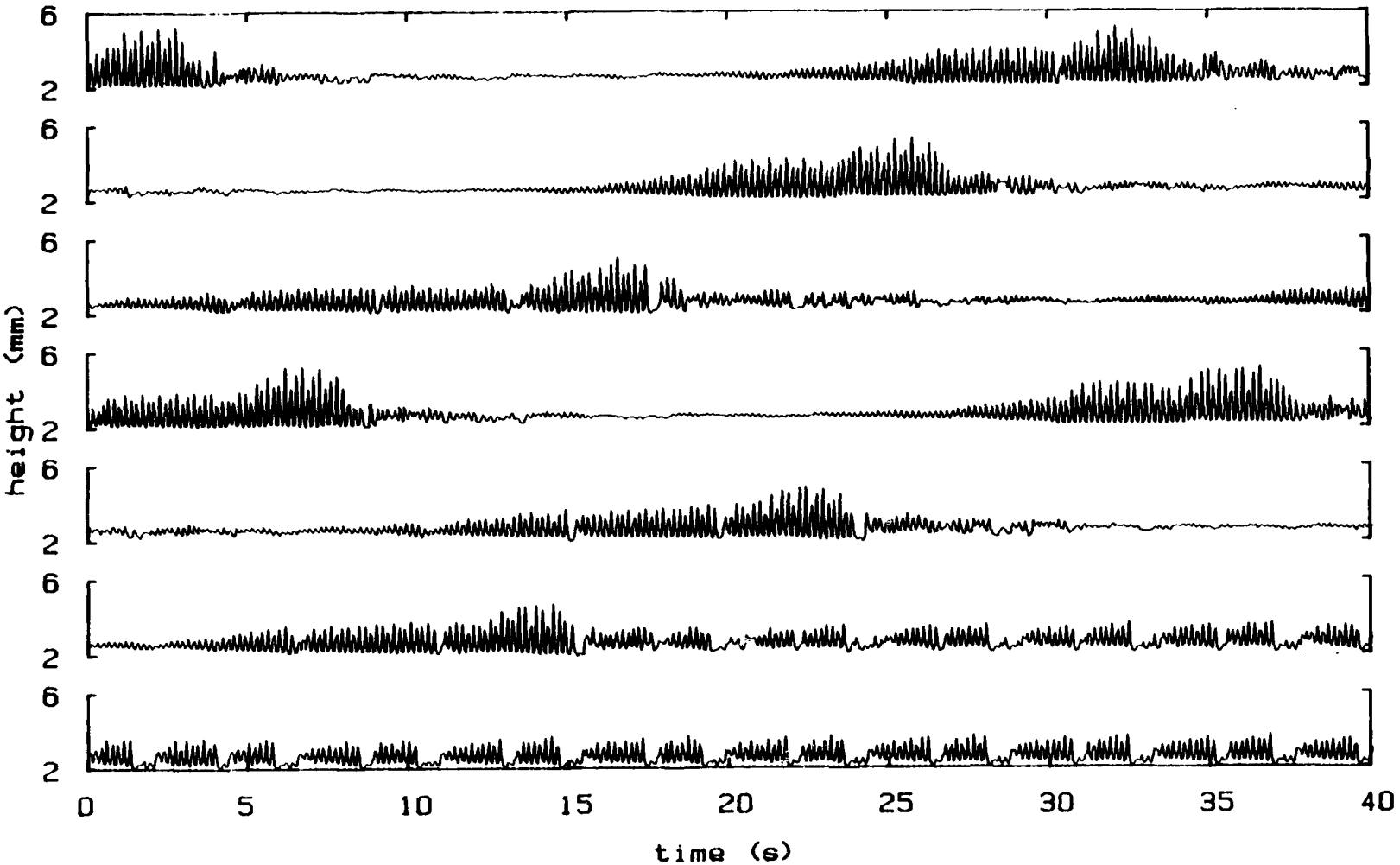


Figure 36. An ultra deep modulation to cockscomb transition in 2.56 mm of helium at 3.95 K, driven at 11.000 Hz with 146 μm rms amplitude.

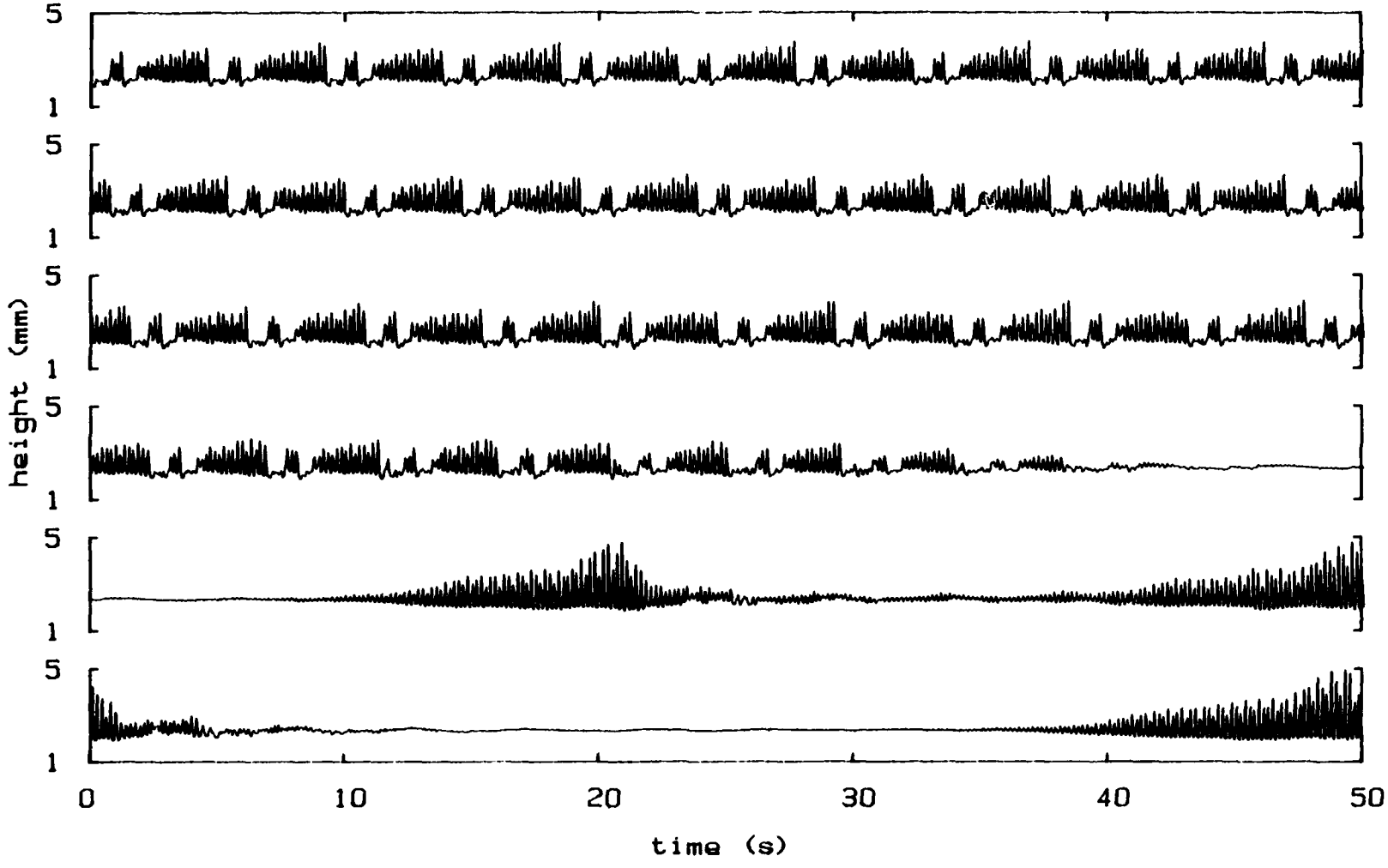


Figure 37. A cockscomb to ultra deep modulation transition in 2.40 mm of helium at 4.04 K, driven at 11.000 Hz with 144 μm rms amplitude.

(if I remember correctly) half wavelengths in the trough. The amplitudes on both side are then at their highest, and the amplitude everywhere in the trough slowly decays to its minimum. The cycle then repeats.

If the drive amplitude is lowered from 429μm to 389μm while f is 11.00 Hz, all f/2 response disappears. If the drive is increased to 450μm, f/2 is regained but without the modulation. If the drive frequency is swept, there is evidence (see p. 149) that the modulations occur in between resonances --at 11.0 Hz, in between the 14th and 15th modes. Thus ultra deep modulations seem to occur at the crossing of the hyperbolas in the drive frequency, drive amplitude plane that mark the thresholds for parametric growth of each mode, as derived by Benjamin and Ursell(1954, without damping) and described in Appendix 2. These ultra deep modulations are probably, therefore, the same phenomena as the "mode competition" seen by Ciliberto and Gollub (1984), which also are slow modulations seen at the crossings of the hyperbolas. Their measurements show that energy oscillates between the two simultaneously parametrically driven modes at the modulation frequency, as is probably happening here for the 14th and 15th modes. Incidently, when the amplitude was raised to 583μm, the water responded with noisy f/14.

The modulations are somewhat like the quasiperiodicity seen in the hanging chain demo described in Appendix 5 which is essentially the spherical pendulum described by Miles (1984 a). A parametrically driven nearly spherical pendulum with the two modes' degeneracy broken

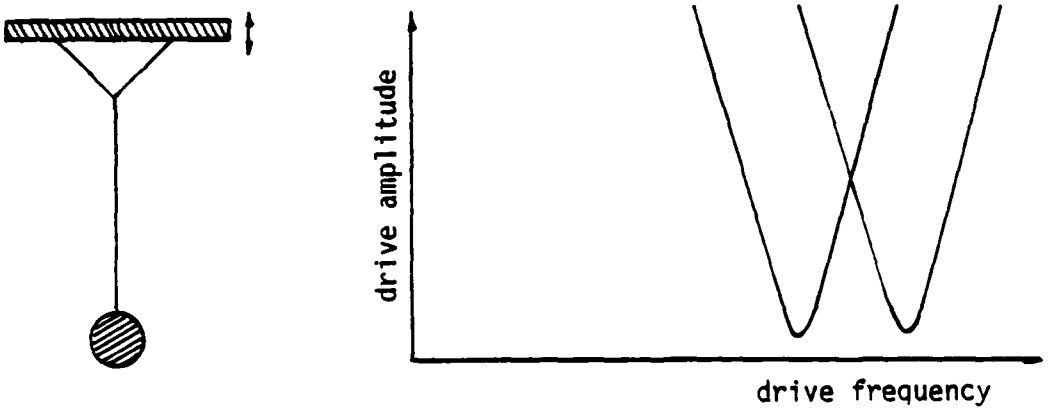


Figure 38. Possible model of ultra deep modulations. A parametrically driven pendulum swings from its support out of the page, and from the knot in the page. At infinitesimal amplitude, the instability hyperbolas for each mode cross.

as in fig. 38 is probably an even closer model of the situation. Identifying the modulations in liquids as occurring at the crossing of the hyperbolas and making the connection to the pendulum is another loose end for the future.

Bursts. After seeing the waveform of fig. 35, I let the experiment run overnight. When I got back, the drive amplitude had drifted down slightly to 402μm and the bursts of f/2 shown in fig. 39 had been recorded. Perhaps it was a bit of external noise or slight increase in the drive amplitude that triggers a burst after a long stretch of quiescent time. This figure suggests that the modulation is a series of these burst, and that the natural starting point of the cycle is the minimum of amplitude, much like the chain demo of Appendix 5.

Speculations. Where do the very long times come from? That they occur near the threshold for f/2 offers a clue. A parametric drive gives exponential growth that adds to the negative growth from viscosity, as explained in Appendix 2. Near the threshold they nearly cancel and the characteristic times become long. The modulation might come from periodic switching between two states, one just barely growing and the other just barely decaying. An old idea was that the two states were related to the two stable states of a bent tuning curve, described in Appendix 1. This led to the measuring of tuning curves with a direct drive, which is the subject of the next section. However, this idea points to the modulations being a property of one mode, and the evidence points to it involving two -- but I cannot rule

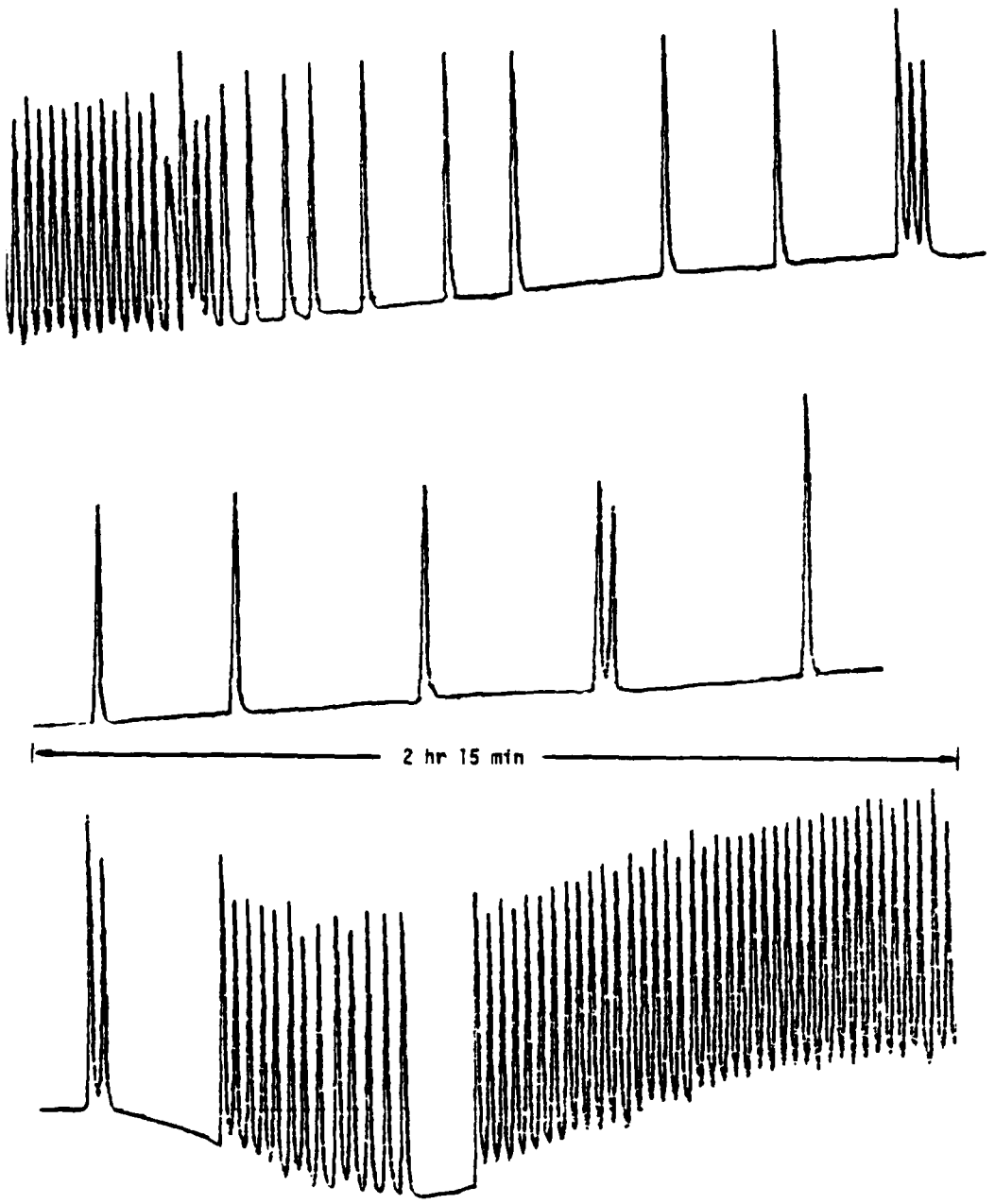


Figure 39. Bursts of amplitude. This is a continuous record.

anything out. This is another loose end.

Another vague fragment of an idea: Perhaps the very long times in the ultra deep modulations come from weak nonlinear coupling. One can think of modes as mechanical oscillators. If the coupling between them is linear, energy can be transferred back and forth between them -- the weaker the coupling the slower the beating -- but one can find the new normal modes (by intuition or diagonalizing a matrix) to use as a basis for description which are like two decoupled oscillators. If the modes themselves are nonlinear, it is useful to think that the resonant frequency becomes a function of amplitude and the tuning curves bend, as described in Appendix 1. Harmonics are present in the response, but maybe they are not important. If the coupling between the modes is nonlinear there is again energy transfer between modes, but if the nonlinearity is weak the energy transfer is slow. Perhaps it is unimportant that the forces between the modes are not sinusoidal; only the net energy transferred over a cycle matters. Then it seems that weak nonlinear coupling would mimic weak linear coupling which gives very slow beating between normal modes. The smaller the amplitude, the weaker the effective coupling, and the slower the beating. There is a lot, though, that I do not understand, like, why would they beat?

## Section 7. Subharmonics and Quasiperiodicity in a Paddle Driven Trough.

### 7a. Data.

Bent tuning curves. After seeing the ultra deep modulations in the annular resonator, we wondered if they were perhaps due to some sort of switching between the two stable states that are possible when tuning curves are bent enough. Bent tuning curves are discussed in Appendix 1. In order to see if the tuning curves for directly driven surface waves bent enough to have two stable states, and if so, which way, waves were driven in the apparatus shown in fig. 40. It should be pointed out that the paddle drives the waves directly, not parametrically, and so response is expected at the same frequency f as the drive. The trough is made of Plexiglas, is 18.4 cm long, 2.5 cm wide, and 5 cm high, and has a paddle 1.3 cm from one end. A shaft epoxied to a loudspeaker drives the paddle. The paddle is made of sheet brass available at hobby stores. Because it fit the trough reasonably well, the paddle was able to drive waves that were so large that they would break, much as they do in the ocean. The third mode is shown breaking in (b) (and the paddle is shown on the opposite side of the trough). It was rather enjoyable to watch the waves slowed down with a strobe light.

Two tinned copper wires that dip into the water detect the height of the surface at the far end of the trough. The conductance between them is proportional to the surface height. Various bridge circuits

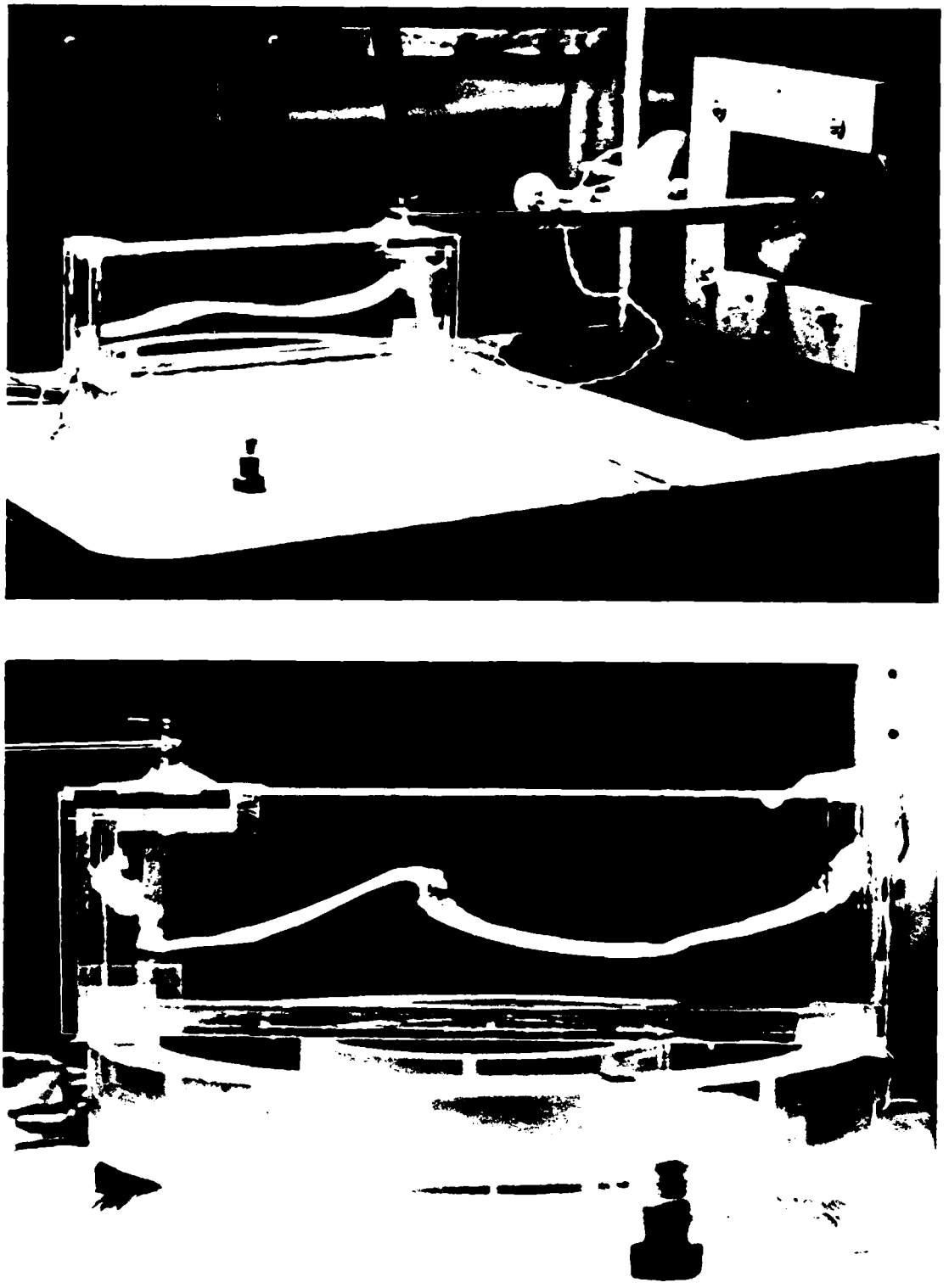

Figure 40. Paddle driven trough driving the third mode.

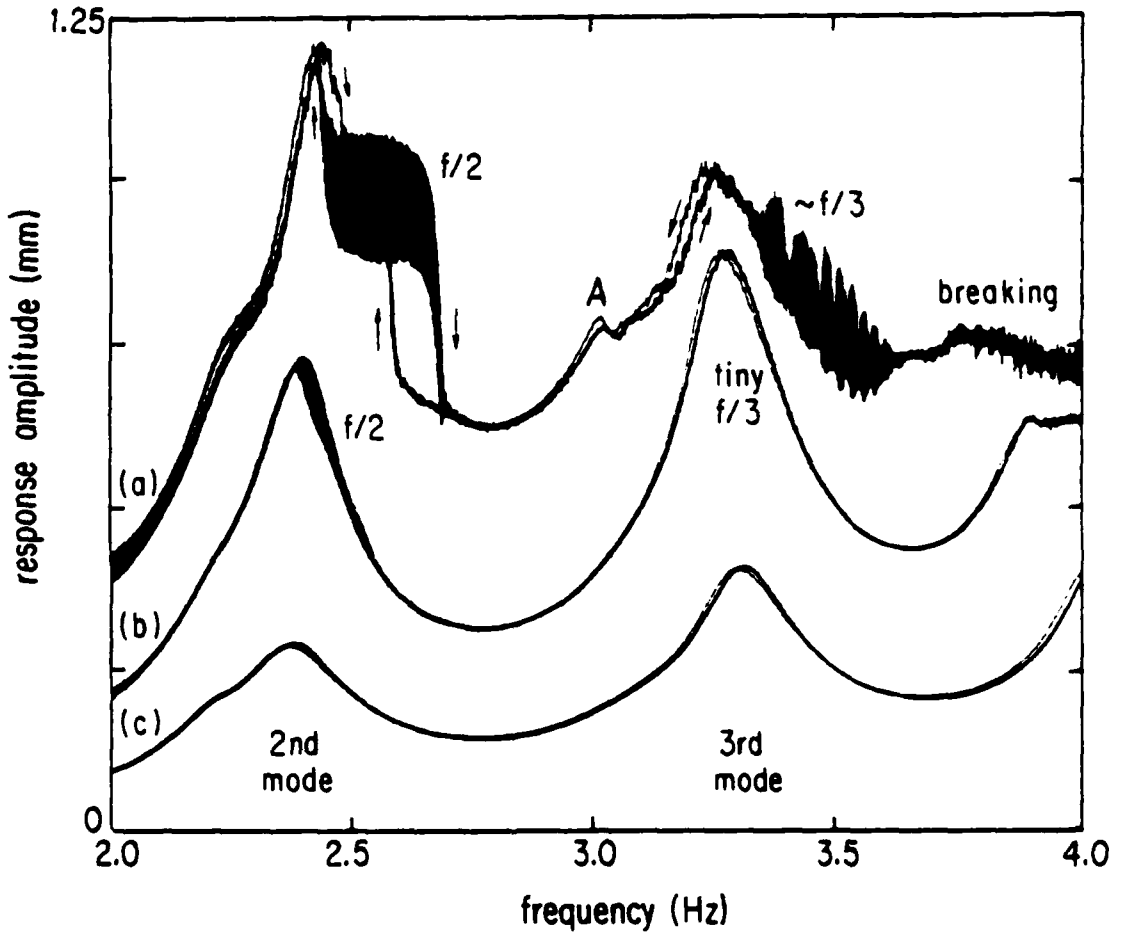


Figure 41. Tuning curves near the second and third modes. The paddle is driven with (a) 1.250 V, (b) 0.625 V, and (c) 0.3125 V.

measured the conductance with enough sensitivity that it was no longer necessary to lace the 200:1 water/Photo-Flo solution with salt. The output of a lock-in amplifier, which follows the bridge, reproduced the surface height vs. time. In addition to being watched on an oscilloscope and FFT analyzer, the absolute value of this signal was filtered with a 1 second time constant to detect the amplitude of the wave. This amplitude is plotted vs. drive frequency as the frequency is swept up and down for various drive amplitudes to obtain the tuning curves of fig. 41.

There were several unexpected features. First, the tuning curves did not bend much at all before the wave broke. The turbulence, which was localized to the steepest part of the wave, causes the amplitude measured at the transducer to be unsteady in time and the tuning curve to have a ragged appearance. The transition to breaking is seen at point A. Likewise, breaking can be seen in the second mode at the highest drive level, and in the fourth mode at the highest and intermediate drive level. At these high amplitudes, though, the second mode bends only slightly to the right, and the third bends slightly to the left; the curves are not even close to showing two stable states. Why did they bend so little and in opposite directions? It turns out, according to Larraza and Putterman (1984) and Miles (1984 b) that the nonlinearity changes from hardening to softening as kh increases past 1.02. By chance, this value lies between the second and third modes. Wu and Rudnick (1985) measure the crossover to occur at 1.0.

Subharmonics at f/2 and f/3. The features that are most prominent are the wide bands to the right of the second and third modes. These are due to another type of subharmonic and quasiperiodic response, that led to a meager understanding of cockscombs in terms of a conspiracy theory, discussed in the next subsection.

First for comparison, the voltage driving the paddle, shown as the lower trace of fig. 42(a), drives the second mode with frequency f of 2.35 Hz. The response, shown in the upper trace, is also at f. A "phase space" for the surface, the response vs. its time derivative, is shown in (b). The extra little wiggle in (a) causes the small loop in (b). At a higher frequency (c) of 2.55 Hz, the surface responds at f/2 (compare with the drive voltage) --every other cycle becomes smaller and delayed, and the phase space plot (d) splits into two loops. This causes the band to the right of the second mode in fig. 41. The width of the band reflects the difference in amplitude of every other cycle of the response. Similarly, the response is f/3 to the right of the third mode when the drive level is reduced. At the same high drive level, the response over a short time looks just like f/3, as shown in fig. 42(e) and (f), but actually it is a bit different.

Braiding. An interesting thing happens to f/3 at higher drive levels --the loci of the extremum look like they are braided; one braid is shown in fig. 43. Every so often, the large heap becomes the middle sized one, the middle one becomes the small one, and the small one becomes the large one. Notice how the loci of the extremum appear

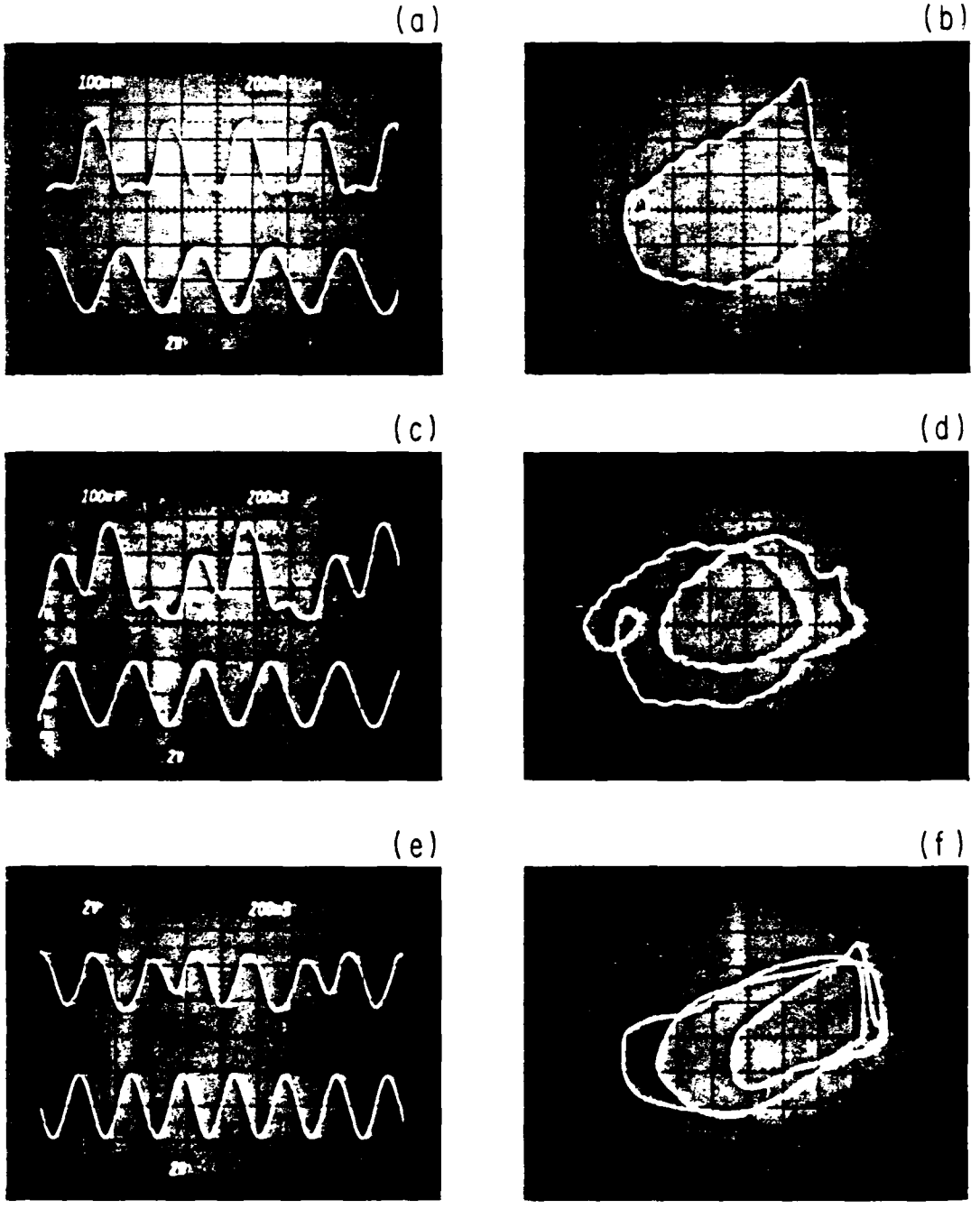


Figure 42. Response at f, f/2, and (nearly) f/3 when the paddle is driven with 1.250 V at 2.35 Hz, 2.55 Hz, and 3.41 Hz.

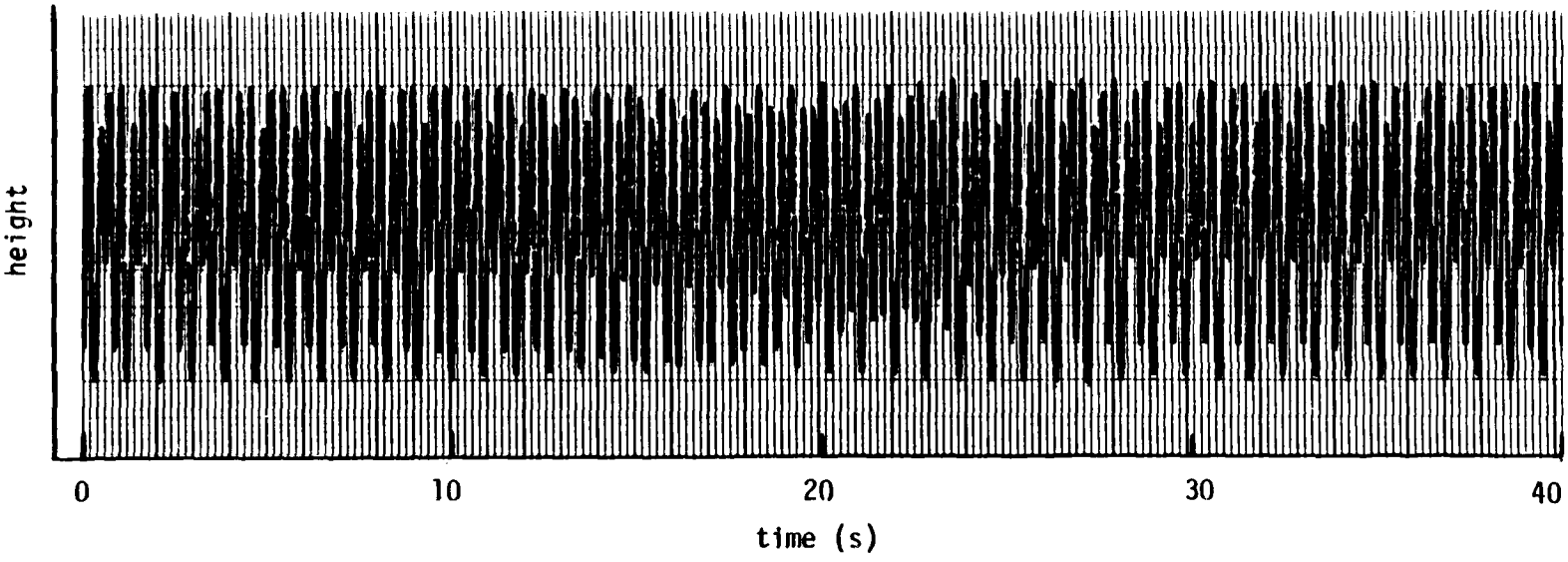


**Figure 43. A braid of f/3 in the paddle driven trough.**

to exponentially approach the transition. Each of the dips in the band to the right of the third mode in fig. 41 is a braid.

The time between the transitions can either be regular or erratic to the eye. I made a return map for the erratic transition times (return maps are discussed on p. 112) but there was not enough data to show much structure.

Another way of thinking about braiding when it occurs with periodic transition times is that it is a modulation with frequency $f_m$ near f/3 that is not quite phase locked onto f. It is another quasiperiodic phenomena. Quasiperiodicity is discussed on p. 109, and phase locking is discussed in Appendix 4. During a transition the modulation slips in phase with respect to the drive; it leads f/3 by one cycle of f. Thus $f_m$ is $f/3+\varepsilon$, with $\varepsilon>0$ where I explored. Perhaps the physics of braiding is similar to that of the smooth modulations of Sec. 8; perhaps not. This is yet another loose end.

(An experimental point for paddle builders: The shoulder on the left side of the second mode in fig. 41, and at other frequencies not shown, was due to water escaping from below the paddle, twice per cycle, because the paddle moves in an arc and the bottom of the trough is flat. This drove the fourth mode at twice the drive frequency. The problem was later corrected by putting a round bottom below the paddle and making the paddle thicker which effectively isolates the water on either side.)

7b. Conspiracy theory.

The subharmonics in the paddle driven trough can be understood qualitatively in terms of a "conspiracy theory." It goes like this:

Consider driving the trough near its second mode. If the wave had small amplitude it would have two height nodes as shown in fig. 44(a). But, at higher amplitudes, the troughs of the wave broaden and the crests compact, so that the wave has more the appearance of two heaps of water traveling back and forth. One cycle is shown in (b). The nodes partially disappear; there is no part of the surface that remains motionless. The anti-nodes become the places where the heaps meet and add: at center of the trough, and at the ends where they meet with their own reflections.

Let's consider, now, how these heaps interact. Each feels the influence of the other through two competing effects. First, one heap locally raises the water level for the other where they meet, which, for other than the deep water limit, locally increases the wave speed. This shortens the round trip time for the heaps, increasing the nonlinear resonant frequency for the second mode. Second, when a pulse of water travels on a surface, water moves from the back of the pulse to the front giving the fluid a velocity in the direction of propagation of the heap. When the two heaps meet, each presents a fluid velocity in a direction opposing the motion of the other. They slow each other down through the Doppler effect, increasing the round

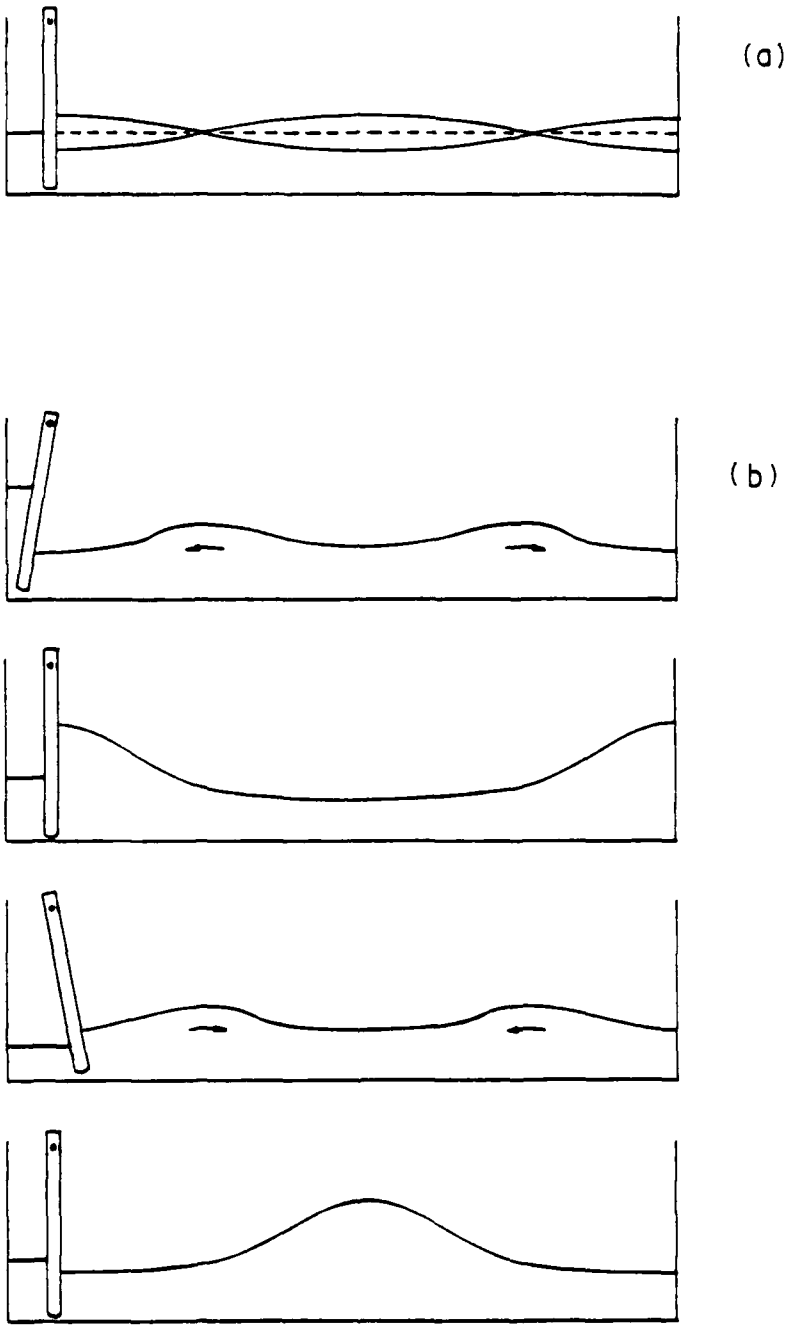


Figure 44. The shape of water in the trough; (a) at small amplitudes, (b) at larger amplitudes.

trip times, decreasing the nonlinear resonant frequency for the mode. I claim this effect dominates the first, for no good reason other than it explains what I see.

As in the small amplitude case, the paddle delivers the most energy if it is phased to move forward while the water is at its highest, maximizing the product of the force on the water with the paddle's velocity. If the trough is driven at a frequency slightly above the second resonance, however, the paddle completes a cycle before the heaps have had time to fully complete a round trip. The amplitude of the heaps suffers because the phase of the heap's arrival lags behind that of the forward motion of the paddle. Now, consider what happens if one heap should become slightly larger than the other, due to a fluctuation. The large heap slows the small heap more that the small heap slows the large. The small heap lags behind the paddle more than it did, is less able to draw energy from the paddle, and so, becomes even smaller. Meanwhile, the large heap is delayed less, becomes better phased with the drive, and so grows even larger. With the right conditions two heaps of the same size are unstable; they spontaneously split into a large and small one, as in fig. 42(c), causing the f/2 subharmonic.

Below the second resonance, the small heap would be better able to take energy from the drive if delayed, and the large heap would not. A split in the relative size of the heaps decreases at these frequencies, which is why the subharmonic occurs to the right of the second resonance. It is interesting to note that because of

dispersion, twice the frequency of the first mode is also to the right of the second mode. The subharmonic occurs when its component at f/2 is in resonance with the fundamental mode of the trough.

The small heap can be seen becoming more and more delayed as it grows smaller and smaller, and the opposite occurring to the large heap, by watching the subharmonic develop on the oscilloscope; the final results were already shown in fig. 42. More directly, this delay mechanism can be seen by video taping the trough, playing the tape back frame by frame, and plotting the positions of the heaps and paddle vs. time as in fig. 45. The large heap, represented by circles, leaves the paddle while the paddle is moving forward, which is the optimal phase for transferring energy, and completes a round trip in time to meet the paddle again. The small heap, represented by triangles, only makes it halfway back by the time the paddle moves forward again -- the paddle then creates another fresh small heap. Unlike what occurs with the large heap, the old and new small heaps do not constructively interfere, so the small heaps stay small.

The same idea probably applies near the third resonance where there are now three heaps. Two of them conspire to keep the third one delayed and small. The rich get richer and the poor get poorer.

Elements of this conspiracy theory might work towards understanding the parametrically driven cockscombs of Sec. 5. The cockscombs can be thought of as a traveling collection of heaps that winds along the circumference of the annulus, reflects off the

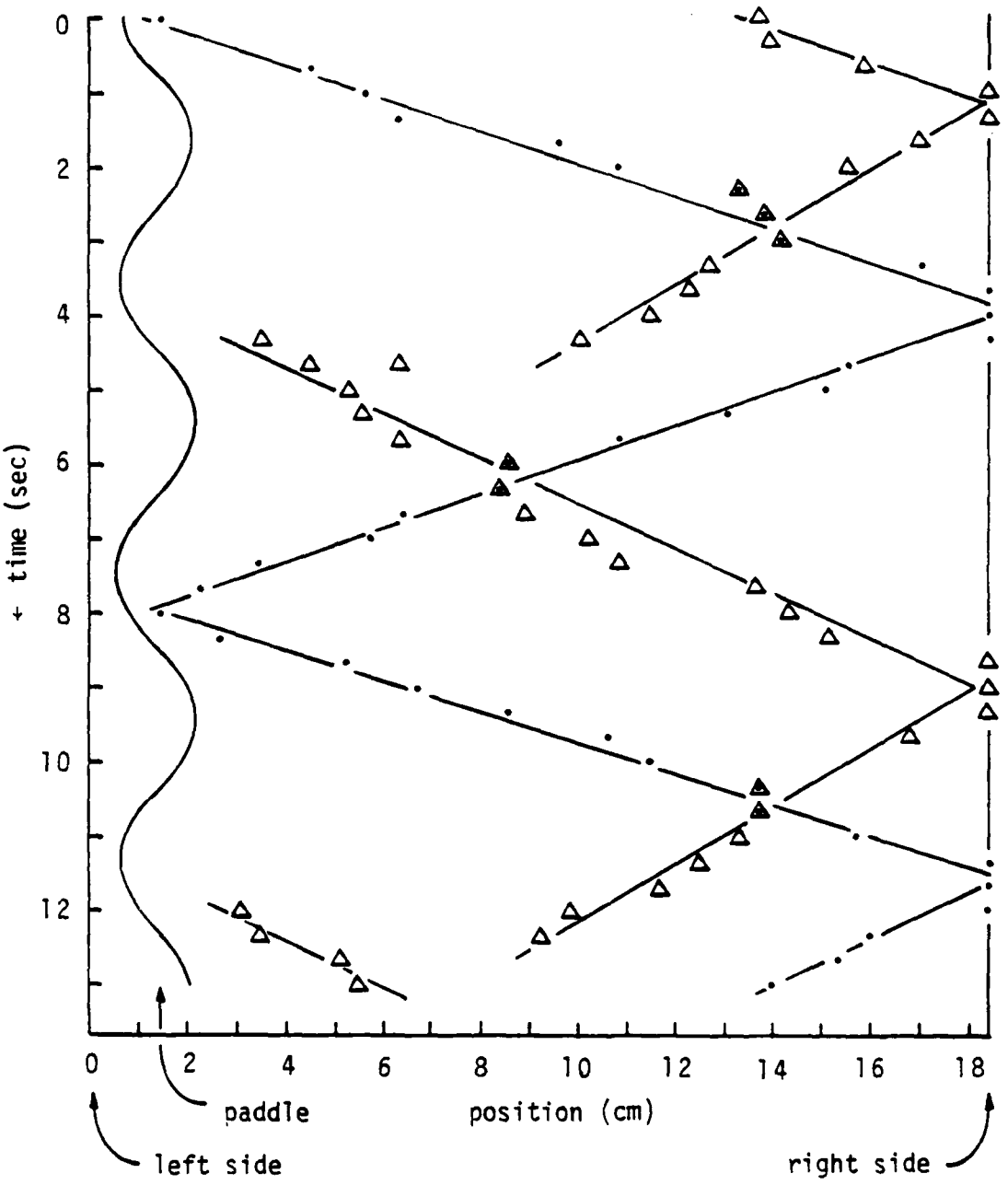


**Figure 45. Trajectories of the large heaps (circles) and small heaps (triangles) during f/2 subharmonic. Straight lines are guides to the eye.**

barrier, and passes through itself on the way back. Each heap interacts in turn with all the other heaps, including itself when it reflects off either side of the barrier. A pair of heaps passing through each other can best absorb energy from the oscillating trough if their juncture occurs at the proper moment -- when the trough's acceleration changes sign from down to up (pp. 3 and 191) -- so again, the flow of energy into a heap is sensitive to the delays it suffers from all the other heaps.

Consider for example the smallest heap as it reflects off the barrier. It has been considerably delayed by all the other heaps (which barely felt its influence) so that it mounds up on the barrier too late to gain energy from the drive. It therefore stays small. (The barrier is not critical, though; cockscombs were seen early on without it.) This delay can be easily seen in most cockscomb waveforms -- fig. 25 on p. 67, for instance. At the sudden drop, note that the time between the small heap and the previous large one is quite a bit longer than the time between any of the larger heaps.

## Section 8. Smooth Modulations.

### 8a. Smooth modulations in helium, and quasiperiodicity.

The forth major type of behavior seen during these experiments is being called "smooth modulations" because, as can be seen in fig. 46, the envelope of the f/2 measured at the barrier smoothly rises and falls, unlike the cockscombs which rise and fall suddenly. However, smooth modulations and cockscombs share a feature not found with ultra deep modulations -- they occur at frequencies near that of the lowest mode of the trough.

Smooth modulations were seen principally in superfluid helium because they appear to be the preferred instability in troughs of high Q driven with low amplitude, but they occur in normal helium and water as well. Thus the modulation is not a superfluid effect.

The most striking feature of the modulation is that the ratio of the drive frequency f to the modulation frequency $f_m$ is seldom an integer, nor even a rational number formed by the ratio of small integers, but rather (with a stretch of the imagination) an irrational number. This implies that the motion never repeats, and precludes any understanding of the mechanism in terms of subharmonics (as in Landau and Lifshitz, Mechanics, 1976, pp. 90-92, or Marion, 1970, p 171).

The spectrum shown in fig. 47 results from digitizing the

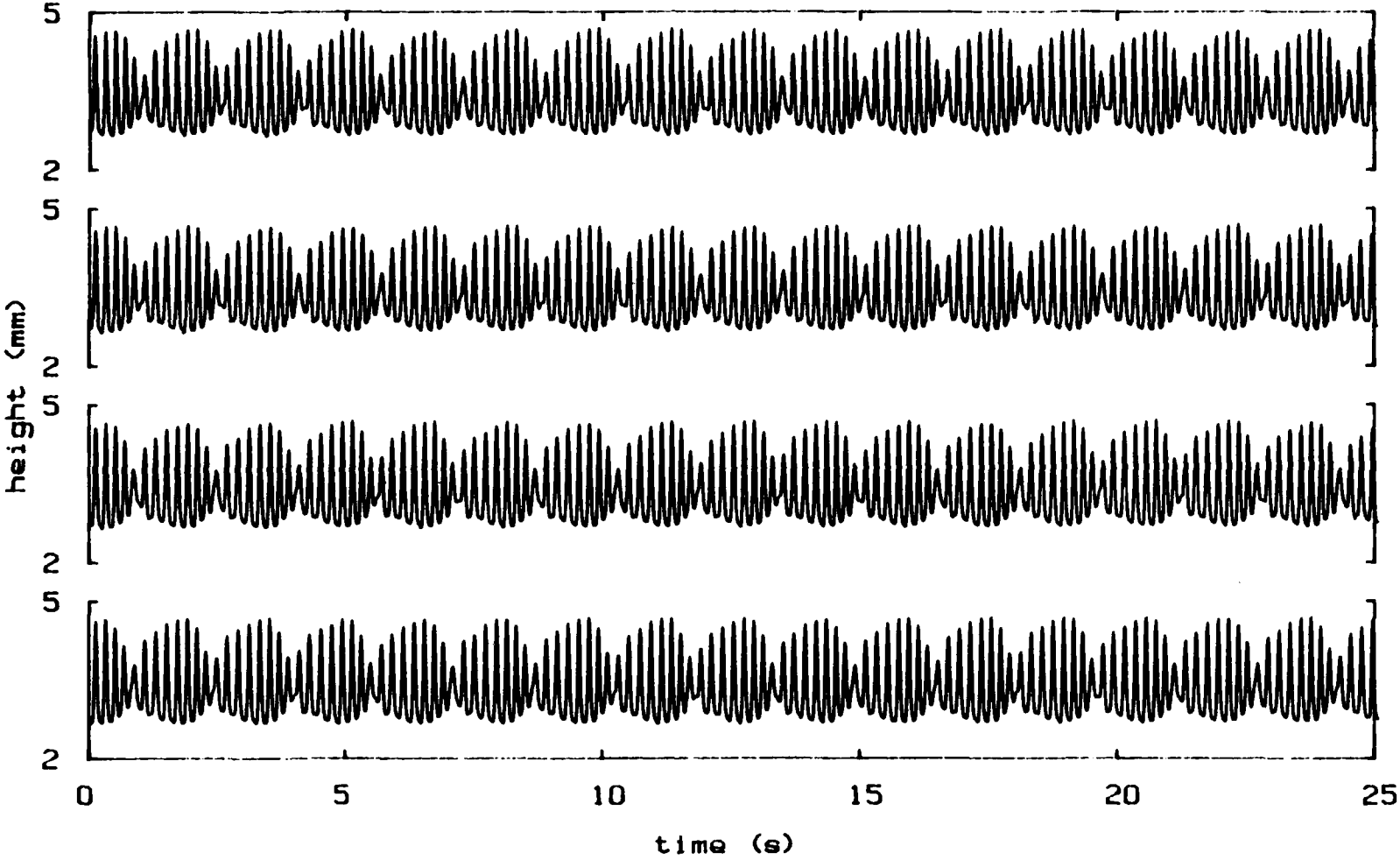


Figure 46. Smooth modulation in 3.47 mm of helium at 3.21 K. The trough is driven at 10.000 Hz with 24.8 μm rms amplitude.

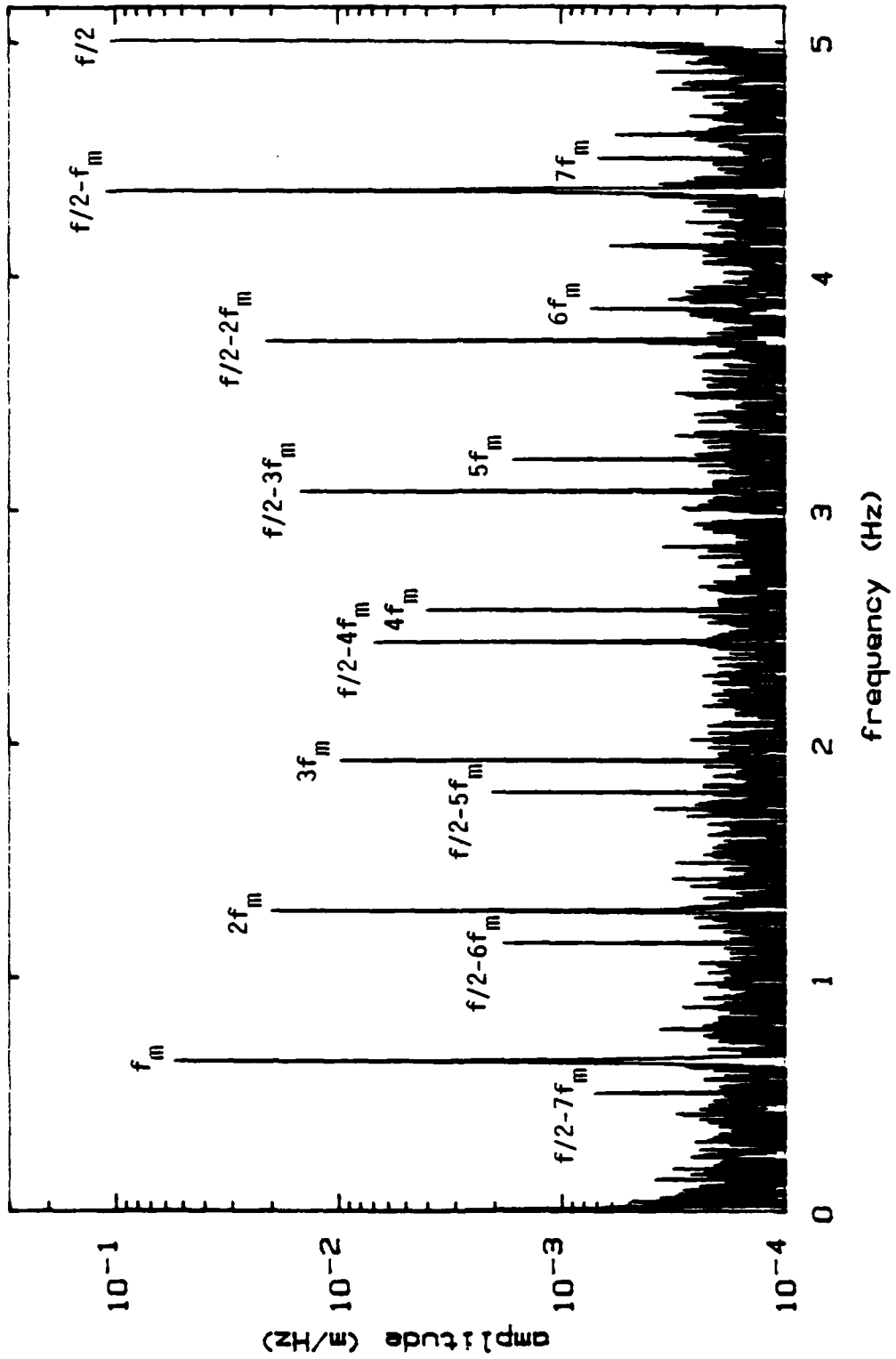


Figure 47. Spectrum of the smooth modulation of the previous figure.

previous waveform over a longer time (8192 points taken at the drive frequency of 10 Hz), and gives the ratio of the frequencies $f/f_m$ as 15.570. A series of peaks -- $f_m$ and its harmonics, $2f_m$, $3f_m$ ... -- extend from low frequency, while a similar series -- f/2 and the difference frequencies, $f/2-f_m$, $f/2-2f_m$ ... -- extend down from high. Had the modulation been a subharmonic of f/2, the two sets of peaks would lie on each other, but clearly they do not. The FFT suggests that $f_m$ is independent of f. Knowledge of both f and $f_m$ is sufficient to determine the frequencies of all the major peaks.

That the ratio $f/f_m$ is not the ratio of small integers is shown by constructing a return map, fig. 48. It is constructed by sampling the surface height at a frequency of f/2 (which in this case is every other point in the time record) and plotting one sample $x_n$ versus the previous sample $x_{n-1}$. Had the motion repeated after a certain number of samples there would have been as many distinct dots, but instead there is essentially a continuous line. The phase of the modulation smoothly slips with respect to the drive so that the motion, although regular, never quite repeats.

Of course, any number a computer generates must be rational, but one does not have to stretch the imagination much to suppose that if the waveform could be measured for an infinite amount of time, the ratio $f/f_m$ would be found to be irrational. A more definitive test is to see the ratio change smoothly as a parameter does the same. This is shown in conjunction with cockscombs on p. 165. Nonlinear dynamicists like to call the presence of irrationally related

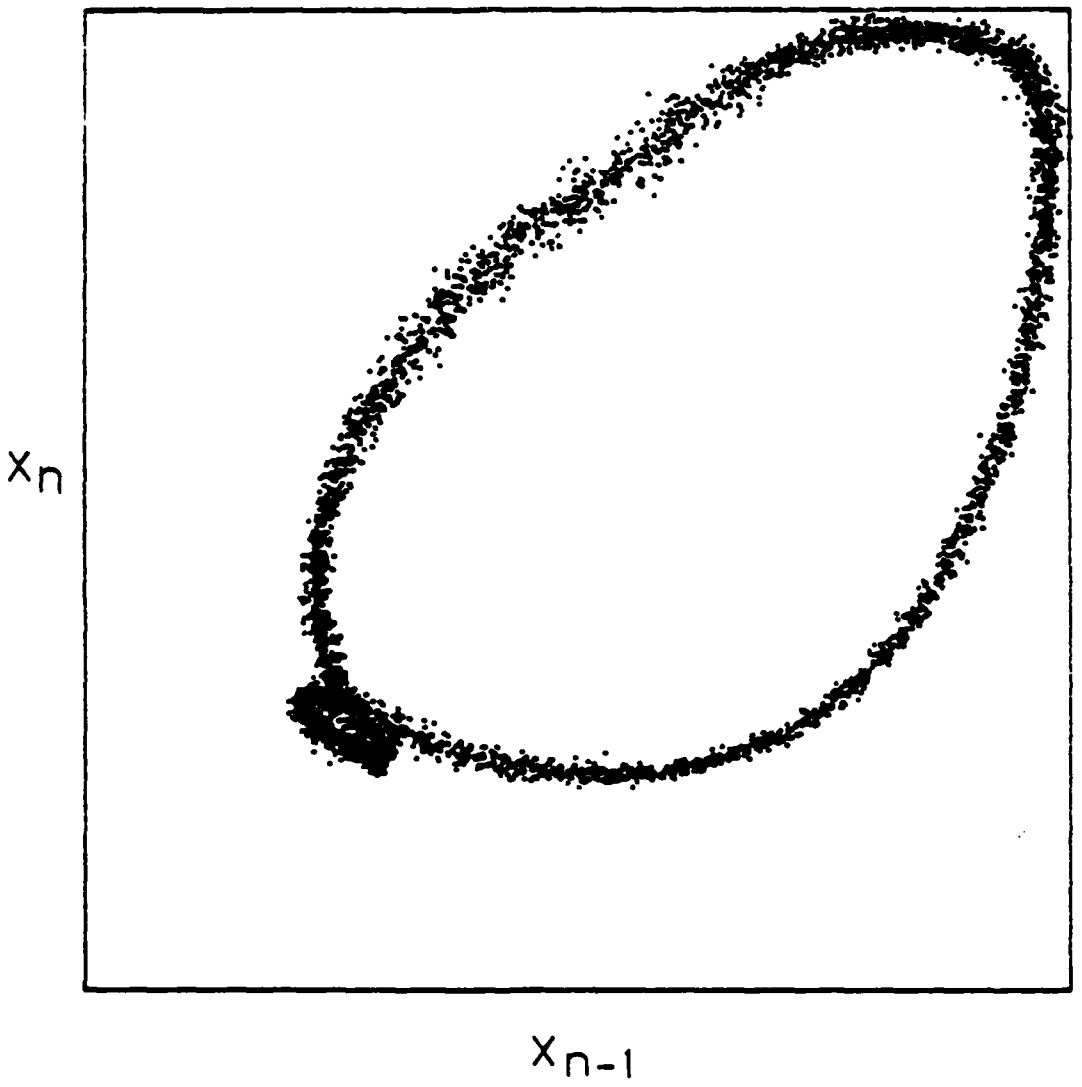


Figure 48. Return map of the smooth modulation of the previous two figures.

frequencies "quasiperiodicity," although double or multiple periodicity would be a better name, and the transition to this state from steady f/2 a "Hopf bifurcation."

Such quasiperiodic response is surprising (to me at least) as one might expect the same response for each cycle of the drive. The drive is still needed to supply energy, but it is the system that determines the frequency of the modulation, as if it had a mind of its own. This is not unheard of -- an electronic signal generator takes energy at 50 or 60 Hz and converts it to any frequency dialed -- but it is curious that hydrodynamics can do the same.

The amplitude of the drive in the helium experiment could be swept up and down by the computer while the drive frequency is held fixed (see p. 61 for details). In the data to be presented next, the amplitude was incremented every five seconds to rise at a rate of 7.00 nm(rms)/second. Every micrometer of rms amplitude, the sweep was halted to take a time record and store it on floppy disk, after which the sweep resumed. After the amplitude reached a maximum value, it was similarly swept back down to check for hysteresis and repeatability. The time records are 4096 samples of the surface height at the barrier taken at a frequency of 4f, commensurate with the drive, along with the values of various experimental parameters. While this is going on, the envelope of the waveform on a one second time scale is recorded on a strip chart recorder (p. 57) so that long term behavior and the values of various thresholds can be monitored. This business, by the way, is the hard part of the thesis.

Figure 49 shows the location of three sweeps in the parameter space of drive frequency and drive amplitude. The other two parameters where held constant: the temperature at 1.22K, and the equilibrium height at 4.20 mm. The hyperbola is the calculated threshold for parametric growth of the 15th mode at zero response amplitude (Benjamin and Ursell, 1954, supplemented with damping, as in Appendix 2) -- but decreased by a factor of $10/(2)^{1/2}$ to agree better with the measured thresholds of f/2. It might be that the drive levels in these sweeps were actually higher than are presented here by this factor. This might have been caused by an incorrectly set knob, but there is no way of telling now. (This does not seem to be a problem in the data to be present later in Sec. 9.) Other explainations are possible. Without being able to see into the dewar, it is easy to make a mistake.

With this caveat, just above 3.4 μm rms, the surface responds at f/2 as expected for parametric resonance (described further in Appendix 2 and Sec. 9). Figure 50 shows a time record, FFT, and return map for f/2. The return map can be idealized as a single point which can be thought of as an "attractor" of dimension 0; nearby initial conditions off this point converge onto it as the steady state is approached.

Above 4.4 μm, the smooth modulation appears, as shown in fig. 51. The oscillations inside the envelope, which looks like a string of sausages, remain at f/2. The ratio $f/f_m$ here is $34.55 \pm 0.03$ measured

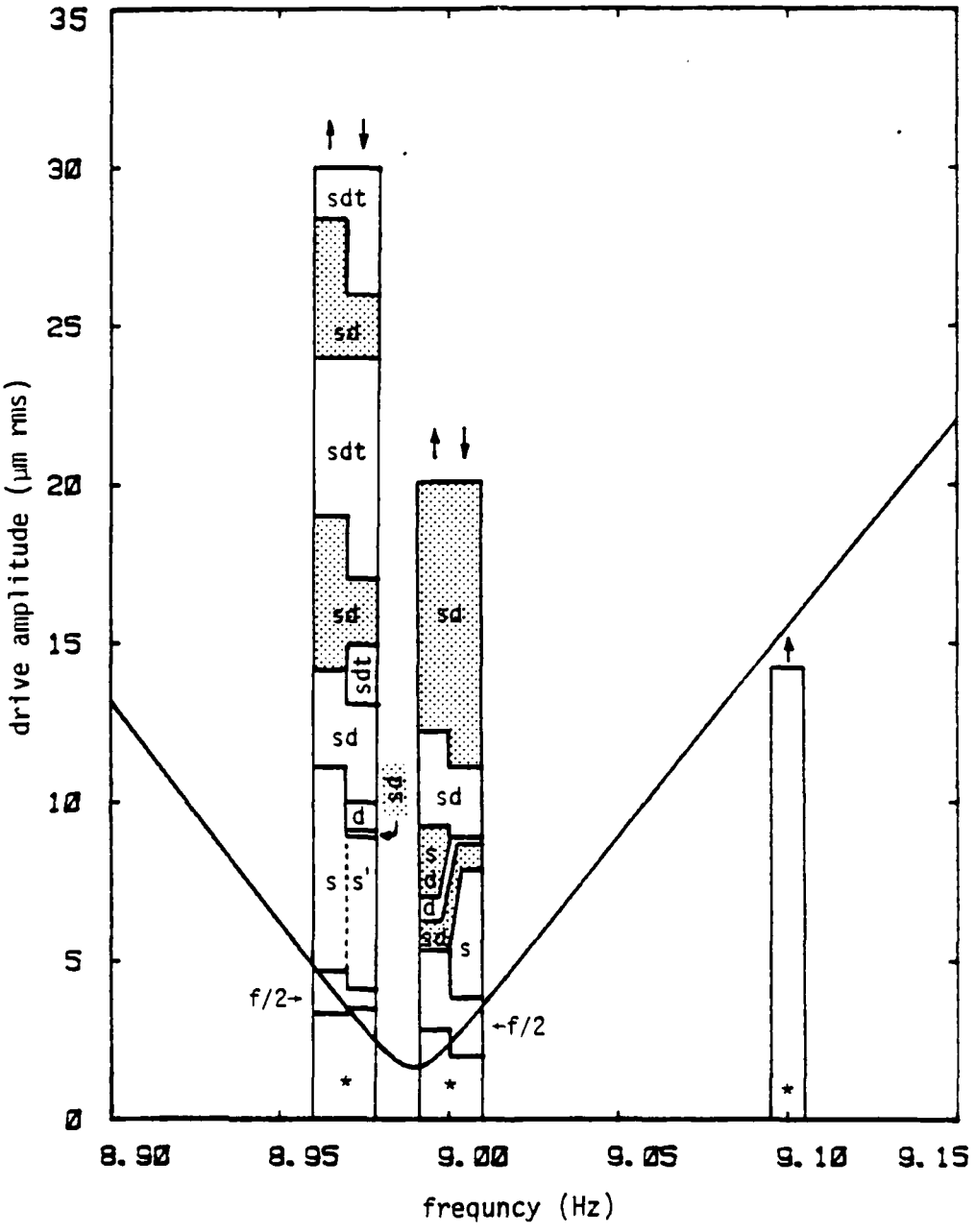


Figure 49. Three drive amplitude sweeps at 8.970 Hz, 9.000 Hz, and 9.100 Hz. Arrows show the directions. Single, double, and triple sausaged smooth modulations are denoted by s,d, and t. Shaded regions mark where modulations phase locked. The s' refers to a single sausaged modulation with slowly oscillating amplitude; * refers to negligible response.

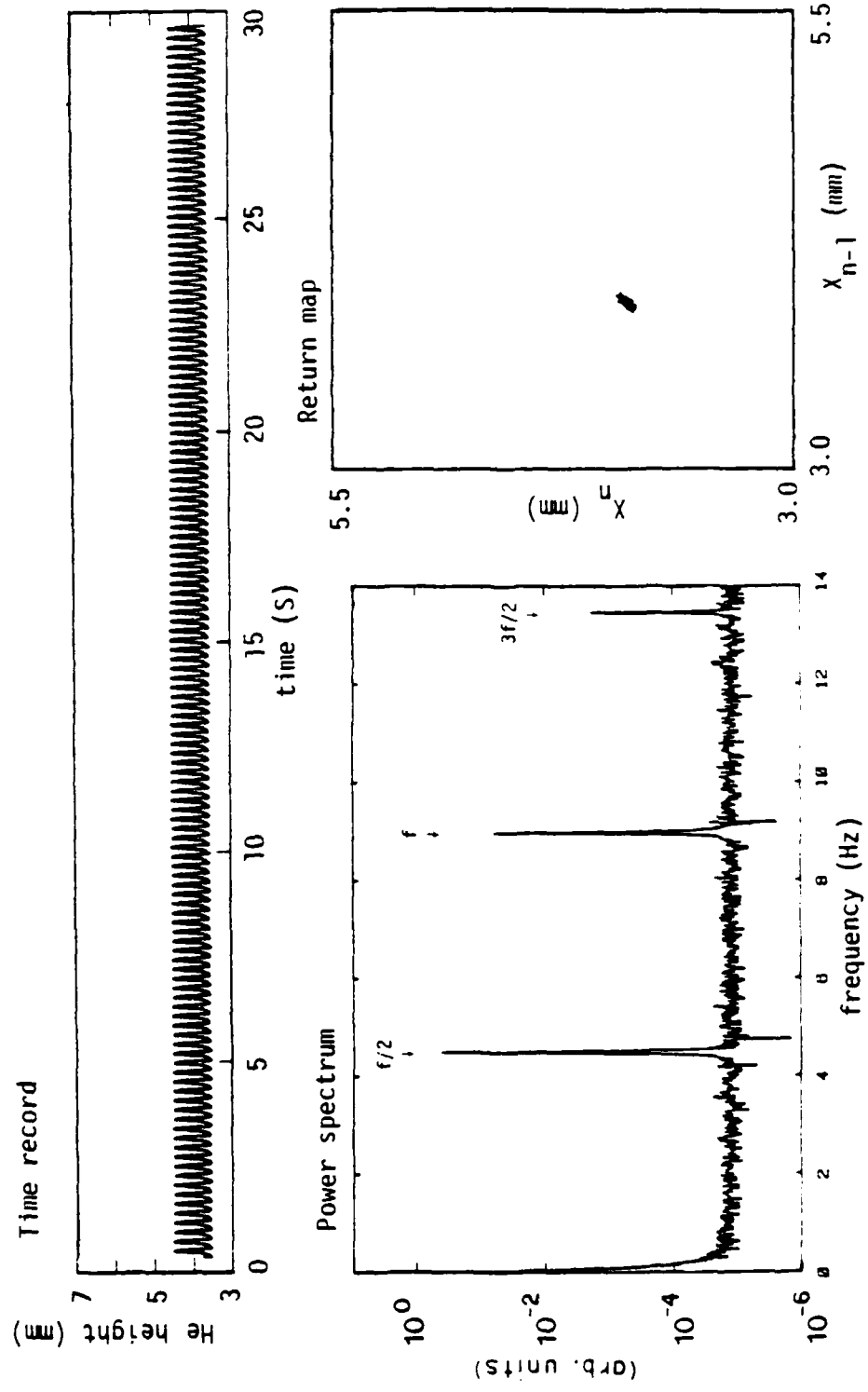


Figure 50. Steady f/2 with 3.8 μm rms drive amplitude. The parameters 8.97 Hz, 1.22 K, and 4.19 mm are held constant for this and the next seven figures.

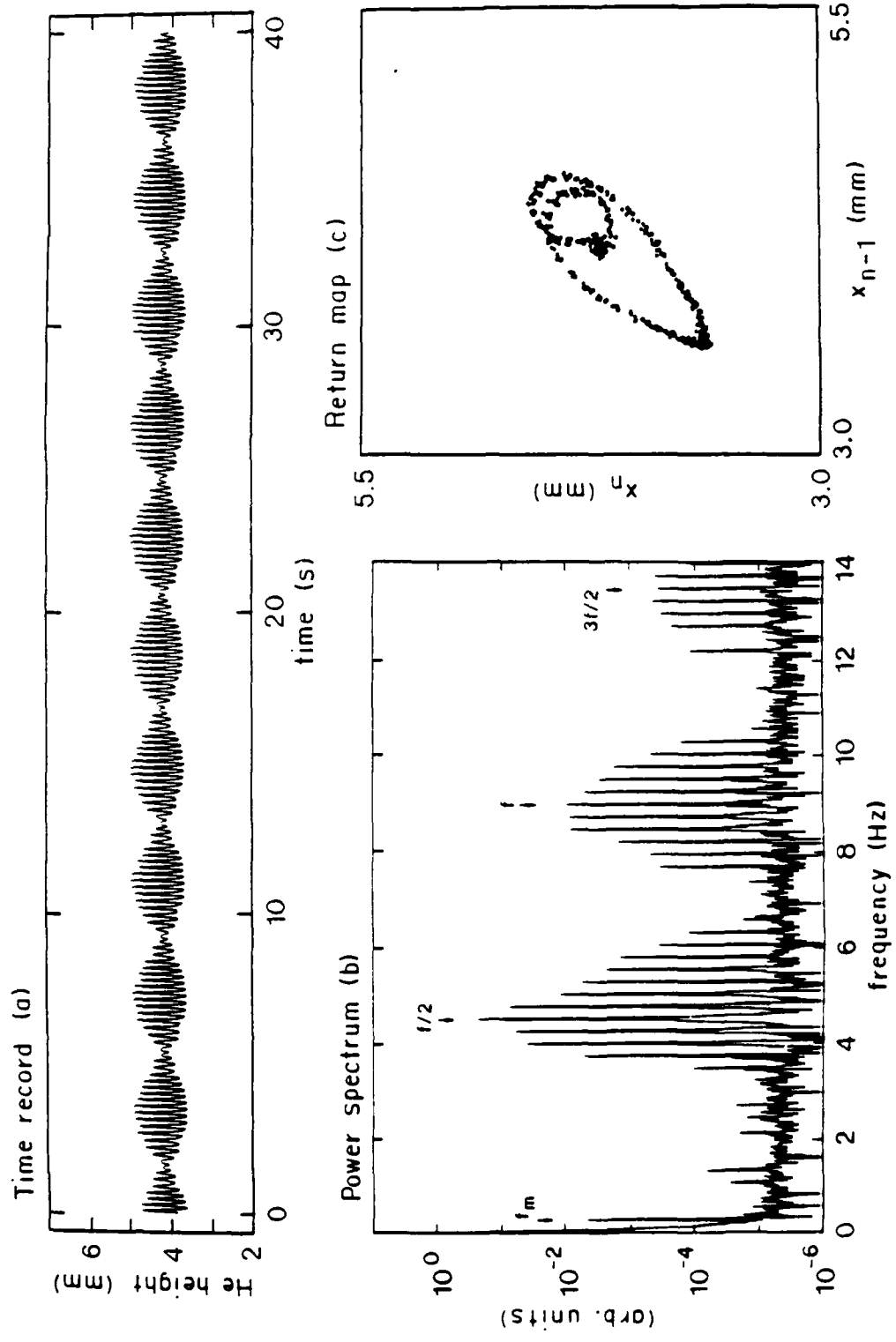


Figure 51. Single sausaged smooth modulation with 9.2 μm rms drive amplitude.

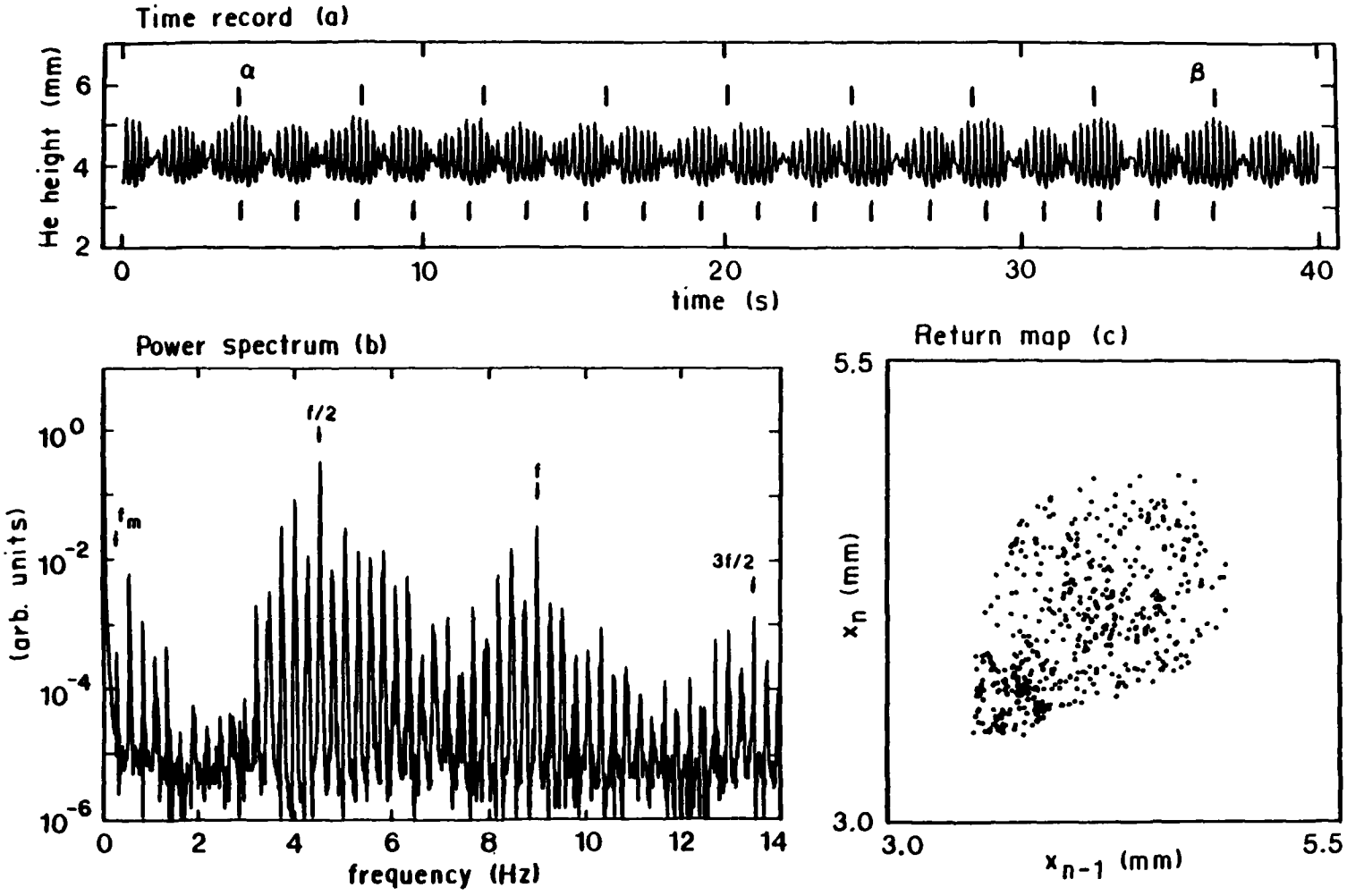


Figure 52. Simultaneous single and double smooth modulations out of phase lock, with 12.2 μm rms drive amplitude.

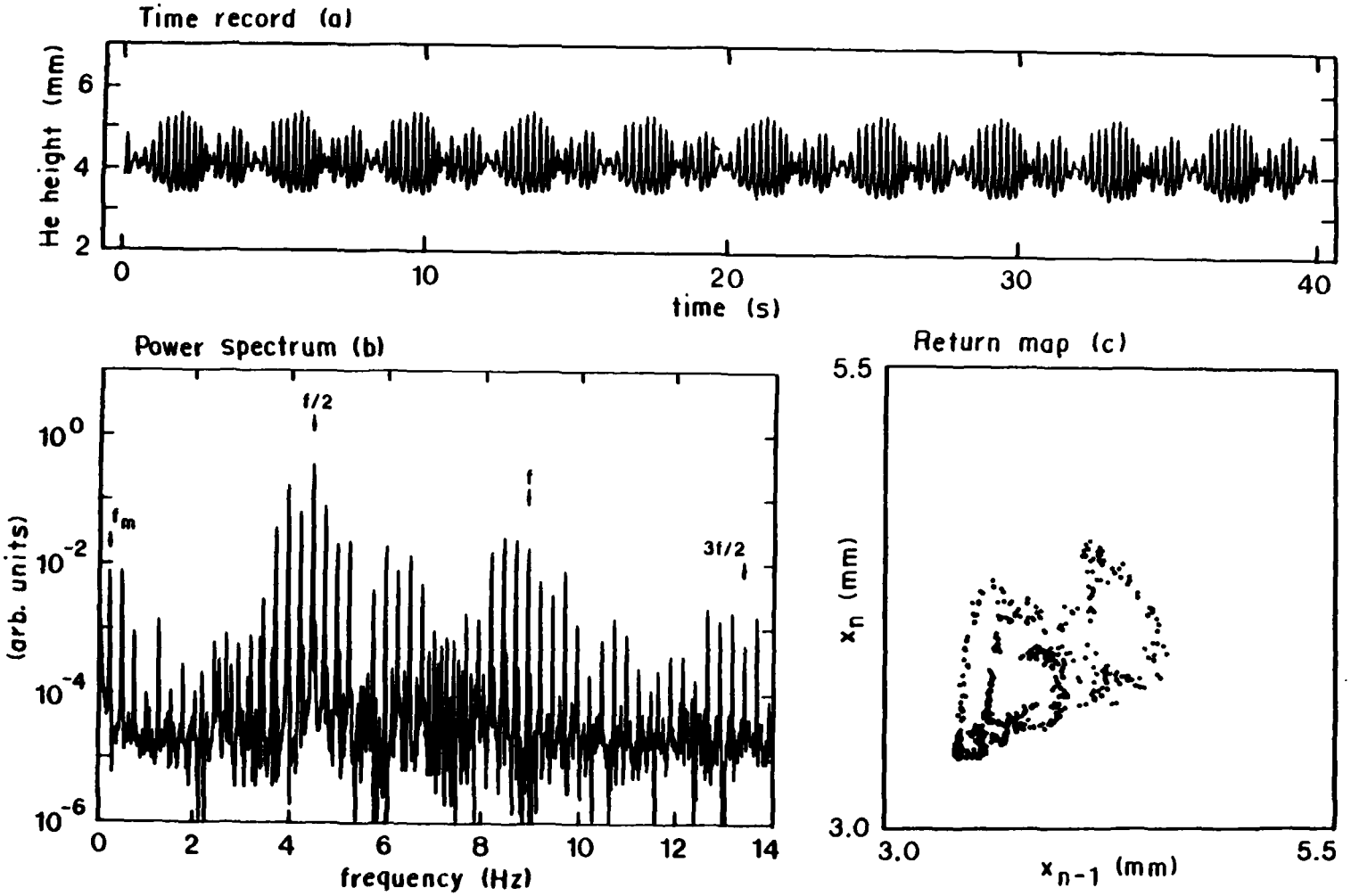


**Figure 53. Single and double sausaged modulations phase locked, with 16.2 μm rms drive amplitude.**

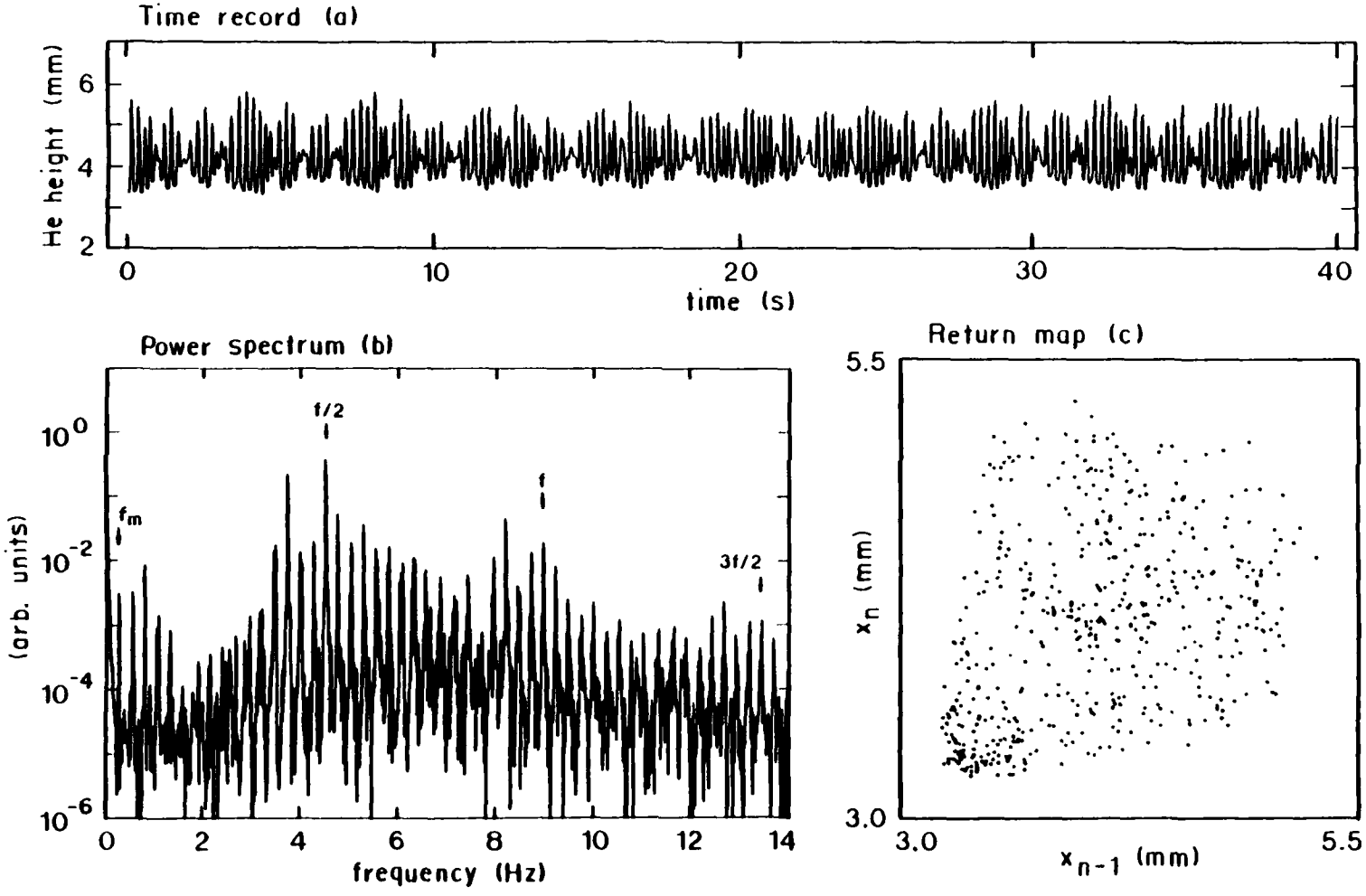


**Figure 54. Single, double, and triple modulations out of lock, with 22.2 μm rms drive amplitude.**

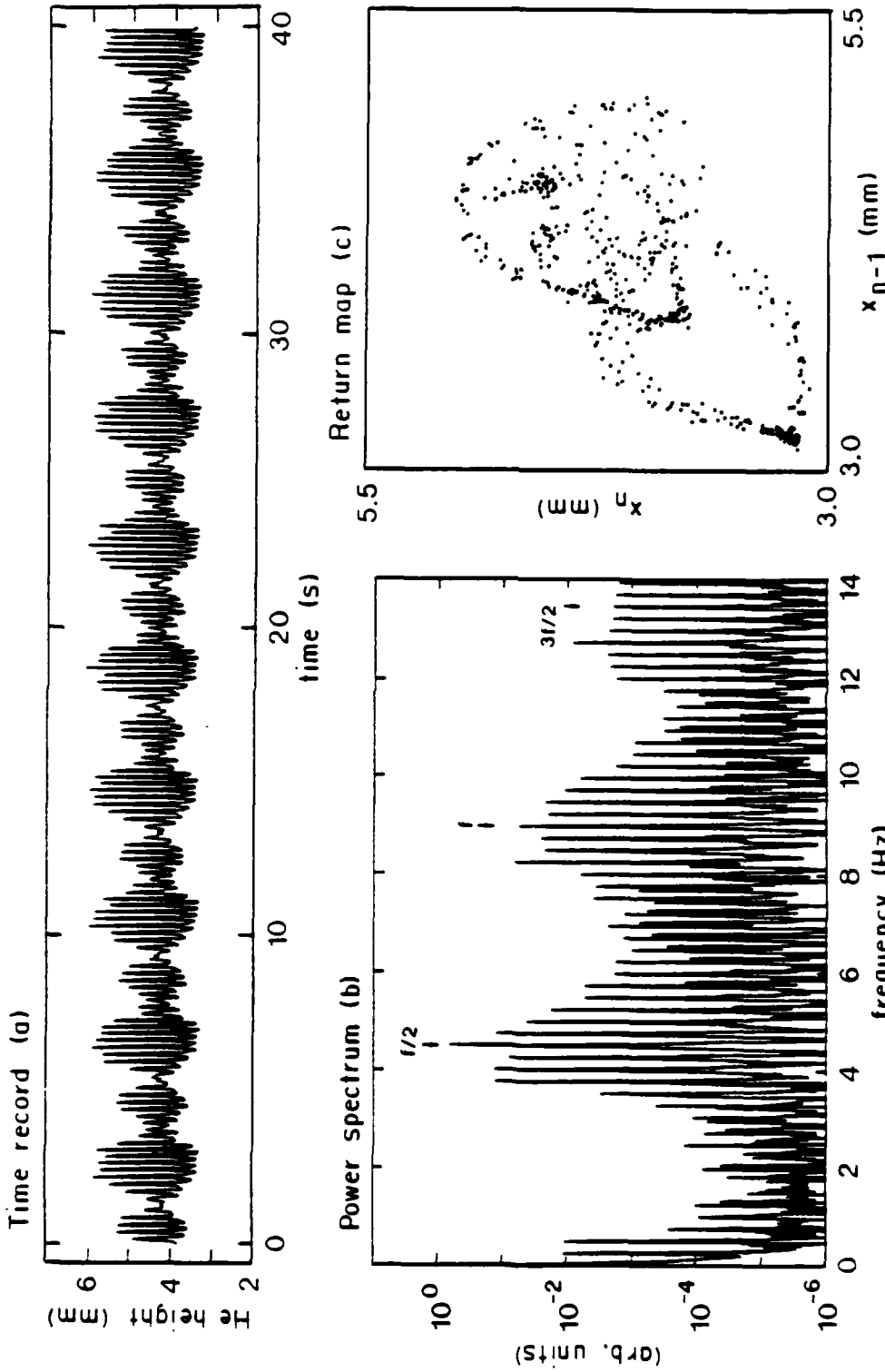


Figure 55. Smooth modulations phase locked, with 25.1 μm rms drive amplitude.

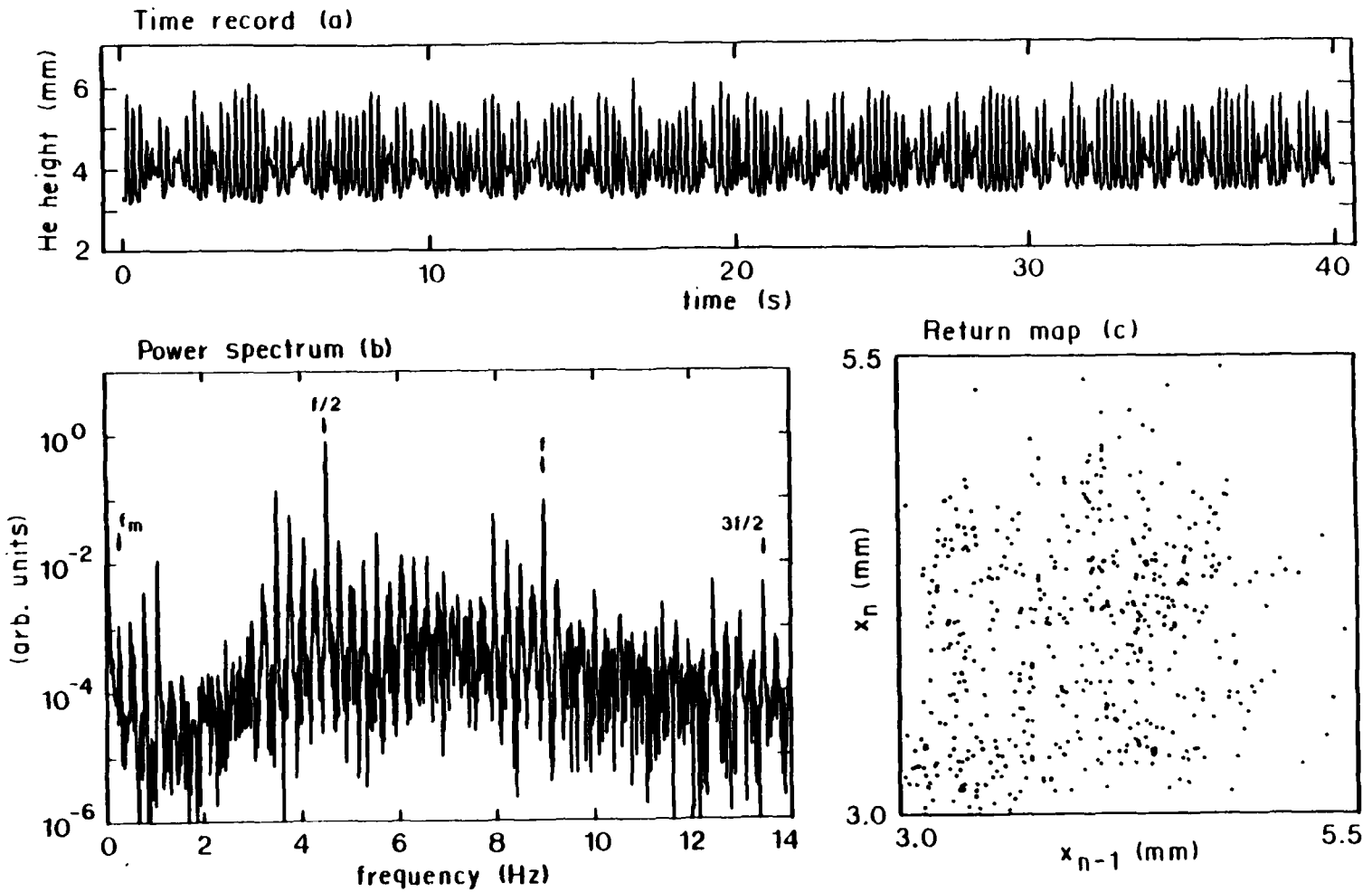


**Figure 56. At least three modulations out of lock, with 29.1 μm rms drive amplitude.**

by counting cycles in the time record (however, see below). The return map shows the Hopf bifurcation; the attractor has gone from a point to a line twisted into a loop. This jargon means that the motion picks up another independent frequency. That the dimension of the line is one means that the number of independent frequencies present in the response other than those tied to the drive (f/2 and its harmonics) is one.

With further increase in the drive amplitude something else happens, as shown in fig. 52. Another independent modulation frequency appears and beats with the first. This second modulation has nearly two "sausages," at the locations of the lower tick marks, for the first modulation's one, at the upper tick marks. They are superimposed and seen to slip in phase between $\alpha$ and $\beta$, which like the tick marks were placed by eye. The slight splitting of peaks in the spectrum also shows the beating. The return map is a two dimensional blur, not because this is chaos, but because the motion has picked up another frequency.

In general, two self-maintained oscillators, like these modulations, should be able to pull each other into synchronism if the coupling between them is strong, or if their frequencies are close. Their frequencies "feel" the phase difference between them, so that their phases may lock together, making the frequencies identical. This mechanism is detailed in Appendix 4. The modulations do indeed phase lock in a two to one ratio, as fig. 53 shows. The waveform no longer shows beating and the return map is no longer blurred because

the two sets of sausages have stopped slipping in phase. That the return map appears as a contorted line, rather than distinct dots, shows that the modulations, although locked to each other, have not locked onto the drive.

Phase locking competes with quasiperiodicity in the battle to make the motion more complicated. In this not-too-far-removed-from-naturally-occurring system, nonlinearities first make life difficult by creating incommensurate frequencies, but then at larger amplitudes (which probably means larger couplings) the independent frequencies lock up. Phase locking orders the motion. When the various motions phase lock, there are fewer independent numbers one must keep track of.

The interplay of quasiperiodicity and phase locking continues on through higher drive levels of the trough. In fig. 54, an additional unlocked quasiperiodic modulation appears with three sausages. In fig. 55, the modulations are phase locked, although it is unclear whether the third modulation is still present because it is difficult to see three sausages in the waveform. In fig. 56, the modulations unlock again. Notice that a noise floor seems to rise in the spectrum, however this may be an artifact of not enough frequency resolution for the long periods in the waveform. At still higher amplitudes on other runs, either turbulent waveforms yet to be characterized or cockscombs are seen.

For heuristic reasons, the smooth modulation in fig. 51 was

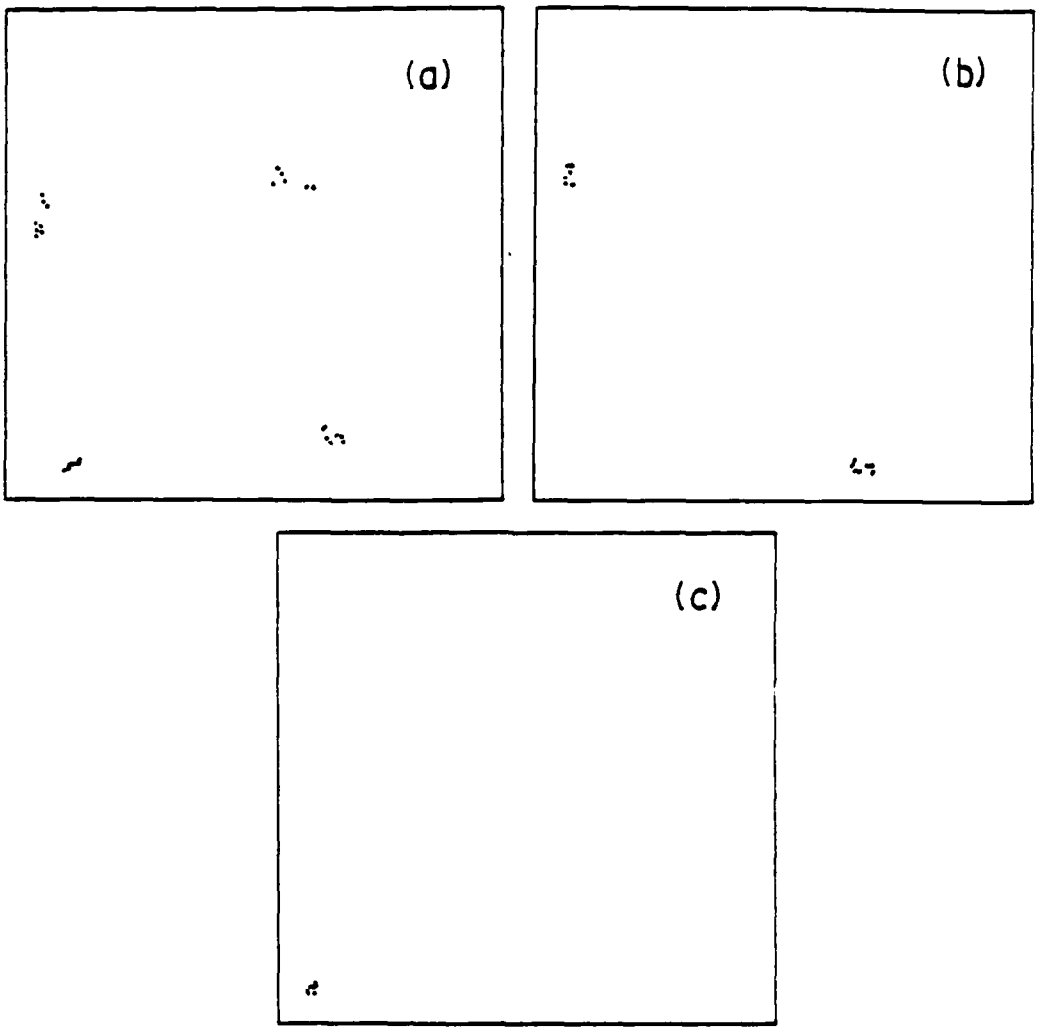


**Figure 57. More return maps for figure 51.**

presented as being quasiperiodic, but actually it has phase locked onto the drive. The motion repeats every fourth modulation, as shown by the return maps of fig. 57, constructed by sampling once (a) every modulation, (b) every other modulation, and (c) every fourth modulation. Hence, the ratio $f/f_m$ is actually 34.500, or better stated, $f_m$ is $\frac{4}{69}$ f/2. (Incidently, my previous specification, from examining the time record, of $f/f_m$ as $34.55\pm.03$ shows that I tend to set error bars too small.) However, it is still easier for me to believe that the modulation occurs through some mechanism that allows $f/f_m$ to be an irrational number, and that the modulation phase locked because of some small coupling to the drive, than to believe that the energy transfer down to the subharmonic depends on the 69th harmonic of the response being in resonance with the 4th harmonic of f/2.

Remarkably, nonlinear hydrodynamics creates self-maintained oscillators that can take energy from a simple sinusoidal drive and distribute it to several lower, independent frequencies. Phase locking competes with this tendency towards complication, orders the motion, and reduces the number of degrees of freedom. They go hand in hand — as is explained in Appendix 4; phase locking should be expected since there will be residual coupling between the modulations. So the physics is in understanding the source of the independent frequencies. To find it, an experiment was performed in water, where, unlike helium, the waves can be seen.

## 8b. An Experiment in Water.

A similar experiment in water provides spatial information on the modulations. The ninth mode of a glass trough, 2.6 cm wide by 38 cm long filled to 2.9 cm height, is parametrically driven by vertically oscillating the trough at 8.6 Hz with amplitude 0.94 mm with a large loudspeaker. The water contains some non-dairy coffee creamer (which is very white) to contrast against a black background. The surface profile is video taped and played back frame by frame. Those frames where the water at the right side of the trough is at its crest (occurring at f/2 which was luckily almost exactly every seventh frame) is traced onto clear plastic sandwich wrap. The trace of the profile is then digitized with 64 points taken by hand using the computer and plotter. The experiment was not set up carefully. I ended up analyzing a practice tape more and more intending to go back and do it right, which never happened.

In spite of these caveats, the time evolution of the surface strobed at nearly f/2, fig. 58, shows the nature of the modulation: Even though the drive is uniform in space, there is a region of large amplitude which oscillates at $f_m$ between the left and right sides of the trough.

The surface profiles were then Fourier transformed using as the basis the linear normal modes, which are each cosines of a certain number of half wavelengths, rather than the full wavelength sines and cosines of the usual Fourier series. The time dependence of each spatial mode, however, could not be unambiguously determined without

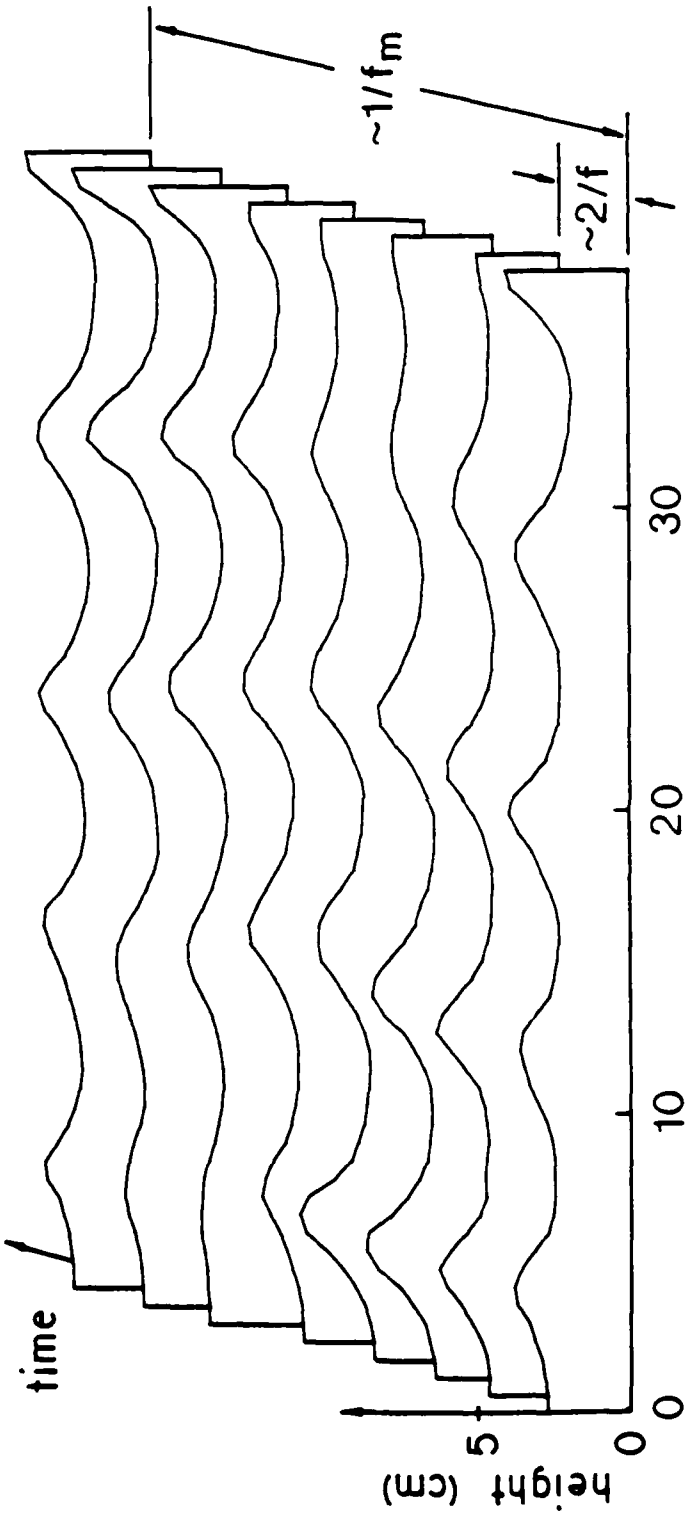


Figure 58. Surface profiles of water through one cycle of a smooth modulation.

digitizing the surface many times per cycle of the drive over many cycles of the modulation. In all, about a hundred times more data is needed — too much to take by hand.

The information is on the tape, but I was at that time under orders to not take any more data and write up this thesis. So the following system, which is fully described in Appendix 6, was put together to feed the existing video tape to the computer, without writing any software or building any electronics (except for soldering four resisters together). (I learned a lesson: by working around the temptation to build something, I got a system that works better, sooner.)

Figure 59 shows a simplified TV picture. A horizontal band and a vertical band, superimposed on the picture, are set to select a particular position in the trough to be digitized by the computer. A ramp voltage $V_{ramp}$ starts when the electron beam crosses the band as it scans down the picture. The voltage $V_{bright}$ follows the brightness of the picture in the vertical band, but only where the two bands cross. The computer, then, recognizes the height of the oscillating surface by measuring $V_{ramp}$ when the black to white transition in $V_{bright}$ occurs. As the surface oscillates up and down, the computer measures a higher or lower voltage on the ramp, and so generates a series of height measurements at a particular position in the trough at the TV picture scanning frequency of 60 Hz. The vertical band acts just like the height transducers used in helium, so the same helium software can be used. A pulse dubbed onto the audio track of the tape

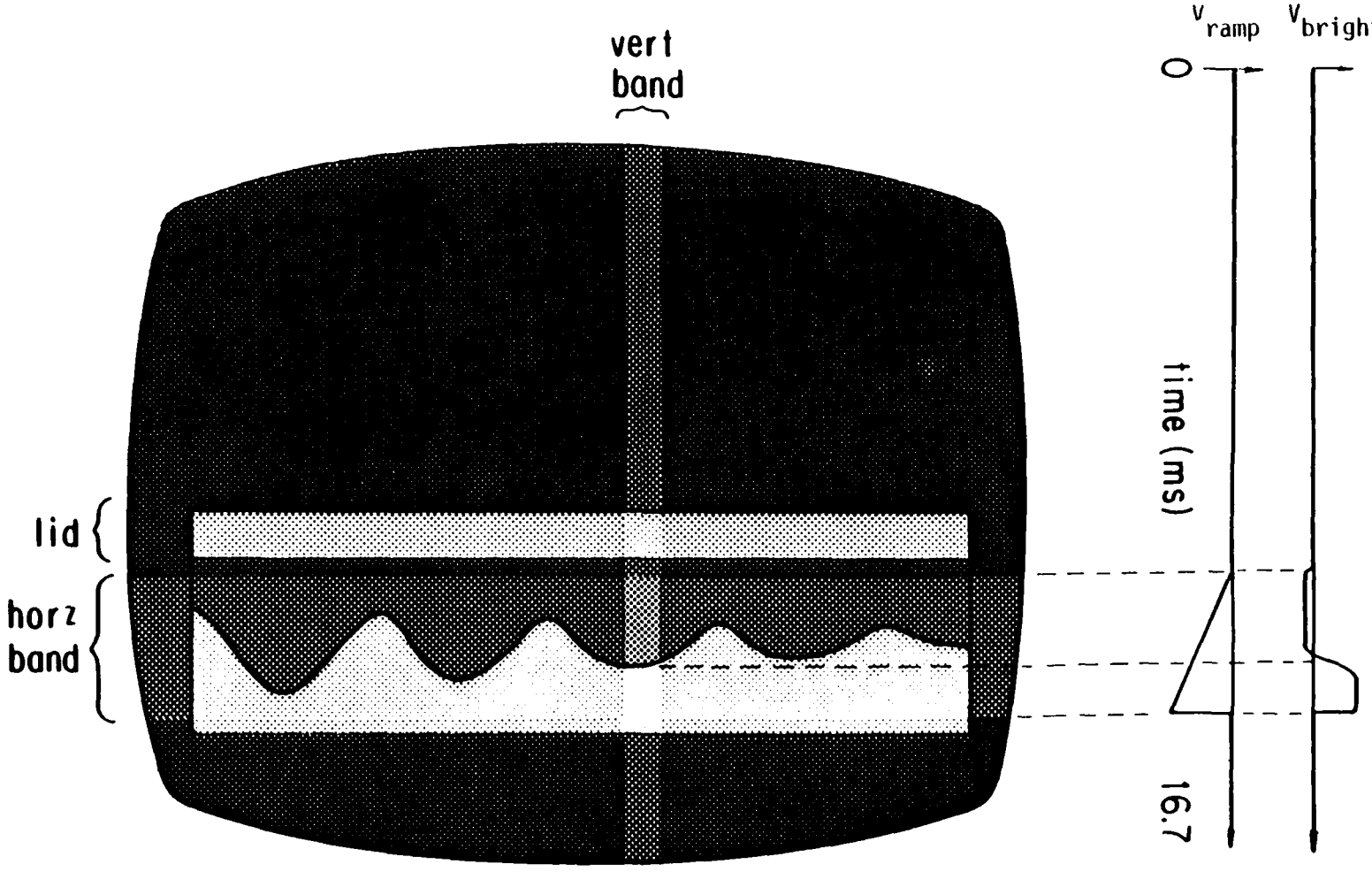


Figure 59. A method for digitizing a video tape.

initiates the digitization.

The procedure then goes like this: The vertical band is placed at the left edge of the trough, the tape is played, and the audio pulse starts the computer digitizing the height there for 2048 fields. When done, the tape is rewound, the band is moved to the right a little, and the process is repeated. This is done at 32 positions along the trough. Thus I end up with 32 time records taken along the trough all starting at the same time.

Figure 60(a) is the height vs. time at the left side of the trough while (b) is from the right. Note how the large amplitude oscillates between the left and right sides of the trough.

To get the spatial Fourier coefficients as a function of time, the first element of each time record is collected and decomposed into the first 32 linear normal modes, as described earlier, then the second, the third, and so on. Each mode can now be shown vs. time in fig. 61. I find it remarkable how different each of the modes look -- they could have come from different experiments. These time records for the spatial modes are then Fourier analyzed in time to get each mode's frequency spectrum, shown in fig. 62. Modes not shown had very little energy in them.

One should remember how poorly the original data was taken before treating this data quantitatively, however. Unlike smooth modulations in helium, the troughs in fig. 60 extend lower than the crests extend up. It is as if something were "clipping" the top of the waveform.

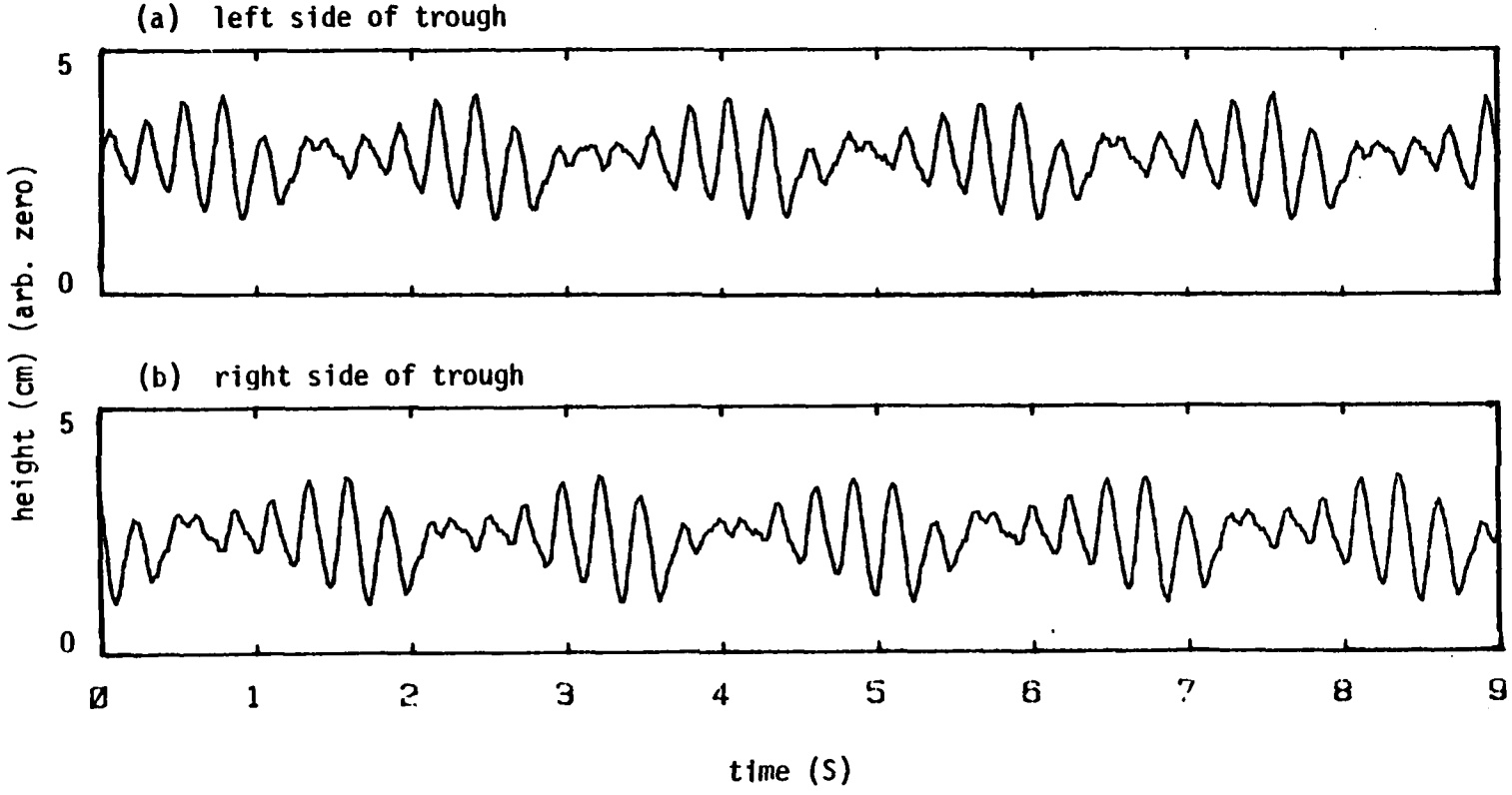


**Figure 60. Smooth modulation in water on (a) left and (b) right sides of the trough.**

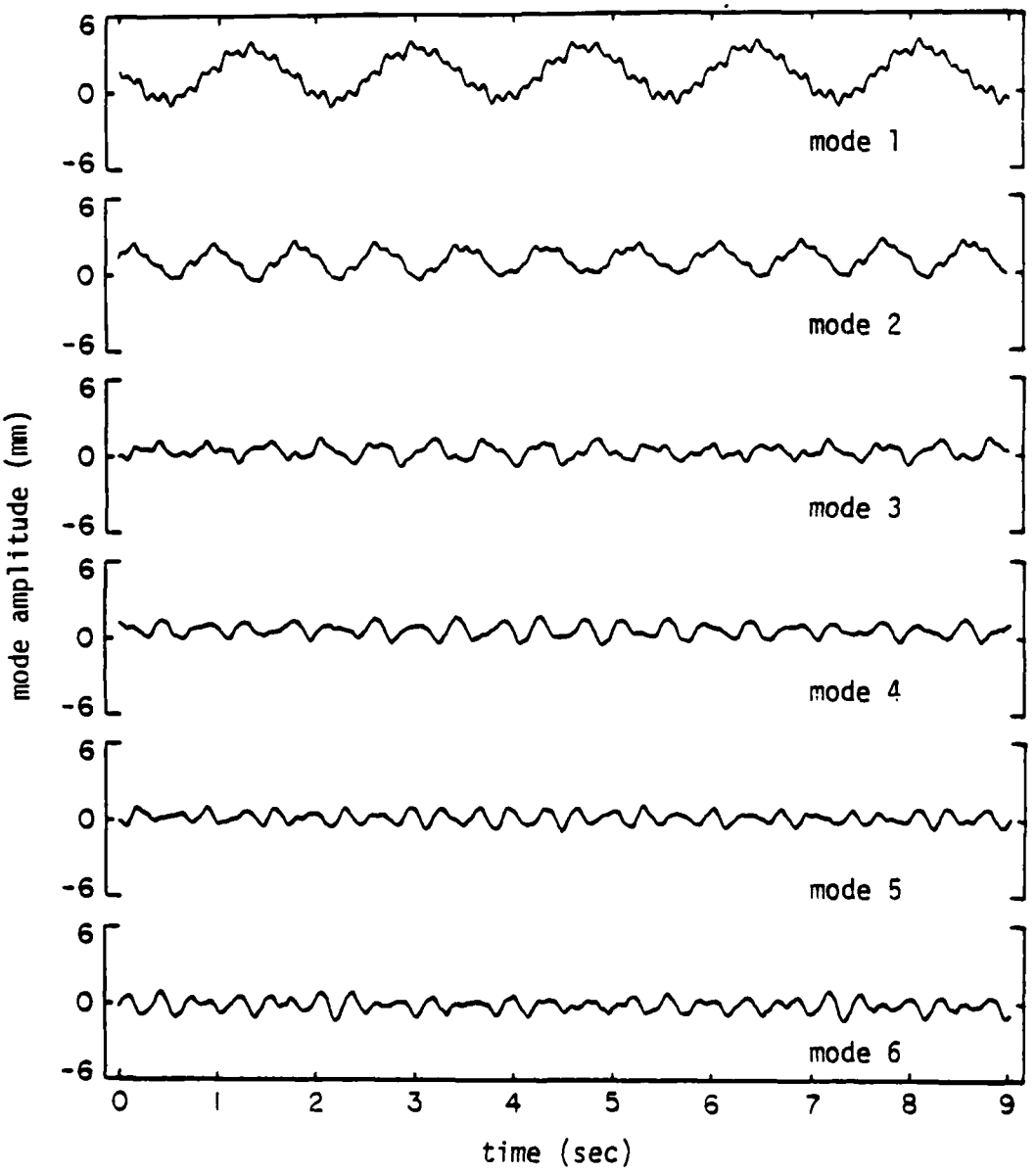


**Figure 61(a). Spatial modes of the trough vs. time during a smooth modulation.**

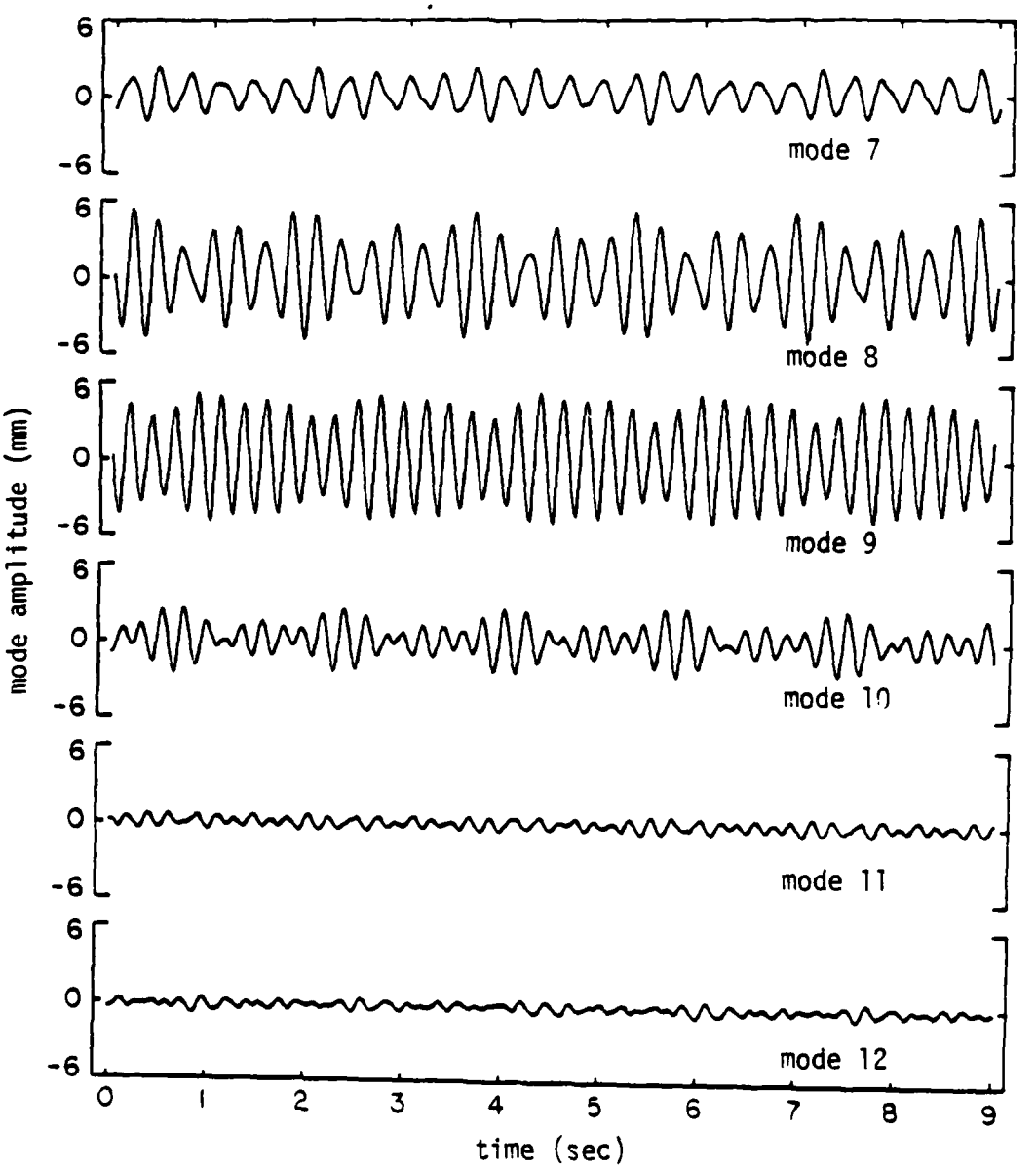


**Figure 61(b). Spatial modes of the trough vs. time during a smooth modulation.**

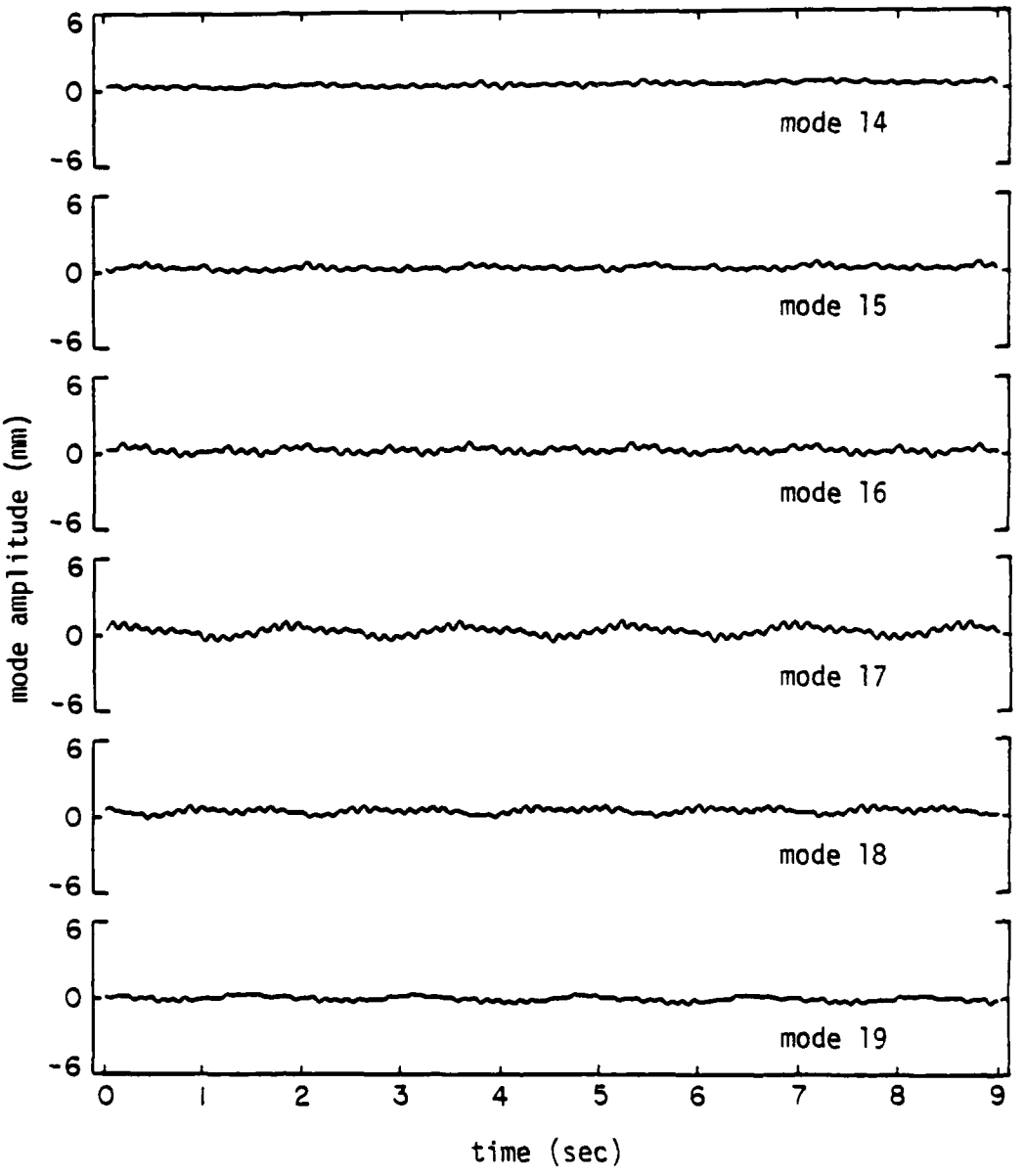


**Figure 61(c). Spatial modes of the trough vs. time during a smooth modulation.**

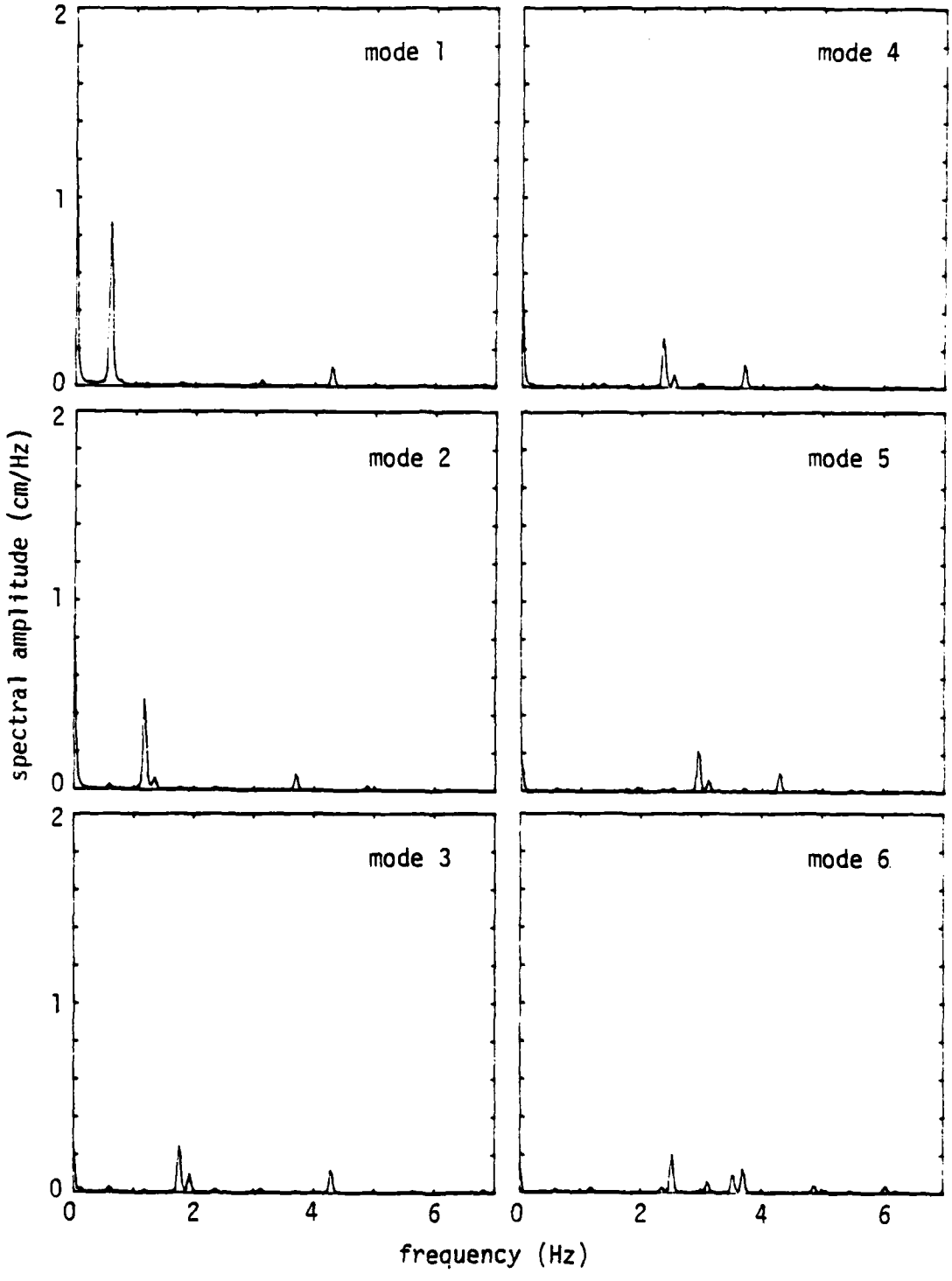


**Figure 62(a). Frequency spectrum of each spatial mode.**

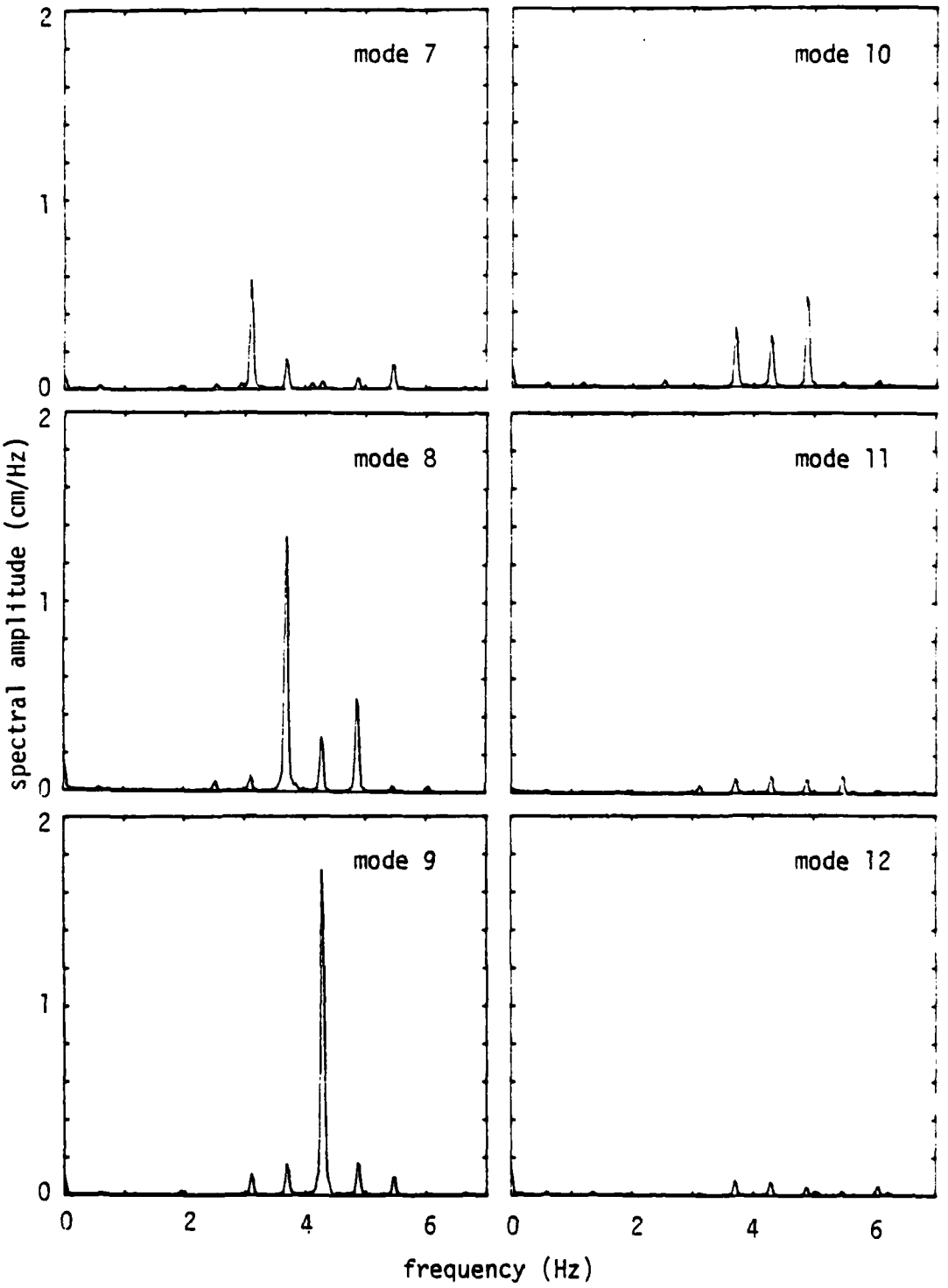


**Figure 62(b). Frequency spectrum of each spatial mode.**

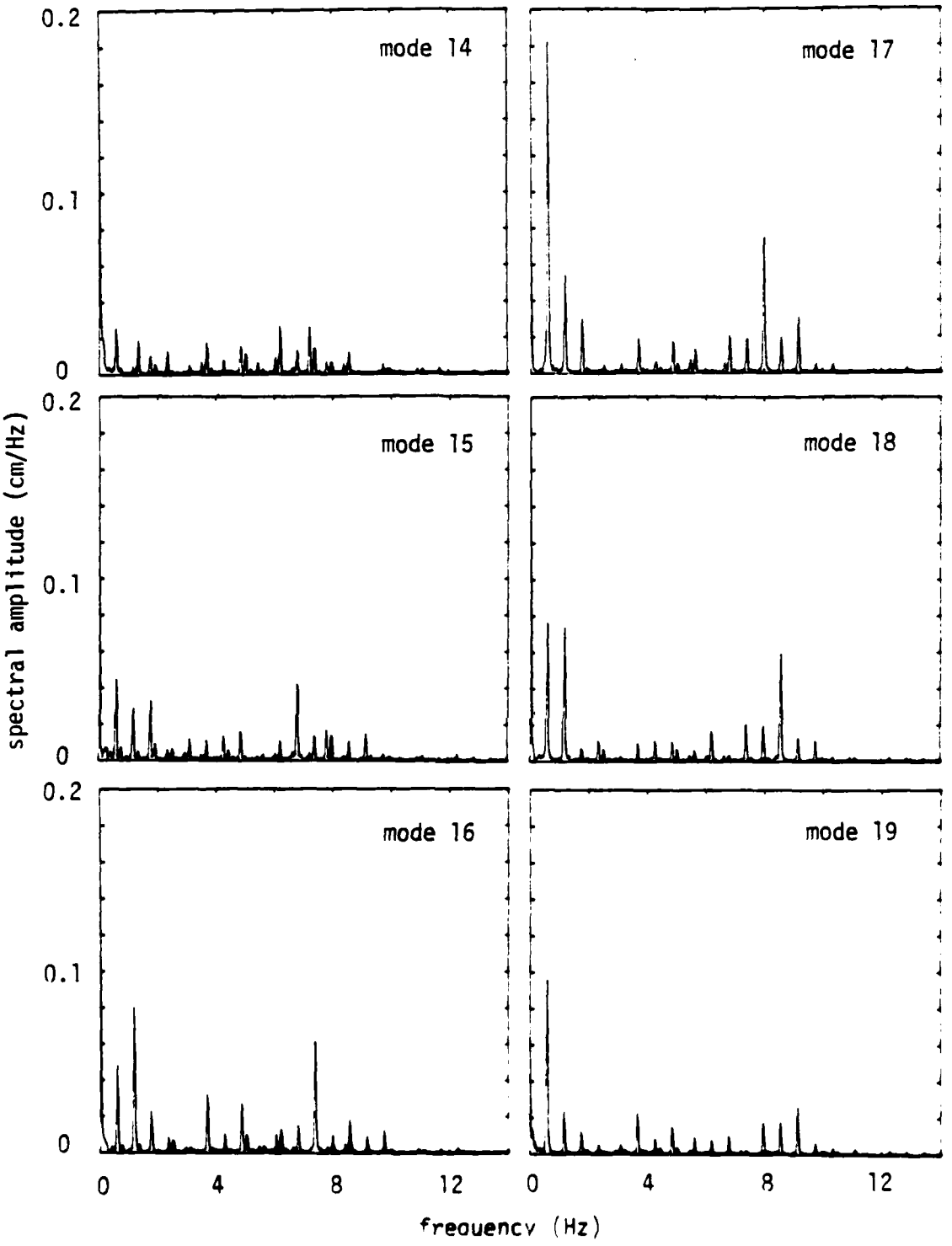


**Figure 62(c). Frequency spectrum of each spatial mode. Note change of scale.**

(Perhaps this is the source of the f/2 in the first mode.) I take this as evidence for wetting problems at the walls -- white stuff from the creamer, probably fat, was collecting there -- and as justification for doing the experiment in helium.

Interpretation. Now for some physics and speculation: Most of the energy is in the first, eighth, and ninth modes. The fundamental oscillates at the modulation frequency $f_m$. The ninth mode is the driven mode and its amplitude is fairly constant in time. Somehow, it seems, the first and eight modes can take energy out of the ninth. There is a satisfying numerology here; the wavevectors of the first and eight modes add up to the ninth's, forming a what I'll call a resonant triad. The largest peak in the spectrum of the eight mode is at $f/2-f_m$, so the main frequencies of the modes add up too. The ratio of dominant frequencies in the first, eight, and ninth modes is 1 : 6.3 : 7.3.

An approximate theory that obtains the amplitudes of all the modes iteratively seems natural to me. The ninth mode is presumably replenished by the drive; its amplitude is determined primarily by the nonlinearities of the ninth mode, as described in Appendix 2, and the drain of energy to the other modes just looks like more nonlinear damping. Then, hopefully, some way can be found for the first and eight modes to be coupled together so that they are unstable to growth at infinitesimal amplitudes, with a growth rate that depends on the amplitude of the ninth mode. This is where the physics is. If the growth rate balances dissipation, the smooth modulation forms. This

determines the drive amplitude and frequency needed to see the modulation. Another nonlinearity will then stop the growth, setting the amplitude of the first and eight modes in such a way that the sum of their frequencies is f/2. What exactly determines $f_m$ is an open question, but it should be close the resonant frequency of the first mode. Additionally, perhaps, another triad made from the first, tenth, and ninth modes can form simultaneously, but because the 1,8,9 triad and the 1,10,9 triad share the fundamental, they would lock together and their amplitudes would be tied to the same nonlinearity. The amplitudes and phases of the other modes might then be set by higher order interactions. For instance the amplitude of the second mode $A_2$ would depend on the amplitude of the first $A_1$ as $A_1^2$, $A_3$ would be even higher order and depend on $A_1A_2$, $A_7$ would depend on $A_1A_8$ and $A_9A_2$, and so on. Incidently, the nonlinear couplings between the modes can be found in a paper by Miles (1976). Hence, the response in all the other modes is set and the motion is determined.

At higher drive levels additional resonant triads probably become excited, for instance, 2,7,9 or 3,6,9. These triads would each respond at their own independent frequencies, the triad with the second mode producing waveforms with two sausages as in Figs. 52 and 53, the triad with the third mode producing three sausages as in fig. 54. Waveforms with 1, 2, or 3 sausages, singly or combined, have all been seen. Figure 46 was actually a waveform with just two sausages, as evidenced by $f_m$ being close to the frequency of the second mode. This suggests that the proper, physical variables for

the return maps are not $x_n$, $x_{n-1}$, $x_{n-2}$ ..., popular because they are easy to generate from computerized data, but rather the amplitudes and their time derivatives (or the phase) of the lowest modes of the trough. These ideas still need to be tested.

## Section 9. Frequency and Amplitude Sweeps -- Hysteresis.

### 9a. Sweeps in Water.

The first ultra deep modulations, described in Sec. 6, were seen when the probe was used to shake water in the Plexiglas annular trough (Sec. 3) at 11 Hz with an amplitude of 429 μm rms. The drive amplitude and frequency were later swept in this neighborhood, with water at a height of 6.07 mm. When the frequency was swept the drive voltage was held constant. For a given voltage, the displacement of the trough is controlled by its inertia when the frequency is well above the probe's main resonant frequency of 5 Hz (the resonance due to the mass of the trough being supported by springs). Hence, the acceleration amplitude of the trough is held approximately constant.

The results are figs. 63-65. Plotted vertically is the absolute value of the oscillating height at the barrier low pass filtered with a 1 second time constant (p. 57). Steady f/2 response causes a steady line while a cockscomb or other modulation causes a wavy line or band. Starting with the second trace (b) of fig. 63, the frequency is swept up at a rate of 3 mHz/S, with a constant drive voltage such that the drive amplitude is 589 μm rms when f is 11 Hz. A cockscomb at f/26 starts off at 10 Hz, which switches to f/28, then unlocks from the drive (see Appendix 4 on phase locking) but stays near f/28, denoted by f/~28, and so on as f is increased. Past 12 Hz, 16 and 17 half

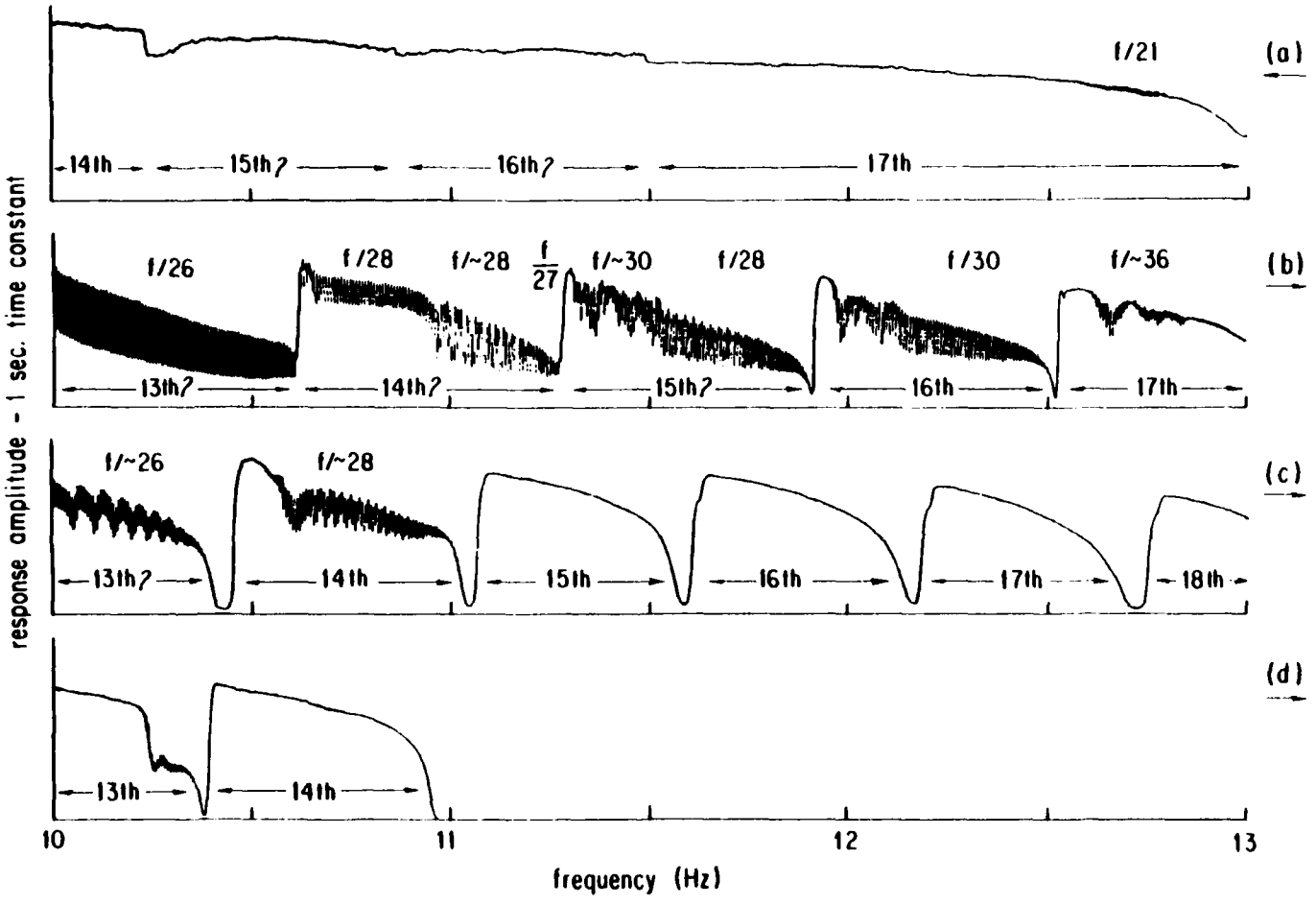


Figure 63. Drive frequency sweeps at 3.0 mHz/sec sweep rate in 6.07 mm of water. Direction and rms drive amplitude at 11 Hz: (a) down, 589 μm; (b) up, 589 μm; (c) up, 530 μm; (d) up, 471 μm.

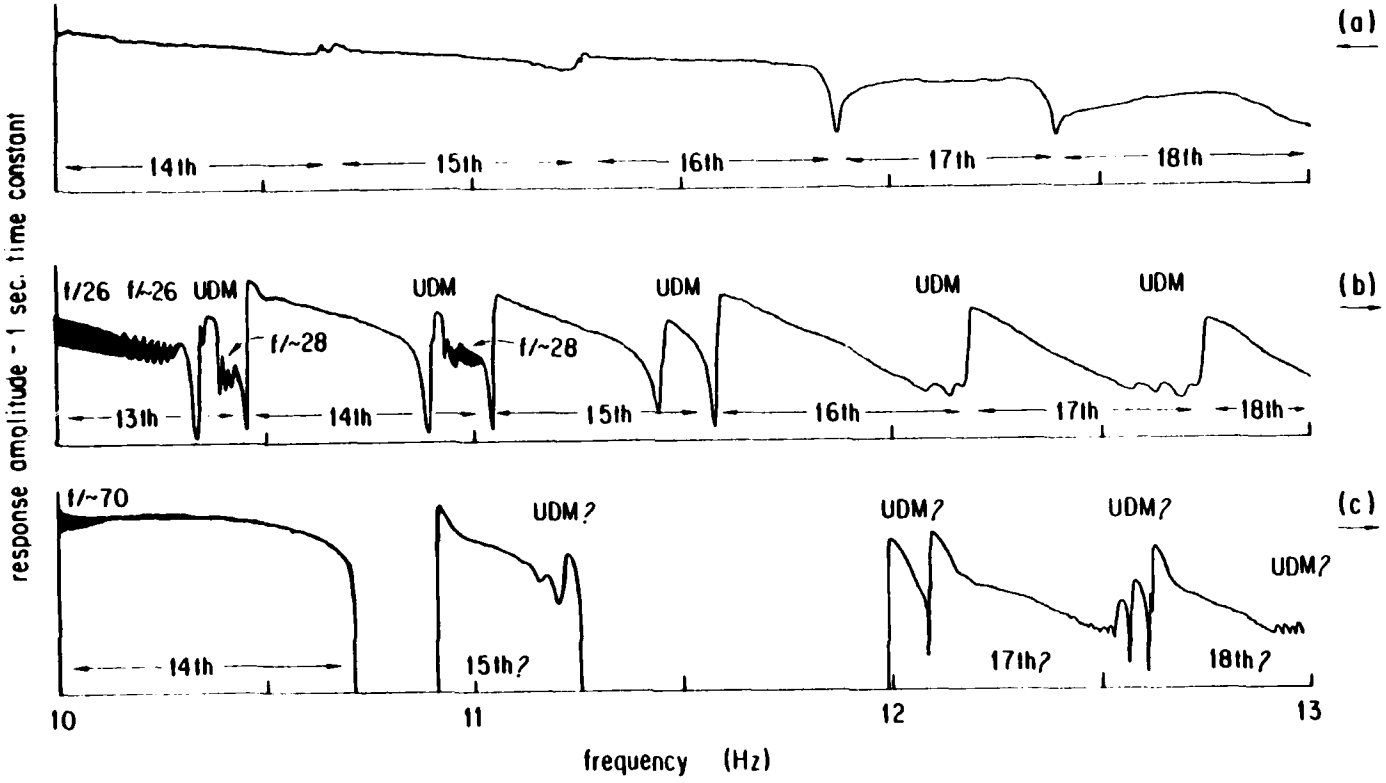


Figure 64. Drive frequency sweeps with 530 μm rms drive amplitude at 11 Hz in 6.07 mm of water. Direction and sweep rate: (a) down, 1.0 mHz/sec; (b) up, 1.0 mHz/sec; (c) up, 0.15 mHz/sec.

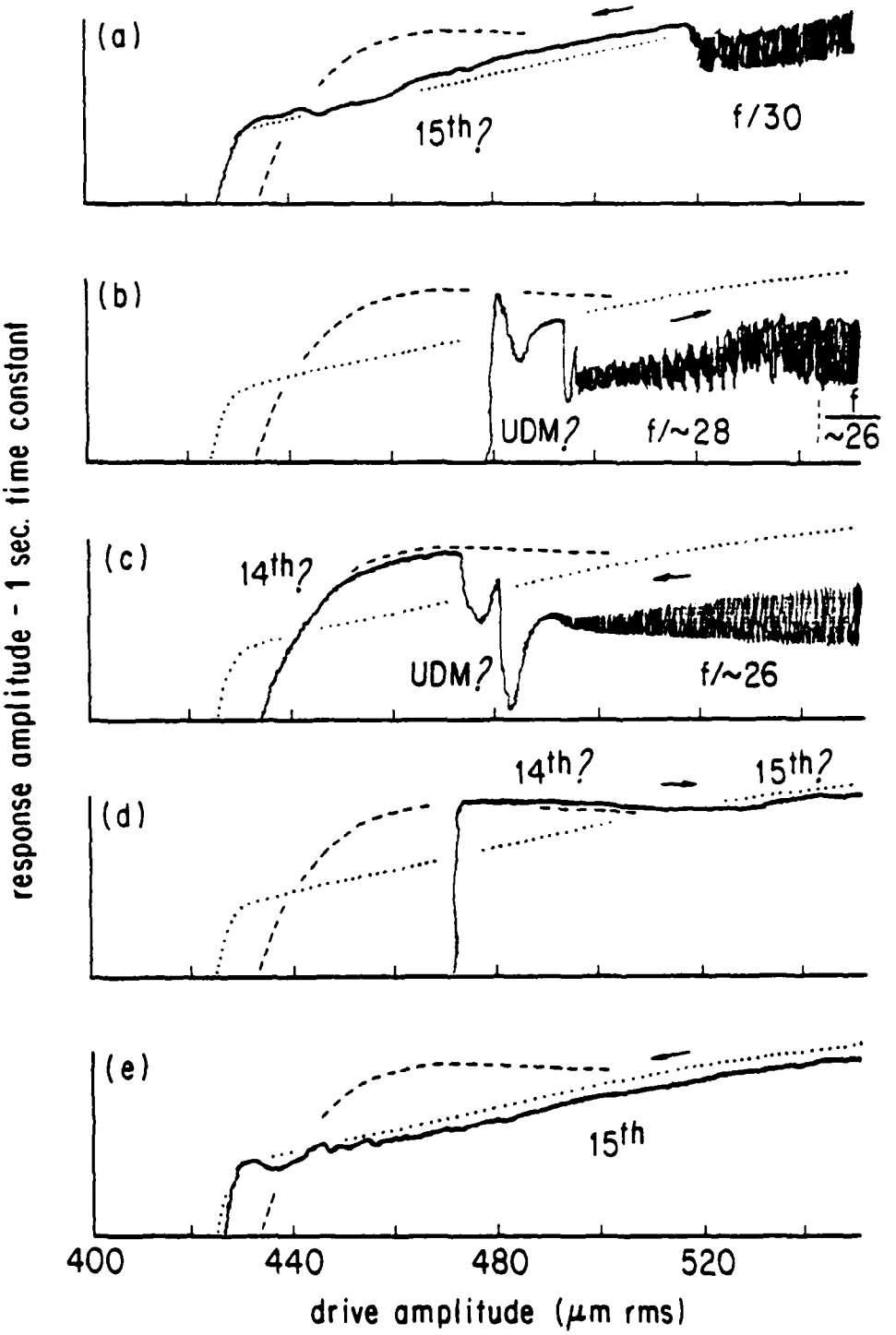


Figure 65. Consecutive drive amplitude sweeps, holding f at 11.000 Hz, in 6.07 mm of water. Direction and sweep rate: (a) down, 200 nm/s; (b) up, 200 nm/s; (c) down, 200 nm/s; (d) up, 100 nm/s; (e) down, 100 nm/s. Dotted and dashed lines are guides to the eye for the 15th and (presumably) 14th modes.

wavelengths were counted in the trough (with the aid of the conical mirror shown earlier in fig. 32), meaning that the 16th and 17th modes of the trough were excited, also notated in the figure. Features with question marks were not noted when the data was taken, but were inferred at the time of this writing.

However, when the frequency was ramped back down, the result was trace (a). The structure disappeared. This was quite repeatable -- and terribly confusing.

If the drive amplitude at 11 Hz is lowered to 530 μm and 471 μm rms, the results for upward frequency sweeps are (c) and (d). If the sweep rate for trace (c) is lowered to 1 mHz/S, the result is trace (b) of fig. 64. At this rate, one cycle of an ultra deep modulation (UDM) was apparent as the amplitude on one side of the barrier rose well before the other. Again though, if f is swept down (at the lower rate), the structure disappears in (a). A very slow trace, at 0.15 mHz/S, at the same intermediate amplitude, is recorded in (c). Amplitude sweeps at 11 Hz are shown in fig. 65.

For an ever so long amount of time I could not understand these sweeps. The reader probably will not either, until he turns to Appendix 2 on parametrics.

Welcome back. These sweeps make more sense when one can imagine the cross sections of the instability regions described in the

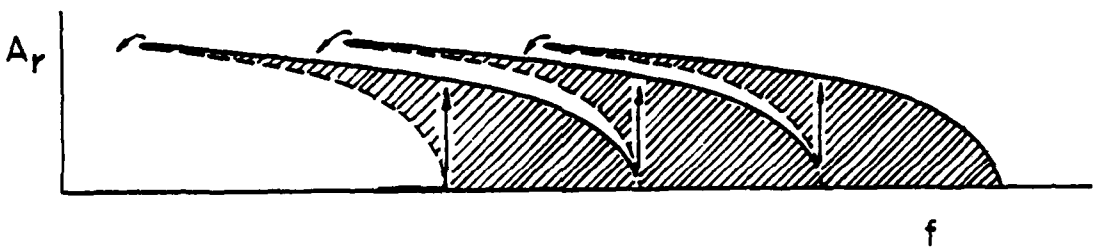


**Figure 66. Instability regions suggested by the water frequency sweeps.**

Appendix, one for each mode, as sketched in fig. 66. (Benjamin and Ursell, 1954, show that each mode separately has an instablity "V" at infinitesimal response amplitude.) The regions flop over each other to the left, like the feathers on a wing. When the frequency is swept up, the response follows one mode's region down to low amplitude, bangs into the next and pops up to the top, giving the large jumps in fig. 63(b). But, as the frequency is swept down the response hops over the tops of the regions. Notice how the 17th mode in fig. 63(a) overlaps the 15th mode in (b); the instability regions overlap at least three deep.

Notice that the ultra deep modulations occur in between modes. This is good evidence that these modulations are probably the same as the "mode competition" of Ciliberto and Gollub (1984). Notice also, the nice phase locking transition for the f/26 cockscomb on the 13th mode in trace (b) of fig. 64. This is compelling evidence that these modulations can be quasiperiodic.

The f/~70 on the 14th mode of trace (c) of the same figure was a small smooth modulation at 0.35 the fundamental frequency of the trough (the fundamental is calculated to be 0.403 Hz), modulating f/2 that has every other cycle slightly different (i.e. f/4). It has never been seen since.

## 9b. Sweeps in Helium.

The purpose of the last helium run was to verify the existence of

these instability regions. Again, either the drive amplitude $A_d$ or drive frequency f was swept, this time by the computer (p. 61). The temperature was 2.11±0.01 K and the helium height was 4.02 mm. While the frequency was swept (at 1 mHz/S), the computer held the drive amplitude constant in spite of the probe resonance and probe temperature drifts (p. 61). The response amplitude $A_r$ (again, the absolute value of the surface oscillations at the barrier, filtered with a 1 second time constant) was sampled by the computer every five seconds. Too much detail was lost in the computer records because this time was too long, but the information was recovered from the strip chart (p. 57) that was running continually, as usual. A 3-dimensional projection of $A_r$ vs. $A_d$ f was made on a X-Y recorder (p. 57) so that the regions could be visualized during the run. The phase shift of the response relative to the drive (p. 191) was measured (p. 57) as a curiosity. Every so often a time record of the surface height on one side of the barrier was recorded. The transducer on the other side of the barrier, with its own set of electronics, was also monitored on the oscilloscope. By noting whether the signals from the two sides of the barrier were principally in phase or out, it could be determined whether the driven mode was even or odd.

The region near the tenth and eleventh modes was explored, and everything was nice and stable. The records of $A_r$ vs. f are projected in fig. 67. Arrows mark the sweep direction (and upward sweeps are drawn with slightly heavier lines). Modulations cause the uneveness

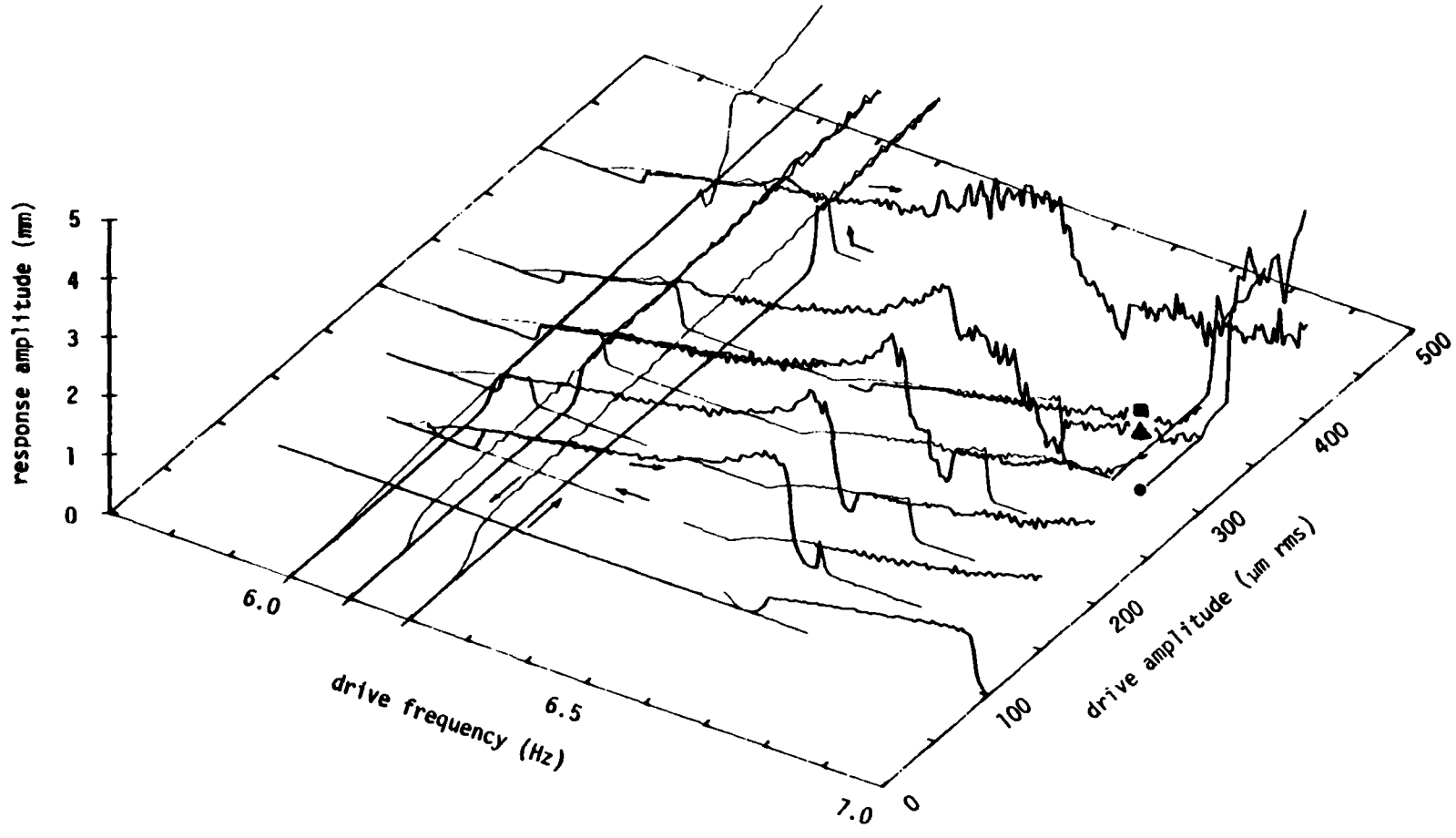


Figure 67. Raw projected frequency and amplitude sweeps in helium.

of the traces at large $A_r$.

This plot is a bit tough to decipher so fig. 68 is offered as a guide to the large scale features. The instability regions for the tenth and eleventh modes flop over each other as described in Appendix 2, but this time to the right. Some $A_d$ sweeps (not shown) go up the crotch between the two hyperbolas on the $A_d$ - f plane, underneath the surface from the tenth mode. If the tenth mode's hyperbola is met, the response jumps up to the top surface. This surface can be left by lowering $A_d$ and falling off an edge to the $A_d$ - f plane, or by lowering f and smoothly sliding down the surface to the $A_d$ - f plane, or by increasing f until falling off the edge, this time switching to the eleventh mode. The eleventh mode can also be reached by going up the crotch by increasing $A_d$, then making a right turn by increasing f. The expected f/2 parametric response occurs along the left and lower parts of the surfaces of each mode, where $A_r$ is low. But this is unstable at increased $A_d$ and f, where $A_r$ is higher.

The instability regions for helium and water bent in opposite directions. As was described on p. 98, tuning curves for gravity waves are supposed to bend to the right or left depending on whether kh is below or above 1.02. The value of kh for the eleventh mode in helium is 0.43, well below the transition, while for the fourteenth mode in water kh was 0.88.

Figure 69 is my best guess of the boundaries of the various behaviors seen for the tenth (a) and eleventh (b) modes. Data was

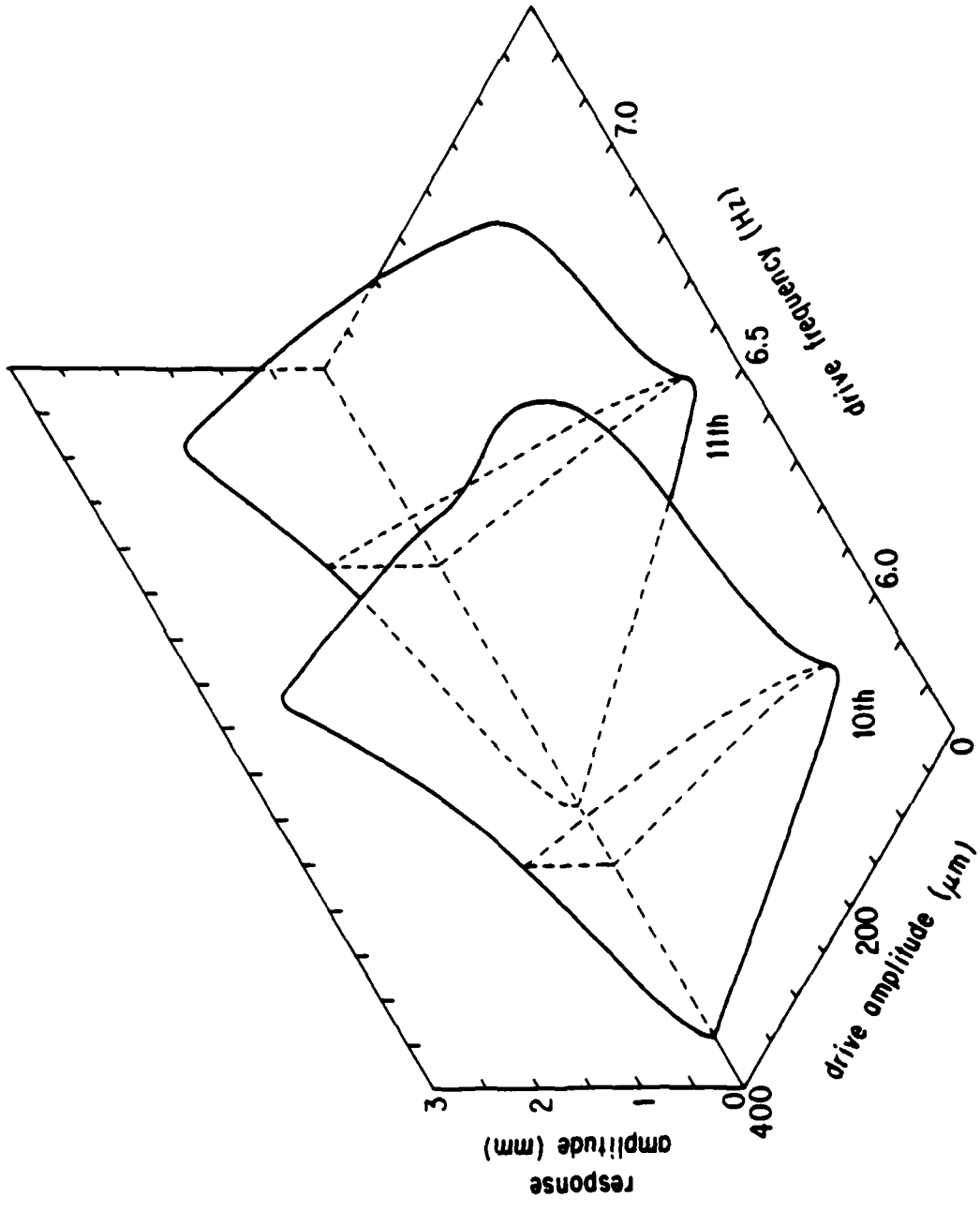


Figure 68. Idealized instability regions for the 10th and 11th modes, from data.

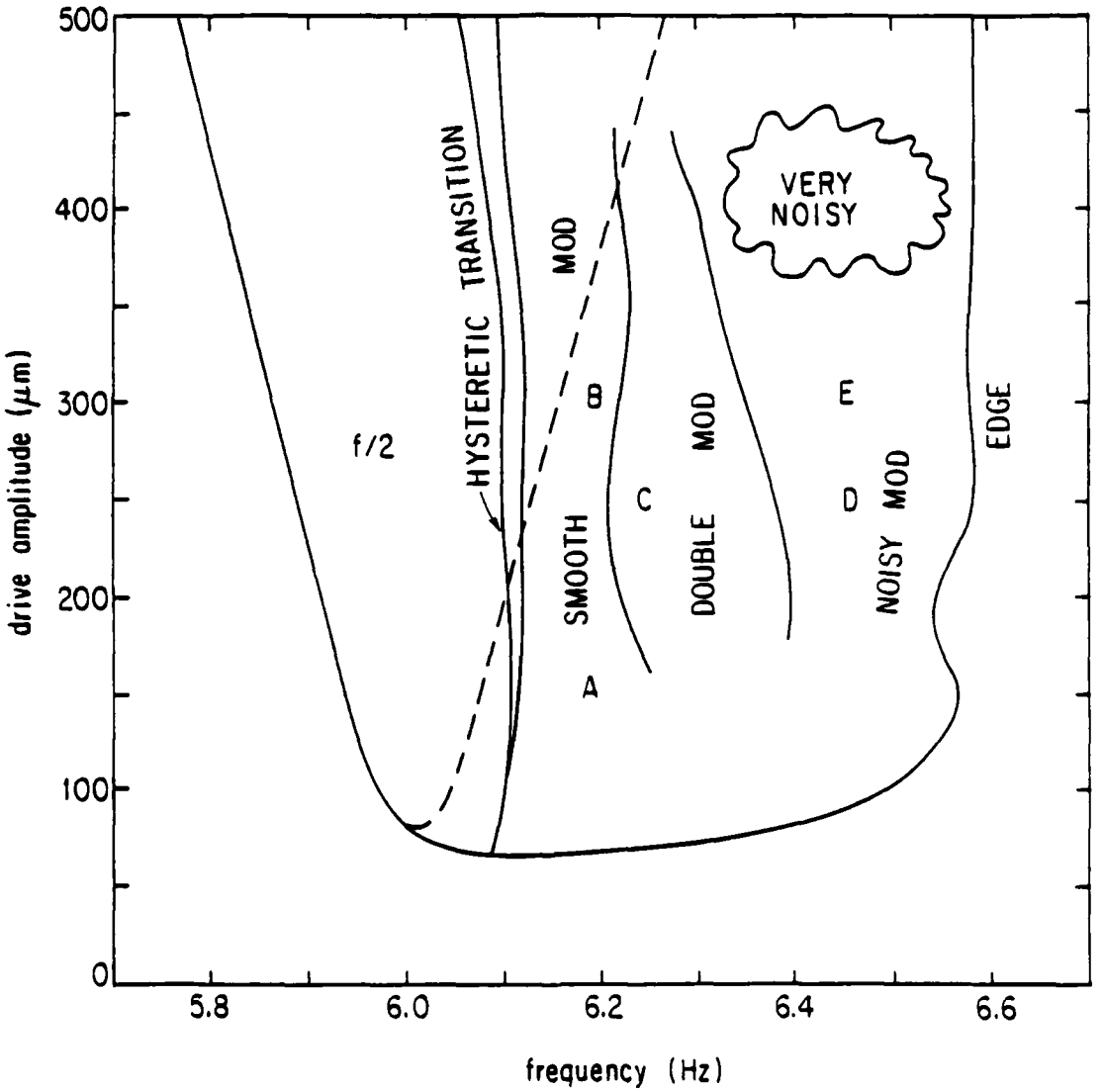


**Figure 69(a). Modulation boundaries for the 10th mode.**

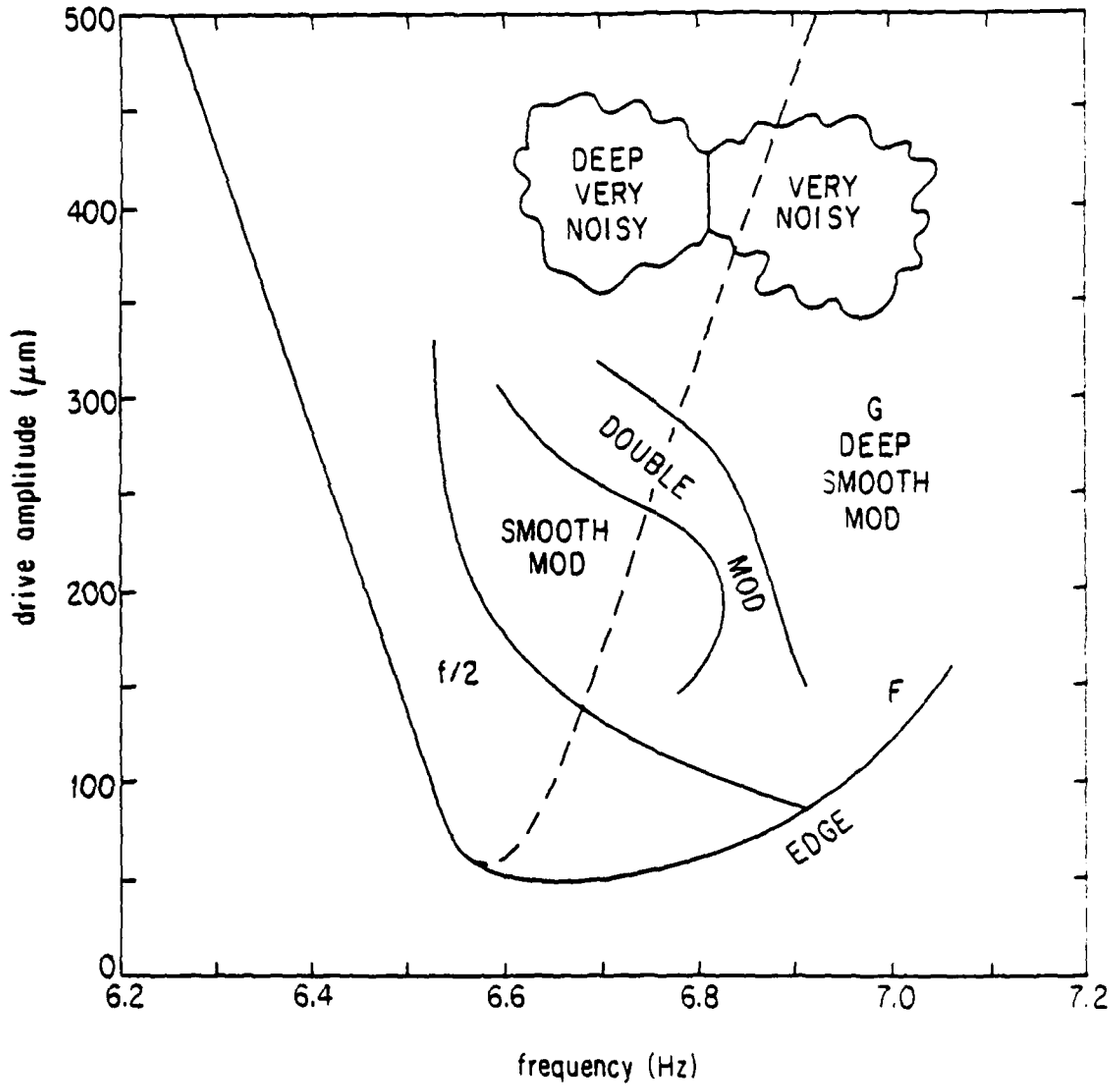


**Figure 69(b). Modulation boundaries for the 11th mode.**

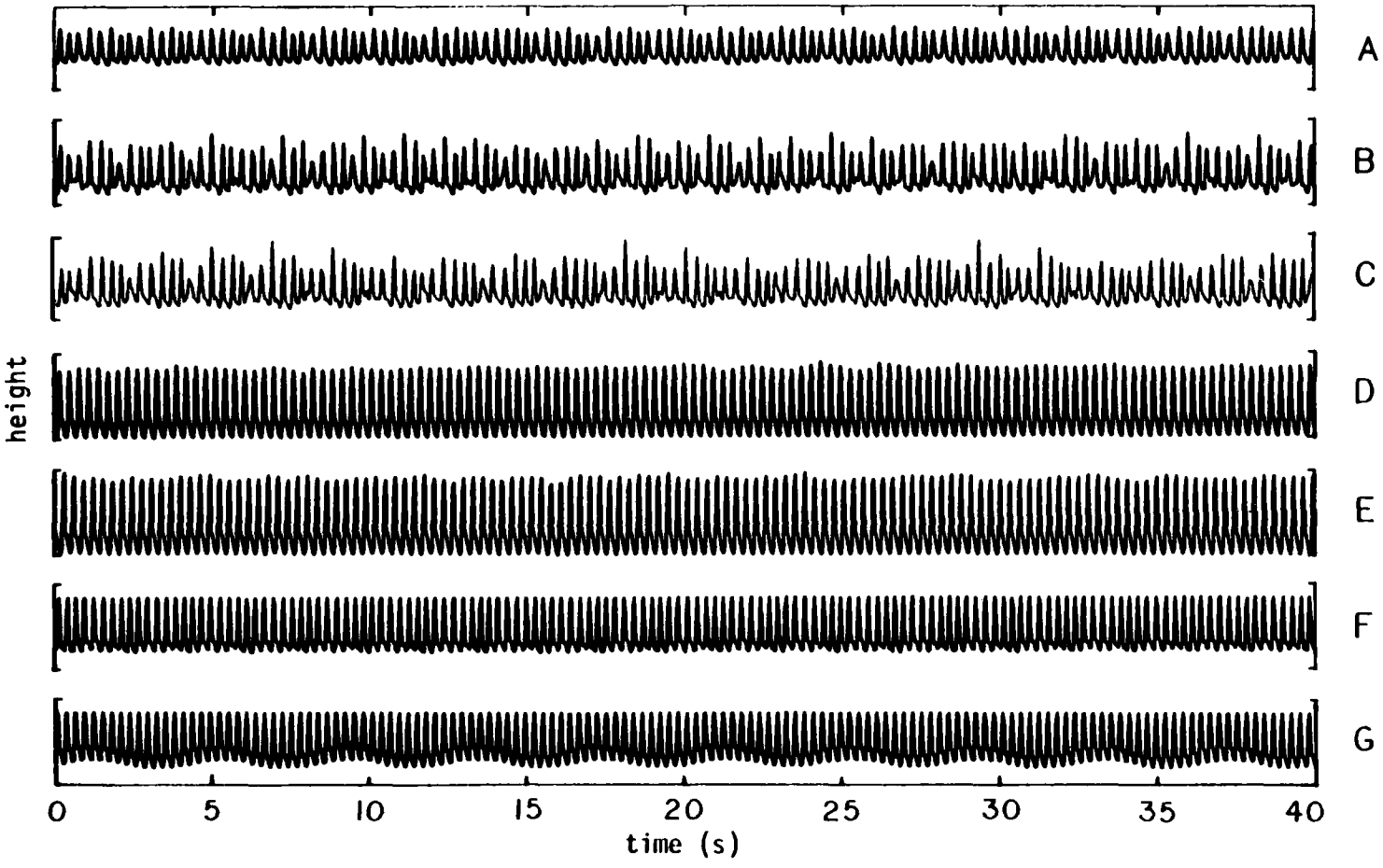


**Figure 70. Time records taken during the helium frequency sweeps. (F and G are clipped.)**

Table 2
Periodicities of Time Records

| Record | Drive Amplitude (μm rms) | Drive Frequency, f (Hz) | Modulation Frequency, $f_m$ (Hz) | $f/f_m$ |
|---|---|---|---|---|
| A | 150 | 6.1847 | 0.5496 | 11.253 |
| B | 300 | 6.1988 | uncharacterized | - |
| C | 250 | 6.2500 | 0.08929 and 0.5357 | 70 and 70/6 |
| D | 250 | 6.4500 | small noise floor | - |
| E | 300 | 6.4588 | small noise floor | - |
| F | 150 | 7.0000 | 0.5366 | 13.05 |
| G | 300 | 7.0000 | 0.2512 | 27.87 |

reduced from the computer records, strip chart, X-Y chart, and time records to make these plots. The point here is to show that this nice simple fluid in a simple container shaking sinusoidally can have lots and lots of structure. Some transitions were probably missed, especially those that run parallel to the f axis since only six $A_d$ sweeps were made. The capital letters indicate the positions on the $A_d$ - f plane that the time records shown in fig. 70 were taken. Unfortunately, some of these records are clipped, but their periodicity still can be determined from their FFT's, which is listed in Table 2.

Three distinct states exist for the same drive parameters in the neighborhood of 6.9 Hz and 300 μm rms. The states shown by the circle, square, and triangle in fig. 67 can be reached by: circle -- going up the crotch between the 11th and 12th modes; square -- starting in the crotch between the 10th and 11th modes and sweeping f up; and triangle -- starting in the crotch between the 9th and 10th modes, sweeping f up, following the 10th mode's surface until falling off the edge, and, for some unknown reason, "punching through" the 11th mode's surface into another state. In nonlinear dynamics jargon, there are at least three domains of attraction for the same parameter values.

## Section 10. Smooth Modulations vs. Cockscombs

Cockscombs are more likely to be seen than smooth modulations in water in the small plastic annular trough, in normal helium, or at high drive amplitudes. The opposite is true of water in the large glass trough, superfluid helium, and low drive amplitudes. Thus, cockscombs seem to be the preferred instability for low Q, high drive amplitude systems, while smooth modulations are preferred in high Q, low drive amplitude system. The high Q systems allow data to be taken near the tip of the hyperbolas described in Appendix 2, with lower drive levels. Perhaps this is the necessary condition to see smooth modulations.

### 10a. Shock ideas.

Smooth modulations were presented as three wave interactions, on p. 140, while cockscombs were suggested to be solitons on, p. 77, or the result of a conspiracy theory on, p. 106. But, it is difficult to tell whether the waveform analyzed with video tape, fig. 60 on p. 133, was a smooth modulation or a cockscomb since the envelope is rather asymmetric; it takes quite a bit longer to rise than it does to fall. Are smooth modulations and cockscombs different limits of the same thing?

Perhaps the rounded envelope of the smooth modulation distorts

into the squarish envelope of the cockscomb, leaning forward then dropping precipitously, as if the modulation develops a shock front. This is incompatible with the soliton idea, where an extra $180^{o}$ "kink" of phase would suddenly appear, though remember that the extra phase shift was not seen under cursory examination of the video tape described on p. 79.

They share some common features. Both have frequencies near the fundamental of the trough. Either can oscillate independently of or phase lock onto the drive -- typically cockscombs lock but smooth modulations do not. And both become more complicated as the drive amplitude is increased; smooth modulations develop more "sausages" and cockscombs develop more "sudden drops" with more drive.

Only once -- perhaps -- by eye did I see a gradual transition from smooth modulation to cockscomb, playing with water in the glass trough; unfortunately I made no measurements. This remains a particularly loose loose end. However, in helium smooth modulations do occur at low drive amplitude and cockscombs at high. The change in behavior was always seen to be discontinuous, perhaps because the system jumps to another overlapping sheet of a different mode, discontinuously slipping in or out an extra half wavelength of f/2 to be modulated, as described in Sec. 9.

## 10b. Simultaneous Smooth Modulations and Cockscombs

Smooth modulations and cockscombs can exist simultaneously and

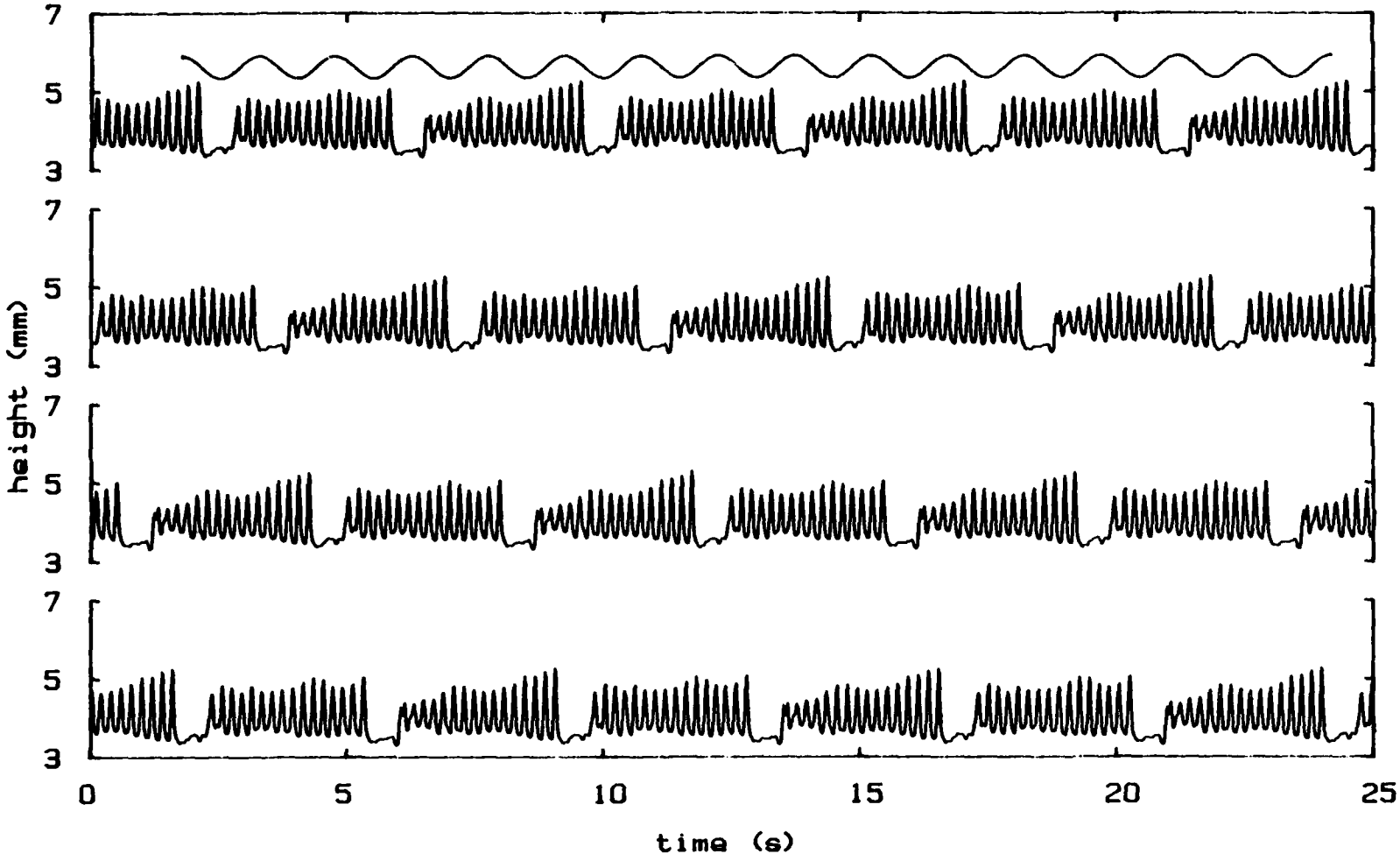


Figure 71. Simultaneous smooth modulation and cockscomb phase locked, in 3.47 mm of helium at 3.21 K driven at 10.200 Hz with 24.4 μm rms amplitude. The sine curve is a guide to see the smooth modulation.

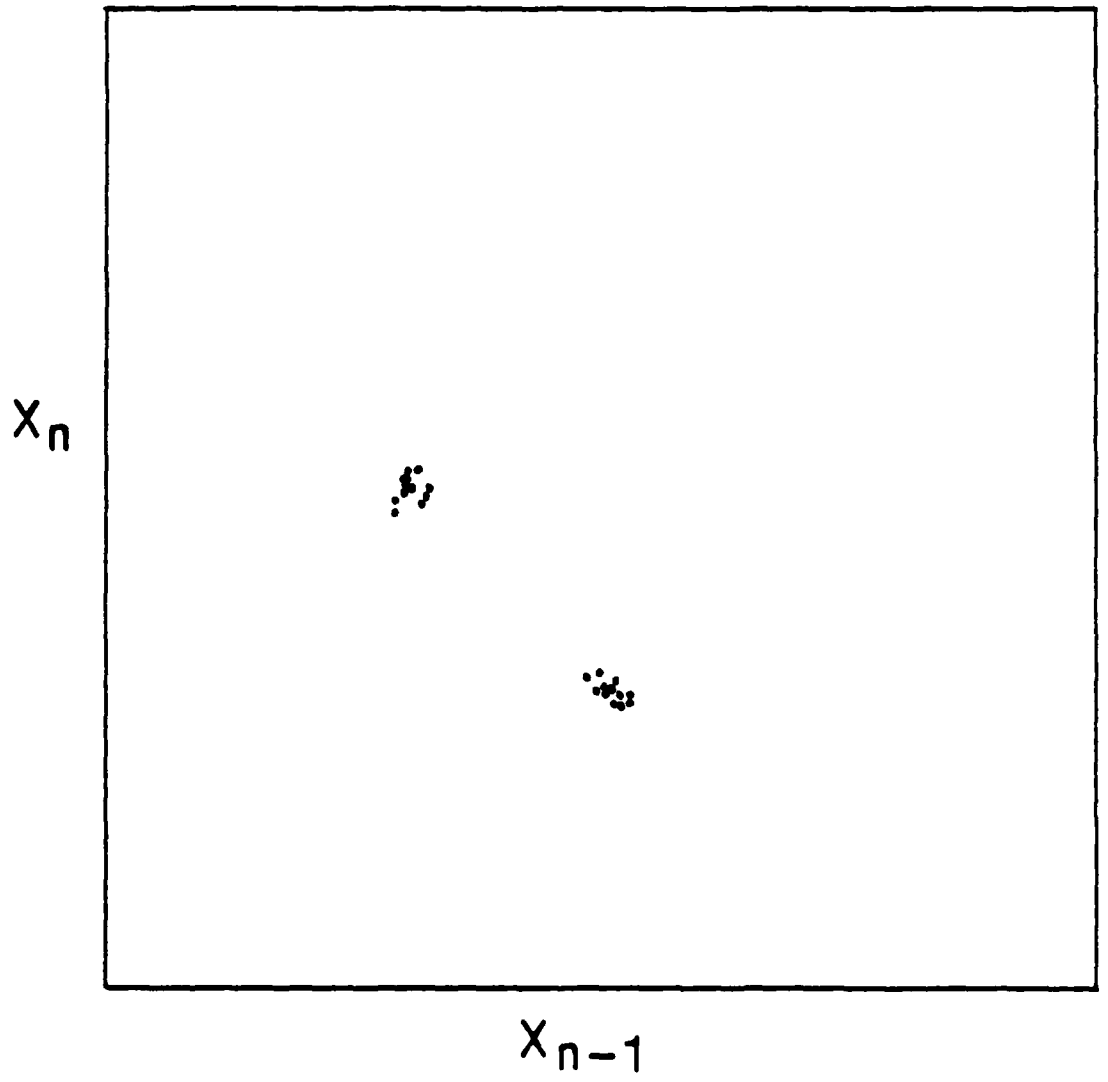


Figure 72. Return map for the previous figure, made by sampling once per cockscomb.

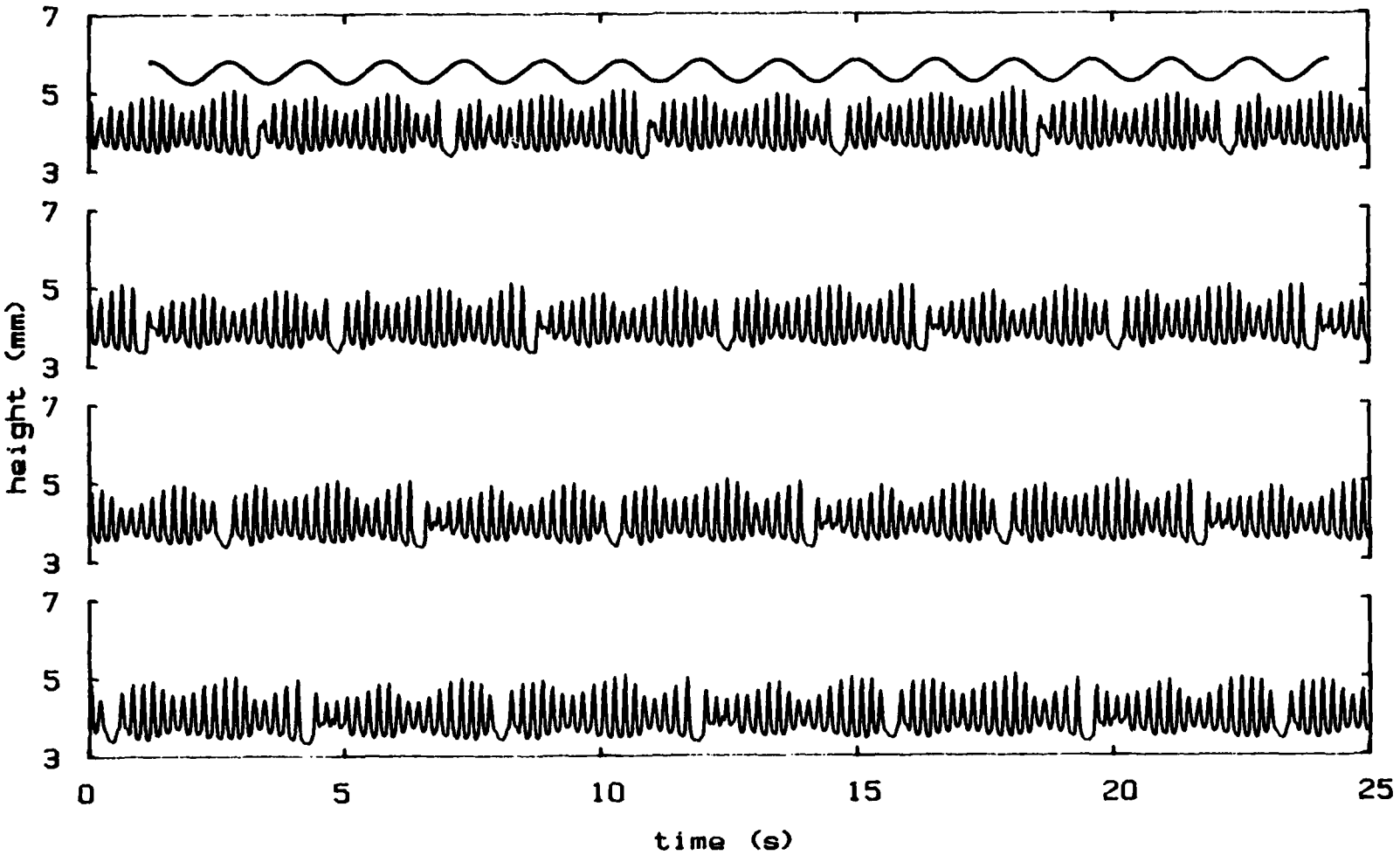


Figure 73. Simultaneous smooth modulation and cockscomb unlocked, in 3.47 mm of helium at 3.21 K driven at 10.000 Hz with 24.8 μm rms amplitude. The sine curve is a guide to see the smooth modulation.

turn out to be remarkably decoupled. Figure 71, obtained by driving the helium resonator at 10.20 Hz, shows a (presumably) double sausaged smooth modulation and cockscomb phase locked in a 5:2 ratio with the cockscomb phase locked to the f/2 of the drive in a 19:1 ratio. The sine wave in the figure is a guide to help the eye see the smooth modulation. The return map of fig. 72, made by sampling every 19th cycle of f/2, shows that all the frequencies are indeed locked. Had any of the frequencies been unlocked, the dots would not have clustered in two groups. That there are two groups shows that every other cockscomb is different -- the effect of the five cycles of the modulation that occur during two cycles of the cockscomb.

I first interpreted this waveform as a cockscomb that underwent a period doubling bifurcation, but I no longer do because when the drive frequency was changed to 10.00 Hz, braiding in the continually running strip chart (not shown) indicated that one frequency had unlocked. The smooth modulation, again indicated by the sine wave, and the cockscomb are seen unlocked in fig. 73. The ratio of their frequencies, obtained by counting cycles in the time record, is now 2.484. That the ratio can be so close to 5/2 and yet not locked to it shows how little coupled these two phenomena can be. The smooth modulation apparently cares little that the cockscomb so nearly zeros the amplitude. The cockscomb, however, stayed locked onto the drive (determined by noting the positions of the sudden drops relative to the drive).

It is not unreasonable that a cockscomb is more likely than a

smooth modulation to lock onto the drive, because of the sharp edge of the cockscomb's sudden drop. Whether the drop lands on a crest or trough of f/2 substantially affects the cockscomb's shape, and probably therefore its frequency, which is the key condition for phase locking as emphasised by Appendix 4. A smooth modulation, lacking sharp features, is little changed by shifting its phase relative to the drive. Pippard discusses a similar case on p. 405 of his book (1978). Relaxation (square wave) oscillators are more likely than class C (sine wave) oscillators to lock subharmonically to an external frequency.

Later in the same run, a phase locking transition was seen on the strip chart when the drive amplitude was swept with the drive frequency held fixed at 10.00 Hz, the temperature again at 3.21 K, and the height at 3.47 mm. The beat frequency seen in the strip chart is plotted in fig. 74. It has the classic phase lock signature of two frequencies smoothly approaching each other, becoming identical over a finite range, and departing again as some parameter, here the drive level, is smoothly varied. (The beat frequency is arbitrarily plotted going from above to below the axis.) In the phase locked region, the waveform was a triple cockscomb with every other cycle different, shown in fig. 75. In the unlocked region, fig. 76, it is hard to tell what is happening, but notice big and little chunks of the cockscomb labeled B and L. Twice in the record the sequence changes from LBLB to BLBL or back. This may be a smooth modulation interacting with a cockscomb again -- the parameters are nearly the same -- but I cannot

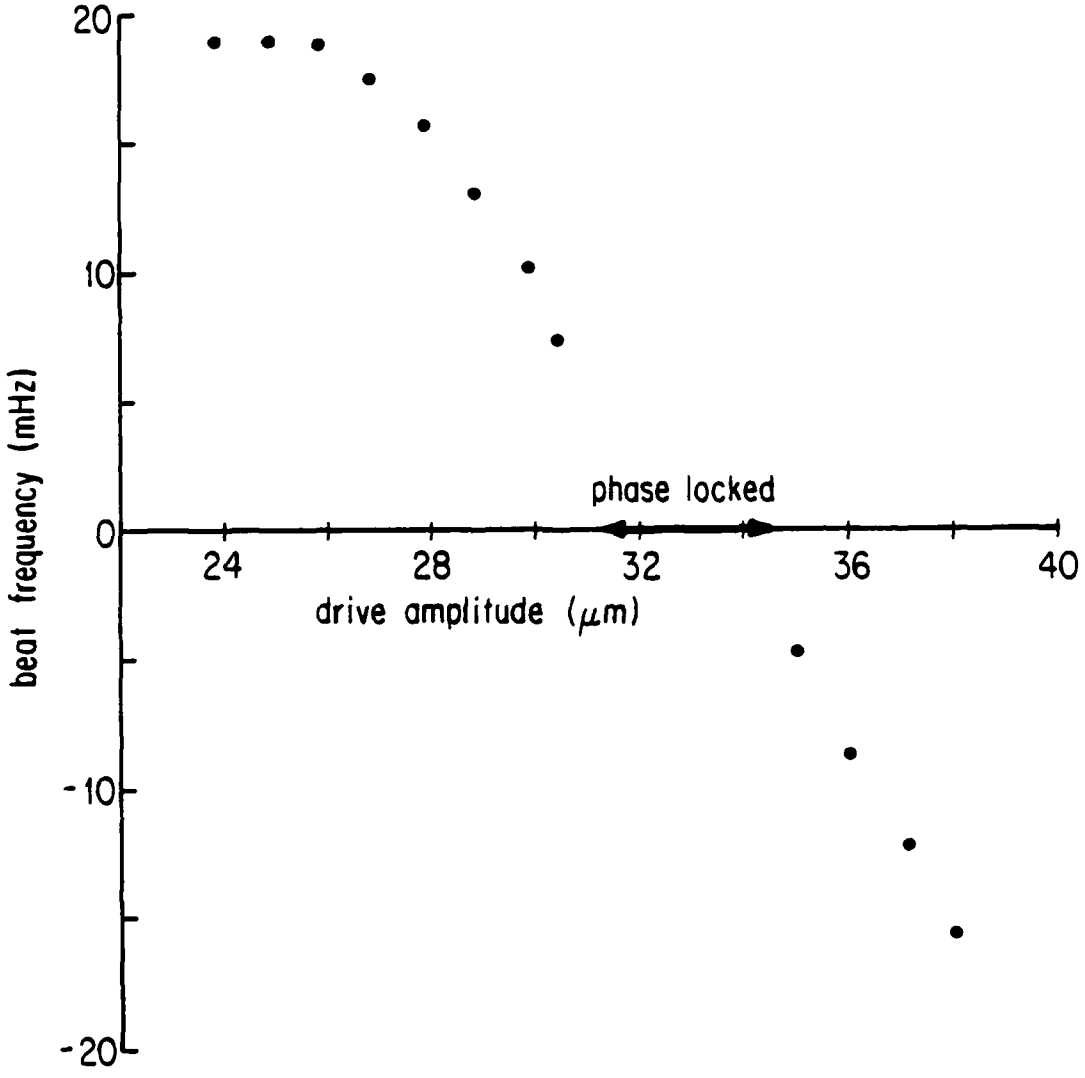


**Figure 74. Phase locking transition in 3.47 mm of helium at 3.21 K driven at 10.000 Hz.**

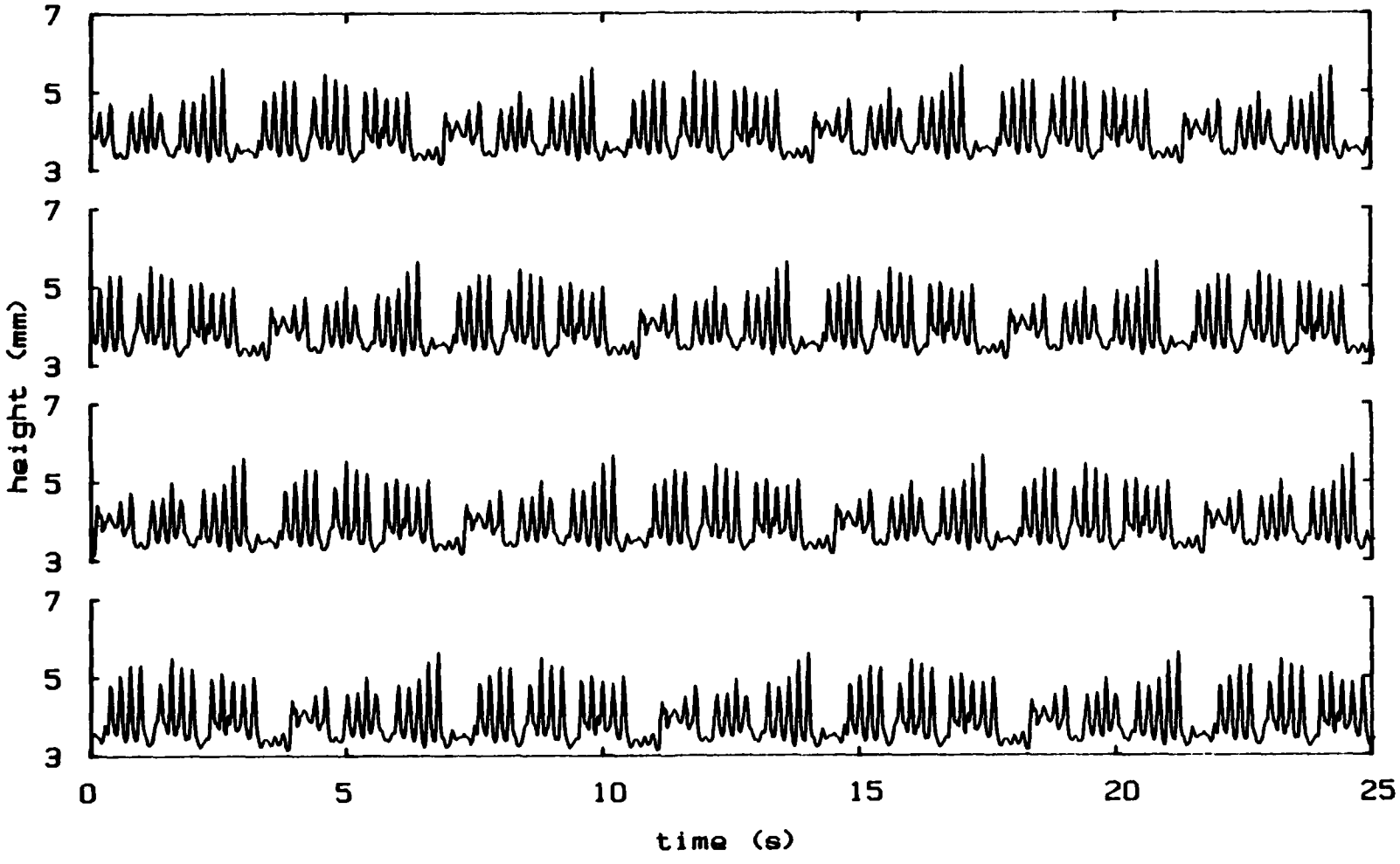


Figure 75. A waveform in the locked region, at 32.9 μm rms amplitude.

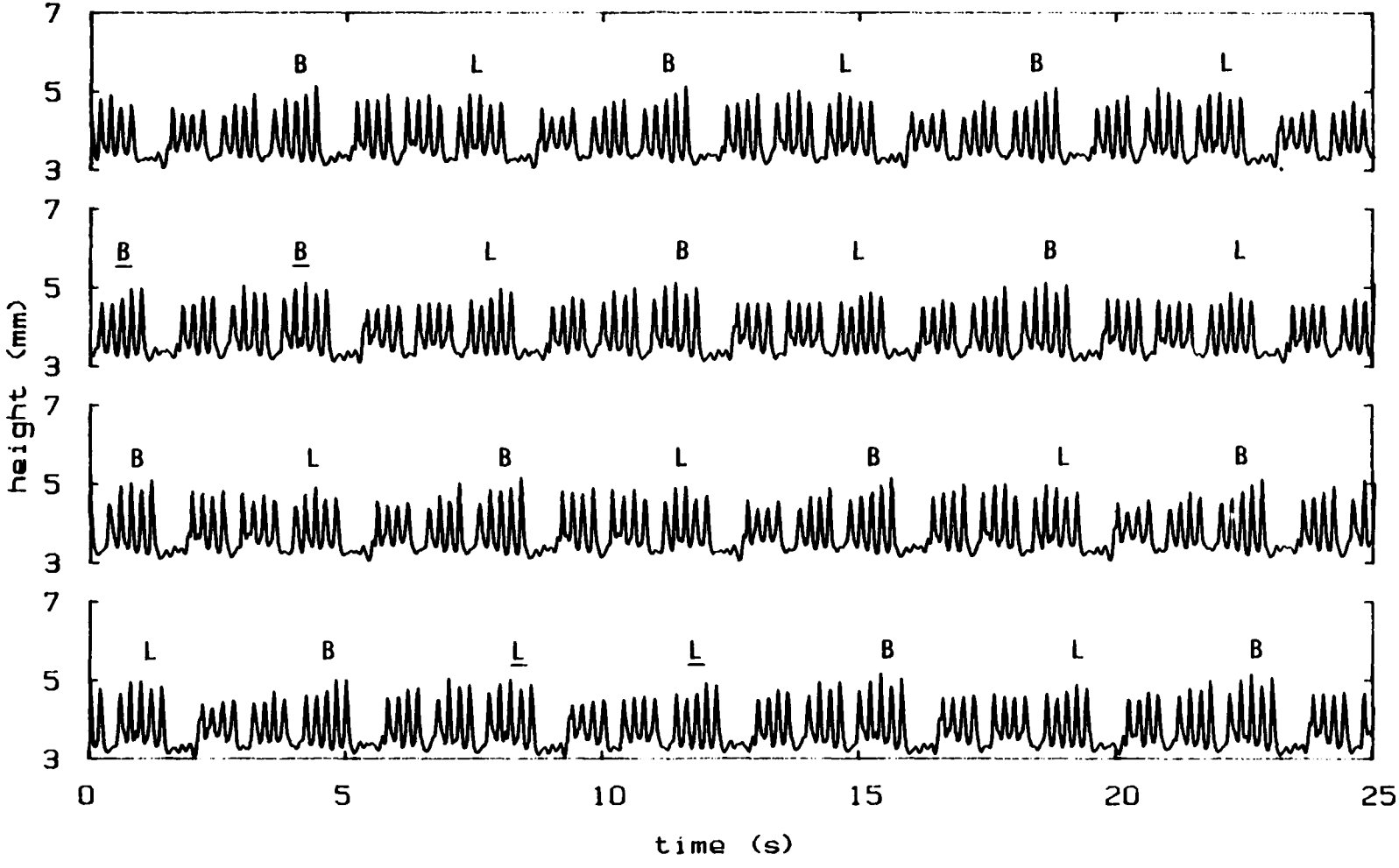


**Figure 76. A waveform in the unlocked region, at 25.8 μm rms amplitude.**

say. A phase locking transition like this (or the one mentioned on p. 149) is the most compelling argument that quasiperiodicity, described in Sec. 8, exists in this system.

## Section 11. Loose Ends and Future Experiments.

Spatial observations are crucial. Long ago I should have stopped using the annular resonator when using water -- you can't see what's going on. As this was only lately appreciated, an embarrassing large number of questions remain in this experiment. Many can probably be quickly resolved by applying the technique of digitizing a video tape made with a straight glass trough, used with smooth modulations on p. 127 and Appendix 6, to the other types of behavior.

What are the sudden drops? This is the outstanding question on cockscombs. Are they a "kink" soliton with $180^0$ across them, or a gradual rise then sudden fall of the spatial phase, or something else? One good video could settle this.

Are the ultra deep modulations a slow transfer of energy back and forth between two adjacent modes? This is perfect for the video technique.

Are double sausaged smooth modulations due to a triad involving the second mode? Just find one in water, apply the technique, and see whether the second mode predominates over the first.

The conspiracy theory offered for the subharmonics of the paddle driven trough could probably be enhanced with a modal description, which would be provided by the video technique. Perhaps the nature of

the braiding would then become clear.

After exploiting the video technique to clarify the physics of the various modulations, the locations and nature of the transitions to the various modulations should be mapped in the drive amplitude - drive frequency plane using helium, because helium is free of wetting problems at the walls. Do ultra deep modulations really occur at the crossings of the instability hyperbolas and is the value of kh (and therefore the type of nonlinearity) important? Where do smooth modulations of various numbers of sausages occur? Where do they phase lock? Are the smooth modulation transitions hysteretic and can they display the period doubling route to chaos in a very narrow range? Do smooth modulations gradually turn into cockscombs as the drive amplitude is increased? How and where do cockscombs acquire and discard various numbers of sudden drops?

An experiment which should still be done, and one that my mentor is especially keen on, is a very slow drift through the lambda point, particularly while observing chaos.

The chaos that is always seen at large enough drive amplitude should be characterized and some connection to the work done by nonlinear dynamicists should be made. It would be nice to see a so-called strange attractor and to know its dimension.

The pendulum on p. 91 could be easily constructed, parametrically driven, and studied. Perhaps it is a good model of ultra deep modulations.

On a theoretical level, what determines the response amplitudes, response frequencies, and drive thresholds of the various modulations? Can the data from the smooth modulation videos on p. 134 be shown to be a solution of the Navier-Stokes equation merely by substitution?

By far, not all of the parameter space of drive amplitude, drive frequency, liquid height, and temperature (when using helium) has been explored. Several other behaviors were glimpsed and not cataloged here; there are probably many more.

There is a generous amount of work for the next person.

## REFERENCES


T.B. Benjamin and F. Ursell, 1954, "The stability of the plane free surface of a liquid in vertical periodic motion," Proc. Roy. Soc. London, Ser. A 225, 505-515.

S. Ciliberto and J.P. Gollub, 1984, "Pattern competition leads to chaos," Phys. Rev. Lett. 52, 922-925; and 1984, "Chaotic mode competition in parametrically forced surface waves," preprint submitted to J. Fluid Mech.

M. Faraday, 1831, "On a peculiar class of acoustical figures; and on certain forms assumed by groups of particles upon vibrating elastic surfaces," Philos. Trans. Roy. Soc. London, 299-340.

D. Heckerman, S. Garrett, G.A. Williams, and P. Weidman, 1979, "Surface tension restoring forces on gravity waves in narrow channels," Phys. Fluids 22, 2270-2276.

J. Heiserman and I. Rudnick, 1976, "The acoustic modes of superfluid helium in a waveguide partially packed with superleak," J. Low Temp. Phys. 22, 481-499.

J.S. Imai and I. Rudnick, 1969, "High-frequency acoustical interferometer," J. Acoust. Soc. Amer. 47, 1144-1147.

L.D. Landau and E.M. Lifshitz, 1959, Fluid Mechanics 1st ed. (Pergamon Press, Oxford).

L.D. Landau and E.M. Lifshitz, 1976, Mechanics 3rd ed. (Pergamon Press, Oxford).

A. Larraza and S. Putterman, 1984, "Theory of non-propagating surface-wave solitons," J. Fluid Mech. 148, 443-449.

G.B. Lubkin, March 1981, "Period-doubling route to chaos shows universality," 17-19.

J.B. Marion, 1970, Classical Dynamics of Particles and Systems, 2nd ed. (Academic Press, New York).

J. Mathews and R.L. Walker, 1970, Mathematical Methods of Physics, 2nd ed. (W.A. Benjamin, Inc., Menlo Park, California).

L. Matthiessen, 1868, Pogg. Ann. 134; and 1870, Pogg. Ann. 141.

J.W. Miles, 1976, "Nonlinear surface waves in closed basins," J. Fluid Mech. 75, 419-448.

J.W. Miles, 1984(a), "Resonant motion of a sperical pendulum," Physica 11D, 309-323.

J.W. Miles, 1984(b), "Parametrically excited solitary waves," J. Fluid Mech. 148, 451-460.

A.B. Pippard, 1978, The Physics of Vibration, Vol. 1, 1st ed. (Cambridge Univ. Press, New York).

Lord Rayleigh, 1883(a), "On maintained vibrations," Philos. Mag. 15, 229-235; and 1894, The Theory of Sound 2nd ed. (Dover, New York, 1945), Sec. 68 b; and 1887, "On the maintenance of vibrations by forces of double frequency, and on the propagation of waves through a medium endowed with a periodic structure," Philos. Mag. 24, 145-159.

Lord Rayleigh, 1883(b), "On the crispations of fluid resting upon a vibrating surface," Philos. Mag. 16, 50-58.

Lord Rayleigh, 1896, The Theory of Sound 2nd ed. (Dover, New York, 1945), the cutoff frequency for aerial vibrations in a rectangular tube is discussed in Sec. 268.

J. Wu, R. Keolian, I. Rudnick, 1984, "Observation of a nonpropagating hydrodynamic soliton," Phys. Rev. Lett. 52, 1421-1424.

J. Wu and I. Rudnick, 1985, "Amplitude dependent properties of a hydrodynamic soliton," to appear in Phys. Rev. Lett.

AD-A157 958 MODULATIONS OF DRIVEN NONLINEAR SURFACE WAVES ON WATER AND LIQUID HELIUM-4(U) CALIFORNIA UNIV LOS ANGELES DEPT OF PHYSICS R M KEOLIAN JUN 85 TR-44 N00014-85-K-0370 3/3

UNCLASSIFIED F/G 20/4 NL

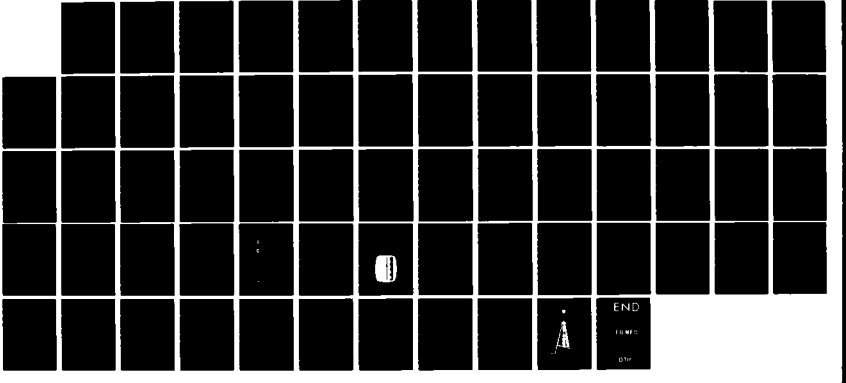

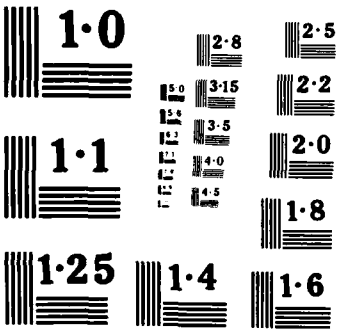

## Appendix 1

### Bending of Tuning Curves

At small but finite amplitudes, driven nonlinear oscillators -- for instance, a mass on a nonlinear spring, a pendulum, or the modes of surface waves -- can display hysteresis with a direct drive; there are two stable states for the oscillator over a range of drive amplitude and frequency. The hysteresis can be conveniently understood in terms of bent tuning curves, which, as usual, is fully and clearly explained in Pippard's book (1978, p. 12 and p. 248), and also in Landau and Lifshitz Mechanics (1976, p. 87).

It is helpful to consider the potential energy of the oscillator. Consider a mass that moves in a one dimensional potential well that deviates at large amplitudes from the parabolic shape it has at small, as in fig. 77. In (a), the well bends upward from the parabola and the mass completes a round trip in less time at high amplitude than at small because of the steepening walls or extra restoring force. This is called a hardening nonlinearity. The inverse of the round trip time is the nonlinear resonant frequency, which, plotted as line $f_{nl}$ in fig. 78, bends to the right. If instead the well bends downward, as in fig. 77(b), the round trip time increases at higher amplitude and $f_{nl}$ would bend to the left. This is a softening nonlinearity. Because the amount of time the mass can spend near a softening turning

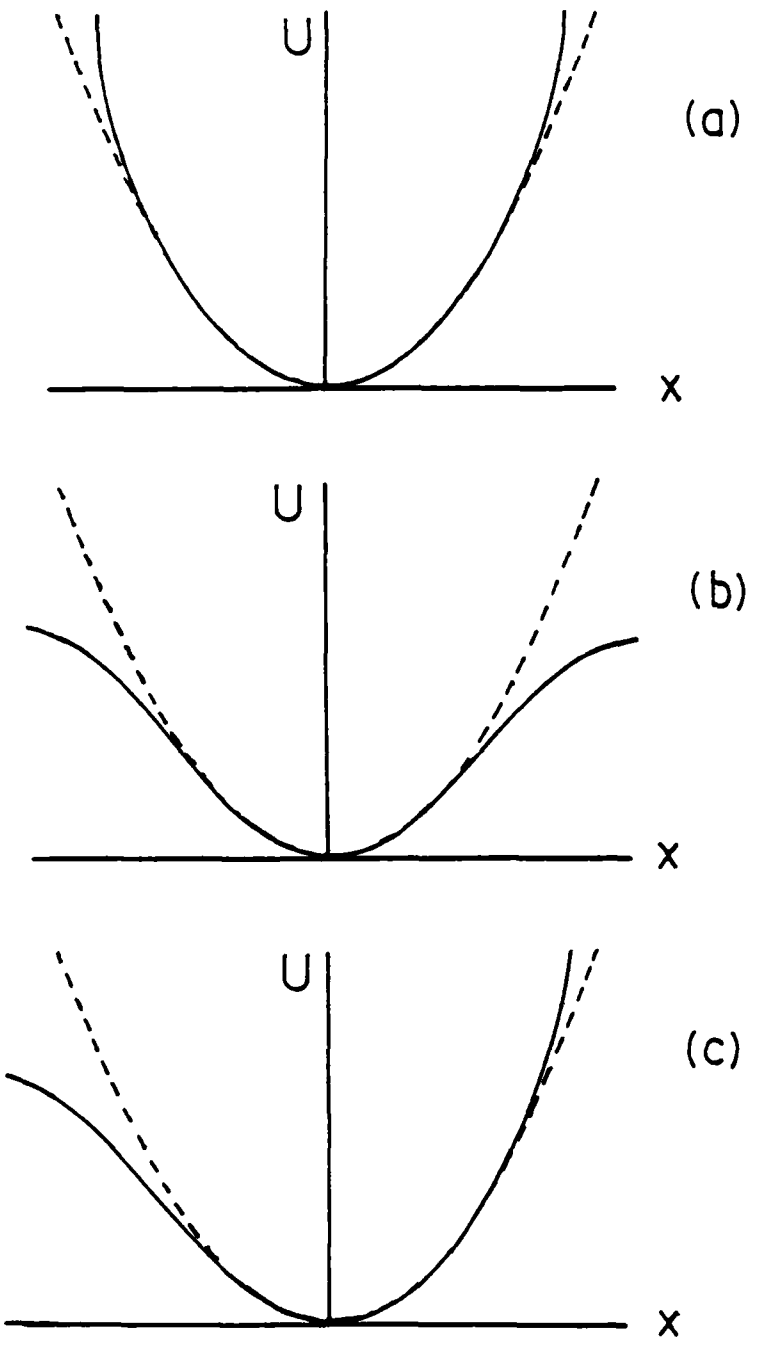


**Figure 77. Some potential wells for a one dimensional oscillator.**

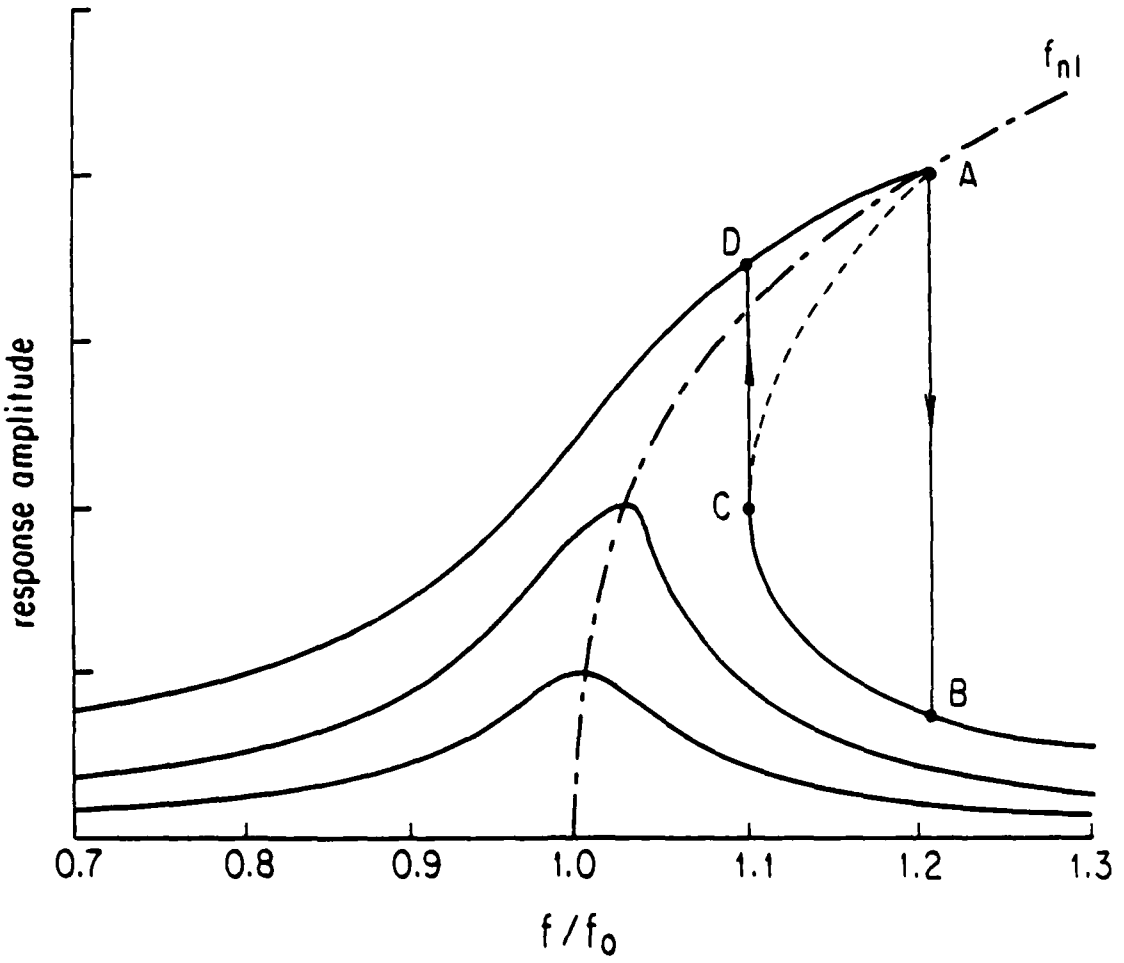


**Figure 78. Tuning curves for a hardening nonlinearity, drawn with a Q of 10.**

point can be quite long, but the time saved near a hardening turning point can at most be half the small amplitude period, asymmetric wells like (c) tend to be softening on the whole. (A more complicated well is discussed in Appendix 3.)

Let us now give the mass some linear damping and drive it directly, rather than parametrically, with a sinusoidal force. At infinitesimal drive amplitude, the tuning curve -- the response amplitude plotted vs. drive frequency for fixed drive amplitude -- has the familiar form, the lowest curve of fig. 78. As the frequency is swept, the phase of the oscillator shifts from $0^{o}$ to $180^{o}$ with respect to the drive from the left to right sides of the resonance. The tuning curve can be thought of as the locus of points of no amplitude growth. The amplitude grows inside and decays outside the curve until the curve is met. (Actually, the amplitude is not enough to specify the state of the oscillator so this presumes it already has the equilibrium phase.)

If the drive level is increased to a value less than is needed for something more complicated to happen, the motion is periodic with the period of the drive, though not strictly sinusoidal. The amplitude of the mass still goes through resonance as the frequency is swept, but now at a resonant frequency that changes with response amplitude. A family of tuning curves for various drive amplitudes are sketched in fig. 78, and bend to the right, following $f_{nl}$.

At high enough drive amplitude, something interesting happens:

the tuning curve can bend over enough to become triple valued. If the frequency is increased from below resonance, the response amplitude follows the highest curve until point A of fig. 78. As the frequency is increased beyond this, the amplitude suddenly and irreversibly drops to B, accompanied by a jump in the oscillator's phase with respect to the drive. The amplitude then follows the curve on to higher frequencies. If the frequency is then lowered, nothing special happens when point B is crossed, but there is another discontinuous jump from C to D. At frequencies between the two jumps, the amplitude can have either of two values depending on the drive's past history. The amplitude is unstable on the dashed line; if the amplitude should fluctuate above or below the line, it grows or decays to the upper or lower branch, because amplitudes grow when they are inside tuning curves and decay when they are not (presuming again that the oscillator already has the proper phase).

The apparatus shown in fig. 79 demonstrates a tuning curve that hardens. A loudspeaker horizontally drives a pair of rubber bands, knotted together and stretched vertically to slightly over their unstretched length. As the drive frequency is slowly increased into the first resonance, the knot oscillates vigorously with an amplitude of several cm. With such a large amplitude, the tension in the rubber bands increases substantially, giving an additional restoring force which starts off cubic in the displacement. Increase the frequency beyond around 40 Hz, and the amplitude will dramatically drop to only 1 cm. Lower the frequency, and the amplitude rises slightly, then

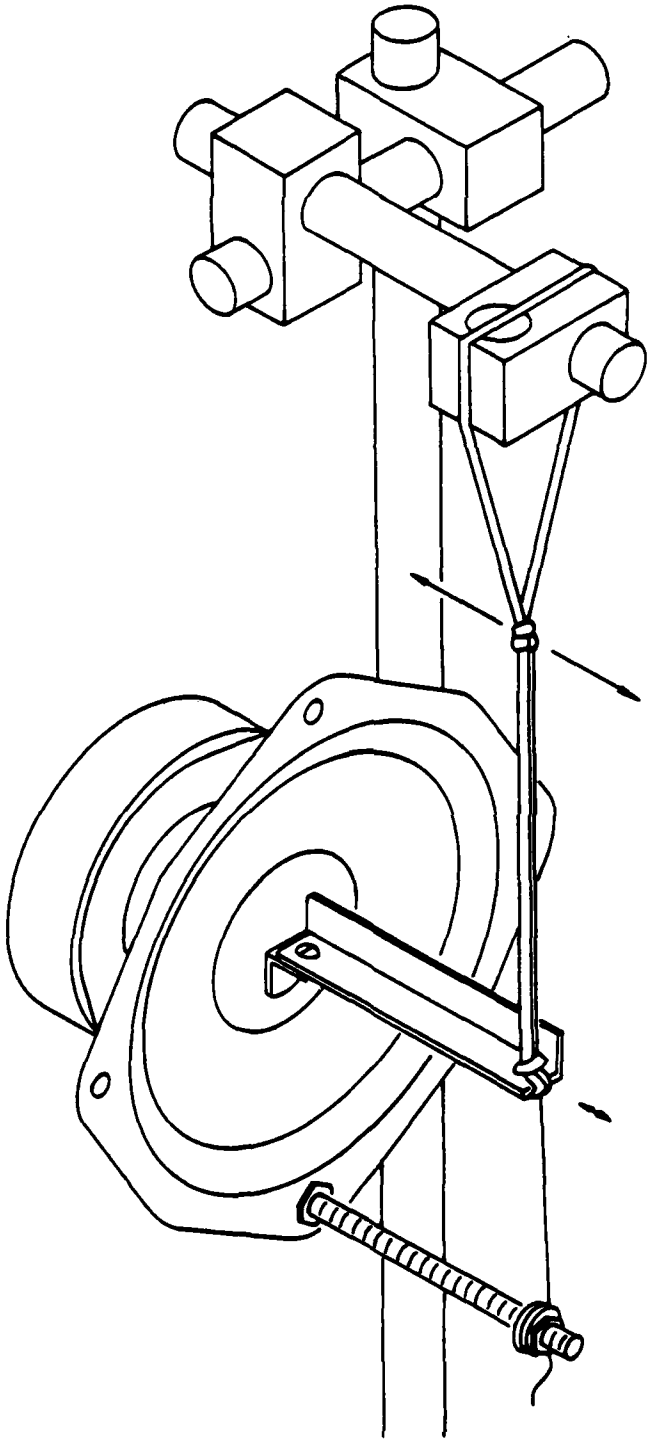

Figure 79. Apparatus to demonstrate bent tuning curves.

suddenly jumps to the upper branch at around 36 Hz. Bring the frequency back to 38 Hz and the amplitude will be large. Squeeze the rubber band and it will go to the small amplitude state. Pluck it, and the amplitude will again be large.

A couple tricks to make sure it works: Spread the top rubber band out in the plane of the speaker cone as shown to break the degeneracy between the driven mode and the other mode with sideways motion perpendicular to the shaft. If you do not, you will have a nice demo of quasiperiodicity, similar to the hanging chain in Sec. 5. By making the initial tension in the rubber bands small, the nonlinear effect is made large. Select a loudspeaker with sufficient excursion; the drive amplitude is a few mm. I like to epoxy a small bracket with a threaded hole to the speaker cone, so that the shaft and other demos can be easily interchanged. A string attached to a bolt below the shaft balances the tension in the rubber bands to keep the voice coil in the speaker from rubbing. Finally, a sheet of black paper behind the rubber bands makes them more visible.

## Appendix 2

## Parametrics

From what I can tell, there are a handful of ideas that keep coming up with nonlinear oscillators, and one of the most important is parametrics: the transfer of energy from one system by oscillating a parameter of another, first recorded by Faraday. For example, energy can be fed to the horizontal motion of a pendulum by vertically oscillating its point of support (take a peek at fig. 88 of the next Appendix), or a mass can be made to oscillate on a spring by oscillating the value of the spring constant, without directly applying a force to the mass. Parametrics turns up in directly driven nonlinear oscillators, too -- Landau and Lifshitz (Mechanics, 1976, page 90) discuss the parametric resonance that occurs between various nonlinear terms when a mass on a spring undergoes subharmonic response. In the case of quasiperiodicity of the spherical pendulum described in Appendix 5, I don't know if it is a general principal, or even a correct one, but I like to think of the extra frequency that appears in the motion as being due to the two modes taking turns parametrically driving each other. And I suspect that most of the threshold behavior seen in many nonlinear systems is somehow tied to the thresholds for growth associated with parametrically driven systems.

Experimentally, parametrics provides a good way of obtaining large response out of a system. If it works at all, the response grows exponentially until something limits the growth. Nonlinearities are guaranteed to be important.

The early drive amplitude and frequency sweeps in water long remained a mystery until I studied parametrics. The information came from Pippard (1978), Landau and Lifshitz Mechanics (1976), Benjamin and Ursell (1954), and Mathews and Walker (1970). This Appendix is meant to supplement Pippard with some more figures.

Consider for the moment a lossless, linear, one dimensional system with resonant frequency $f_0$ -- for instance, a mass on a spring. There is no external force applied directly to the mass. Instead, perturb the system with drive amplitude $A_d$ and drive frequency f by oscillating one or more of the parameters that determine the resonant frequency -- for instance by giving the spring a time dependent spring constant $k(1+\beta\cos 2\pi ft)$, $\beta$ proportional to $A_d$. Then if f is close enough to $2f_0$, any initial fluctuation will set the mass oscillating with frequency f/2, with a response amplitude $A_r$ that increases exponentially in time. The range of frequencies for parametric growth increases linearly with $A_d$, starting from zero when $A_d$ is zero, as shown by the V shaped wedge in fig. 80(a). (Note the zero positions of $A_d$ and $A_r$ and that only the small region of frequency near $2f_0$ is shown.) The exponential growth rates are given by a family of hyperbolas on the $A_d$ - f plane inside the wedge, shown by the dotted line. The deeper the drive is in the wedge, the faster the amplitude

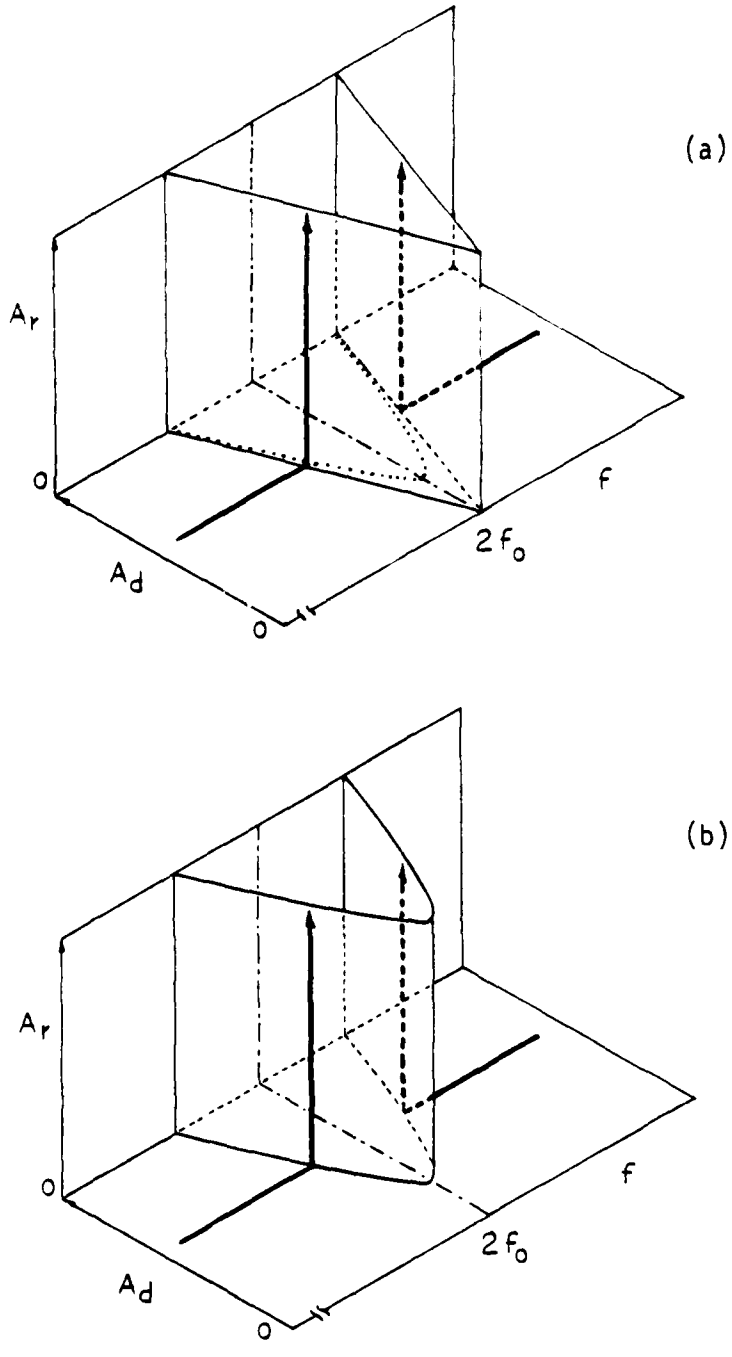


**Figure 80. Parametric instability regions for a linear system (a) without damping and (b) with linear damping.**

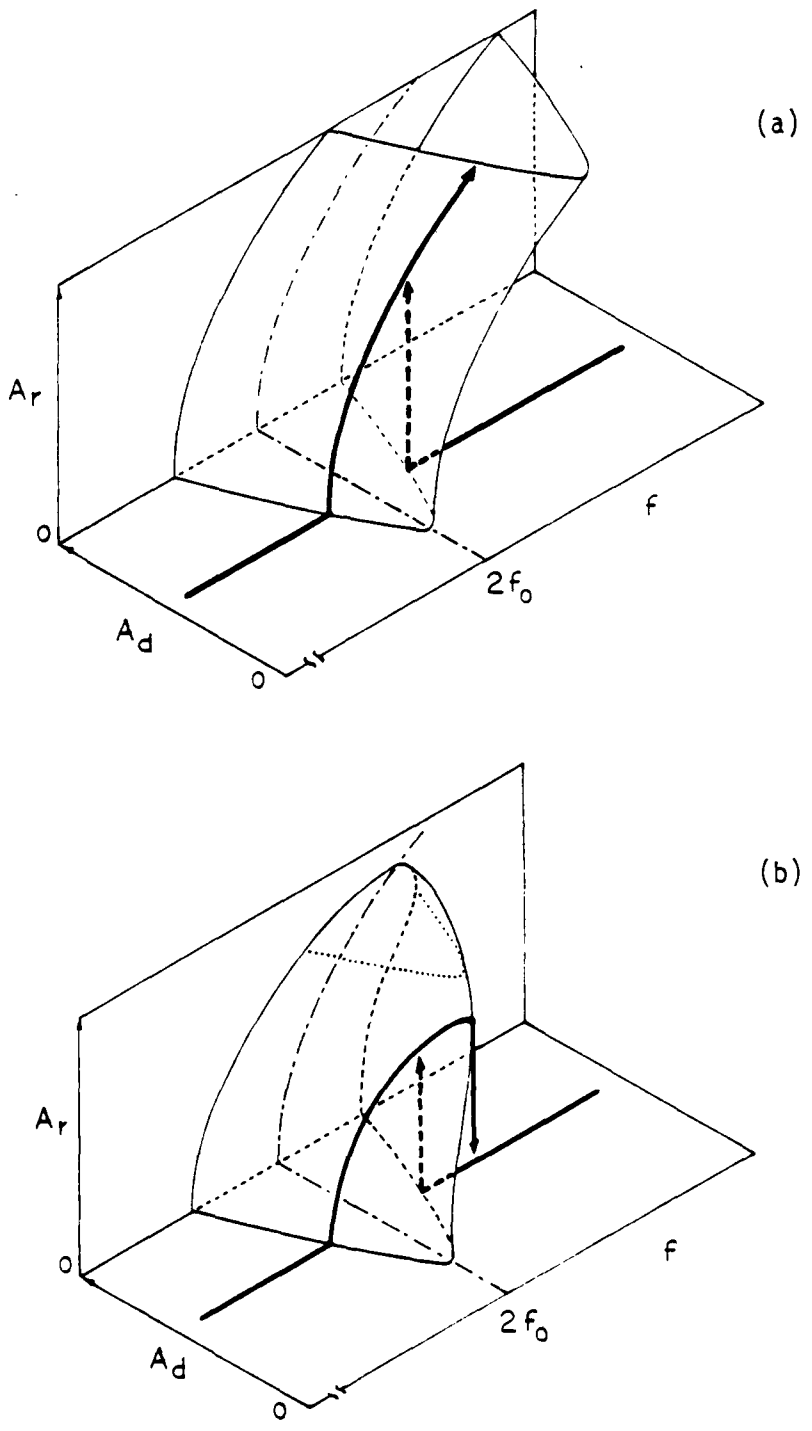


**Figure 81. Parametric instability regions for a nonlinear system (a) with linear damping and (b) with nonlinear damping.**

grows. Outside the wedge $A_r$ remains constant. Following the heavy lines, if the mass starts at rest and f is swept towards the wedge from either side while holding $A_d$ constant, the response amplitude stays small until the wedge is reached. Inside the wedge, $A_r$ rises to infinity.

If the mass m is now subjected to linear viscous damping force -bv, the motion is the same as before, except that it is multiplied by the exponential decay it would suffer if it were to free decay, $e^{-bt/2m}$. (The damping term drops out of Newton's second law with a change of variable from x(t) to $x(t)e^{-bt/2m}$ just as it would without the parametric drive.) Hence, the hyperbola with the parametric growth rate just balanced by the decay due to dissipation marks the new threshold for net growth, shown in fig. 80(b). The distance from the tip of the hyperbolic cylinder to the f axis is proportional to the dissipation; in appropriate unitless variables, the distance is a constant of order 1 (depending on the system) divided by Q, the quality factor. Inside this hyperbola the final state has infinite amplitude. Outside it, the amplitude decays to zero. This is shown again by the frequency sweeps.

The next level of complication is to add a nonlinearity to the spring, since no spring is linear to an infinite amplitude. The nonlinear resonant frequency then bends one way or another depending on the nonlinearity, as described in Appendix 1. It is shown bending to the right by the dash-dot line in fig. 81(a), and the hyperbolic cylinder instability region "flops" over following it. Sweeping up

the frequency from the left, the response amplitude is now finite near $2f_0$. As the frequency is swept up, $A_r$ follows the upper branch, rising ever higher as the frequency increases. Now, however, there is a lower branch with zero $A_r$ which can be reached by going around the tip of the hyperbola. As there are two states of $A_r$ for a given drive, the system is hysteretic. If the instability region should be reached by sweeping the frequency down from the lower branch, $A_r$ starts to rise, but as it does so it is even deeper in the instability region, and so rises even faster, until it punches through to the upper branch.

The system is still unphysical because $A_r$ can become infinite should f do the same. One reasonable possibility, however, is that dissipation goes up with response amplitude; the damping also becomes nonlinear. The minimum drive amplitude for net growth increases as response amplitude increases, so, the distance from the tip of the dotted hyperbola of fig. 81(b) to the f axis increases as $A_r$ increases. Nonlinear damping pushes the instability region backwards. Now, if the frequency is swept up the response amplitude rises to a maximum value, comes down a little, then irreversibly falls off the edge if the nonlinearity in the spring is sufficiently large compared to the nonlinearity in the damping. Coming back, the response bumps into the instability region and suddenly rises. This hysteresis loop with nonliner damping resembles the upper curve of fig. 78 of the previous appendix with a direct drive and linear damping, but there is a measurable distinction. For a direct drive, $A_r$ rises smoothly vs. f

from zero; for a parametric drive, $A_r$ rises sharply past a threshold.

Limits on $A_r$ other than these simple nonlinearities are possible. In a way, this dissertation is a study of some alternatives.

Let's look more closely at the linear case without damping. The $A_d$ - f plane of fig. 80 is reproduced in fig. 82(a). Floquet has a theorem that says that the motion has the form $e^{-ipt}P(t)$, where p is a complex constant and P(t) has the period of the drive. The imaginary and real parts of p are plotted in fig. 82(b) and (c) for a particular drive level, shown by the horizontal line in (a). As usual, two solutions to Newton's second law are needed to match initial conditions. Outside the V formed by the two straight diagonal lines in (a) the two roots are in the real part of p; inside the two roots are in the imaginary part.

Outside the V, the motion is somewhat, though not quite, like a transient that cannot decay. The motion is quasiperiodic; it asymmetrically beats against the drive in a subtle way described nicely in Pippard. If damping is added to the system, the imaginary part of p picks up a negative constant, shifting the origin of Im(p) to the horizontal line b/4πm of (b), and the motion beats and decays away at the same time.

Inside the V, the motion is phase locked to the drive at f/2 (see Appendix 4 for more details on phase locking). The straight part of Re(p) is a signature of this. Because of the phase locking, the response can take energy from the drive and grow exponentially, at a

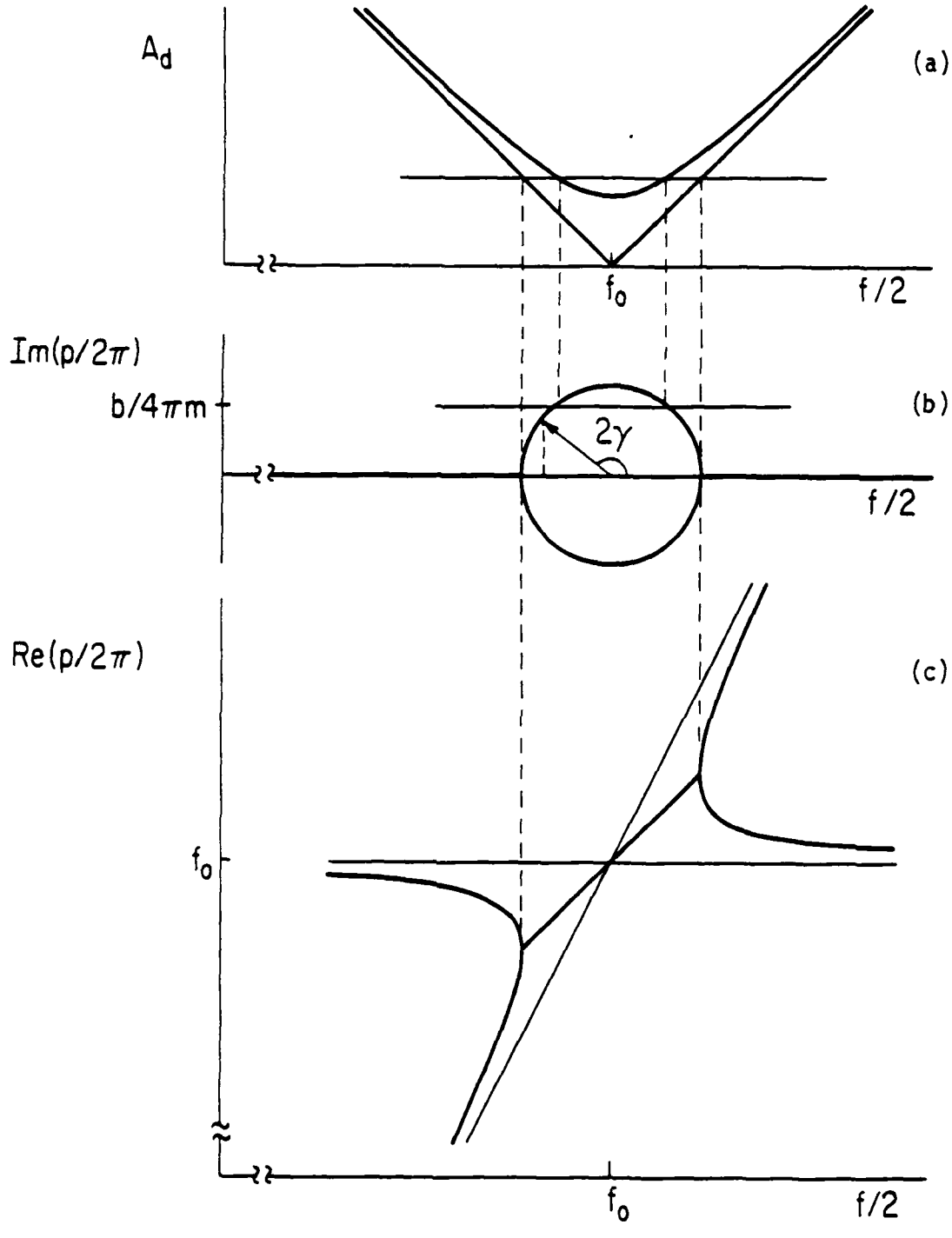


**Figure 82. Growth rate (b) and frequency (c) of parametrically excited motion for a drive amplitude given by the horizontal line in (a).**

rate given by the positive root of Im(p). There is another independent solution, necessary for matching initial conditions, with just as large exponential decay as the system gives its energy to the drive. With damping in the system and the origin of Im(p) shifted to the horizontal line, there is a positive root to Im(p) and net exponential growth only if the drive is within the hyperbola of (a).

Thus with damping there are three regions of behavior. Inside the hyperbola there is a growing and a decaying solution, both phase locked onto the drive. Between the hyperbola and the V, both solutions decay, but are still phase locked. Outside the V, the solutions are no longer phase locked to the drive, and decay at the free decay rate.

One can think in the $A_d$ - f plane: nonlinearities in the inertia or stiffness of the system move the hyperbola sideways as the response grows, and nonlinearities in the dissipation push the hyperbola away from the f axis as the response grows. The response grows until the outline of the hyperbola just touches the $A_d$ - f point given by the drive. Typically, the distance the hyperbola moves in either direction is second order in response amplitude. It is interesting to note that if the point is close enough to the tip of the hyperbola, the distance the hyperbola needs to move sideways is second order in the distance it needs to move away from the f axis in order to touch the point. Hence, close to the tip nonlinearities in the damping typically dominate over nonlinearities in the spring, and frequency sweeps are not hysteretic.

The phase $\gamma$ of the response with respect to the drive is given by half the angle shown in fig. 82(b) for the frequency directly below the arrowhead. Curves of constant phase are plotted in fig. 83(a). This phase gives a warning that the response is about to fall off the cliff in fig. 81(b). For most of the rise of $A_r$, the system hugs the left side of the V and $\gamma$ is nearly $90^\circ$. But near the cliff the dissipation dominates and the system is near the tip of the hyperbola, where $\gamma$ is $45^\circ$. This phase was measured, mostly for my amusement, in the last helium run described on p. 150.

The curves of fig. 83(b) are drawn to help physically interpret the meaning of these phase angles. The resonant frequency $f_0(t)$ is shown oscillating between being stiff and compliant, using terminology appropriate to a mass on a spring. For reference, the vertical position x and velocity v of a trough of liquid or a pendulum's point of support are also plotted if these are the systems in mind. (These systems are excited by effectively oscillating the acceleration of gravity, which oscillates $f_0$.) Comparison of the curve of zero $\gamma$ with $\delta f_0(t)$ shows that the spring is stretched while the drive is making it stiff. The mass on the spring increases its resonant frequency as much as possible with this phase. It does not matter that the spring is also being made compliant -- the mass does not feel it when it is not stretched. Conversely, the mass lowers its frequency as much as possible with $90^\circ$ phase shift by extending the spring while it is being made compliant. However, since these two phases give motion

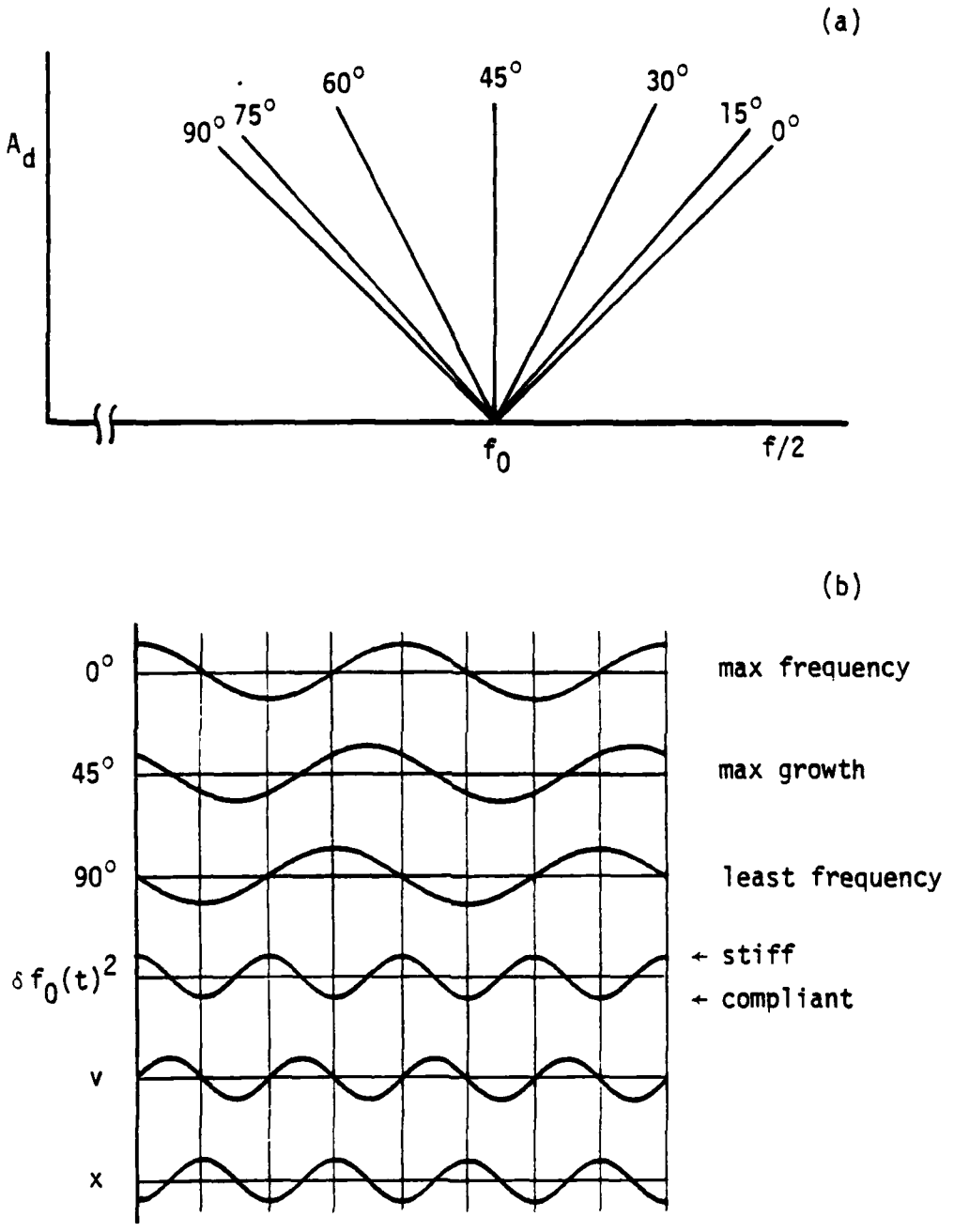


**Figure 83. Phase of parametrically excited motion with respect to the drive.**

that is symmetric with the drive under time reversal, no net work is done on the system. The mass has the maximum growth rate with $45^{o}$ phase shift. The spring is compliant as the mass is on its way out, and stiff on the way back in, so net work is done on the mass. The drive does its work by stiffening the spring while it is stretched (or by giving a pendulum's point of support positive velocity while the pendulum's transverse velocity, and centrifugal force, are high).

Drive frequencies well outside the neighborhood of $2f_0$ can also parametrically excite a system. Consider, once again, the mass on a spring of spring constant $k(1+\beta\cos 2\pi ft)$. There are lots of unstable (exponential growth) regions in the $\beta(2f_0/f) - (2f_0/f)^2$ plane, reproduced from Mathews and Walker (1970) in fig. 84. The V described so far is the tiny region above 1 on the $(2f_0/f)^2$ axis. Note that high drive frequency is towards the origin in this plot. The width of the second unstable region is second order in $\beta$, the width of the third is third order, and so on, and when dissipation is thrown in, the minimum drive needed for net growth gets squeezed up in these regions (Landau and Lifshitz, Mechanics, p. 83), so I have always ignored these other regions in my experiments.

Curiously, near the origin, hence high f, there is a shaded stable region that penetrates to negative $(2f_0/f)^2$. This corresponds to a negative restoring force. This is the region of the infamous inverted pendulum demo, which can be seen by inverting the apparatus described in Appendix 3 and driving the speaker hard, with several millimeters at around 30 Hz. The pendulum will defy gravity and stand

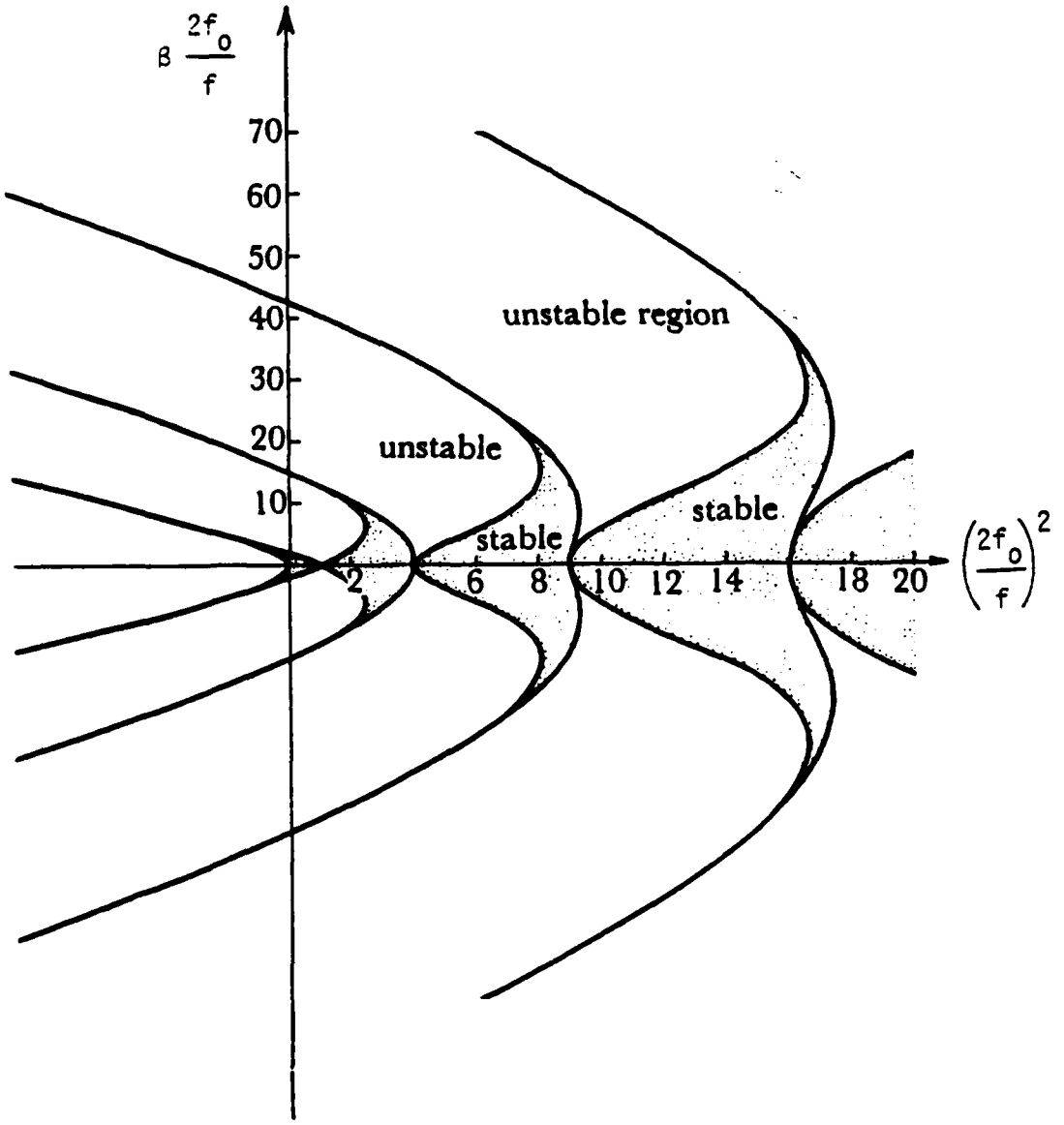


**Figure 84. Other parametric instability regions.**

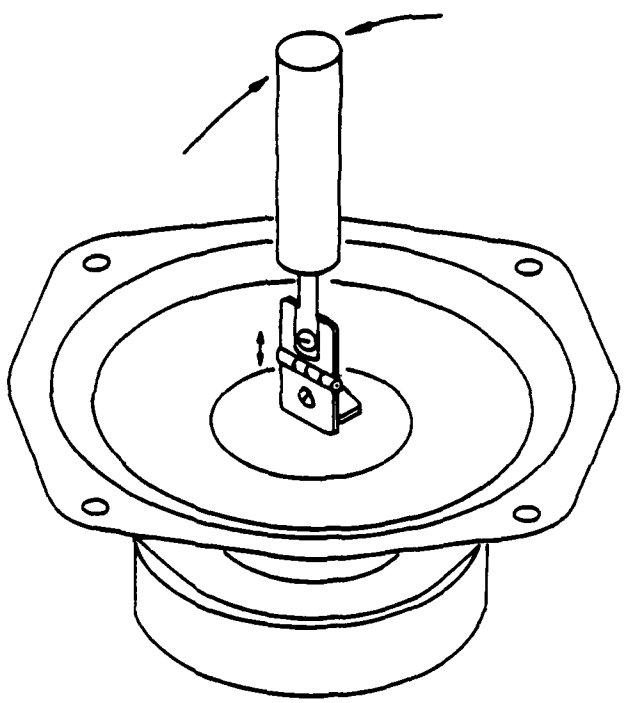

**Figure 85. Inverted pendulum demonstration.**

on end (fig. 85). This effect has some interesting technical applications -- vibration stabilization, strong focusing of particle accelerators, and particle beam weapons (see the cover of Physics Today, August, 1983).

A bit of free physics ought to be mentioned here. By rotating fig. 82(c) counterclockwise $45^{\circ}$, one (me at least) can finally understand where electron bands at the edge of a Brillouin zone in crystalline solids come from; the electron wave function's physics in space is the same as the pendulum's in time. Outside the V the wave function cannot phase lock onto the lattice, and so it neither grows nor decays. The electrons go merrily on their way. Inside the V, the ion potential is strong enough and the electron and lattice wave vectors are close enough that the electron wave function phase locks to the lattice and grows (or decays) exponentially in space. After normalization to finite probability, however, the wavefunction cannot go very far at all. Perhaps it can be appreciable near a surface, or in thin films, but not in the bulk. Hence there is a band, the straight region of fig. 82(c), without propagating states.

For fun, the relay in fig. 86 switches in a bit more capacitance to the LC circuit. Suppose one drove the relay at twice the average $f_0$. If the voltage parametrically builds up, where does the energy come from? What limits the growth?

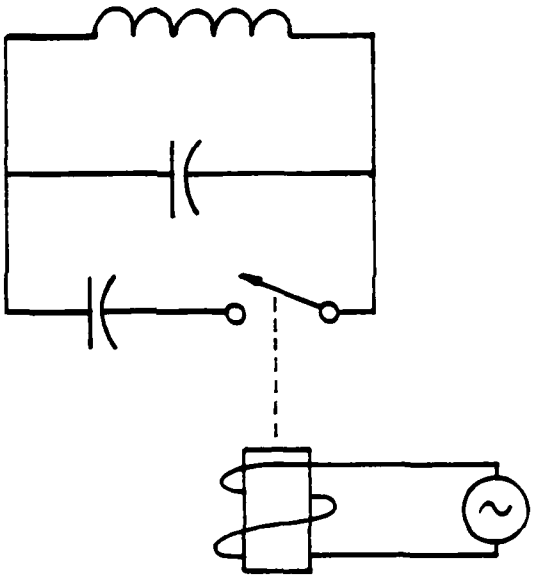

Figure 86. A parametrically driven LC circuit?

## Appendix 3

### Doubly Bent Tuning Curves

If tuning curves can bend, what keeps them bending twice, or more? For example, the frequency sweeps made in helium and shown in fig. 67 on p. 151 (especially at 200 μm rms near the tenth mode) show tuning curves that bend to the right at low response amplitude, but start to bend upward a little before the edge of the instability region is reached, just before the response falls down. Such a sweep is reproduced schematicly as the heavy line of fig. 87(a).

The sweep can be understood by imagining a marble rolling in the well sketched in (b). Since the well becomes steeper at intermediate amplitudes than the parabolic shape of the well at infinitesimal amplitudes, the marble initially traverses the well in less time as the amplitude rises. The resonant frequency, drawn as the (arbitrarily picked) dashed line in (c), starts to bend to the right. At higher amplitude, however, the marble visits what looks like the side of a "hill" in the potential well. If the potential possessed a local maximum, the marble would spend more and more time there as the turning point approached the summit, causing the resonant frequency to bend back to the left. The potential, however, can remain monotonic for the frequency to bend back to the left as long as it is flat enough near the marble's turning point.

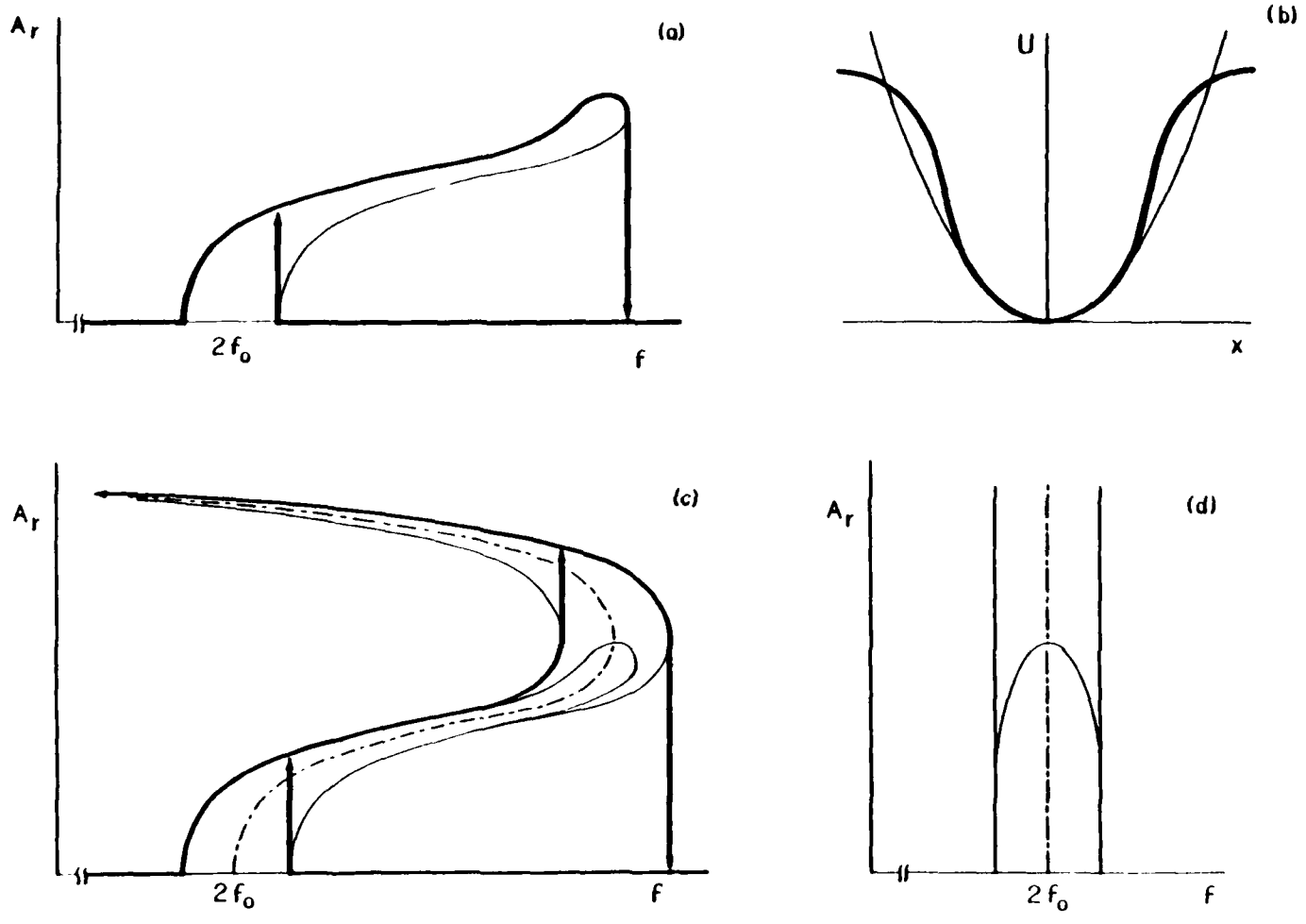


Figure 87. Doubly bent tuning curves: Curve (a), resembling some data in helium, might come from a well like (b) which would doubly bend the curve (d) as in (c).

The shape of the parametrically driven frequency sweep (a) was made by using the dashed curved line of (c) to translate to the right and left the curved line of (d), which describes a sweep in a parametrically driven system with nonlinear damping but with resonant frequency that is independent of response, i.e., in a system with a parabolic well.

Imagine what would happen if the damping stayed linear to higher amplitude. Starting near the origin in (c), the response would stay small as the frequency was swept upward until the instability region was reached. This state can also be reached by sweeping down from high frequency. Following the heavy line, the response then climbs up the surface of the instability region. A point is reached where the response jumps up irreversibly, and then starts to fall with increasing frequency. This is the signature that warns that an edge will be reached where the response irreversibly drops to zero if the frequency continues to increase. But instead, the response can be made to rise if the frequency is decreased.

There is hysteresis galore here; for a range of frequencies there are three stable states. Also, there is no way of reaching the upper state by just dialing up a particular drive amplitude and frequency -- the system must be "prepared" with a particular recipe first. One can easily imagine a long series of these "switchback" states caused by all kinds of bumps and wiggles in the potential well.

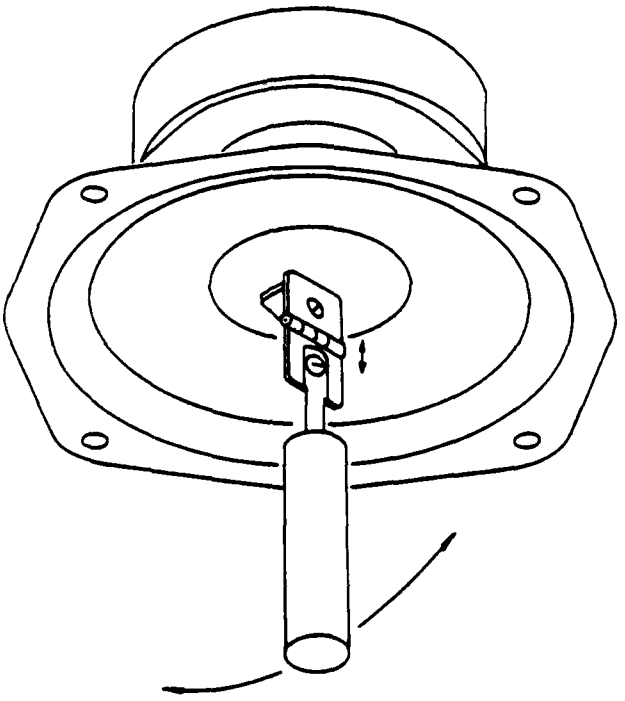

Figure 88. Apparatus to demonstrate parametric excitation and a doubly bent tuning curve.

A doubly bent curve that bends first to the left and then to the right, as well as parametric excitation, can be demonstrated with the apparatus of fig. 88. A rigid pendulum hangs from a small nylon hinge (obtainable from a radio controlled model airplane store) attached to a oscillating speaker, which effectively oscillates the acceleration due to gravity. Remember that the tuning curve for a pendulum bends to the left because its potential is sinusoidal, which diverges down from the appropriate parabola. But when the amplitude gets so high that the pendulum hits the rim of the speaker, the potential goes up very high -- and the tuning curve bends over to the right.

The response of the pendulum is visible to the eye, but for the data of fig. 89 it is more convenient to measure the velocity amplitude of the pendulum at its lowest position. This is done by letting the pendulum interrupt a red laser beam that would otherwise shine on an ordinary light emitting diode of roughly the same color. Amazingly, these diodes will supply very little voltage in ambient light but supply nearly a volt through a MΩ output impedance when hit by the laser, enough to drive a counter/timer and oscilloscope without any amplifier. The drive amplitude here is 9.2 mm peak to peak.

If the pendulum is driven just above 5 Hz and given a little nudge, it oscillates a little as it decays. The same thing happens just below 4 Hz. At 4.5 Hz, however, the oscillations grow to a finite amplitude because the tuning curve initially bends to the left. As the frequency is lowered the amplitude rises. At 4 Hz, the amplitude is high enough that the pendulum starts to hit the rim of

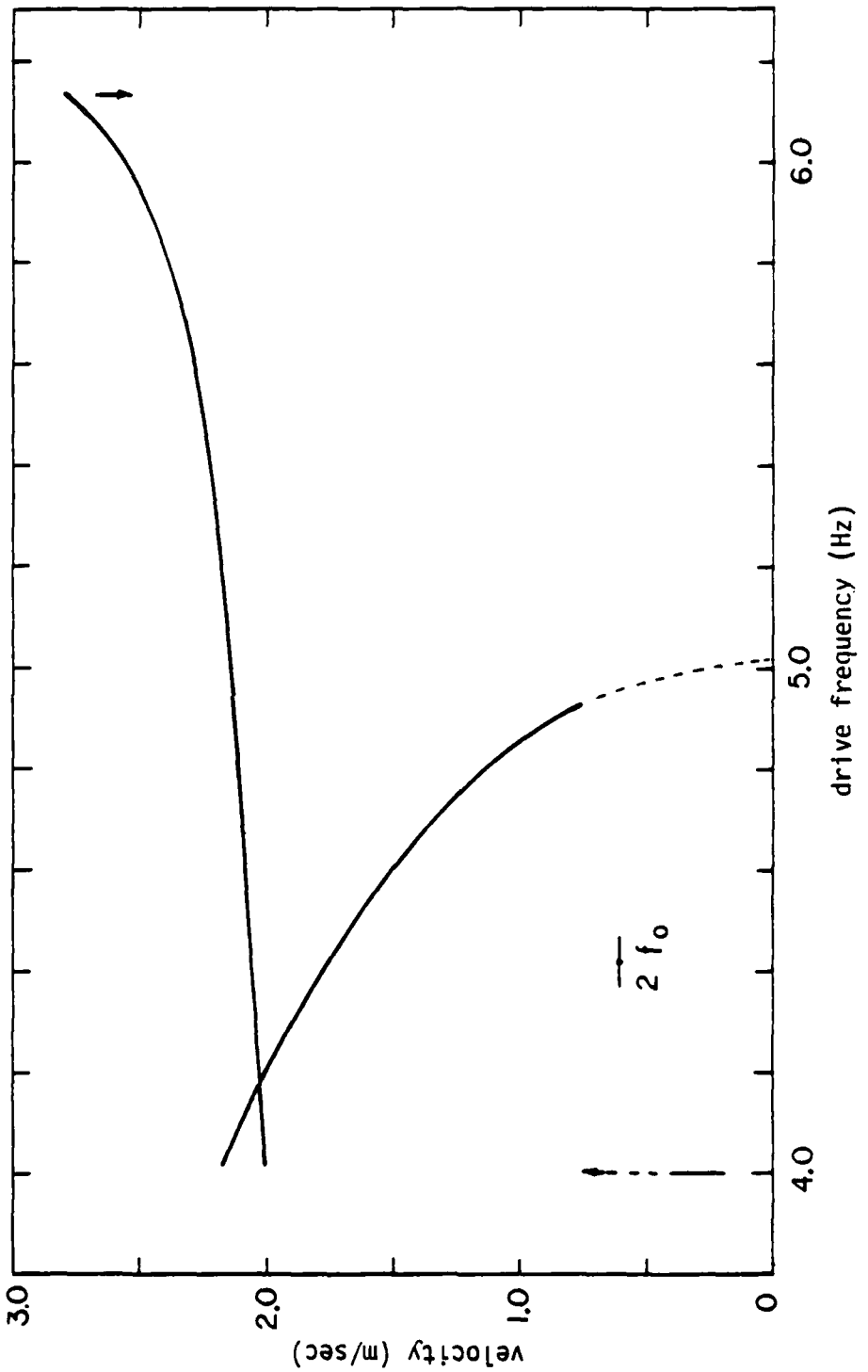


Figure 89. Velocity amplitude data showing a doubly bent tuning curve.

the speaker which causes the tuning curve to bend back to the right. If the frequency is now raised, the pendulum is in a new state banging against one side of the rim, then the other. From 4 Hz to 6 Hz, the pendulum is in this banging state that can only be reached by first decreasing the frequency (or by giving the pendulum such a big nudge that it start off banging into the rim). The pendulum is banging back and forth like mad around 5 Hz where there was no response before, but gives up above 6 Hz and drops to zero response.

For these measurements, I forgot to decrease the frequency below 4 Hz in the banging state. There may not be much significance to the velocity amplitude curves crossing in fig. 89, the displacement amplitude does not. There is probably a phase shift that explains the lower velocity when the displacement amplitude was larger.

The original motivation for thinking about doubly bent curves was the upward bending of the frequency sweeps of fig. 67 in helium, but fig. 89 shows this effect also. Maybe I made a mistake. It happens.

## Appendix 4

### Phase Locking

In general, two self-maintained oscillators, like the smooth modulations of Sec. 8, should be able to pull each other into synchronism if the coupling between them is strong enough or if their frequencies are close enough. Pippard, in his remarkable book (1978), explains this entrainment, or phase locking as it is sometimes called, in detail. Phase locking occurs in many systems. Two metronomes on a light platform suspended by strings can force each other to tick in unison, the moon's spin and orbital frequencies are phase locked, two people walking together unconsciously adjust their pace until their feet hit the ground simultaneously, and a television picture does not roll if the vertical hold knob has set the TV's vertical sweep frequency close enough to lock onto the station's sweep frequency.

Indeed, as was shown in fig. 53 on p. 120., when the drive amplitude is further increased the second modulation phase locks to the first. The large and small sausages stop slipping in phase, and the return map is no longer blurred. Phase locking transitions were also shown on pages 149 and 165.

Two things are common to all of the examples mentioned in the first paragraph. They involve at least one oscillator that is

self-maintained, that is, its frequency is free to respond to outside influences since its frequency is determined internally, and the frequency of the oscillator depends, at least slightly, on the phase shift between it and the other oscillator.

Because the frequency of one oscillator depends on its phase relative to the other, the oscillators may settle into a state where they maintain a constant phase difference. If so, they have identical frequencies. To see this, consider the simplified case of a maintained oscillator of frequency $\omega_0$ locking onto another oscillator of fixed frequency $\omega_i$. If there is no coupling, the instantaneous phase difference between the oscillators $\theta$ increases at a constant rate, the difference of the frequencies. An analogy that will be useful is a marble rolling on a flat surface through a viscous liquid while being pulled by a constant force proportional to the detuning $\omega_0-\omega_i$, where the displacement of the marble represents $\theta$.

The key point in phase locking is that somehow the frequency of the maintained oscillator depends on $\theta$. For example, consider a grandfather pendulum clock. The motion of the pendulum determines the frequency $\omega_0$ of the clock. An extra sinusoidal force at $\omega_i$ applied to the pendulum looks like an extra impedance (Pippard, p. 393), and the reactive part of that force, proportional to $\cos(\theta)$, changes the frequency of the clock. If the force adds in or out of phase with the restoring force of gravity, as far as the clock is concerned, gravity has increased or decreased, causing $\omega_0$ to vary as $\beta\cos(\theta)$, where $\beta$ is the range that the frequency can be made to change.

Let's expand the analogy to include the coupling. The rate at which the marble rolls is the frequency difference of the oscillators, which now depends on $\theta$. Again, let the marble be controlled by viscosity (its inertia is unimportant) so that it rolls at a rate proportional to the forces on it. Then represent the coupling with a force proportional to $\beta\cos(\theta)$, added to the one proportional to $\omega_0-\omega_i$, by putting the marble on the washboard of fig. 90.

The dynamics then go like this: By applying a strong enough horizontal force, the marble will roll over the humps of the washboard, slowing at the tops, but slipping over them nevertheless. But if the force is reduced until the marble does not make it over a hump the marble will stop and be trapped in a well. The phase difference stops increasing. This represents the transition from the out of lock, quasiperiodic state to the phase locked state. Note that trapping the marble does not depend on the sinusoidal shape of the wells, and that no matter how shallow the wells there is a horizontal force weak enough that the marble will be trapped. In other words, the smallest dependence of the frequency of the oscillator on its phase relative to the other guarantees phase locking for close enough tuning (in this simplified model). Once the modulations have been shown to be quasiperiodic one should expect to see phase locking.

The grandfather clock (and the examples in Pippard on p. 392 and p. 398) suggests how the frequency of one modulation might depend on its phase relative to the other. Various modes of the trough

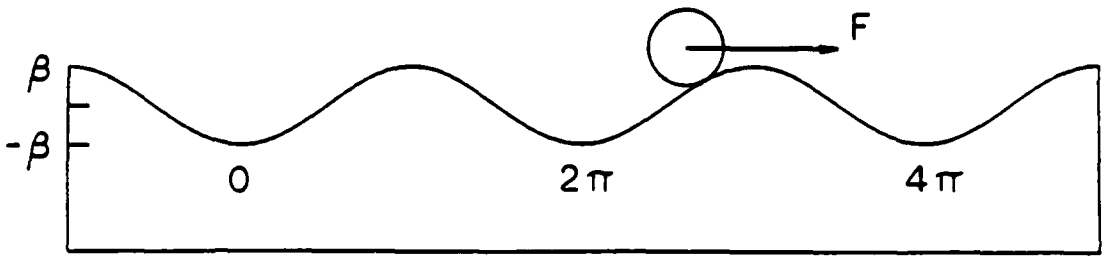


Figure 90. A washboard model for phase locking. The marble's position represents the phase difference between two oscillators. A constant horizontal force F represents the detuning of the oscillators, $\omega_0-\omega_i$. For small enough detuning, the phase may settle into one of the sinusoidal wells separated by $2\pi$. When the phase is constant, the oscillators have identical frequencies.

participate in the modulations. Since the modes are nonlinearly coupled together (Miles, 1976), they can exchange energy, to an extent and direction determined in part by their relative phases. The modes of one modulation present a complex impedance to the modes of the other -- and the frequencies of those modes, and therefore the modulations, will be shifted by the reactive part of that load.

Phase locking transitions are often hysteretic -- the range of frequencies that initiates lock can be less than the range that maintains it. So far, the washboard model lacks hysteresis since the critical amount of force needed to keep the marble moving is the same amount as is needed to release the marble from its well. Hysteresis can be put in by allowing the coupling, and therefore the depth of the wells, to change. One way is to imagine the washboard to be made of some magic material that smooths out in response to the marble rolling over it, but relaxes, increasing the depth of the wells, as the marble slows down. The coupling depends on the frequency difference of the oscillators. This is how electronic phase lock loops (quickly mentioned on p. 59) are typically hysteretic. Another way the coupling strength may change is shown by Pippard. Quickly stated, the coupling depends inversely on the maintained oscillator's amplitude, but the amplitude may grow because of the nonreactive component of coupling force, the component in quadrature with $\theta$, doing work on the oscillator. The amplitude, and therefore the coupling, ends up being different for the locked and unlocked states. It is unclear from the data whether the smooth modulation phase locking transitions are

hysteretic —this is another loose end — but they may easily be. The coupling strength for the modulations probably behaves like the systems described by Pippard.

## Appendix 5

### Quasiperiodicity Demonstrations

A hanging chain. Quasiperiodicity -- motion that has Fourier components at frequencies that are (in principle) irrational multiples of each other, caused for instance by the motion developing an instability at a frequency unlocked to the drive frequency -- was seen in all four phenomena reported in this dissertation: smooth modulations and cockscombs can exist out of phase lock with the drive; the frequency of ultra deep modulations is so low that it is probably unrelated to the drive; and the braiding seen in the paddle driven trough can be interpreted as a modulation occurring close to but not quite f/3. Quasiperiodicity is discussed further on p. 109. To convince myself that quasiperiodicity might actually exist, and that I wasn't nuts, I wanted to see it in a simpler system. Seth Putterman and others were telling me that quasiperiodicity can come from energy sloshing back and forth between nonlinearly coupled normal modes of a system, so I set up the hanging chain drawn in fig. 91.

Eighteen cm of the kind of beaded chain that is sometimes used in key chains or pull chains for lamps is driven by the speaker in one direction, call it x, but additionally it is free to move in the perpendicular direction, call it y. At small drive amplitude, the modes in either direction are decoupled, and the chain responds only

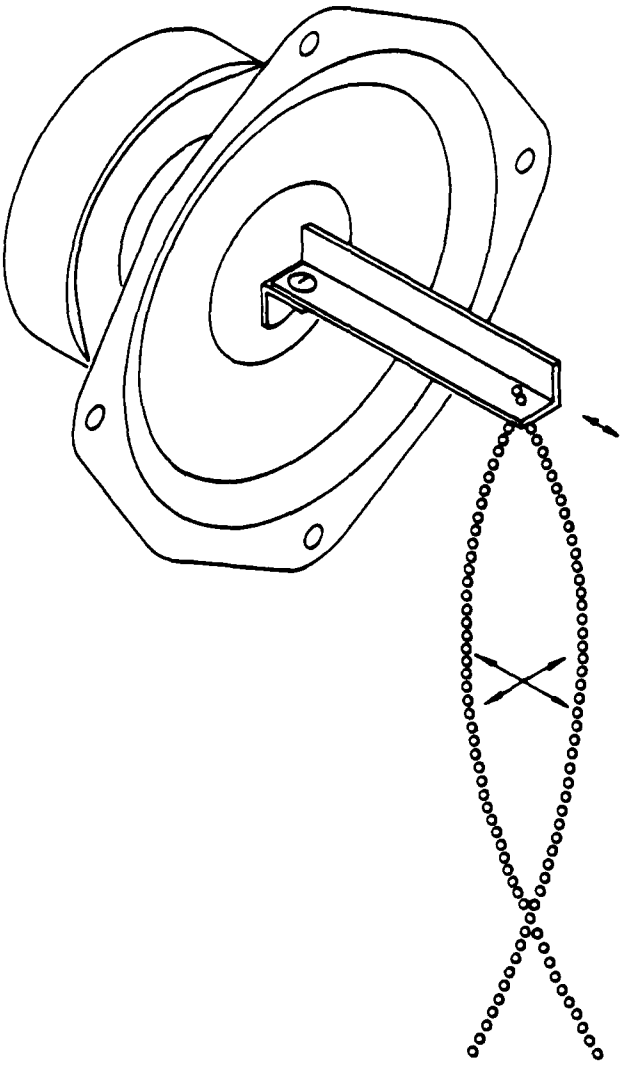

**Figure 91. A driven hanging chain that demonstrates quasiperiodicity.**

in x. The chain also responds in only the x direction when driven with larger amplitude on the low side of the second mode (which has one node as shown in the figure) at around 2.9 Hz. But when the frequency is raised a bit to around 3.3 Hz, motion in the plane is unstable and the chain whips around in pretty much a circle one way or the other; both x and y modes are excited, $\pm 90^{\circ}$ out of phase. This isn't quasiperiodicity, but it's neat anyway.

I like to think that each mode parametrically excites the other (although, to tell the truth, I am not completely sure of this). Motion in x at f gives tension oscillations in the chain at 2f, which is just the right frequency to parametrically drive motion in y at f. Circular motion will be shown to be the phasing between the modes where each increases the frequency of the other. With this phasing, the frequency can be increased quite a bit, to 5 Hz, and the circular motion can still be driven at resonance.

In between these two behaviors, at around 3.1 Hz with a drive amplitude of around 1.5 mm, the behavior is even more interesting; it repeatedly goes through the cycle shown in fig. 92. Starting from rest, the chain oscillates in a plane in the x direction, its amplitude increasing. After x builds up, the plane of motion rotates one way or another; y picks up motion in phase (or $180^{\circ}$ out of phase) with x. Then the motion opens into an ellipse, which progresses to nearly a circle, then into another ellipse oriented $90^{\circ}$ from the first. The ellipse then collapses and the cycle starts over. Variations on this cycle are possible, too.

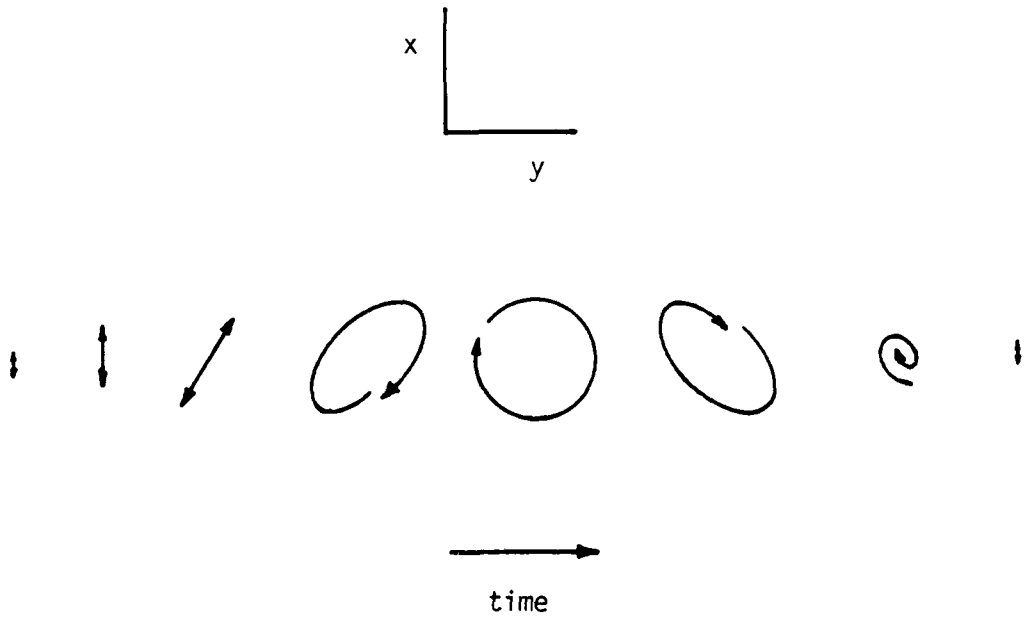


**Figure 92. Quasiperiodic modulation of the motion of the hanging chain.**

Parametrics explains quite a bit of this. Suppose x is as shown in fig. 93. Then the tension oscillations in the chain that are due to x are high when the x velocity is high (because of the centrifugal force and the component of gravity along the chain). The oscillating tension oscillates y's resonant frequency and beyond a threshold y will be driven, as described in Appendix 2. The various phases that y can have relative to the tension control the frequency and growth rate of y, and gives the trajectories of the chain shown to the side of the figure. The solid and dotted lines are equivalent states, allowed because of the 2:1 frequency ratio in parametrics or the left-right symmetry of the problem. Comparing fig. 92 to fig. 93, the orientation of the first ellipse of the cycle indicates that energy is flowing from x to y. The second ellipse, which occurs after the circle, indicates that energy is flowing out of y to x, and presumably back into the drive (if y's load on x can change x's phase with respect to the drive enough). This is not a complete understanding, but it is nice to be able to visualize the energy flows.

In 1962 and 1984(a), Miles analyzed essentially the same problem, a pendulum that can move in two directions, and showed that in addition to being quasiperiodic, the motion can be chaotic. Perhaps the chaos is associated with the moment near the start of the cycle when the plane of motion has to decide which way to rotate. Small influences, due to the previous trajectory of the chain or slightly different initial conditions, greatly effects the future motion of the

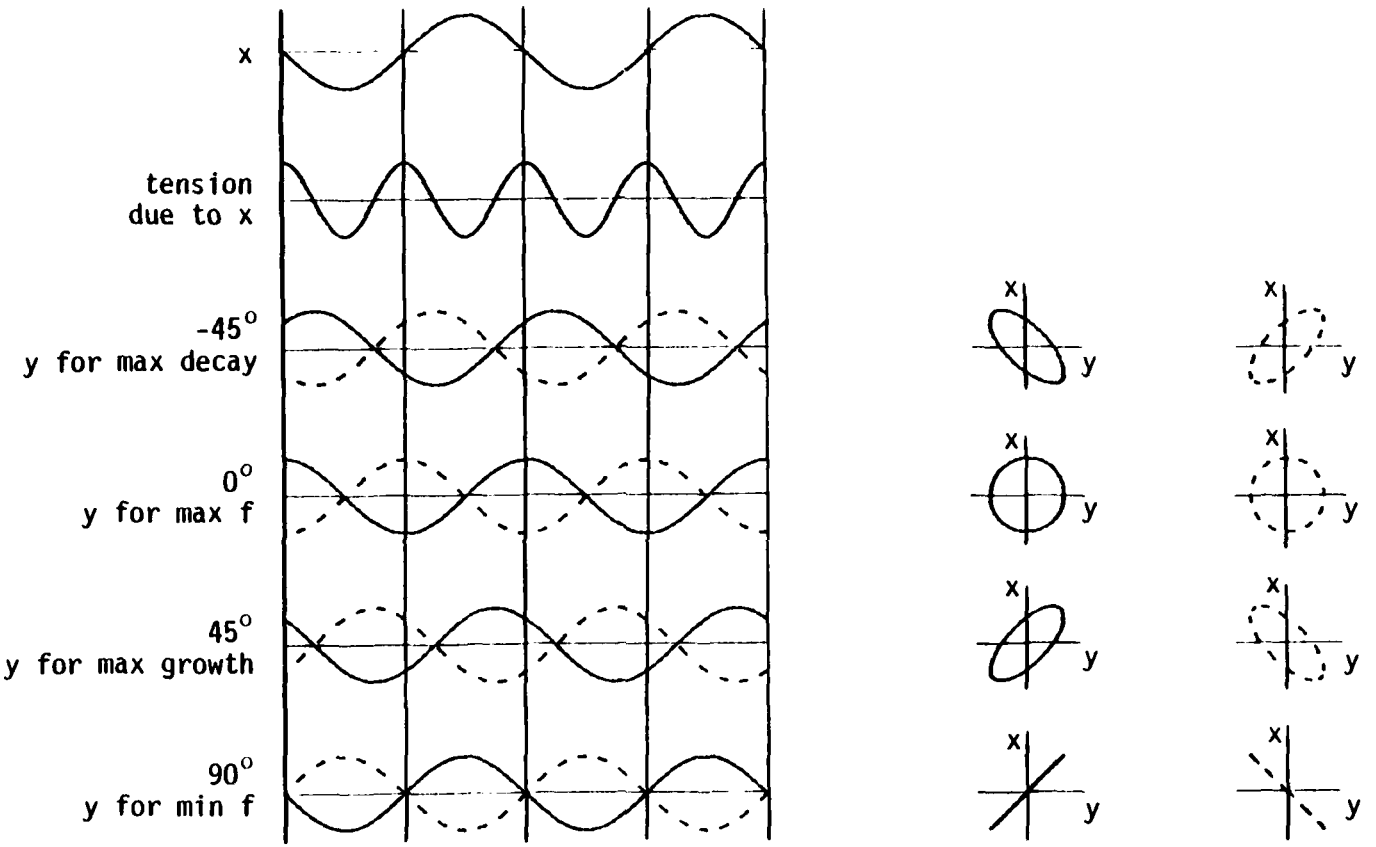


**Figure 93. Parametric coupling between degenerate modes of the chain.**

chain. Sometimes the chain can be seen changing directions apparently at random, though external noise may be the cause.

The chain is not unlike the ultra deep modulations of Sec. 6. Two modes interact and the bursts on p. 92 show that there is a natural starting point to the motion -- when the amplitude is small everywhere. After this point, the modulation must decide which side of the barrier is going to have the initial growing amplitude. Unlike the chain, the modulation is parametrically driven and the nonlinearities may or may not be the same.

Quasiperiodicity by loading the drive. Another type of quasiperiodicity can be seen in the inverted pendulum demo of Appendix 2. If the drive amplitude is carefully lowered once the pendulum is up, the pendulum will slowly fall to one side. But as it does it loads the speaker less and the speaker amplitude builds back up. The restoring force goes up and catches the pendulum, pushing it back up. In its vertical position, the pendulum loads the speaker a bit more, the speaker amplitude drops a little, and the cycle repeats. This sort of oscillation, were the response of an oscillator modulates its drive, guarantees that the driving force has a Fourier component in common with the velocity of the response, which allows for transfer of energy (similar considerations in the case of subharmonics are treated by Pippard, p. 278). It could have been a problem on the probe, with the water or helium waves modulating the position of the voice coil in the gap of the loudspeaker giving a quasiperiodic modulation to the drive -- but I watched for this and do not think it was.

## Appendix 6

### Video Tape to Computer Interface

The method used to digitize the video tape of the water surface, described on p. 130, is elaborated here. This method of obtaining the surface height vs. position and time eliminates the need for dozens of transducers. The system was assembled from electronics laying around the lab; substitutions and rearrangements are possible.

One needs to first understand video signals. Inside the picture tube, an electron beam scans the image in lines from left to right at 15.750 Khz and stacks these lines from top to bottom forming "fields" at 60 Hz. One field of the closed circuit video signal (before RF modulation) is sketched in fig. 94. The upper part carries brightness information, white being more positive. The lower part carries timing pulses to synchronize the horizontal and vertical sweeping of the beam. These pulses were decoded to select the particular part of the surface of interest. Horizontal timing pulses occur when the beam flys back between lines. The doubling in the frequency of the pulses and their subsequent increase in duty cycle marks the start of a new field (at the upper left corner of the picture) and the start of a new vertical sweep.

The system is block diagramed in fig. 95. The collection of

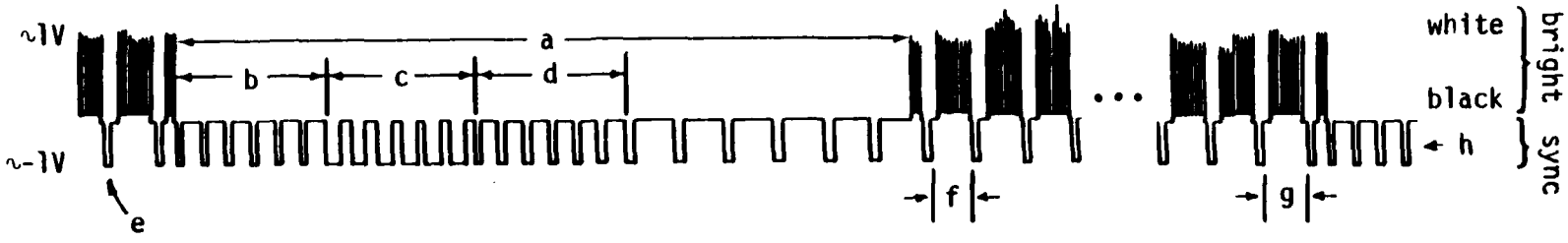


Figure 94. A typical video signal. (a) The start of the field (this is the black bar at the top of a TV picture that can be seen if the picture is rolling), (e) a horizontal sync pulse, (b) and (d) sync pulses at double the frequency, (c) sync pulses with increased duty cycle, (f) and (g) the first and last lines of the picture, and (h) the threshold level used to strip the sync pulses from the video signal.

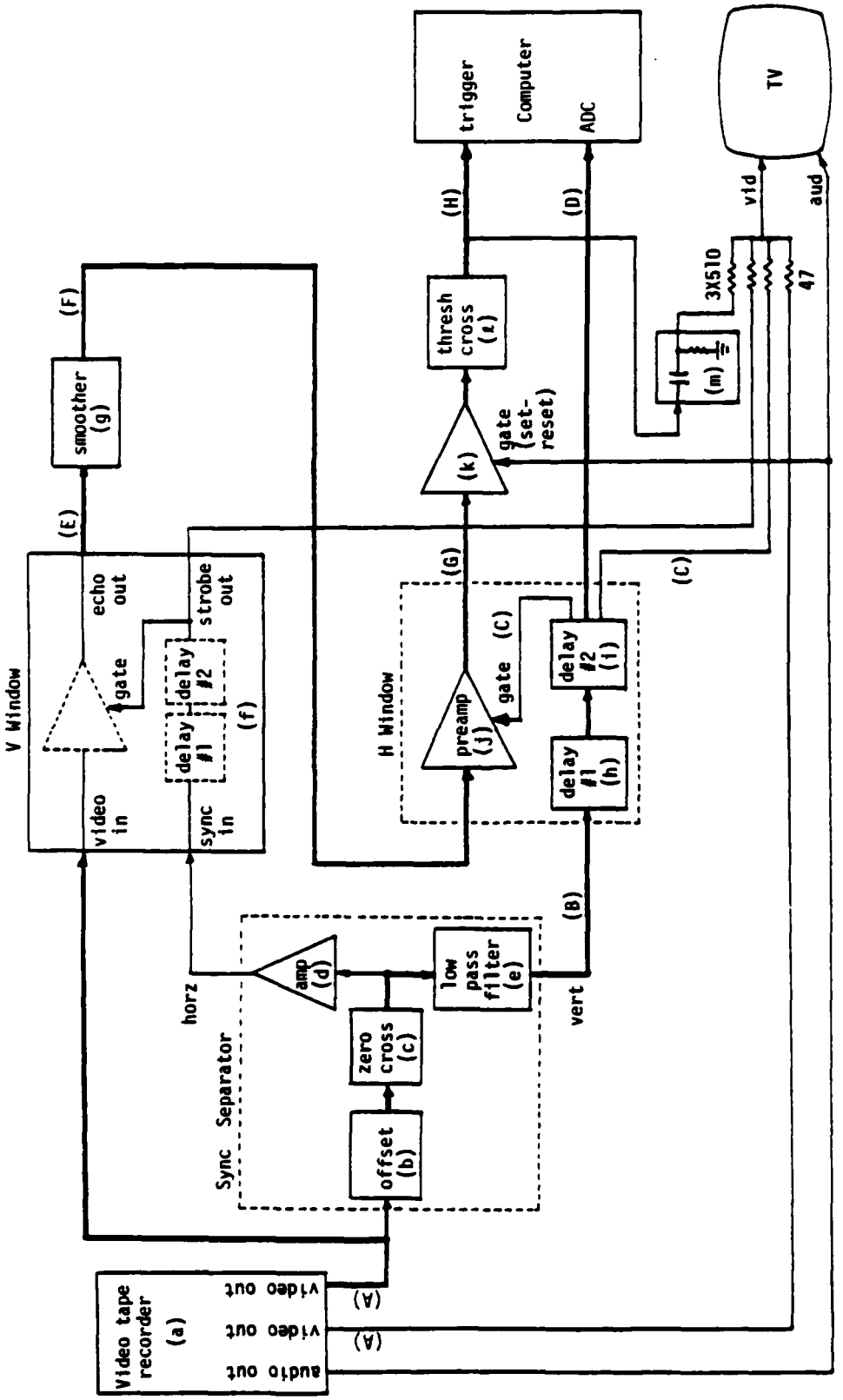


Figure 95. Block diagram of the interface.

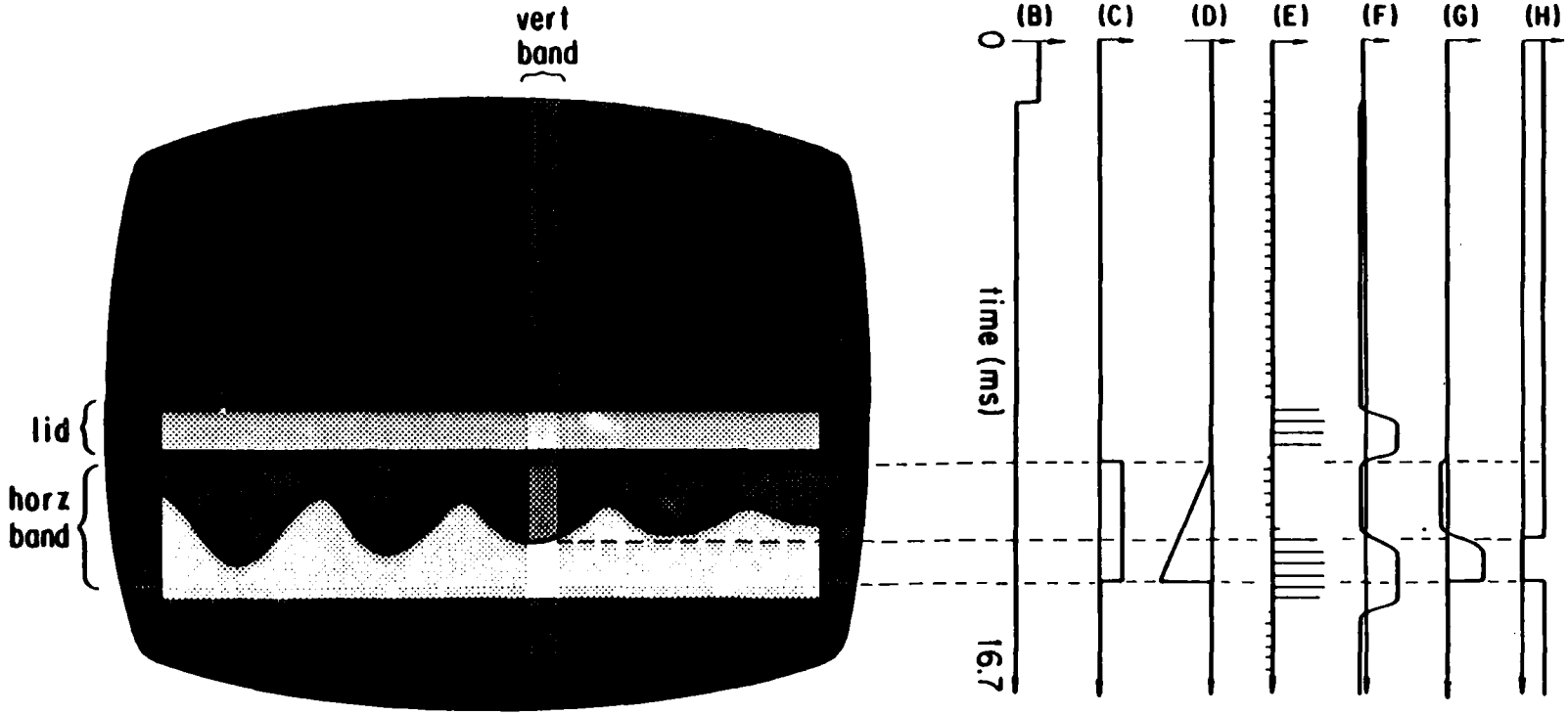


Figure 96. Simplified TV picture and timing diagrams.

Table 3. Equipment List for Video Interface

a) Panasonic VHS recorder.

b) * Offsetter.

c) * Zero cross detector.

d) Wavetek 186 waveform generator in trigger mode. Frequency set to 50 KHz to
set length of output pulse.

e) Krohn-Hite 3200 4-pole low pass filter set to 5 KHz.

f) Maytec 2470 attenuation recorder.

g) Krohn-Hite 3200 4-pole low pass filter set to 3 KHz.

h) Wavetek 116 waveform generator in trigger mode. Frequency set to around 100
Hz.

i) Wavetek 116 waveform generator in trigger mode. Frequency set to around 260
Hz.

j) Ithaco 1201 preamp with gate. Gain at 200, low pass filter set to 10 KHz.

k) General Radio 1396-A tone burst generator.

l) * Divide by $2^n$, n set to 0.

m) * Pulse shaper.

* Homemade electronics. See Appendix 7.

circuits called the Synch Separator detects the timing pulses, and the V and H Window circuits generate the vertical and horizontal bands on the TV monitor. Lower case letters refer to the entries in Table 3 that lists the equipment used for each block. The capital letters refer to the voltages of fig. 96 which are drawn to be coincident with the vertical scan of the simplified TV picture shown.

The offsetter and zero-cross detector of the Synch Separator strip the timing pulses off the video signal by detecting when it passes below a selected threshold. The average level of these pulses, the output of the low pass filter, goes up at the start of the field (because of the increased duty cycle and frequency of the pulses) triggering delay #1 which in turn triggers delay #2 of the H Window. The length of #1's output pulse determines the position of the horizontal band from the top of the screen, while the length of #2's pulse determines the width of the band. Delay 2 also sends a ramp to be digitized by the computer's analog to digital converter (ADC) at the proper time.

Meanwhile, the horizontal timing pulses are amplified to reliably trigger the Maytec 2470 (f), which serves as the vertical window, at the start of each line. The Maytec, an ultrasonic pulse-echo system component designed to select a particular echo out of a stream of echos, here passes the portion of the video signal occurring within a window of width 2.2 μS, set by its Delay #2, that starts after a selectable delay time, set by Delay #1, from the horizontal timing pulse. These tiny bursts of video signal are low pass filtered by the

Smoother to give a signal that follows the brightness in a thin vertical band a selected distance from the left edge of the screen. The Preamp in the H Window gates this signal so that only the portion coincident with the horizontal band can get through. This signal must next pass through another Gate that stays open after it receives an audio pulse placed on the tape at the start of the section to be digitized. The rise in this signal caused when the beam scans the bright water surface makes the digital output of the Threshold Cross detector fall. The ADC then digitizes the ramp. The higher the surface, the sooner the ramp is measured, so the higher the number recorded. Thus, the element of surface a particular distance from the left is digitized once per field, at 60 Hz, starting with the field containing the audio pulse.

Bright bands are superimposed on the TV picture to show where in the trough the digitization is taking place and the status of the delays by summing the gating signals of both Windows with the video signal, taken from another isolated output so as not to contaminate the video signal going to the Maytec. A thin dark line that oscillates with the portion of the surface at the crossing of the bands is also superimposed on the picture by adding the falling edge of the ADC trigger. The signals are also monitored on an oscilloscope, not shown.

## Appendix 7

### Schematics of Homemade Electronics

Schematics of most of the homemade electronics used in the experiment are presented here for your amusement.

Some notes:

Bridges and lockin. The bridge circuit is essentially as described on p. 50, except that op amps are used to buffer and invert signals, instead of a transformer. The MC1494L is a four quadrant multiplier made by Motorola. The current coming out of pin 14 is proportion to the product of the voltages on pins 9 and 10, or pins 9 and 13.

Preamps. These four preamps have 100 MΩ input impedance, low enough noise to do the job (around 20 $nV/Hz^{1/2}$), DC to 150 KHz response -- and don't cost $2000 apiece.

AC to DC converters. Converter 1, made by our electronics shop, has a simple RC low pass filter. It monitored the liquid surface. Converter 2 has a four pole Butterworth filter for lots of filtering with quick response which can be set to 1 or 0.3 Hz. It monitored the drive amplitude.

Divide by $2^n$. The CD4040BC is a cascade of 12 CMOS JK

flip-flops.

3D to 2D projection box. This is a more convenient but complicated version of the circuit described on p. 57. The capacitors smooth the computer's digital to analog output.

Graphics controller. This is not shown because it is not in the signal path, it is complicated, and no one should make another. I built it for therapy. It is essentially a graphics card for a terminal.

Bridge - Part 1

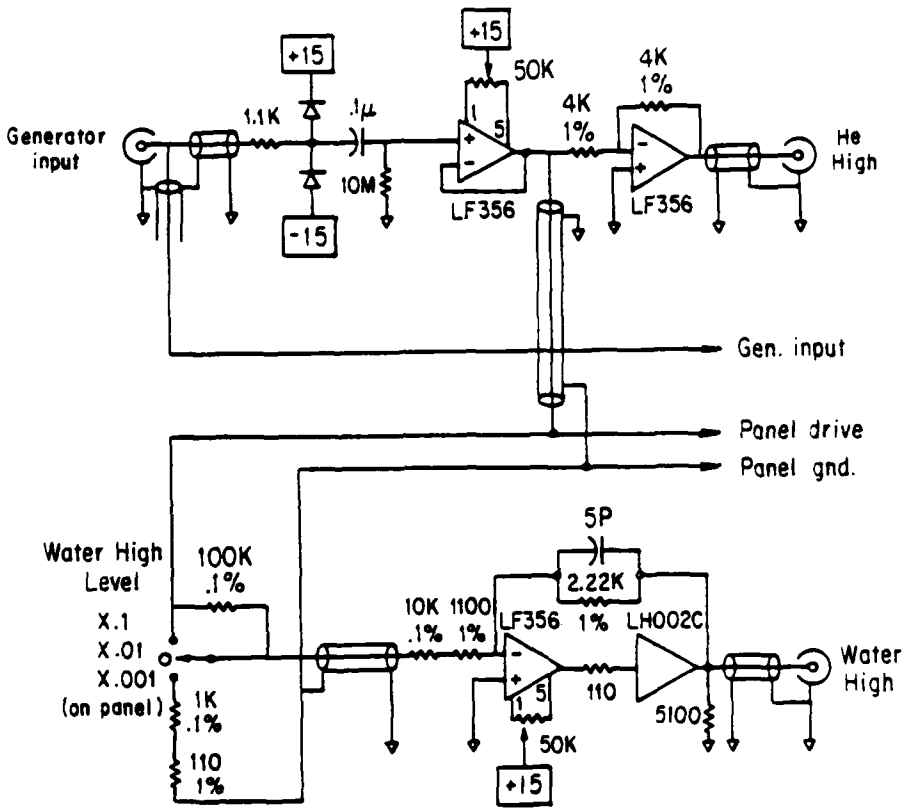


**Figure 97(a). Bridge.**

Bridge - Part 2

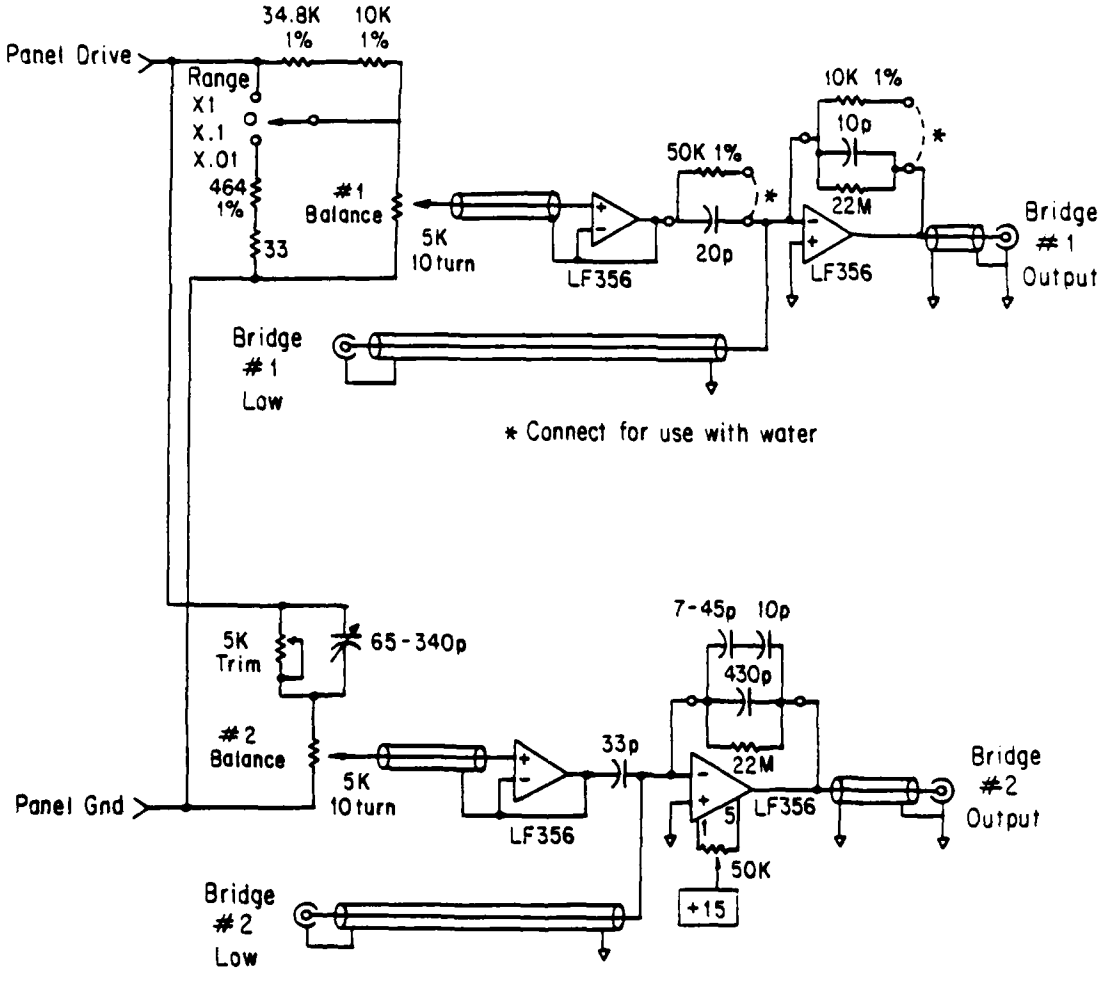


**Figure 97(b). Bridge.**

Bridge - Part 3

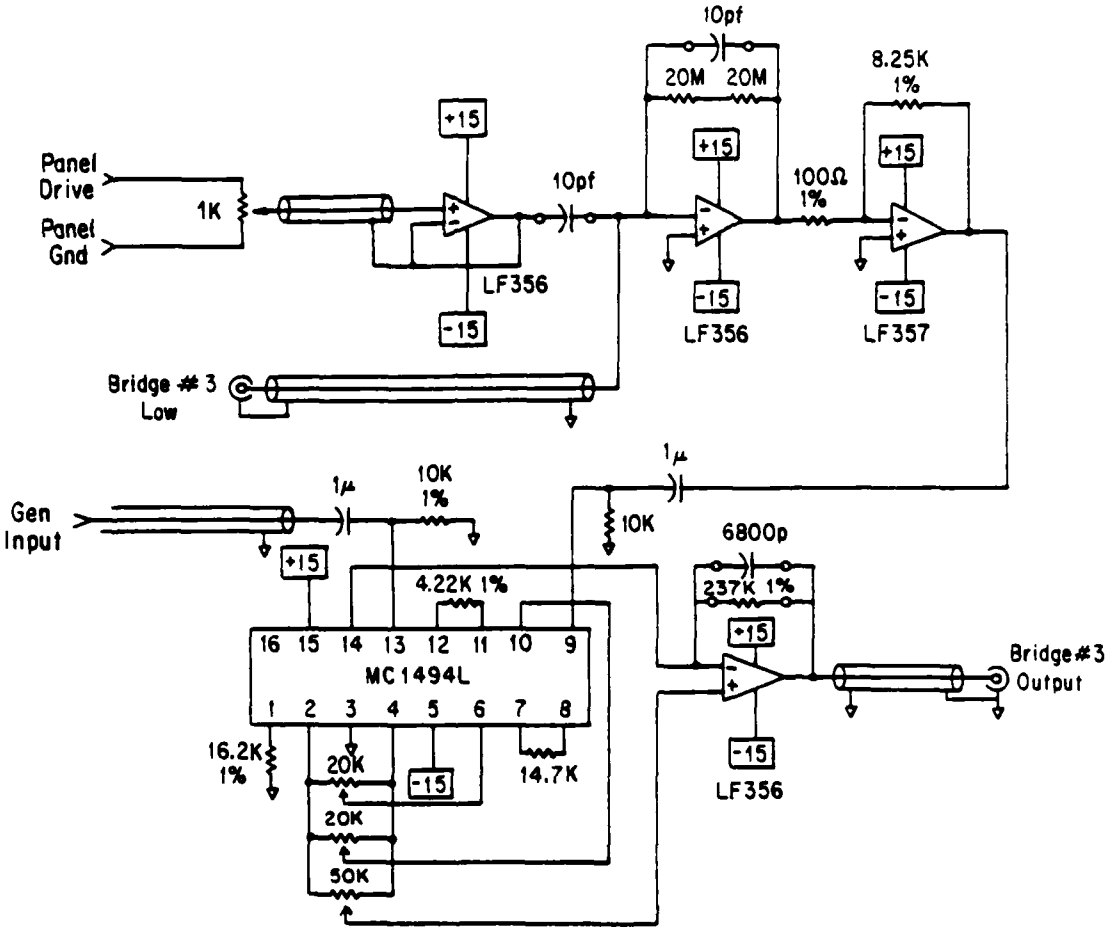


**Figure 97(c). Bridge.**

Preamps

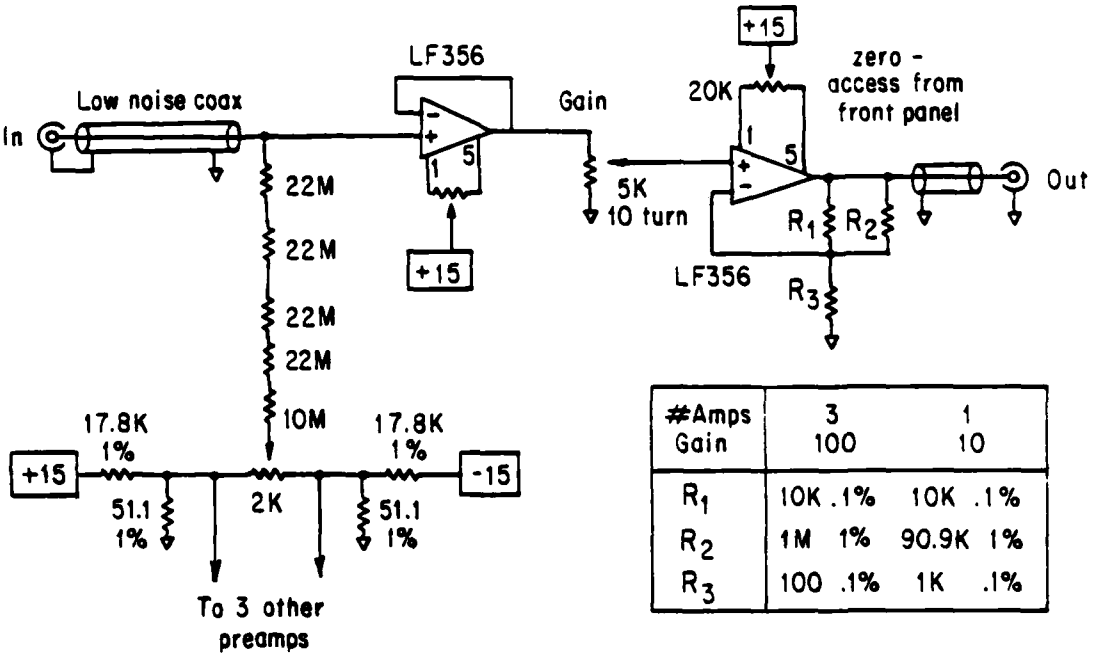


| #Amps<br>Gain | 3<br>100 | 1<br>10 |
|---|---|---|
| $R_1$ | 10K .1% | 10K .1% |
| $R_2$ | 1M 1% | 90.9K 1% |
| $R_3$ | 100 .1% | 1K .1% |

**Figure 98. Preamps.**

Lock - in Amplifier

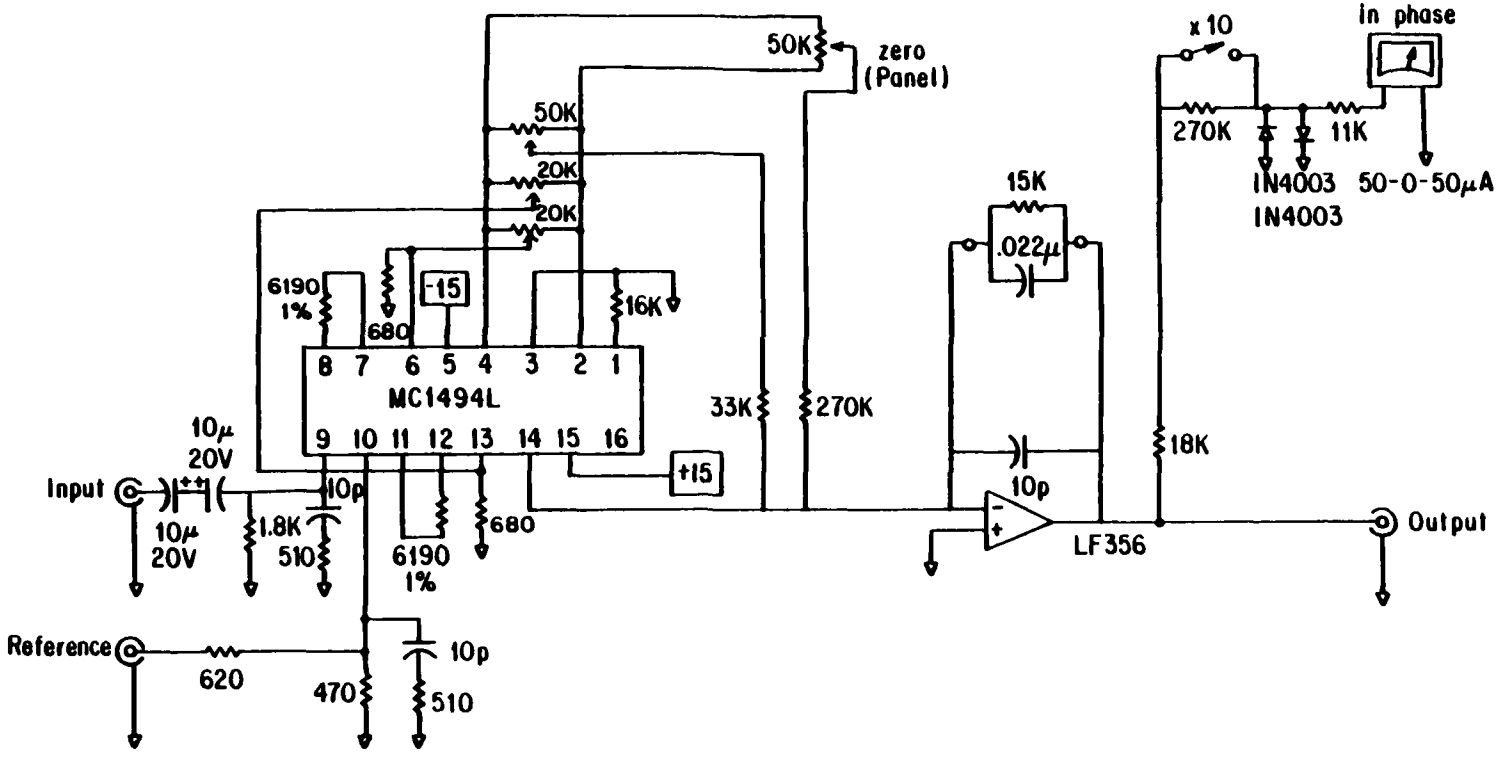


Figure 99. Lock-in amplifier.

AC to DC Converter # 1

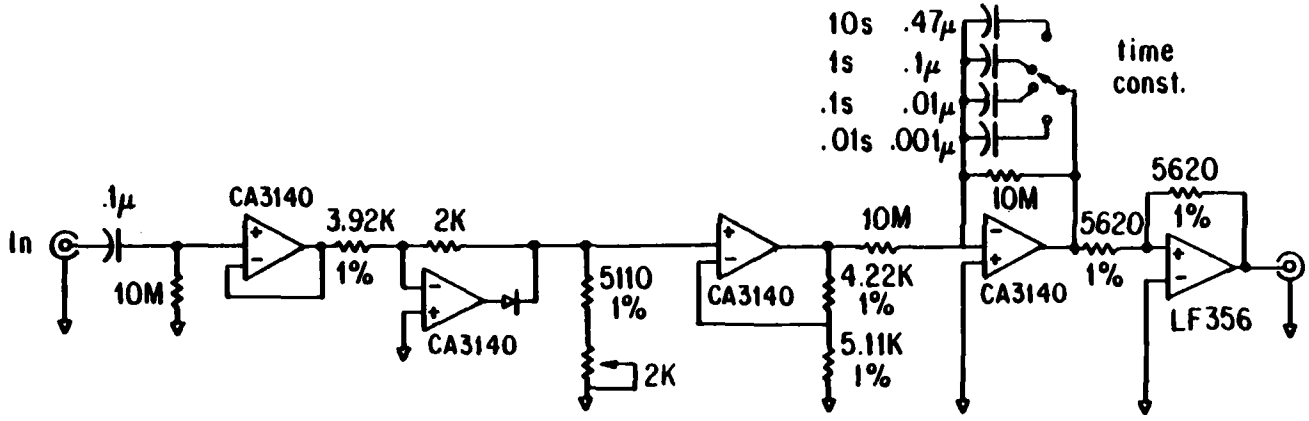


Figure 100. AC to DC converter #1.

AC to DC Converter #2

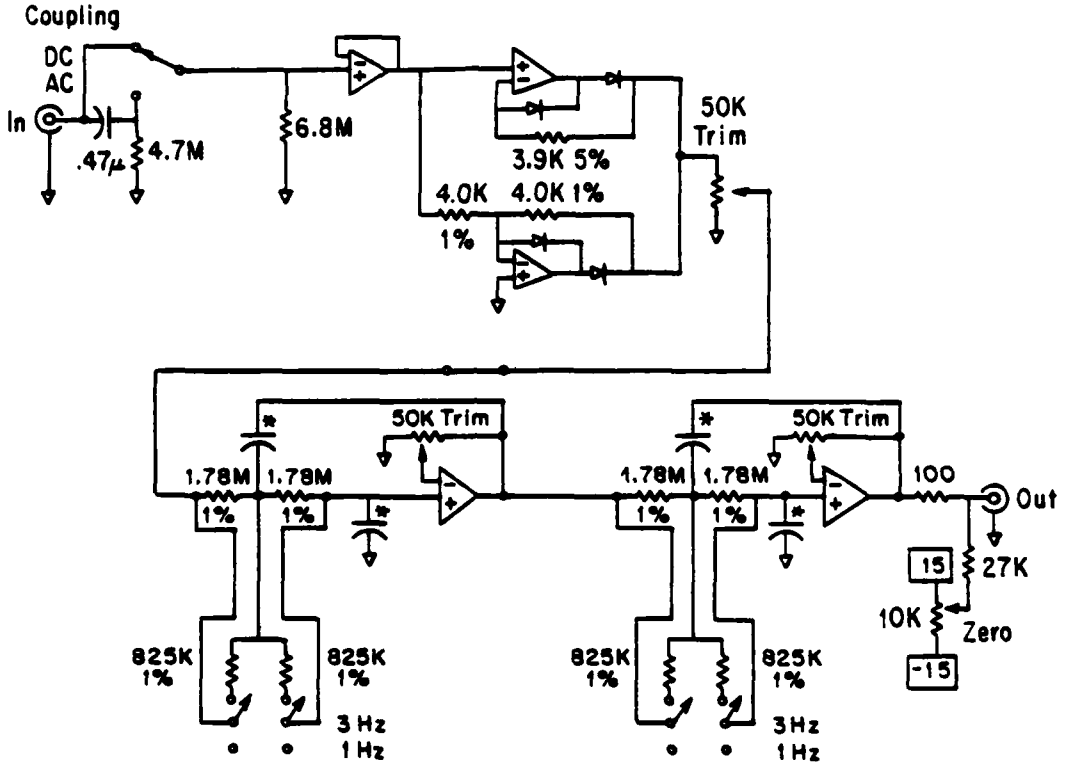


Figure 101. AC to DC converter #2.

Differentiator

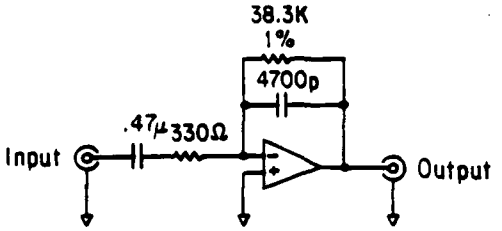


Zero Cross Detector

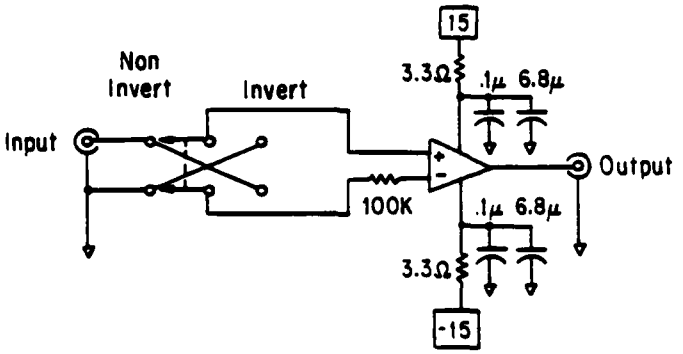


Pulse Shaper

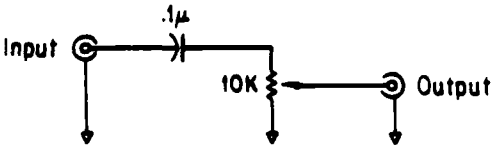


Offsetter

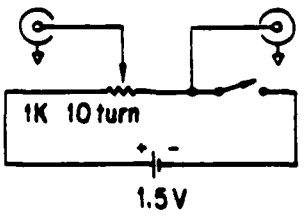


**Figure 102. Differentiator, Zero cross detector, Pulse shaper, and Offsetter.**

Divide by $2^N$ ($2^0$ to $2^{11}$)

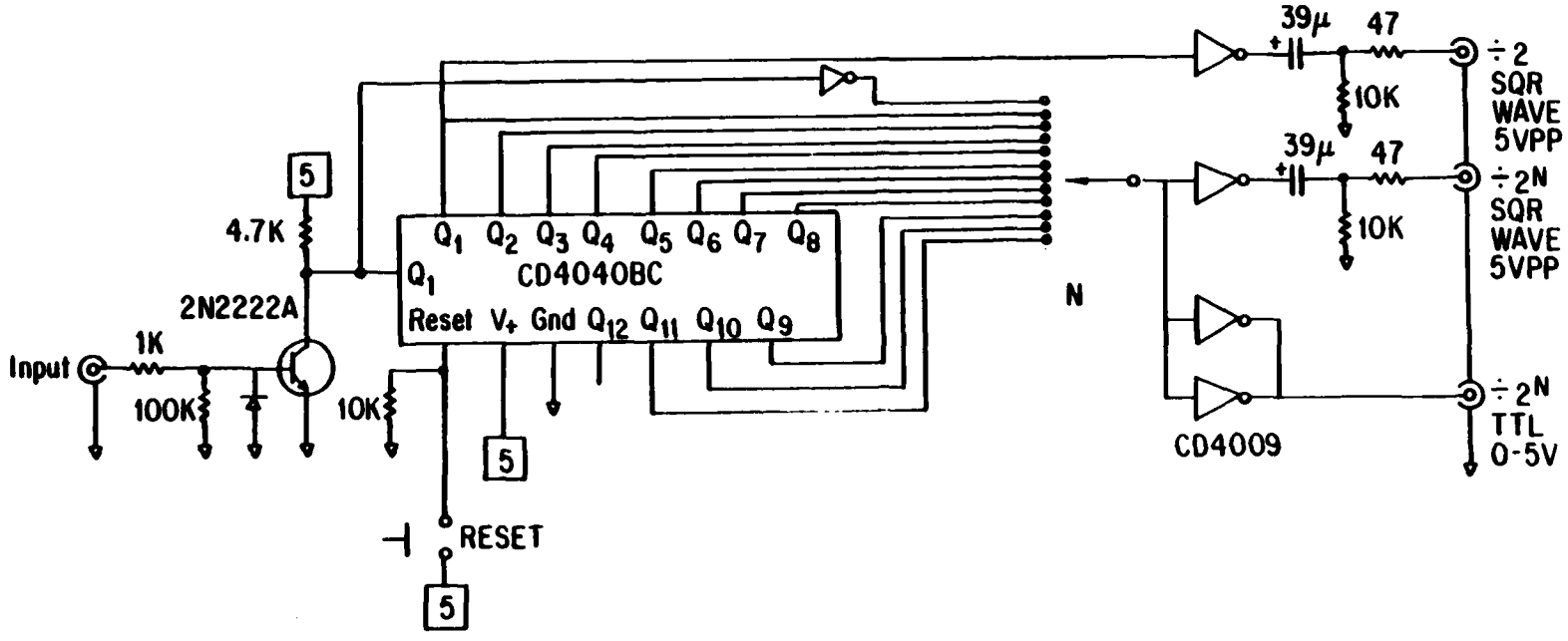


Figure 103. Divide by $2^n$.

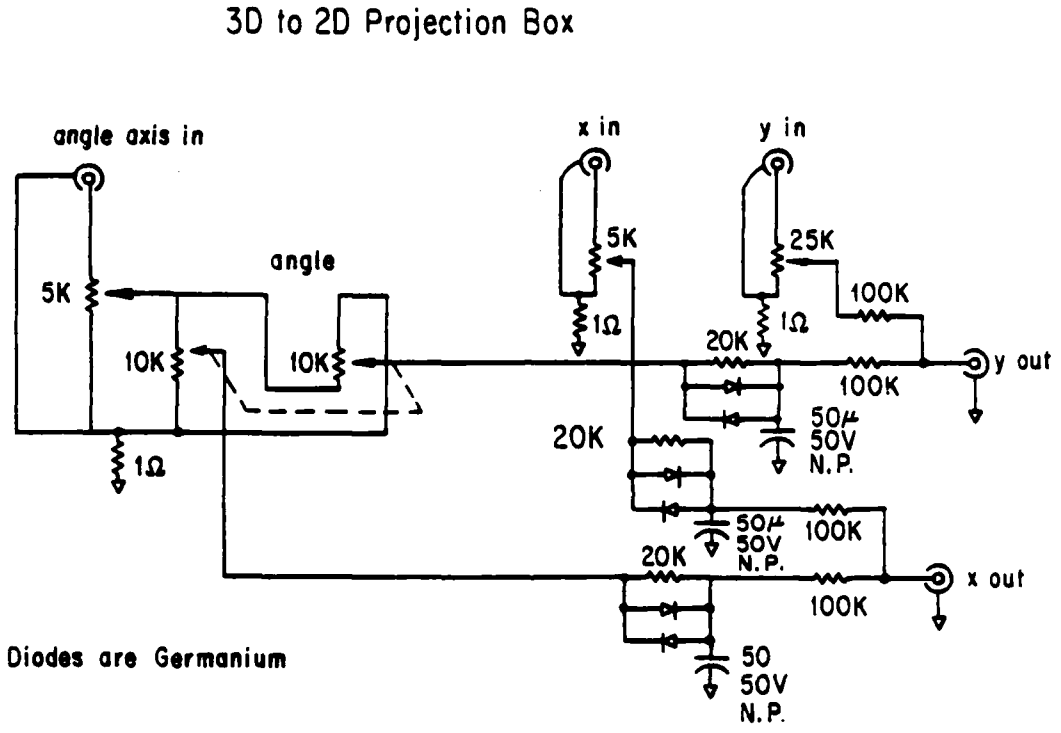


**Figure 104. 3D to 2D projection box.**

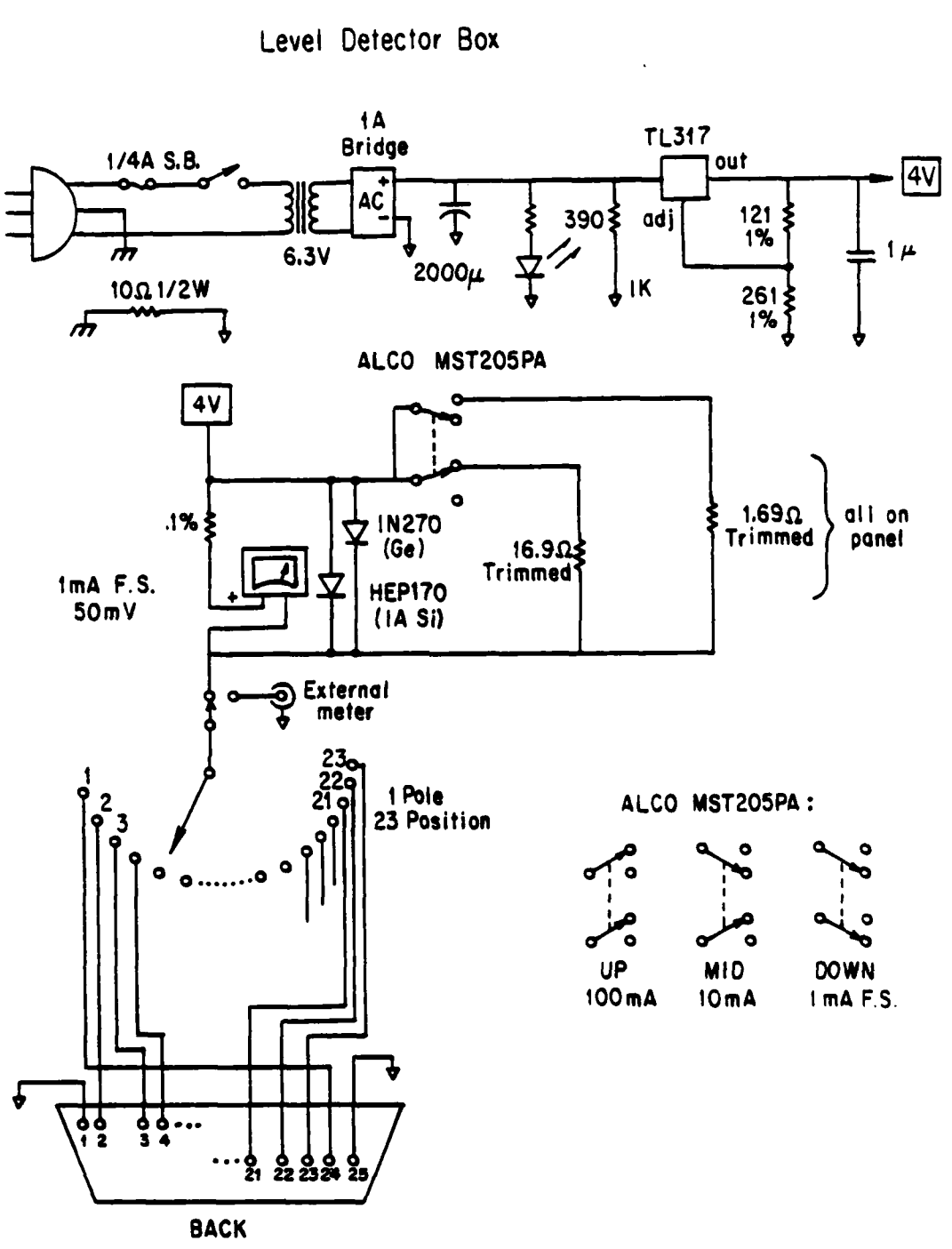


**Figure 105. Level detector box.**

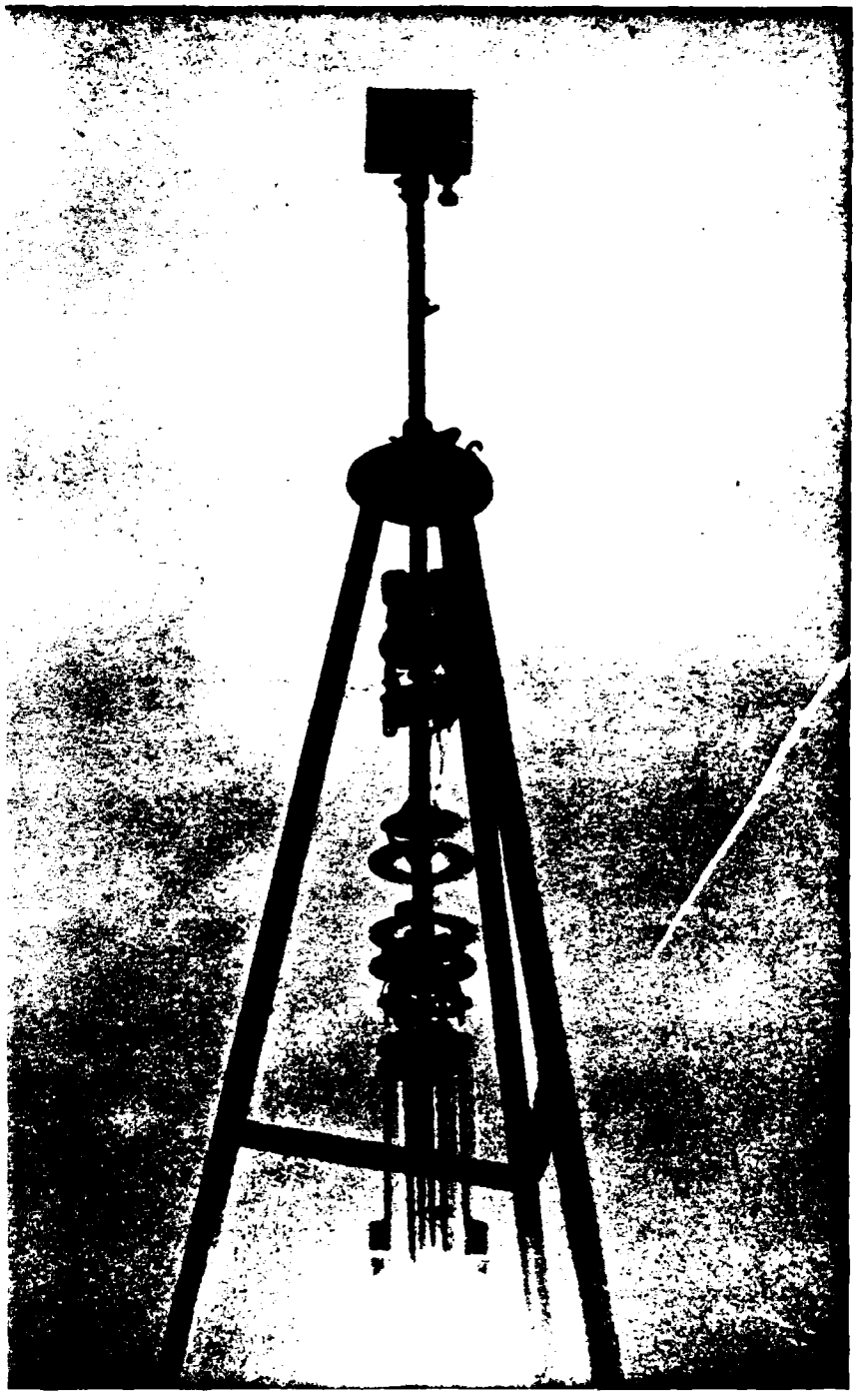

Figure 106. Probe in its launch configuration.

END

FILMED

10-85

DTIC